Role of the chemokines CCL17 and CCL22 in the immune defence against *Salmonella* infection

Anna Belen Erazo

ORCID ID:
0000-0002-2317-675X

from Guayaquil, Ecuador

Submitted in total fulfilment of the requirements of the joint degree of
Doctor of Philosophy (PhD)
of
The Medical Faculty
The Rheinische Friedrich-Wilhelms-Universität Bonn
and
The Department of Microbiology and Immunology
The University of Melbourne

Bonn/Melbourne, 2020

Performed and approved by The Medical Faculty of The Rheinischen Friedrich-Wilhelms-Universität Bonn and The University of Melbourne

1. Supervisor: Prof. Dr. Christian Kurts

2. Supervisor (shared): Prof. Dr. Irmgard Förster
Prof. Richard A. Strugnell, PhD
Nancy Wang, PhD

Date of submission: 31st of October 2019

Date of the oral examination: 3rd of March 2020

LIMES Institute, Director: Prof. Dr. Waldemar Kolanus

Table of Content

Abbreviations

A	act	Activated
	AF	Autofluorescent
	alum	Aluminium phosphate
	AMP	Adenosine monophosphate
	APC	Antigen-presenting cells
	ATP	Adenosine triphosphate
B	β_2m	Beta two microglobulin
	BatF3	Basic leucine zipper transcriptional factor ATF-like 3
C	CCL	Chemokine ligand
	CCR	Chemokine receptor
	CFU	Colony-forming unit
	CI	Confidence interval
	CNS1	Conserved nucleotide sequence 1
	conc	Concentration
	CTLA4	Cytotoxic T-lymphocyte-associated protein 4
D	DAMP	Damage-associated molecular pattern
	DC	Dendritic cell
E	eff	Effector
	EGFP	Enhanced green fluorescence protein
F	FAE	Follicle-associated epithelium
	FCS	Foetal calf serum
	Fig	Figure
	FLT3L	FMS-like tyrosine kinase 3 ligand
	FOXP3	Forkhead-box protein P3
G	GALT	Gastrointestinal associated lymphoid tissue
	GATA3	GATA binding protein 3
	GF	Growth factor
	GI	Gastrointestinal
	GSK	GlaxoSmithKline
H	h	Hours
	HIV	Human Immunodeficiency Virus

I	IFNγ	Interferon gamma
	IFNγ-R	Interferon gamma receptor
	IL	Interleukin
	ILC	Innate lymphoid cell
	IPEX	Immune dysregulation, polyendocrinopathy, enteropathy, X-linked
	IRF4	Interferon regulatory factor 4
	IRF8	Interferon regulatory factor 8
K	KLRG1	Killer Cell Lectin Like Receptor G1
	KO	Knock out
L	LB	Luria-Bertani
	LC	Langerhans cell
	LD	Live-Dead
	LP	Lamina propria
	LPS	Lipopolysaccharides
M	M cell	Microfold cell
	MDC	Macrophage-derived chemokine
	MDR	Multidrug-resistant
	MFI	Mean fluorescence intensity
	MHCI	Major histocompatibility complex class I
	MHCII	Major histocompatibility complex class II
	min	Minutes
	mLN	Mesenteric lymph nodes
	MP	Mononuclear phagocytes
	MOI	Multiplicity of Infection
N	NK cell	Natural killer cell
	NKT cell	Natural killer T cell
	Nramp1	Natural resistance-associated macrophage protein 1
	nTD	Not *Salmonella* Typhi diagnosed
P	PAMP	Pathogen-associated molecular pattern
	PBS	Phosphate-buffered saline
	PCM	Paracoccidioidomycosis
	PCR	Polymerase chain reaction

	PP	Peyer’s patches
	PRR	Pattern recognition receptor
	PV	Pre-vaccination
R	RBC	Red blood cell
	RORγT	Retinoic acid-related orphan receptor gamma T
S	SCV	*Salmonella*-containing-vacuole
	SED	Subepithelial dome
	SPF	Specific pathogen-free
	STM	*Salmonella enterica* Serovar Typhimurium
	STY	*Salmonella enterica* Serovar Typhi
T	T_{conv}	Conventional T cell
	TARC	Thymus and activation-regulated chemokine
	Tbet	T-box–containing protein expressed in T cell
	TCR	T cell receptor
	TCV	Typhoid conjugate vaccine
	TD	*Salmonella* Typhi diagnosed
	TF	Transcription factor
	TGFβ	Transforming growth factor beta
	TGFβ-R1	TGFβ receptor type-1
	Th	T helper cell
	TLR	Toll-like receptor
	TNFα	Tumour necrosis factor alpha
	T_{reg}	Regulatory T cell
W	WHO	World Health Organization
	wt	Wild type

List of Tables

List of Figures

Abstract

The chemokines CCL17 and CCL22 are both ligands of the chemokine receptor CCR4, which is expressed on dendritic cells (DC) and a variety of different effector T cells including regulatory T cells (T_{reg}). Both chemokines are mainly produced by DC, but also by macrophages. CCL17 promotes numerous inflammatory and allergic diseases, whereas CCL22 is rather associated with an immunosuppressive milieu. These differential roles are reflected by preferential recruitment of distinct subsets of T cells to site of inflammation. While CCL17 facilitates chemotaxis of effector T cells and supports DC-T cell interactions as well as DC migration towards CCR7-ligands, CCL22 induces chemotaxis of T_{reg} cells. In addition, CCL22 signalling induces a more rapid desensitisation and internalisation of CCR4 than CCL17, suggesting biased agonism of CCL17 and CCL22. The functionality of CCL17 and CCL22 should, therefore, be considered in combination as well as individually in the context of immune-related diseases. The role of CCL17 and CCL22 in infectious diseases has not been well understood. The central hypothesis was that CCL17 and CCL22 play important but potentially different roles during bacterial infection. This was modelled using a well-studied bacterial pathogen, *Salmonella enterica* serovar Typhimurium (STM). It was hypothesised that CCL17 expression may direct the migration of STM-infected DC from the gut to draining lymph nodes a key bottleneck in early infection that controls bacterial dissemination to systemic sites. It was further hypothesised that CCL22 may play a role in immune regulation through the induction of T_{reg} cells. These regulatory cells may have downstream effects on Th1 responses, which are critical for the control of *Salmonella* infection.

In the first part of the thesis, the role of CCL17$^+$ DC in the transmission of STM was investigated. Histological analysis of CCL17 reporter mice revealed that CCL17-expressing cells co-localised with *Salmonella* in the dome area of Peyer's patches (PP). Further, CCL17-expressing DC contributed to dissemination of STM from PP to the mesenteric lymph nodes (mLN). Within the mLN, STM were found within CCL17$^+$ DC as well as in other DC, monocytes and macrophages. Analysis of the STM$^+$ DC subpopulations revealed that all DC subsets carried STM, but the CD103$^+$ CD11b$^-$ DC could be identified as the main STM-containing population. STM infection triggered upregulation of CCL17 expression in specific intestinal DC subsets in a tissue-specific manner. Interestingly, the $CD103^+$ DC subsets upregulated CCL17 in the PP, whereas $CD103^-$ DC subsets upregulated CCL17 in the mLN.

In the second part of this thesis, the role of CCL17 and CCL22 in the induction of antigen-specific $CD4^+$ T cell responses was investigated. CCL17/CCLL22 double-deficient, CCL17- and CCL22 single-deficient, and wild type mice were analysed after live-attenuated STM TAS2010 vaccination, vaccination/challenge and in steady-state. Mice deficient in both chemokines, CCL22 and CCL17, demonstrated a reduction of effector T_{reg} cells. This promoted an enhanced STM-specific Th1 immune response characterised by an expansion of Th1 T cells, resulting in a more favourable effector T_{reg}/activated T_{conv} ratio and a significantly improved vaccine efficacy to challenge with virulent *Salmonella*.

In conclusion, the work presented within this thesis showed the contribution of $CCL17^+$ DC in the dissemination of STM and identified CCL22 as a potential target to improve vaccine approaches.

Declaration

The work that is presented in this thesis was conducted at the University of Bonn, the laboratory of Professor Dr. Irmgard Förster and at the University of Melbourne, the laboratory of Professor Richard A. Strugnell. The research work was funded by grants obtained from the National Health and Medical Research Council and the Deutsche Forschungsgemeinschaft. Anna Belen Erazo was supported by the Melbourne International Fee Remission Scholarship.

This is to certify that,

(i) the thesis comprises only my original work towards the PhD except where indicated in the preface,

(ii) due acknowledgement has been made in the text to all other material used,

(iii) the thesis is less than 100,000 words in length, exclusive of tables, maps, bibliographies and appendices.

Anna Belen Erazo

Preface

My contribution to the experiments within each section was as follows:

Section 3.1: 100%
Section 3.2: 100%
Section 3.3: 100%

I acknowledge the important contributions of others to experiments presented herein:

Section 3.2: Nancy Wang, PhD; Adrian Semeniuk
Section 3.3: Prof. A. Pollard; Jennifer Hill, PhD

Acknowledgments

The present work reflects the incredible support I have received from many individuals throughout; supervisors, advisors, colleagues, friends and family. I sincerely thank everyone for your encouragement and support during this fantastic journey.

First of all, I want to thank Prof. Irmgard Förster for allowing me to undertake my PhD thesis in her laboratory and for the chance to work and grow very independently as a scientist. She always provided me with valuable input and feedback and supported me in any possible way on this challenging journey of a joint PhD at two different institutions and continents. Besides, I want to thank Prof. Richard Strugnell for allowing me to work in his lab. His direct, focused but also relaxed attitude made him a great supervisor. I also want to thank Prof. Cristian Kurtz for agreeing to be my examiner.

Further, I would like to thank everybody from the Förster and Weighardt laboratory. You are the best lab a PhD student can wish for! In particular, I want to thank Heike, who always provided me with new perspectives and good advice on my work. A big thanks goes to Philip, who spent countless hours with me in the S2 room; I really enjoyed our conversations, discussions and our shared love for cats. I also thank Lorenz for being such an enthusiastic and inspiring person. Every time he talks about science, there is just no other possibility than loving it. And of course, I thank everybody else I did not name in person!

Then I would like to thank my second lab, the Strugnell laboratory, who welcomed me from the very beginning as one of their one. The great experience I have made in Melbourne would not have been possible without you guys! Especially, I want to thank Nancy, who has been incredibly supportive. Her never-ending help with organisation and experiments, and her always useful advice has made my PhD a successful experience. I also thank Karthik for becoming such a good friend, even though he did not like to clean up his lab space. I thank Adrian for being the person he is. And I thank everybody else in the Strugnell lab.

I am very grateful to our collaborators in Oxford, Prof. Andrew Pollard and his lab. I am thankful for so many people I have met during my PhD in Bonn and Melbourne, and that have supported me. Further, I have to thank the animal

caretakers at the LIMES and at the Peter Doherty for doing a great job. I also thank Marie and Lucie.

Most importantly I would like to thank my husband, Lars, for his continuous love and faith in me. Even though he may not always understand what I do he always knows what I need. I thank my family and parents for their never-ending support and for making me the person I am today.

List of Publications

- Fülle L., Steiner N., Funke M., Gondorf F., Pfeiffer F., Siegl J., Opitz F.V., Haßel S.K., **Erazo A.B.**, Schanz O., Stunden H.J., Blank M, Gröber C., Händler K., Beyer M., Weighardt H., Latz E., Schultze J.L., Mayer G., and Förster I.;
  RNA Aptamers Recognizing Murine CCL17 Inhibit T Cell Chemotaxis and Reduce Contact Hypersensitivity In Vivo, Mol Ther 26, 95, 2018.

- Fülle L., Offermann N., Hansen J.N., Breithausen B., **Erazo A.B.**, Schanz O., Radau L., Gondorf F., Knöpper K., Alferink J., Abdullah Z., Neumann H., Weighardt H., Henneberger C., Halle A., Förster I.;
  CCL17 exerts a neuroimmune modulatory function and is expressed in hippocampal neurons, Glia. 2018 Oct;66(10):2246-2261.

There are more things in heaven and earth, Horatio,
Than are dreamt of in your philosophy.

Hamlet (1.5.167-8)
William Shakespeare

1 Introduction

1.1 The immune system

We are constantly exposed to microorganisms, some we need, some we live with and some can cause disease and still we only fall ill rarely. How are we able to permanently defend ourselves? When we eventually get infected, how do we overcome the invader and recover? And how come, that once we encountered many infectious pathogens we show lifelong protection against the diseases they cause?

The immune system is a very complex construct of physical barriers, such as the skin and the intestinal epithelium, chemical barriers, such as the low pH in the stomach, enzymatic and humoral factors, including antimicrobial peptides, complement and antibodies, and cellular components. These cellular elements comprise innate immune cells, such as macrophages, granulocytes and natural killer cells, as well as T and B cells representing adaptive immune cells, which provide a much more focussed and potent immune response (Fig 1.1.1). When the physical and chemical barriers, which form the first line of defence, are breeched, the cells of the innate immune system take over. In other circumstances where the microbe has some capacity to resist innate effectors, inflammation can result and together with innate immune cells serves to activate the adaptive immune cells (Murphy and Weaver, 2017).

Inflammatory inducers, which may be either pathogen-associated molecular patterns (PAMP) or damage-associated molecular patterns (DAMP), bind to pattern recognition receptors (PRR) expressed by immune cells, epithelial cells and other cells, and alarm the immune system (Murphy and Weaver, 2017). Several classes of PRR have been characterised, including Toll-like receptors (TLR), nucleotide-binding oligomerization domain (Nod)-, leucine-rich repeat–containing receptors (NLR) or RIG-I-like receptors (RLR) (Murphy and Weaver, 2017). PRR can be categorised based on their structure and specificity, but most importantly by their localisation in defined cellular compartments, including the plasma membrane, lysosomes, endosomes and the cytosol. Current evidence supports the view that PRR-mediated sensing shapes the adaptive immune responses. The different pathways of microbial-recognition by the innate immune system reveal elements of the pathogen’s pathogenesis – presence, location, viability, replication and virulence. Each of these factors, alone and in combination, are essential for the commitment of downstream effector responses (Iwasaki and Medzhitov, 2015).

Dendritic cells (DC) are innate immune cells with phagocytic capacity, but have a unique setting within the immune system since they link innate and adaptive immune responses (Fig 1.1.1). When DC PRR are activated via PAMP, the cells are stimulated to take up the pathogen and degrade it intracellularly. Pathogen degradation results in the presentation of small pathogen-derived peptide fragments (antigens) via the major histocompatibility complex (MHC) on the DC surface. Macrophages and B cells can also act as antigen-presenting cells (APC) under certain circumstances. Once DC have taken up antigens at the site of infection they may leave the tissue and migrate to secondary lymphoid organs, such as the draining lymph nodes (LN) or the spleen. Here, DC will present pathogen-specific antigens to T cells, via MHCII for CD4$^+$ T cells and MHCI for CD8$^+$ T cells. The MHC-antigen complex activates the antigen-specific T Cell receptor (TCR), providing the first signal for the priming of naïve T cells. Stimulation of PRR also triggers the DC to express co-stimulatory molecules on the cell surface, which provides the second signal required for T cell activation (Murphy and Weaver, 2017).

Activation of naïve T cells leads to their proliferation and differentiation into effector T cells. The fate of these activated T cells depends on the DC subset that is driving the response, and the microenvironment that can differ in abundance of particular cytokines, co-stimulatory signals and strength of antigenic stimulation (Eisenbarth, 2019). Effector T cells have a variety of functions (Fig 1.1.1). CD8$^+$ cytotoxic T cells for example recognise virus-infected cells and kill them. CD4$^+$ T cells, also known as T helper (Th) cells further differentiate into functionally distinct subsets. Th1 effector cells support the activation of macrophages to enhance their killing of intracellular pathogens. Mucosal barrier immunity against pathogens such as helminths is promoted by Th2 effector cells.

The control of infection by certain kinds of fungi and bacteria is facilitated by Th17 cells, particularly at barrier sites (Murphy and Weaver, 2017).

B cell activation requires both binding of the antigen by the B cell receptor and interaction of the B cell with antigen-specific Th cells. A specific type of antigens can also induce T cell independent B cell activation (Fig 1.1.1). One of the main functions of B cells is the production of pathogen-specific antibodies. The binding of these antibodies to the pathogen promotes the elimination of the pathogen by phagocytic cells and the complement system (Murphy and Weaver, 2017).

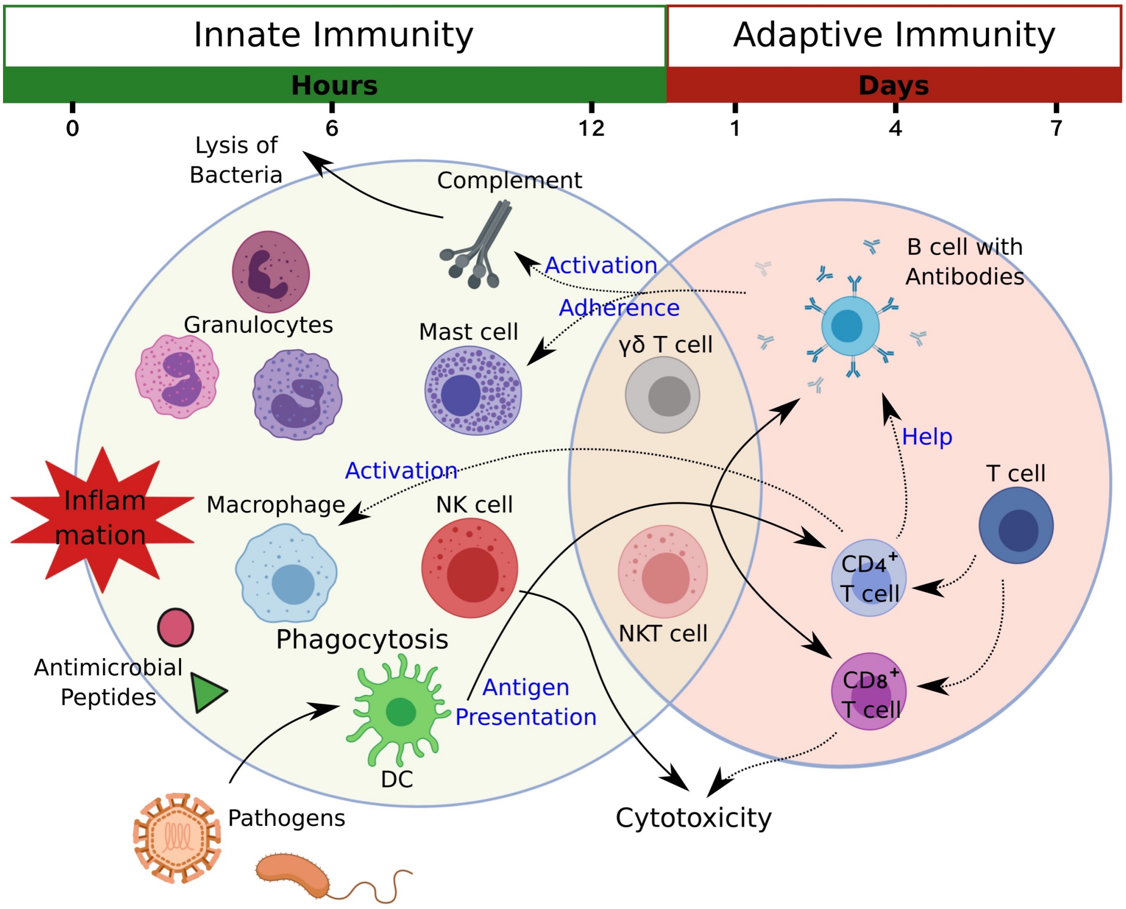

Figure 1.1.1: Key interactions between the innate and adaptive immune response Innate immunity represents the first line of defence against many pathogens. It is fast acting but has only limited specificity. Innate immune cells include DC, macrophages, mast cells, natural killer (NK) cells and granulocytes (basophils, eosinophils and neutrophils). They act either by directly engulfing the microbe or through the production of immune mediators (cytokines, chemokines etc.). On the other hand, there are the slow acting but highly specific adaptive immune responses. The two central cell types in adaptive immunity are T and B cells. In addition, NK T cells and γδ-T cells possess both innate and adaptive immune features.

T and B cells play a key role in the generation of pathogen-specific effector pathways that eliminate pathogens or pathogen-infected cells; and with the development of an immune memory that can quickly eliminate the pathogen in case of re-infection. Consequently, adaptive immune responses are the basis for effective immunisation against infectious diseases.

1.1.1 Immunity in the gut – a question of balance

The gastrointestinal (GI) tract is a unique organ system. It has evolved to digest food and take up nutrients while maintaining immune homeostasis. The gut-associated lymphoid system must balance protection against harmful microbes, while supporting tolerance against harmless food, commensals and self-antigens. Active tolerance comprises induction of anti-inflammatory responses that can be either antigen-specific or non-specific. In addition, tolerance involves deletion of autoreactive cells or induction of anergy in T cells. Oral tolerance is typically induced by elevated levels of ILI0 and TGFβ produced by CD4$^+$ regulatory T cells (T$_{reg}$) leading to the inhibition of effector T cell response. A Th2 response also supports the generation of tolerance in the gut (Mowat et al., 2004; Wawrzyniak et al., 2017). The various mechanisms which collectively result in immunological tolerance protect the mucosa from detrimental inflammatory immune responses.

The distinctive architecture of the GI tract enables both nutrient absorption and immune homeostasis. The gut has a large overall surface area generated by extensive folding over multiple levels. The large surface area permits optimal nutrient uptake whilst holding the largest number of immune cells in the body. In order to block microbe-entry and reduce pathogen-caused damage, the GI tract has an effective repertoire of protective mechanisms including physical barriers, antimicrobial molecules and specific cell immune responses (Mason et al., 2008). The gut-associated lymphoid tissue (GALT) consists of distinct inductive and effector sites. Inductive sites include specialised clusters of lymphoid follicles named Peyer's patches (PP) and mesenteric lymph nodes (mLN). PP are mostly localised at the distal part of the small intestine and are macroscopically detectable ‘nodules’. They are connected to the mLN by lymphatic vessels and have a structural arrangement similar to lymph nodes. PP are made up of large B cell follicles, flanked by smaller T cell areas and surrounded by the subepithelial dome (SED) comprised of several cell populations including macrophages and DC (Mason et al., 2008; Mowat and Agace, 2014) (Fig 1.1.2). The SED is separated from the gut lumen by the follicle-associated epithelium (FAE). This monolayer of epithelial cells is characterised by the presence of microfold (M) cells, which constantly take up molecules and particles from the gut lumen by endocytosis or phagocytosis and transport this material to specialised APC within the underlying SED through transcytosis. DC and macrophages take up this material and process it for antigen presentation to T cells (Murphy and Weaver, 2017).

The mature DC migrate into the T cell zone of the PP or to the draining mLN in a CCR7-dependent manner, where they encounter and prime naïve T cells (Jang et al., 2006; Murphy and Weaver, 2017) (Fig 1.1.2). Together, DC and T cells stimulate B cells and initiate class switching to IgA. Once T and B cells have been activated in the PP, some lymphocytes migrate directly into neighbouring areas of the lamina propria (LP). Most of these cells, however, leave the PP and mLN through the lymphatics, and ultimately end up in the thoracic duct. From there the activated lymphocytes circulate in the bloodstream and selectively re-enter the intestinal mucosa via small blood vessels, where they accumulate as effector cells in the LP (Murphy and Weaver, 2017) (Fig 1.1.2).

The LP is one of two main compartments in the gut where effector T and B cells are found. The LP contains many different types of immune cells, including IgA-producing plasma cells, conventional $CD4^+$ and $CD8^+$ T cells with effector and memory functions, innate lymphoid cells, DC, macrophages and mast cells. In contrast, a second compartment which is formed by the lymphoid components of the intestinal epithelium consists mainly of intraepithelial lymphocytes (IEL). These T cells have a wide range of regulatory and effector activities (Mowat and Agace, 2014).

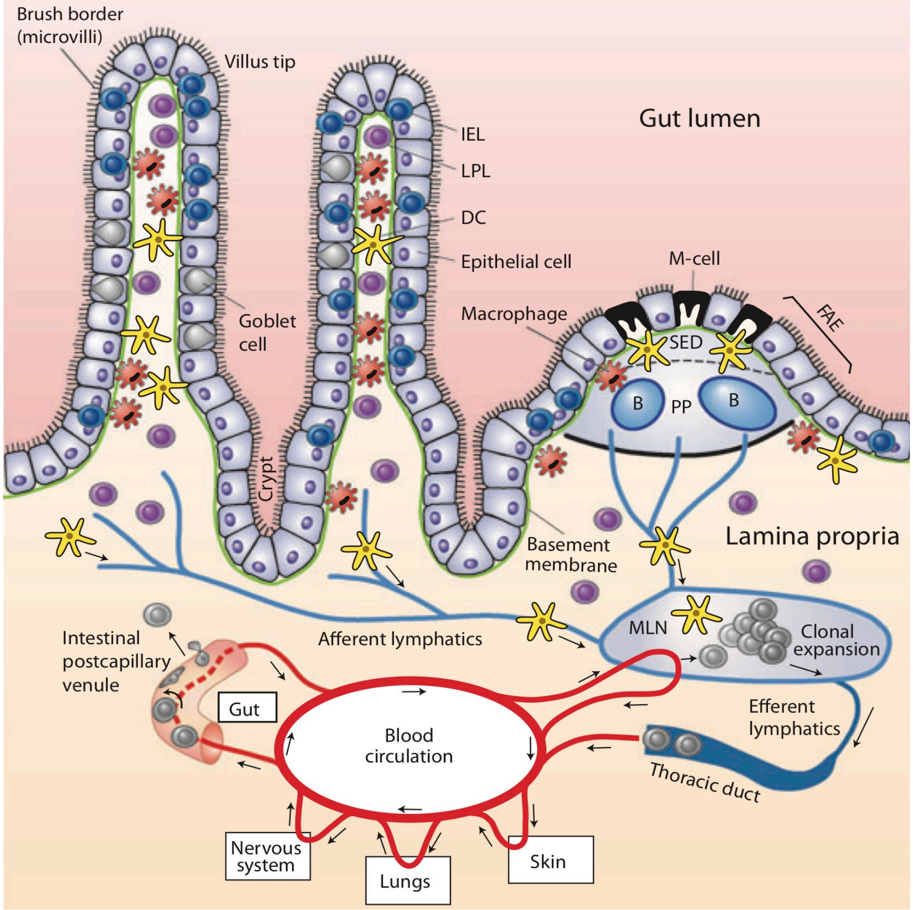

Figure 1.1.2: Architecture of the intestinal lymphoid compartments and lymphocyte trafficking

A monolayer of intestinal epithelial cells separates the gut lumen from the lamina propria. The epithelium in the small intestine forms crypts and villi. The epithelium of the crypts contains Paneth cells producing antimicrobial molecules. Goblet cells produce mucus covering the epithelium. Inductive intestinal sites comprise mLN and PP. PP consist of B cell follicles flanked by T cell regions localised beneath a subepithelial dome (SED), rich in macrophages and DC. The SED is separated from the gut lumen by a M cell containing follicle-associated epithelium (FAE). DC take up antigen via a variety of different routes and migrate to the T cell areas in the PP or to the draining mLN in order to prime naïve T cells. If a naïve T cell recognises its cognate antigen presented by a DC, in combination with co-stimulatory signals, it is activated. The activated T cells are transported via efferent lymphatic vessels to the blood. The specific homing molecules direct the activated T cells towards their final destination. The activated T cells are further guided to their effector compartment by different chemokines and adhesion molecules (Figure adapted from Marsal and Agace, 2012).

1.1.1.1 Intestinal DC and macrophages – who is who?

Intestinal mononuclear phagocytes (MP), comprising DC, macrophages and monocytes, are crucial for both immune homeostasis and induction of active immune response. Importantly, DC and macrophages perform distinct yet complementary functions in the intestine. The absence of specific identifying markers made it difficult in the past to exactly classify different intestinal MP, because the markers used, including CD11c, CD11b, MCHII, CX3CR1 and CD103, could not distinguish between most subtypes. Intestinal macrophages as well as DC express very similar levels of CD11c, CD11b and MHCII. Furthermore, not all DC in the intestine express CD103 and only a subset express CX3CR1. In order to distinguish these cells correctly from macrophages it is essential to use macrophage-specific markers like CD64 or F4/80 (Cerovic et al., 2014; Joeris et al., 2017).

Intestinal DC can be classified as lineage (CD3, CD19, NK1.1) negative cells that express CD11c and MHCII but, in contrast to macrophages, do not express CD64. They are FMS-like tyrosine kinase 3 ligand (FLT3L) dependent for their development from DC precursors in the bone marrow, and have only a short lifespan in tissue of a few days (Joeris et al., 2017). The DC compartment in the gut is highly heterogenous but can be subdivided depending on the expression of CD103 and CD11b, forming 4 intestinal DC subpopulations: CD103^{+} CD11b^{-}, CD103^{+} CD11b^{+}, CD103^{-} CD11b^{+} and CD103^{-} CD11b^{-} (Cerovic et al., 2014; Joeris et al., 2017). Importantly all 4 subsets migrate via the lymph from the intestine to the mLN and are able to present antigen to naïve T cells and to induce CCR9 expression on dividing T cells *in vitro*. (Cerovic et al., 2013) (Fig 1.1.3). Hence, each population has the potential to stimulate and regulate adaptive immune responses.

Studies investigating the lymphatic and splenic DC populations in the body demonstrated that DC can be split into two distinct populations, namely cDC1 and cDC2 which are developmentally dependent on IRF8 and IRF4, respectively (Schlitzer et al., 2013, 2015). The composition of the intestinal DC compartment is more complex, but the same approach can be applied in principle. The CD103^{+} CD11b^{-} intestinal DC represent the cDC1 and are dependent on BATF3 and IRF8 for their development (Edelson et al., 2010; Persson et al., 2013). Like TLR-activated CD103$^+$ DC in other tissues, they efficiently cross-present soluble antigen and can prime effector CD8$^+$ T cells (Cerovic et al., 2013). The CD103$^+$ CD11b$^-$ intestinal DC also support Th1 cell differentiation in mLN, characterised by IFNγ (Luda et al., 2016), and are required for optimal induction of T_{reg} cells in the intestine (Esterházy et al., 2016; Welty et al., 2013).

The CD103$^+$ CD11b$^+$ intestinal DC represent the cDC2 and are dependent on IRF4 for their development (Persson et al., 2013; Schlitzer et al., 2013). They are crucial for Th17 homeostasis, since depletion of this subset results in a decrease of Th17 cells in the intestine (Persson et al., 2013; Schlitzer et al., 2013; Welty et al., 2013). T_{reg} cells are not affected by the depletion of CD103$^+$ CD11b$^+$ DC alone, but mice lacking both CD103$^+$ CD11b$^+$ and CD103$^+$ CD11b$^-$ DC subsets display a profoundly altered intestinal T_{reg} population (Welty et al., 2013). While the role of CD103$^+$ CD11b$^+$ intestinal DC in Th17 homeostasis is very clear, the function of these cells in the context of Th1, Th2 and T_{reg} cells has to be further investigated. Some data suggested a role of CD103$^+$ CD11b$^+$ DC subset in Th1 immune response (Cerovic et al., 2013), while other data rather suggested a function in Th2 immune response (Joeris et al., 2017).

The CD103$^-$ CD11b$^+$ intestinal DC population is highly heterogeneous, some of these DC are IRF4-dependent, while others are not (Scott et al., 2015). Nevertheless, previous studies showed that they are closely related to CD103$^+$ CD11b$^+$ intestinal DC since their transcriptome differs only by 100-200 genes (Joeris et al., 2017). In addition, the absence of TGFβ-R1 signalling in CD11c$^+$ cells results in an accumulation of CD103$^-$ CD11b$^+$ DC and a reduction of CD103$^+$ CD11b$^+$ DC, indicating that CD103$^+$ CD11b$^+$ DC develop from CD103$^-$ CD11b$^+$ DC (Joeris et al., 2017). *In vitro* CD103$^-$ CD11b$^+$ DC are able to prime the development of IFNγ-producing T cells and IL17-producing T cells (Cerovic et al., 2013; Scott et al., 2015).

The CD103$^-$ CD11b$^-$ intestinal DC subset represents the least abundant intestinal DC population. Relatively little is known about these cells. They most likely represent a population of PP-resident DC that can migrate to the mLN (Cerovic et al., 2014). *In vitro* CD103$^-$ CD11b$^-$ DC are able to prime IL17-producing T cells (Cerovic et al., 2013) (Fig 1.1.3).

Table 1.1.1: Intestinal DC subsets – summary of markers, ontogeny and functions

Phenotype		Ontogeny		Function	
Common marker	Subset-specific marker	GF	TF	Common	Specialised
CD11c$^+$ **MHCII$^+$** CD64$^-$ F4/80$^-$ Ly6C$^-$ CD3$^-$ CD19$^-$ B220$^-$ NK1.1$^-$	**CD103$^-$** **CD11b$^-$**	FLT3L-dependent	?	CCR7-dependent migration to mLN Presentation of soluble proteins	Th17
	CD103$^-$ **CD11b$^+$**		IRF4 ?		Th17 Th1
	CD103$^+$ **CD11b$^+$**		IRF4		Th17 Th2/Th1? T$_{reg}$
	CD103$^+$ **CD11b$^-$**		IRF8 BatF3		Th1 Cross presentation T$_{reg}$

GF: growth factor, TF: transcription factor

Intestinal macrophages can be defined as lineage (CD3, CD19, NK1.1, Ly6G) negative cells that express CD11c and MHCII, but in contrast to DC also express CD64. They are developmentally independent of FLT3 signalling but require the colony-stimulating factor 1 receptor (CSF-1R). Unlike many other tissue-resident macrophages, which develop from embryonic precursors, those in the intestine require constant replenishment by blood monocytes (Joeris et al., 2017). After arrival in the intestinal mucosa, Ly6C$^+$ blood monocytes undergo a process of local differentiation, first acquiring MHCII before losing Ly6C, resulting in a series of phenotypic intermediates known as the monocyte ‘waterfall’ (Fig 1.1.3) (Cerovic et al., 2014).

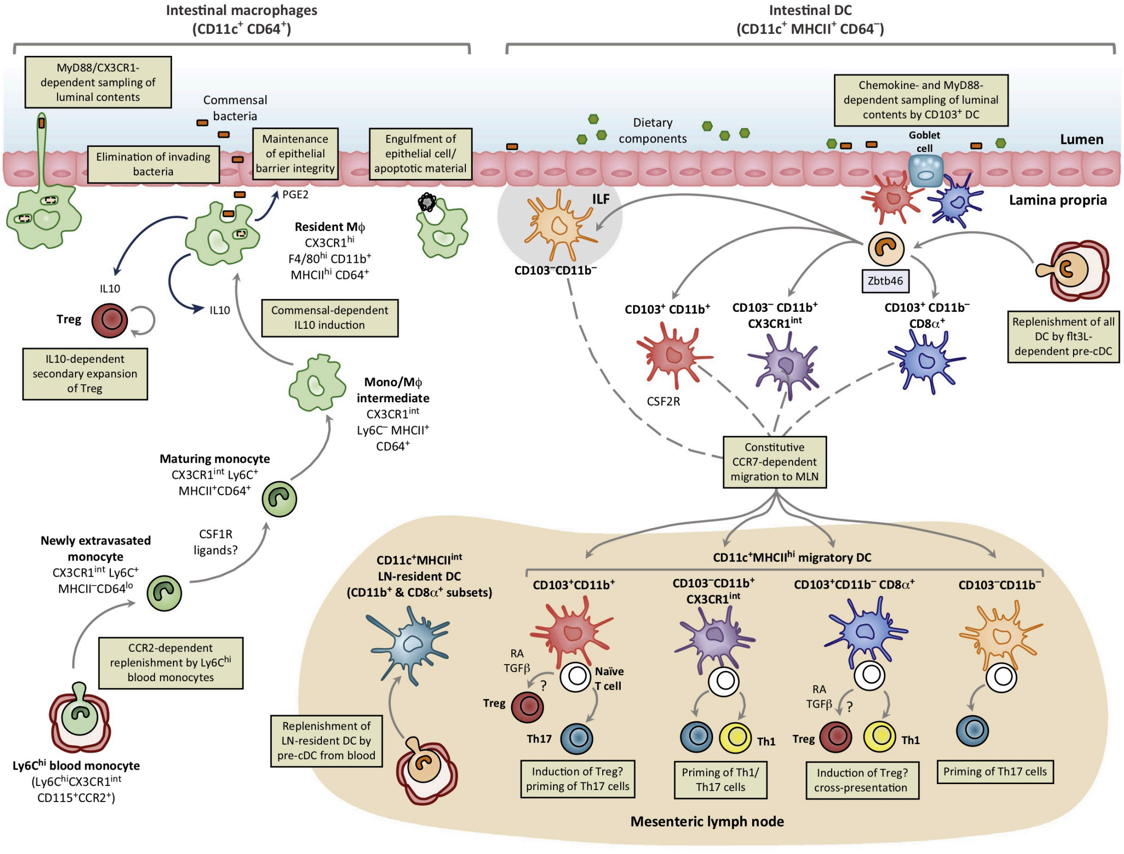

TRENDS in Immunology

Figure 1.1.3: Distinct phenotype, ontogeny and function of intestinal DC subsets and macrophages
Ly6C$^+$ blood monocytes continuously replenished intestinal macrophages. After entering the intestinal mucosa Ly6C$^+$ monocytes undergo differentiation into tissue-resident macrophages. Intestinal macrophages reside near the endothelium and are perfectly equipped to take up apoptotic cells and any invading microbes. In addition, they can extend cellular processes and sample the luminal content. Since they cannot migrate to the mLN it is rather unlikely that they are able to prime naïve T cells. However, they continuously secrete IL10 thereby, facilitating the survival and secondary expansion of T$_{reg}$ cells. In contrast to macrophages, intestinal DC do not express CD64 or F4/80. They derive from a FLT3L-dependent DC precursor and develop into 4 functionally different populations, dependent on their expression of CD103 and CD11b. They are able to acquire luminal antigen via a variety of different routes. Following antigen uptake, all subsets of intestinal DC are able to migrate to the mLN in a CCR7-dependent manner. In the mLN the different DC subsets are able to induce differential T cell responses (Figure adapted from Cerovic *et al.*, 2014).

At steady-state, intestinal macrophages have a lifespan of several weeks and these cells are not able to migrate from the gut to the mLN and have little or no ability to prime naïve T cells (Cerovic et al., 2014; Joeris et al., 2017; Murphy and Weaver, 2017). Intestinal macrophages are positioned immediately under the epithelium, ideally located to clear apoptotic cells and to take up and degrade any organisms that penetrate across the epithelial barrier, maintaining intestinal homeostasis (Cerovic et al., 2014; Joeris et al., 2017). However, unlike macrophages in other parts of the body, intestinal macrophages are relatively unresponsive to activating stimuli such as IFNγ, TLR ligands or pathogen uptake. They do not produce significant quantities of pro-inflammatory cytokines, reactive oxygen or nitrogen species in response to inflammatory stimuli (Bain et al., 2013; Platt et al., 2010; Weber et al., 2011a). This is because they constitutively produce large amounts of IL10 (Bain et al., 2013; Krause et al., 2015), allowing them to limit inflammation while acting as powerful scavengers. Macrophage-derived IL10 is also essential for maintaining antigen-specific tolerance in the intestine since it facilitates the survival and secondary expansion of T_{reg} cells that have migrated back to the intestine after being primed by tolerogenic DC in the lymph node (Hadis et al., 2011). Furthermore, IL10 acts on T_{reg} cells to maintain their suppressive activity in the presence of inflammation (Murai et al., 2009). Intestinal macrophages are involved in the survival and maintenance of other immune cells in the gut. For example, macrophage-derived IL1β produced in response to the microbiota is critical in the differentiation of IL17-producing Th17 cells in the intestine (Shaw et al., 2012) (Fig 1.1.3).

In contrast to intestinal macrophages, monocytes and their intermediates are the main producers of pro-inflammatory stimuli such as IL1, IL6, IL23, TNFα, reactive oxygen or nitrogen species in the inflamed intestine. These pro-inflammatory mediators recruit and activate additional immune effector cells, but also promote tissue damage (Joeris et al., 2017).

Table 1.1.2: Intestinal macrophages and monocytes – summary of markers, ontogeny and functions

Phenotype			Ontogeny		Function
Common marker	Subset-specific marker		GF	TF	Common
Ly6G$^-$ CD3$^-$ CD19$^-$ B220$^-$ NK1.1$^-$	**CD64$^{-/+}$** **CD11c$^-$**	**Ly6C$^+$** **MHCII$^-$**	CFS1-dependent	Runx’3 PU.1	Production of pro-inflammatory mediators in response to TLR ligands etc.
		Ly6C$^+$ **MHCII$^+$**			
		Ly6C$^-$ **MHCII$^+$**			
	CD64$^+$ **CD11c$^+$**	**Ly6C$^-$** **MHCII$^+$**			Scavenging, removal of apoptotic cells and microbes Maintain integrity of epithelial barrier IL10 production Maintenance of T_{reg}

GF: growth factor, TF: transcription factor

Although intestinal DC and macrophages share many markers, they play distinct but complementary roles in the intestine. Migratory DC are responsible for the initial priming and shaping of T cell responses, and tissue-resident macrophages scavenge microbes and cellular debris and may regulate the activity of already primed T cells in the intestine itself.

1.1.1.2 Regulatory T cells – friend or foe?

Together with other specialised immune cells and mechanisms, regulatory T cells (T_{reg}) play a central role in intestinal homeostasis and maintenance of gut health. Sakaguchi and co-workers first showed that $CD4^+$ $CD25^+$ T_{reg} cells can downregulate T cell immune response (Sakaguchi et al., 1995). Since this study researchers have shown that T_{reg} cells suppress activation, proliferation and cytokine production of effector T cells (Sabbagh et al., 2018; Whibley et al., 2019). T_{reg} cells are defined by their expression of the transcription factor forkhead-box protein P3 (FOXP3), which is critical for T_{reg} development and their suppressive function. The critical role of T_{reg} cells in peripheral tolerance is emphasised by the development of detrimental autoimmunity in mice lacking the gene FOXP3 (Whibley et al., 2019). Humans bearing mutations in FOXP3 suffer from the IPEX syndrome (immune dysregulation, polyendocrinopathy, enteropathy, X-linked). This autoimmune disease has in many cases gastrointestinal and skin manifestations, further underlining the important role of T_{reg} cells in the maintenance of homeostasis in barrier organs (Gambineri et al., 2003). Furthermore, T_{reg} cells also ensure a controlled immune response upon pathogen encounter since pathogens often cause excessive acute and chronic inflammation. In order to prevent immune pathology, inflammatory responses are strongly downregulated at the molecular level as well as at the cellular level by T_{reg} cells. On the other hand, excessive suppression by T_{reg} cells can interfere with pathogen clearance and promote infection (Belkaid, 2007; Rowe et al., 2012).

T_{reg} cells can develop in two different ways. Natural T_{reg} cells (nT_{reg}) are thymus-derived and differentiate into $FOXP3^+$ T_{reg} cells subsequent to recognition of self-antigen by the TCR in the thymus. Induced T_{reg} cells (iT_{reg}) are periphery-derived and exit the thymus as naïve $CD4^+$ T cells and develop into $FOXP3^+$ T_{reg} cells following recognition of their cognate antigen, which is usually regarded as non-self (Bilate and Lafaille, 2012). Both T_{reg} populations are present in the gut (Luu et al., 2017). The functions of nT_{reg} and iT_{reg} cells, however, are distinct. Mice deficient for CNS1 (conserved nucleotide sequence 1), which is a FOXP3 regulatory element, lack iT_{reg} cells, but not nT_{reg} cells, and develop spontaneous inflammation in lung and gastrointestinal tissues (Josefowicz et al., 2012). This is consistent with available evidence that indicates that iT_{reg} cells primarily mediate tolerance towards the microbiota and food antigens. For example, through suppression of aberrant Th1 responses to dietary factors (Whibley et al., 2019).

T_{reg} cells can also be categorised due to their activation status, from naïve to effector and memory cells. Upon antigen-encounter, T_{reg} cells undergo different activation states that can be marked by the expression of specific surface proteins such as KLRG1 (Yuan et al., 2014). T_{reg} cells that express KLRG1 also secret higher levels of suppressive molecules such as granzyme B or IL10 and are prone to apoptosis. Moreover, they express chemokine receptors that support migration into non-lymphoid tissues (Cheng et al., 2014). Consistent with these findings, $KLRG1^+$ T_{reg} cells form the dominant T_{reg} population in the lamina propria (Yuan et al., 2014).

T_{reg} cells possess a range of suppressive properties, including the production of anti-inflammatory cytokines such as IL10 and TGFβ, secretion of granzyme and perforin, which induce apoptosis of target cells, and the expression of the inhibitory receptor CTLA4, which can down-regulate the expression of CD80/CD86 on DC (Sabbagh et al., 2018; Vignali et al., 2008; Whibley et al., 2019). T_{reg} cells can also regulate the availability of growth factors such as IL2, and deplete the microenvironment of extracellular ATP via the production of AMP and adenosine, molecules with immunosuppressive properties (Vignali et al., 2008; Whibley et al., 2019). T_{reg} cells do not use one dominant mechanism of suppression, but rather many different mechanisms in order to suppress a vast variety of target cells and microenvironments in which T_{reg} cells act.

All types of T_{reg} cells, both natural and induced, have to be stimulated via their TCR in an antigen-specific fashion to become suppressive (Li and Rudensky, 2016), but their activity towards conventional T cells might not necessarily need to be antigen-specific (Akkaya et al., 2019; Dowling et al., 2018; Göbel et al., 2012; McNally et al., 2011; Olson et al., 2012). Interestingly, T_{reg} cells can experience stimulus-specific differentiation that is regulated by transcription factors characteristically linked to the differentiation of conventional $CD4^+$ T cells. For instance, Tbet controls T_{reg} cell function and migration via CXCR3 during type

1 inflammation, thereby promoting suppression of Th1 response. It is very likely that the very same approach also applies to GATA3 for Th2 T_{reg} cells and RORγT for Th17 T_{reg} cells (Cretney et al., 2013).

1.1.2 Chemokines

Chemokines form a large group of small, secreted molecules that regulate leukocyte trafficking and positioning under physiological and inflammatory conditions. They are defined by the arrangement of specific cysteine residues within the folded protein. The cysteine residues form disulphide-bonds that preserve the structure of the chemokine. Based on the specific position of these cysteine residues, chemokines are classified into 4 subclasses: CC chemokines, CXC chemokines, CX_3C chemokines and XC chemokines (Kufareva et al., 2015). They can also be grouped depending on their expression pattern and role. Homeostatic chemokines are constitutively expressed and facilitate leukocyte mobilisation during normal physiological conditions, whereas inflammatory chemokines are inducible and regulate leukocyte trafficking during inflammation (Cardona et al., 2013). To date, the heterogenous group of chemokines consist of approximately 50 members in humans and mice. Chemokines act via binding to their chemokine receptor(s), which are differentially expressed on leukocytes. Approximately 20 signalling G protein-coupled chemokine receptors have been described (Griffith et al., 2014). Furthermore, a few non-signalling chemokine receptors which are G protein-independent have been described. These non-signalling chemokine receptors appear to regulate chemokine gradients and reduce inflammation by scavenging chemokines (Griffith et al., 2014). Chemokines are promiscuous in their interaction with chemokine receptors. For instance, one receptor often recognises several ligands, and one chemokine can often bind to various receptors (Hughes and Nibbs, 2018). Although chemokines are active as monomers, they also form homodimers, heterodimers, and higher order aggregates, which adds up to the complexity of chemokine signalling (Hughes and Nibbs, 2018).

In the last decade, our knowledge and understanding of chemokine functions has broadened, enabling us to comprehend that chemokines not only work as chemoattractant but rather fulfil many more complex and diverse functions. Studies have proven that the chemokine network exhibits important roles in priming of naïve T cells, in regulatory T cell function and cell fate decisions such as memory and effector cell differentiation (Griffith et al., 2014).

1.1.2.1 CCL17 and CCL22 – a complex relationship

The CC chemokines CCL17, also known as thymus and activation-regulated chemokine or TARC, and CCL22, also known as macrophage-derived chemokine or MDC, act via their CC chemokine receptor 4 (CCR4). CCL17 was described for the first time in 1996 in a study which demonstrated constitutively CCL17 mRNA expression in the human thymus (Imai et al., 1996). Later on, the murine homologue was identified in murine bone marrow derived DC (Lieberam and Förster, 1999). In tissues, cDC2 represent the main source of CCL17 in steady-state (Alferink et al., 2003), but alternatively activated macrophages can also produce CCL17 (Katakura et al., 2004) (Fig 1.1.4). Expression of CCL17 could be described in all major barrier organs as well as in secondary lymphoid tissues, such as lung, skin, intestine and draining LN (Alferink et al., 2003; Heiseke et al., 2012; Yahia et al., 2014). *In vitro* and *in vivo* studies suggested that the major functions of CCL17 are the induction of T cell chemotaxis via the receptor CCR4 (Fülle et al., 2018a; Weber et al., 2011b), the initiation of DC-T cell interactions (Semmling et al., 2010) and the support of DC migration (Stutte et al., 2010) (Fig 1.1.4). CCL17 promotes cutaneous DC emigration from the skin by enhancing responsiveness to the CCR7 (CCL19/21) and CXCR4 (CXCL12) ligands (Stutte et al., 2010). Using a well-established CCL17-deficient mouse model generated in our laboratory, several studies have demonstrated the involvement of CCL17 in the induction or enhancement of a broad spectrum of inflammatory and allergic diseases, including contact hypersensitivity, atopic dermatitis, atherosclerosis, colitis and arthritis (Achuthan et al., 2016; Alferink et al., 2003; Fülle et al., 2018a; Heiseke et al., 2012; Stutte et al., 2010, 2012; Weber et al., 2011b). Comparable to the mouse model, CCL17 is produced upon an inflammatory signal and can be associated with atopic dermatitis, contact hypersensitivity and atherosclerosis (Greaves et al., 2001; Kamsteeg et al., 2010;

Vestergaard et al., 2000) in humans, making the CCL17 murine model particularly useful for modelling these diseases.

The second ligand of CCR4, CCL22, is as well predominantly expressed by DC, but also by macrophages and B cells (Godiska et al., 1997; Rapp et al., 2019; Schaniel et al., 1998; Vulcano et al., 2001) (Fig 1.1.4). Under physiological conditions, CCL22 expression has been reported in the thymus, LN, PP and at a comparatively reduced level in the spleen, lung and colon (Rapp et al., 2019). Furthermore, CCL22 produced by monocyte-derived DC promoted the rapid binding of DC to activated T cells (Fig 1.1.4). These findings emphasise the importance of chemokine-dependent binding of activated T cells to DC in T cell priming (Wu et al., 2001). Until very recently, no CCL22-deficient mouse model was available, which made the research on CCL22 and its potential functions in health and disease more complex. Nevertheless, the involvement of CCL22 in diverse pathologies, ranging from allergic reactions, autoimmunity to tumour growth has been demonstrated using e.g. CCL22 neutralising antibodies or artificially increasing CCL22 (Anz et al., 2015; Bischoff et al., 2015; Curiel et al., 2004; Eby et al., 2015; Montane et al., 2011; Wiedemann et al., 2016). An important feature of CCL22 is the recruitment of T_{reg} cells in humans and mice. In tumour biology, the role of CCL22 in T_{reg} recruitment and associated tumour-specific T cell immunity suppression has been well documented (Anz et al., 2015; Curiel et al., 2004; Gobert et al., 2009; Wiedemann et al., 2016).

The only known receptor of CCL17 and CCL22 is CCR4. It was initially identified in the thymus (Hoogewerf et al., 1996), however, numerous studies have since shown expression of CCR4 on functionally distinct T cell subsets, including activated Th1 cells, Th2 cells, and T_{reg} cells (Andrew et al., 2001; Inukai et al., 2007; Latorre et al., 2019; Miltenyi Biotec, 2015; Morimoto et al., 2005; Sugiyama et al., 2013; Yuan et al., 2007) (Fig 1.1.4). CCL22 dampens inflammation by the recruitment of $CCR4^+$ T_{reg} cells (Curiel et al., 2004; Elhussein Mohamed et al., 2016). Consistent with this theory, it was demonstrated that depletion of $CCR4^+$ T_{reg} cells using an anti-CCR4 antibody can significantly enhance the anti-tumour immune response (Kamada et al., 2019; Sugiyama et al., 2013). In contrast, CCL17 is primarily considered to promote inflammation through the recruitment of immune cells to sites of inflammation (Fülle et al., 2018a; Weber et al., 2011b). The phenomenon that distinct chemokines promote quite different effects, but still bind to the very same receptor, might be explained by the fact that CCL17 and CCL22 engage with distinct binding sites of CCR4 (Santulli-Marotto et al., 2013a, 2013b, 2015). The differential binding of the two chemokines results in the induction of distinct signalling pathways, a phenomenon referred to as biased agonism (Anderson et al., 2016; Rajagopal et al., 2013).

Taken together, CCL17 and CCL22 play a vital role in the immune system, especially in the induction and regulation of T cell immunity. The fact that each of the two chemokines promotes different and sometimes contradictory effects, evokes the question how this relationship between CCL17 and CCL22 might exactly work.

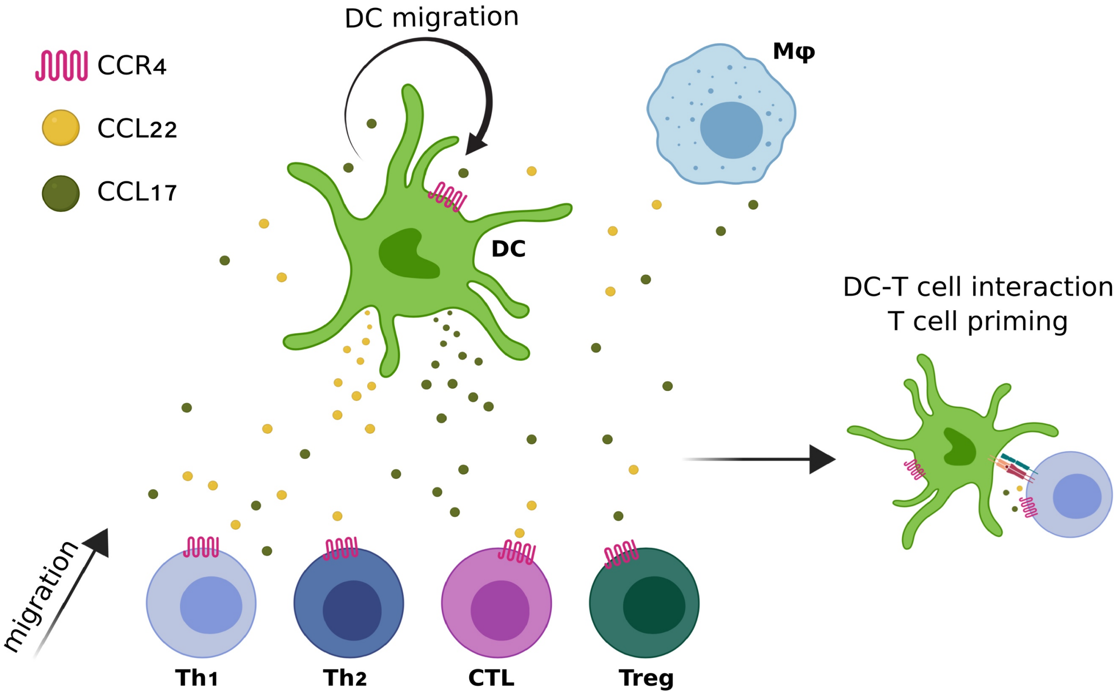

Figure 1.1.4: Origin and functions of CCL17 and CCL22
CCL17 as well as CCL22 are chemokines mainly expressed by DC, but also by macrophages. Both chemokines bind to their receptor CCR4, which is expressed on a range of different T cell subsets, including Th1, Th2, CTL and T_{reg} cells. Binding of the chemokines to their receptor induces T cell migration. In DC, CCL17 can also promote migration of DC towards CCR7 ligands, CCL19 and CCL21. The functions of CCL17 and CCL22 include initiation of DC-T cell interaction, T cell priming and chemotaxis.

1.2 *Salmonella*

Salmonella species (spp.) have been known as a main cause of infectious diseases for more than 100 years. The genus *Salmonella* spp. are Gram-negative, rod-shaped, flagellated, facultative anaerobic and intracellular bacteria closely related to the human gut bacterium *Escherichia coli* (Dougan et al., 2011). The genus *Salmonella* consists of two distinct species – *Salmonella enterica* and *Salmonella bongori* (Brenner et al., 2000) (WHO, 2019). *S. enterica* is genetically highly diverse and adapted to a range of different hosts ranging from cold to warm-blooded animals as well as to harsh environmental conditions (Agnès et al., 2014). Based on the CDC (Centers for Disease Control and Prevention) system, *S. enterica* can be further classified into 6 subspecies (Brenner et al., 2000) (WHO, 2019). About 99% of human disease isolates are accounted for by *S. enterica* subspecies enterica. According to the Kauffmann-White scheme, which is based on the serological identification of H (flagella), O (LPS) and K (capsule) antigens, *Salmonella* subspecies can be further separated into serovars (Dougan et al., 2011), resulting in a nomenclature of which reads as “Genus-Species-Subspecies-Serovar” e.g. *Salmonella enterica* subspecies enterica serovar Typhimurium (shortened to *S*. Typhimurium). Over 2500 different serovars have been identified to date (Brenner et al., 2000) (WHO, 2019) reflecting the wide host range infected by *Salmonella enterica*.

1.2.1 Clinical relevance – infectious diseases caused by *Salmonella* in humans

Salmonella infections can result in a variety of clinical manifestations and disease states. The interactions between a particular *Salmonella* and its host, and therefore disease outcome, is influenced by many factors including serotype, infecting dose, host species, gut flora and immunologic competence. Infection with the same serotype can result in clinically distinct disease outcomes in different hosts (Dougan et al., 2011). Disease range can include anything from asymptomatic carriage to a potentially fatal systemic infection. In humans, *S. enterica* serovars Typhi (*S.* Typhi) and Paratyphi (*S.* Paratyphi) cause typhoid and paratyphoid fever, respectively, which present as febrile, systemic infections. On the other hand, non-typhoidal *Salmonella* (NTS) serovars such as *S.* Typhimurium and *S.* Enteritidis are a frequent cause of gut-associated gastroenteritis in developed countries (Gordon, 2008). *Salmonella* is generally acquired through the uptake of contaminated food or water. It survives the passage through the stomach and replicates in the small intestine (Carter and Collins, 1974). In contrast to non-typhoidal serovars, like *S*. Typhimurium and *S*. Enteritidis, typhoidal serovars *S*. Typhi and *S*. Paratyphi have the capacity to exit the intestinal epithelia, and escape to intestinal lymphoid follicles and draining mesenteric lymph nodes, resulting in systemic disease (Raffatellu et al., 2008a). Typhoid fever is characterised by an asymptomatic incubation period followed by progressively rising high fever from 8-14 days post-infection among other symptoms (Gordon, 2008). It is estimated there are 11-20 million new cases of typhoid fever and more than 120 thousand deaths every year (WHO, 2019) mostly in the developing world (Fig 1.2.1 a). Blood culture is currently the most frequently used diagnostic method for typhoid fever, although it is highly insensitive because the number of blood-borne bacteria is typically very low (Andrews and Ryan, 2015). Diagnosed individuals are regularly treated with antimicrobial therapy with a large spectrum of action combined with restoration of fluid and nutritional deficits (Wain et al., 1998).

NTS serovars usually cause self-limiting gastroenteritis and represent one of the major global causes of diarrhoeal disease with 550 million cases each year, including 220 million cases in children under the age of 5 years (WHO, 2019). Recently, NTS has also been described as a major cause of invasive bacterial disease of humans in many parts of sub-Saharan Africa but also in parts of Southeast Asia (Fig 1.2.1 b), especially affecting HIV-infected adults and immunocompromised children or elderly (Gilchrist et al., 2015; Gordon, 2008; Strugnell et al., 2014). NTS are consistently the most frequent bacterial bloodstream isolates in children and adults presenting with fever in sub-Saharan Africa. Further, invasive NTS (iNTS) serovars have been associated with a case fatality rate of 20% (Feasey et al., 2012; Gilchrist et al., 2015).

In addition, multidrug-resistant (MDR) NTS and typhoid strains are now very common, and fluoroquinolone-resistant typhoid serotypes are emerging, which poses a great challenge in treating typhoid fever in the future (Britto et al., 2018).

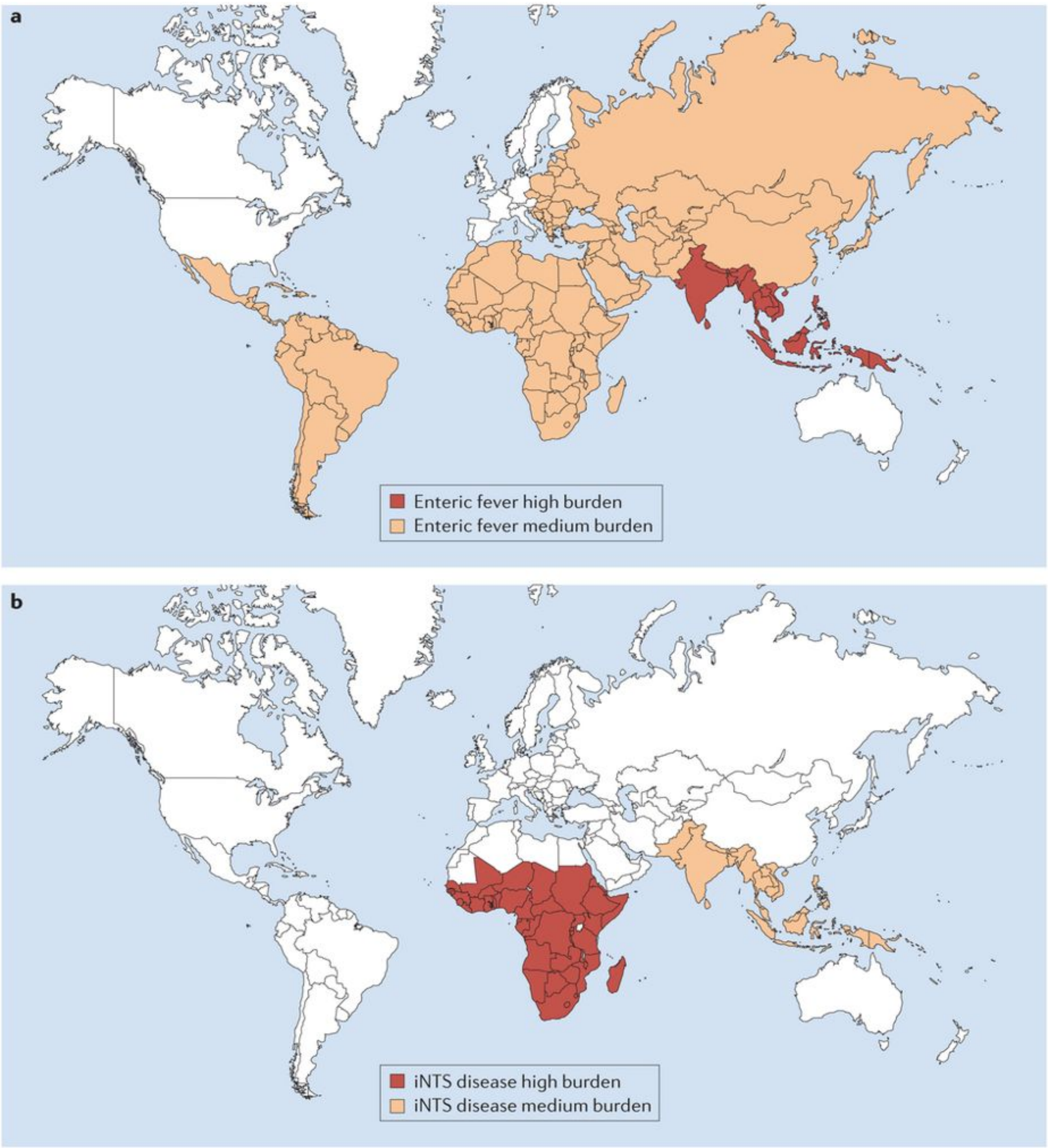

Nature Reviews | Immunology

Figure 1.2.1: The global distribution of invasive *Salmonella* disease
The geographical distribution of enteric fever (a) and invasive non-typhoidal *Salmonella* (iNTS) disease (b). High disease burden is defined as greater than 100 cases per 100,000 population per year, and medium disease burden as 10-100 cases per 100,000 population per year (Figure adapted from Gilchrist *et al.*, 2015).

None of the currently available *S*. Typhi vaccines specifically target NTS or *S*. Paratyphi strains (MacLennan et al., 2014), though there may be some cross-protection from the live vaccine Ty21a (Levine et al., 2007; Meltzer et al., 2006). Furthermore, available *Salmonella* vaccines are not licensed for usage in children under the age of 2 years (MacLennan et al., 2014). Therefore, typhoid fever and invasive NTS represent a major global disease threat in urgent need of extensive investigation, especially in the context of effective vaccine development and/or implementation.

1.2.2 Vaccines – what we have and what we don't have

Considering the increase in MDR *Salmonella*, and the economic costs associated with antimicrobial treatments and reduced economic work power due to illness, effective vaccines are a very desirable alternative to antibiotic therapy.

Three commonly available forms of licensed vaccines targeting *S*. Typhi are currently in use, but neither have been implemented at country level. The injectable Vi capsular polysaccharide (Vi CPS) vaccine (Typhim Vi by Sanofi Pasteur or Typherix by GSK), the orally administered live-attenuated vaccine Ty21a (Vivotif by Crucell) (Gayet et al., 2017; MacLennan et al., 2014) and the typhoid conjugate vaccine (TCV), which is a conjugate of the Vi polysaccharide with several medically relevant proteins (Sahastrabuddhe and Saluja, 2019) such as tetanus toxoid (Mohan et al., 2015). Several TCV developed by various companies are currently in different phases of clinical trials or have been recently licenced (Sahastrabuddhe and Saluja, 2019). All three vaccine types target *S*. Typhi, with no vaccine presently available against the other 3 important invasive serotypes of *Salmonella enterica*, Paratyphi A, Enteritidis and Typhimurium (MacLennan et al., 2014; Sahastrabuddhe and Saluja, 2019).

The Vi-based vaccines consist of purified Vi polysaccharide from *S*. Typhi and are able to confer a 3-year cumulative protection in approximately 55% of the vaccinated adults and children over two years with a single dose (Engels et al., 1998). This type of vaccine, however, does only generate a T cell independent antibody production (MacLennan et al., 2014). Vi conjugate vaccines can overcome this drawback. A single dose Vi-rEPA TCV can elicit strong immune responses in young children including immunologic memory, long-lived elevated anti-Vi antibody titres, and confers 89% vaccine efficacy against typhoid fever (Lanh et al., 2003; Lin et al., 2001). The live-attenuated vaccine Ty21a is able to generate a 3-year cumulative protection in approximately 51% of the vaccinated adults and children over 5, but requires three consecutive vaccine doses (Engels et al., 1998). The exact mechanism of vaccine protection trough Ty21a is still not fully understood, but since Ty21a does not express the Vi capsule its protective effects cannot be attributed to this antigen (Gayet et al., 2017; MacLennan et al., 2014).

The effort to design a better vaccine against *Salmonella* is still ongoing, but the TCA vaccines are promising. Besides achieving optimal vaccine efficacy and long-lasting protection, an optimal *Salmonella* vaccine should confer long-lasting antibody responses, induce potent CD4$^+$ and CD8$^+$ T cell responses, be safe in immunocompromised individuals as well as in young children, not induce bacteraemia, in best case result in cross-protection, tested in large field trials and be cold-chain independent (MacLennan et al., 2014).

1.2.3 A mouse model for invasive *Salmonella* – lessons learned

Salmonella Typhi is a pathogen restricted to its human host. It cannot cause any disease in non-primate vertebrates such as mice (Edsall et al., 1960). In mouse strains, *S.* Typhimurium causes a systemic disease that resembles human enteric fever in many respects (Strugnell et al., 2014). Infection outcome in mice is highly dependent on the expression of a functional *Nramp1* (natural resistance-associated macrophage protein 1) gene (Tsolis et al., 2011). Murine Nramp1 protein expression is restricted to the myeloid cell compartment including macrophages and DC, and affects the ability of the host to control intracellular replication of microorganisms like *Mycobacteria*, *Leishmania* and *Salmonella* that reside within the phagolysosome (Cellier, 2013; Jabado et al., 2000). The commonly used mouse strain C57BL/6 harbours a single point mutation in the *Nramp1* gene (The Jackson Laboratory, 2019) resulting in increased susceptibility to wild type *S*. Typhimurium with mice typically succumbing to the infection within five to seven days. The very short timeframe to lethality does not allow for the study of adaptive immune responses. Alternatively, attenuated *S*. Typhimurium strains, such as those harbouring mutations in important metabolic pathways (e.g. BRD509 (Δ*aroA*)), typically grow slower than wild type *S*. Typhimurium in C57BL/6 and other Nramp1-sensitive mouse strains, resulting in a milder systemic infection that is usually cleared within 10-12 weeks of infection (Kupz et al., 2014). Infection with live-attenuated *S*. Typhimurium strains in mice resembles human typhoid fever in terms of pathogen distribution in organs, which induces protective immunity against a secondary wild type challenge. Hence it is considered to be a good model for investigating and understanding the underlying biology of immunity against *Salmonella* (Mittrucker and Kaufmann, 2000).

Much of our knowledge of immunological processes that are active during *Salmonella* infection and the corresponding underlying cell biology is derived from the murine typhoid model (Dougan et al., 2011; Kupz et al., 2014; Tsolis et al., 2011). In addition, a variety of major virulence factors from *Salmonella* was identified e.g. genes encoded on the *Salmonella* Pathogenicity Islands I and II (SPI-1 and SPI-2), which facilitate the invasion of cells (SPI-1) and intracellular survival in the *Salmonella*-containing-vacuole (SCV) (SPI-2), respectively (Palmer and Slauch, 2017).

The immunobiology of murine *Salmonella* infection bears a good resemblance to human typhoid fever partly because of the high sequence homology between *S.* Typhimurium and *S.* Typhi (99%) (Baker and Dougan, 2007). Furthermore, the two serovars share three important virulence gene clusters that are critical for intestinal invasion, intracellular survival and replication (McGhie et al., 2009). A great limitation of the mouse model for typhoid-like enteric fever is that *S*. Typhimurium causes acute inflammatory diarrhea in humans rather than a systemic illness, and therefore implies a differential type of immune response to *S*. Typhimurium in humans and laboratory mice (Palmer and Slauch, 2017; Santos et al., 2001). Still, the mouse model for typhoid-like enteric fever has provided tremendous insight into the pathogenesis of *Salmonella*.

1.2.3.1 The Trojan horse strategy – how *Salmonella* invades its host and hides within cells

In faecal-oral transmitted diseases like salmonellosis, the first line of defence is represented by the stomach with its low pH of 1.5 and digestive enzymes, serving as an important barrier to infection. On the other hand, enteric bacteria including *Salmonella* have evolved strategies like the Acid Tolerance Response (ATR) to withstand the acidic environment in the stomach (Smith, 2003). The surviving bacteria predominately replicate in the small intestine, where they especially target the Peyer´s patches (PP) (Carter and Collins, 1974). *Salmonella* is able to invade the host via three distinct routes (Fig 1.2.2). In order to cross the protective epithelial barrier, bacteria adhere to and subsequently invade cells. A major route of entry is through M cells in the follicle-associated epithelium (FAE) overlying PP, which transport antigens and bacteria from the lumen to the lamina propria (Fig 1.2.2 (1)). This is thought to be the main route of bacterial uptake from the gut (Broz et al., 2012; Gayet et al., 2017; Palmer and Slauch, 2017). *Salmonella* can also induce its own uptake in non-phagocytic enterocytes through its virulence-associated type 3 secretion system (T3SS) encoded by SPI-1. This needle-like structure allows the direct insertion of bacterial effector proteins into the cytoplasm of cells, facilitating actin rearrangement resulting in bacterial engulfment (Fig 1.2.2 (2)) (Broz et al., 2012; Gayet et al., 2017; Palmer and Slauch, 2017). A third route of invasion is via uptake by macrophages/ DC that reside immediately on the basal side of the gut epithelial linings. These macrophages/DC are thought to extend dendrite-like structures through the tight junction between gut epithelial cells into the gut lumen and take up *Salmonella* cells directly (Fig 1.2.2 (3)) (Broz et al., 2012; Gayet et al., 2017; Niess et al., 2005; Palmer and Slauch, 2017).

Once *Salmonella* has crossed the intestinal epithelial barrier at the site of PP, the bacteria are taken up by phagocytic immune cells like DC and macrophages. Intracellular bacteria replicate within the SCV in the host cytoplasm. Essential for this intracellular phase is a second type three secretion system encoded by SPI-2. While non-invasive strains remain restricted to the intestinal tract, invasive *Salmonella* disseminate from the intestine to the mesenteric lymph nodes (mLN) and further spread to systemic sites, like the liver and spleen (Broz et al., 2012; Palmer and Slauch, 2017) (Fig 1.2.3). It is quite likely that *Salmonella* can spread as free bacterial cells in the circulation (Bravo-Blas et al., 2019), however, they are opsonised by complement factors and quickly cleared (Mastroeni et al., 2009). In addition, there is evidence that bacteria are transported within DC just like in a 'Trojan horse' from PP to mLN from where they can further colonise systemic sites (Bogunovic et al., 2009; Voedisch et al., 2009) (Fig 1.2.3).

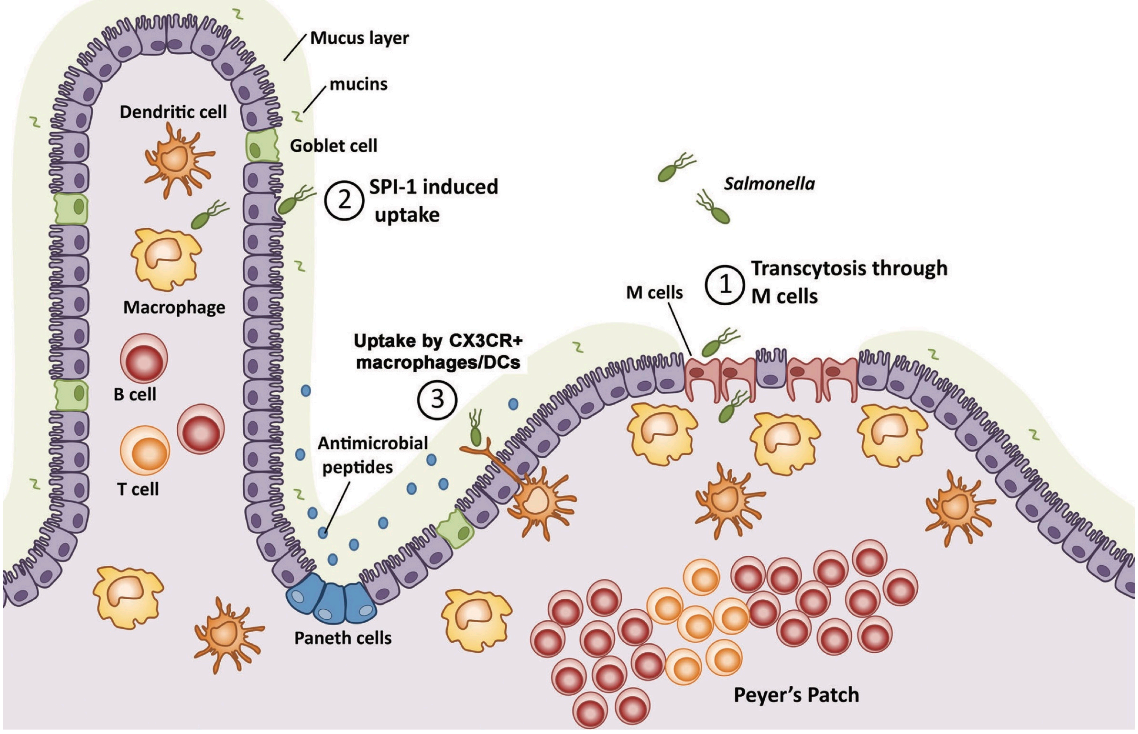

Figure 1.2.2: Schematic representation of the different mechanisms for *Salmonella* to invade the intestinal mucosa

M cell mediated transcytosis at the PP represents the main route of invasion. (1). An alternative route, infecting enterocytes is facilitated via SPI-1 induced uptake (2). A third route of bacterial invasion is represented by macrophages/DC which expand their dendrites through the epithelium and take up bacteria (3) (Figure adapted from Broz *et al*., 2012).

Next to DC, live *Salmonella* are also found inside of neutrophils, inflammatory monocytes and macrophages (Burton et al., 2014). Data indicates that the great majority of viable bacteria in tissues are found within macrophages (Mastroeni et al., 2009). It is also clear that phagocytes affect *Salmonella* in different ways.

Neutrophils are able to kill *Salmonella* very effectively via the production of large amounts of hydrogen peroxide and/or hypochlorite. Also, inflammatory monocytes are able to produce hypochlorite, and are therefore able to efficiently kill the bacteria (Burton et al., 2014). *Salmonella*-containing macrophages have been associated with M2 markers, indicating a reduced ability to kill intracellular bacteria since M2 macrophages are rather associated with tissue repair (Muraille et al., 2014). There is evidence that *Salmonella* promotes M2 macrophage polarisation in the host allowing for long-term persistence in these cells (McCoy et al., 2012). This very effective immune evasion mechanism protects the bacteria from exposure to other more effective phagocytes, as well as from humoral immune response and complement system.

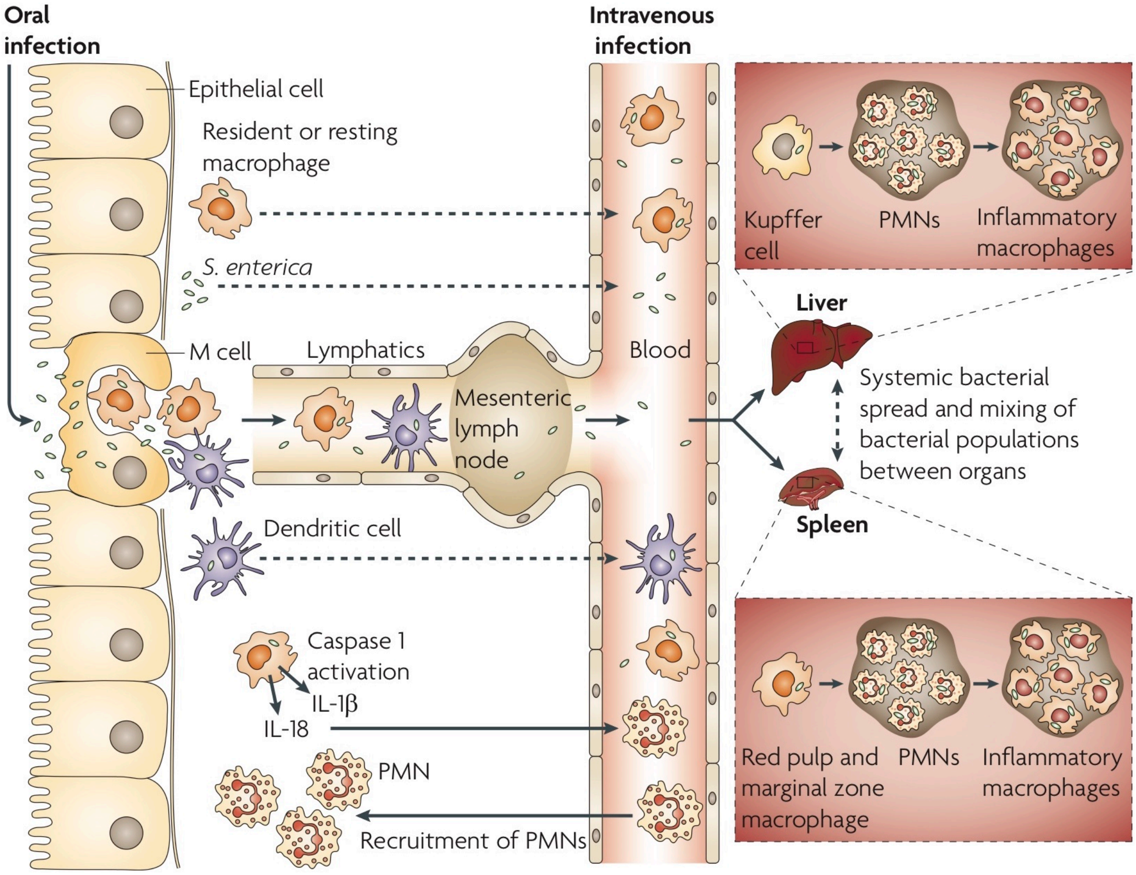

Figure 1.2.3: Dissemination of *Salmonella* in mouse
Salmonella invades enterocytes and M cells and is engulfed by resident macrophages and DC. Caspase 1-mediated cell death of resident macrophages is induced by the bacteria, resulting in the production of IL1β and IL18, which mediate the recruitment of polymorphonuclear phagocytes (PMN). From the intestine, bacteria reach the mLN and the blood and spread to spleen and liver (Figure adapted from Mastroeni *et al.*, 2009).

1.2.3.2 Innate immunity to *Salmonella* – first line of defence

Cellular and molecular components involved in innate immune protection against *Salmonella* have been broadly studied. One of the first hurdles bacteria have to overcome is a thick layer of mucus formed by mucins covering the gut epithelium. In addition to the mucins, antimicrobial peptides are secreted from epithelial cells, which act as peptide antibiotics disrupting the integrity of the bacterial cell membrane. They are mostly induced as part of the inflammatory response to invading pathogens. In order to overcome this rather unfavourable environment, *Salmonella* has evolved strategies to sense these host effectors and to respond by activating counteracting virulence mechanisms (Broz et al., 2012).

Once *Salmonella* has crossed the epithelial barrier it encounters the next stage of innate immune defence, the phagocytic cells of the gut-associated lymphoid tissue (GALT). The bacteria are taken up by DC and macrophages and establish themselves in an intracellular compartment, the SCV. Shielded by the vacuole, *Salmonella* can grow before exiting its host cell and infecting new cells (Jantsch et al., 2011). Although the bacteria remain partially hidden they cannot entirely evade host cell sensing through PRR (Broz et al., 2012). Recognition of *S.* Typhimurium is mostly mediated by TLR2 (peptidoglycan), TLR4 (LPS), TLR9 (DNA) and also TLR5 (flagellin) has been of study interest but since flagella are no longer expressed by intracellular bacteria the relevance is questionable (Broz et al., 2012; Keestra-Gounder et al., 2015). TLR4-deficient mice are very sensitive to *Salmonella* infection, but mice deficient in TLR2, TLR4 and TLR9 partially restore resistance to infection. The reason for these apparently contradictory observations is because TLR signalling is required for SCV acidification, an essential cue for the expression of SPI-2. While the SCV in TLR4-deficient cells are still acidified due to TLR2 and TLR9 activation, the SCV in cells lacking TLR2/4/9 maintain a relatively neutral pH for longer and intracellular *Salmonella* fails to activate SPI-2 expression, leading to partially impaired intracellular growth. Thus, although TLR are clearly essential for defence against bacteria, *Salmonella* also activates intracellular survival mechanisms specifically in response to the activation of TLR signalling (Arpaia et al., 2011; Broz et al., 2012; Keestra-Gounder et al., 2015).

In addition to TLR, other receptors also sense *S*. Typhimurium and form part of an effective innate immune response. The nucleotide-binding oligomerisation domain (NOD)-like receptors (NLR) recognise *Salmonella* PAMP in the cytosol and regulate both inflammation and apoptosis (Keestra-Gounder et al., 2015). NLRP3 activation can be triggered by bacterial mRNA and leads to IL1β secretion e.g. by macrophages (Sander et al., 2012). Furthermore, the complement system also reacts to bacterial invasion by detecting O-antigen repeat units of LPS and contributing to inflammation (Keestra-Gounder et al., 2015).

Interferon gamma (IFNγ) is a cytokine critical for coordinating a protective immune response against intracellular pathogens. It is produced by natural killer (NK) and NKT cells during early phases of host defence and by T helper 1 (Th1) cells and CD8$^+$ T cells during the adaptive immune response to many pathogens. This key cytokine is involved in a wide range of cellular responses and is best known for its immunomodulatory and antiviral properties (Schoenborn and Wilson, 2007). Genes upregulated by IFNγ control important mechanisms in lysosomal activity, anti-viral, apoptotic, and anti-microbial effects such as induction of nitric oxide production. Furthermore, metabolic activity as well as MHC class I and II antigen presentation pathways of antigen-presenting cells (APC) are modulated by IFNγ (Boehm et al., 1997; MacMicking, 2012). The majority of IFNγ regulated proteins are to various degrees vitally important in host defence against *Salmonella* infections. IFNγ production by NK cells (Kupz et al., 2013) and neutrophils (Sturge et al., 2013) contributes to resistance against *Salmonella* infection. Several studies have shown that mutations in the IFNγ pathways or synthesis or blocking of IFNγ results in increased susceptibility to *Salmonella* infection in mice and in humans (Jouanguy et al., 1999; Kupz et al., 2013; Muotiala and Mäkelä, 1990).

The role of the innate immune system is instrumental as indicated by the many ways it contributes to *Salmonella* clearance. TLR- and NLR-activation, complement system, inflammatory cytokines and innate immune cells such as macrophages, DC, NK cells work together alongside several non-conventional T cell subsets. They act in addition to or in synergy with adaptive immune mechanisms in order to fight *Salmonella* infection (Gayet et al., 2017).

1.2.3.3 Dendritic cells – a crosslink between innate and adaptive immunity

Antigen-presenting cells (APC) such as DC and macrophages process and present antigens for recognition by certain lymphocytes. APC are characterised by the expression of the MHCII receptor, allowing them to display exogenous antigens. DC in particular have been described as the key APC for naïve T cell priming. During their maturation, they upregulate surface MHCII, costimulatory ligands, and also acquire the ability to secrete stimulatory cytokines. These three signals are essential for successful T cell activation and differentiation (den Haan et al., 2014; Kambayashi and Laufer, 2014). In the gut, intestinal DC in the subepithelial dome area of PP and the lamina propria act as professional APC. They take up antigens, migrate to the draining mLN and induce T cell priming and differentiation, thus working as a link between innate and adaptive immunity (Gayet et al., 2017). Since salmonellosis is a faecal-oral transmitted disease, the involvement of intestinal DC is implied in the uptake of bacteria and bacterial antigens. As previously described, intestinal DC can be further divided into 4 subsets based on their expression of CD103 and CD11b, whereby all 4 DC subsets can migrate from the intestine to the mLN (Cerovic et al., 2013). In the context of *Salmonella* infection, there is only little knowledge about which intestinal DC subtype would facilitate the uptake, transport and presentation of bacterial antigens. Many different studies have described DC and also macrophages/monocytes as cells that take up bacteria after *Salmonella* infection *in vivo* (Bogunovic et al., 2009; Carden et al., 2017; Farache et al., 2013; Niess et al., 2005; Vazquez-Torres et al., 1999; Voedisch et al., 2009). Only DC, however, have been described to transport bacteria from the gut to the mLN (Bogunovic et al., 2009; Bravo-Blas et al., 2019; Voedisch et al., 2009). Once DC have reached the mLN they can present bacterial antigens and induce naïve T cell priming to initiate adaptive immunity. *Salmonella* has also evolved mechanisms to reduce activation of the adaptive immune system. Infected DC show a reduced migration potential to the mLN (Carden et al., 2017) and they fail to prime naïve T cells due to *Salmonella*-induced programmed DC death and inhibited antigen presentation (Cheminay et al., 2005; van der Velden et al., 2005).

1.2.3.4 Adaptive immunity – T and B cells fighting for bacterial clearance

Innate immunity is an effective first line of defence against pathogen invasion. Still, the formation of a long-lasting, potent and specific protection depends on the induction of both cellular and humoral immunity.

In a systematic approach, Kupz et al. investigated the cellular requirements for the systemic control of attenuated *S.* Typhimurium infection using 13 different mouse strains susceptible to infection (Kupz et al., 2014). The role of $CD4^+$ and $CD8^+$ T cells, B cells, NK and NKT cells as well as IFNγ were evaluated. In line with existing reports, infection of wild type C57BL/6 mice with an attenuated *Salmonella* strain followed a specific pattern: after an initial increase in net bacterial load, a “plateau phase” was reached, which subsequently lead to clearance of infection within 7 to 12 weeks (Fig 1.2.4).

Mice deficient in NKT cells only ($CD1d^{-/-}$) cleared the infection indistinguishably from wt mice. A similar outcome was observed for mice deficient in B cells (μMT) implying that NKT and B cells are not required for bacterial clearance or can be compensated for by other immune cell types. Strains deficient in $CD8^+$ T cells ($β_2m^{-/-}$, $Kb^{-/-}Db^{-/-}$, and 2.43Tg) cleared the infection to the same extent as wt mice, suggesting that the lack of $CD8^+$ T cells alone does not interfere with the host´s ability to clear the bacterial infection. In contrast, mice deficient in $CD4^+$ T cells only (GK1.5Tg and $IAE^{-/-}$) were not able to clear the bacteria and developed a non-lethal chronic infection, indicating that $CD4^+$ T cells are essential for pathogen clearance. Mice deficient in both $CD4^+$ and $CD8^+$ T cells ($(GK1.5Tg \times 2.43Tg)_{F1}$.) were unable to clear the infection and bacterial load eventually grew to a very high level, resulting in lethality at later time points in infection, supporting the concept that in the absence of $CD4^+$ T cells, $CD8^+$ T cells can help to control the infection. In order to study the role of double-negative (DN) T cells and B cells, $Rag1/Je^{-/-}$ mice were used in comparison to $(GK1.5Tg \times 2.43Tg)_{F1}$ mice. Mice additionally deficient in DN T cells and B cells ($Rag1/Je^{-/-}$) had higher CFU counts in spleen and liver at later time points, and became moribund earlier, implying a control-function for DN T cells and/or T cell-independent antibody responses in the late phase of infection. Mice deficient in all lymphocytes including NK cells ($Rag2^{-/-}$ $γc^{-/-}$) in contrast to $Rag1/Je^{-/-}$ mice, which still harbour NK cells, were not able to control the infection and succumbed to early infection within 4 weeks, which was similar to IFNγ$^{-/-}$ mice. These data indicate that NK cells, in the absence of T, B and NKT cells, can provide enough IFNγ during the early phase of infection to establish the “plateau phase” and to limit bacterial growth. Yet, in the presence of other lymphocytes, NK cells and CD8$^+$ T cells seem to be redundant, since mice which were almost deficient in both cell types (IL15$^{-/-}$) cleared the infection indistinguishably to wt mice.

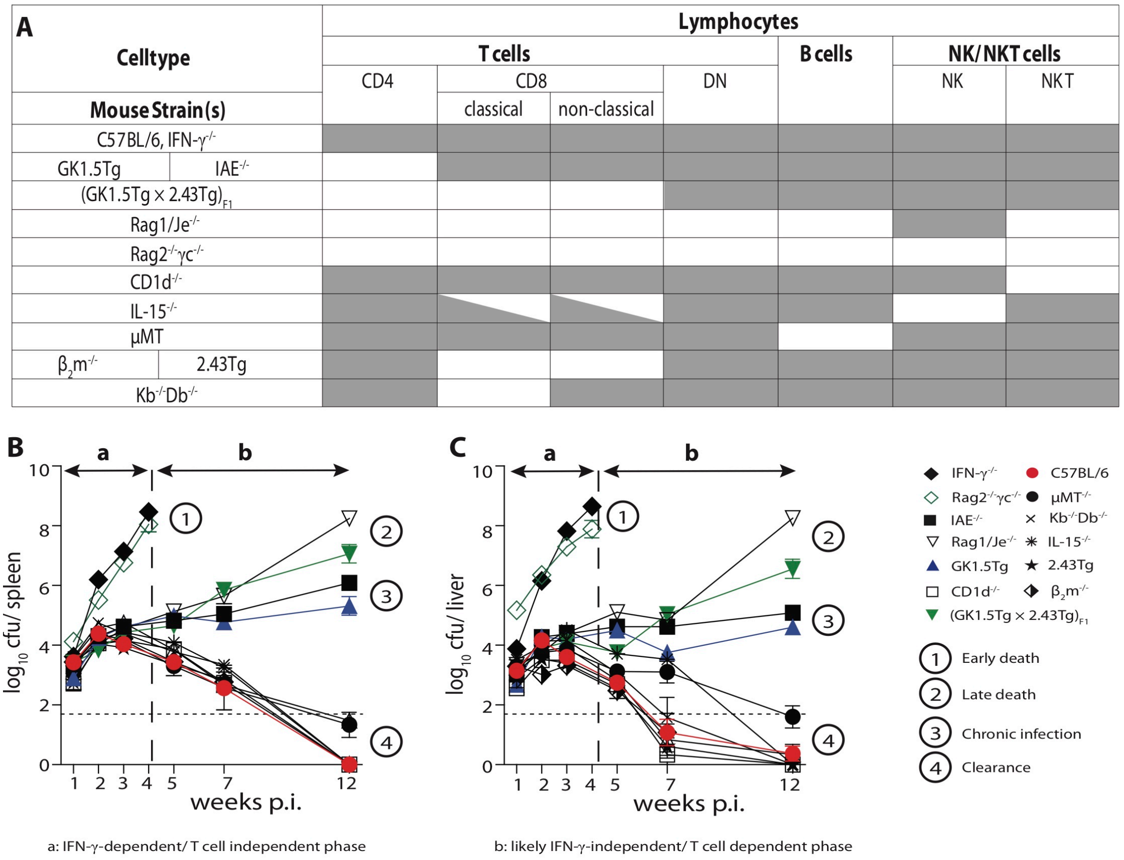

A **Celltype**	**Lymphocytes**						
	T cells				**B cells**	**NK/NKT cells**	
	CD4	CD8		DN		NK	NKT
Mouse Strain(s)		classical	non-classical				
C57BL/6, IFN-γ$^{-/-}$	▨	▨	▨	▨	▨	▨	▨
GK1.5Tg IAE$^{-/-}$		▨	▨	▨	▨	▨	▨
(GK1.5Tg × 2.43Tg)$_{F1}$				▨	▨	▨	▨
Rag1/Je$^{-/-}$						▨	
Rag2$^{-/-}$γc$^{-/-}$							
CD1d$^{-/-}$	▨	▨	▨	▨	▨	▨	
IL-15$^{-/-}$	▨	◣	◣	▨	▨		▨
μMT	▨	▨	▨	▨		▨	▨
β$_2$m$^{-/-}$ 2.43Tg	▨			▨	▨	▨	▨
Kb$^{-/-}$Db$^{-/-}$	▨		▨	▨	▨	▨	▨

a: IFN-γ-dependent/ T cell independent phase

b: likely IFN-γ-independent/ T cell dependent phase

Figure 1.2.4: Assessment of IFNγ production and different lymphocyte subsets in immunity against attenuated *Salmonella* infection
Schematic representation of the presence or absence of different immune cell populations of all mouse strains analysed (C57BL/6 background). White fields display the absence of a specific population and grey fields display the presence of the cell type (A). Mice were infected intravenously with 200 CFU STM BRD509, sacrificed at different time points post-infection and viable bacteria in spleens (B) and livers (C) were evaluated. Early control of infection and initiation of the “plateau phase” relies on IFNγ and lymphocytes but is independent of T, B, and NKT cells (a ↔). Final clearance of bacteria relies on CD4$^+$ T cells (b ↔). 4 distinct outcomes of the infection can be observed: early death (1), late death (2), chronic infection (3), and clearance (4). Dotted lines indicate the cut-off for CFU-detection limits (Figure adapted from Kupz *et al.*, 2014).

Taken together, primary *Salmonella* infection is controlled and cleared through the establishment of an effective immune response comprising IFNγ production and CD4$^+$ T cell expansion. This Th1 response enables mice to develop a robust protective immunity to secondary challenge (Kurtz et al., 2017; Pham and McSorley, 2015).

The specific role of the humoral immune response in murine *Salmonella* infection has been questioned. For instance, mice lacking B cells are able to control primary infection with attenuated bacteria but show reduced protection after wt *Salmonella* challenge (McSorley and Jenkins, 2000; Mittrücker et al., 2000; Nanton et al., 2012). In experiments where serum from *Salmonella* treated mice was transferred to vaccinated B cell-deficient animals prior to challenge the phenotype could be rescued (McSorley and Jenkins, 2000). Although these data indicate that antibodies can participate in protective immunity during secondary challenge, a study comparing B cell deficient mice with antibody-deficient and class-switched antibody-deficient mice demonstrated that B cells have an additional protective function beyond antibody secretion (Nanton et al., 2012). Nevertheless, B cells appear to contribute to the control of *Salmonella* infection in an antibody-independent manner. B cells perform additional functions to antibody production, including cytokine secretion and antigen presentation, which may contribute to anti-*Salmonella* protection (Kurtz et al., 2017; Pham and McSorley, 2015).

In humans, most individuals who overcome *S*. Typhi infection are usually protected from future infections (Marmion et al., 1953). Volunteers receiving the Ty21a vaccine typically develop significant levels of antibodies against O-antigens yet, it is not clear whether this antibody response forms part of protective immunity (Forrest et al., 1991). Likewise, volunteers immunised with the Vi-antigen vaccine, also show significant increases in serum antibodies against the Vi-antigen (Acharya et al., 1987). In contrast, chronic carriers have high titers of serum anti-Vi antibodies in addition to antibodies against the O- and H-antigen. These chronic carriers, however, are not able to clear the infection, questioning the role antibodies might play during infection (Sztein et al., 2014). One explanation could be that anti-*S*. Typhi antibodies predominately capture free invading bacteria, but are not sufficient for clearing bacteria in the intracellular niche (Kurtz et al., 2017).

Similar to B cells, the function of *Salmonella*-specific cytotoxic CD8$^+$ T cells is rather unclear. Commonly, CD8$^+$ T cells are thought not to participate in primary clearance of attenuated *S*. Typhimurium (Kurtz et al., 2017; Pham and McSorley, 2015). Depletion of CD8$^+$ T cells during persistent infection does not lead to an increased bacterial load in systemic organs (Johanns et al., 2010; Nauciel, 1990). Respectively, some studies have shown that β_2m$^{-/-}$ mice, which lack surface MHCI and hence functional CD8$^+$ T cells, can resolve primary infection with attenuated bacteria, suggesting that CD8$^+$ T cells are not crucial for host immunity (Hess et al., 1996). However, β_2m$^{-/-}$ mice are also deficient in the production of non-classical MHCI molecules and CD1, making the role of MHCI restricted antigens in protective *Salmonella* immune response difficult to interpret. Mice that only lack MHCI or CD8$^+$ T cell cytotoxic granules have demonstrated a modest protective role for CD8$^+$ T cells during the resolution of primary infection (Lee et al., 2012a). Taken altogether, these studies indicate that CD8$^+$ T cells likely have a limited functional role in conferring immunity against salmonellosis.

In contrast, the essential role of helper T cells in immunity against *Salmonella* is well established. Multiple studies have shown substantial expansion of *Salmonella*-specific CD4$^+$ T cells and prompt gain of Th1 effector functions, characterised by the ability to secrete IFNγ and TNFα upon restimulation (Johanns et al., 2010; Mittrücker et al., 2002; Srinivasan et al., 2004). These effector Th1 cells can be detected as early as one week post bacterial challenge (Srinivasan et al., 2004). Moreover, activated Th1 cells acquire the capacity to rapidly secrete IFNγ in response to innate signals such as LPS (Srinivasan et al., 2007), and can be activated by cognate and non-cognate stimuli in infected tissue (McSorley, 2014; Pham et al., 2017). Mice deficient in Th1 cells, due to a lack of Tbet, are unable to resolve primary, acute *Salmonella* infection (Ravindran et al., 2005) as are CD4$^+$ T cell deficient mice (Kupz et al., 2014). CD4$^+$ T cells are essential producers of IFNγ during *Salmonella* infection (Lee et al., 2012b; Nelson et al., 2013). IFNγ helps to regulate intracellular bacterial replication in macrophages through the expression of iNOS, which can react to nitric oxide, a free radical that can cause bacterial DNA damage (Blanchette et al., 2003). In line with studies using Tbet$^{-/-}$ and CD4^{+} T cell deficient mice, antibody-mediated depletion of CD4^{+} T cells results in a significant increase in bacterial load in systemic organs (Johanns et al., 2010; Nauciel, 1990). This reduced ability to control *Salmonella* infection is likely due to the loss of IFNγ produced by CD4^{+} T cells, as neutralisation of IFNγ causes bacterial counts to increase in persistently infected mice (Monack et al., 2004). In accordance with these findings, mice deficient in IFNγ or IFNγ-receptor are unable to resolve *Salmonella* infection (Pham and McSorley, 2015).

The critical role of Th1 CD4^{+} effector cells in resolving *Salmonella* infection has been clearly proven in the past. However, despite the efficient expansion of these effector cells during primary *Salmonella* infection, their contribution to bacterial control in early stage of infection is less well understood. Accordingly, mice that are deficient in CD4^{+} or Th1 CD4^{+} cells exhibit uncontrolled bacterial growth 3-4 weeks post-infection (Hess et al., 1996; Kupz et al., 2014; Ravindran et al., 2005), suggesting that Th1 CD4^{+} effector cells may have a minor contribution in regulating bacterial expansion before this point.

There is also strong evidence that CD4^{+} T cells are important mediators of immunity against NTS infection in humans. In HIV-infected individuals, who are deficient in CD4^{+} T cells, non-invasive NTS manifests as a severe, invasive, systemic infection (iNTS) (Uche et al., 2017). Furthermore, antiretroviral HIV therapy has been shown to reduce the incidence of iNTS infection, indicating that CD4^{+} T cells also play a vital role in the immune defence against *Salmonella* infection in humans (Keddy et al., 2017).

Once primary infection with an attenuated *S*. Typhimurium has been cleared, mice develop robust protective immunity to secondary challenge. Studies investigating this acquired immunity propose an important role for CD4^{+} T cells in bacterial clearance (Pham and McSorley, 2015). Transfer of immune spleen cells and immune serum, however, confers only partial protection (Mastroeni et al., 1993). Furthermore, it has been rather challenging to transfer this observed robust protective immunity to naïve mice by adoptive transfer of spleen cells (Benoun et al., 2018). These findings indicate that non-circulating lymphocytes may represent a major component of protective immunity mediated by attenuated *S*. Typhimurium vaccine strains. A recent study of Benoun et al. was able to confirm this idea. Liver-resident Th1 cells could be identified after vaccination and adoptive transfer of these memory cells increased protection against virulent *Salmonella* challenge, demonstrating that non-circulating memory Th1 cells are a critical component of immunity to *Salmonella* infection (Benoun et al., 2018).

Some studies also have suggested other effector CD4$^+$ subsets including Th17 cells and regulatory T cells (T$_{reg}$) to play a role in adaptive defence against *Salmonella* infection. T$_{reg}$ cells suppress adaptive immune responses and either arise from the thymus (natural T$_{reg}$ cells) or develop in the periphery from activated naïve T cells (induced T$_{reg}$ cells), promoted by the presences of TGFβ and retinoic acid, respectively (Lee and Lee, 2018). In contrast, Th17 cells develop from stimulated naïve CD4$^+$ T cells in the presence of TGFβ and IL6 (Bhaumik and Basu, 2017). They are critical in mediating immunity to extracellular pathogens through the recruitment of neutrophils (Curtis and Way, 2009). In the context of *Salmonella* infection, Th17 cells are thought to play an important and protective role in the intestine against extracellular bacteria, whereas Th1 cells are found in the gut as well as at systemic sites (Griffin and McSorley, 2011).

The role of T$_{reg}$ cells in the immune response against *Salmonella* infection has not been well understood. One study from Johanns et al. in 2010 investigated the development of Th1 cells and T$_{reg}$ after *Salmonella* challenge of Nramp1-resistant mice (Johanns et al., 2010). They demonstrated that early after infection, when bacteria are progressively growing, the effectiveness of Th1 responses is reduced, which coincides with increased suppressive potency of T$_{reg}$ cells. In contrast, during the later infection phase, when bacterial numbers decrees, the protective immune response is enhanced and the suppressive potency of T$_{reg}$ cells decreases. They also found that deletion of T$_{reg}$ cells during early infection, when their suppressive potency is strongest, leads to more efficient bacterial eradication (Johanns et al., 2010). Yet, it remains a question to be answered whether suppressive T$_{reg}$ cells can shape the Th1 immune responses against *Salmonella* in a susceptible mouse model or in humans.

In summary, $CD4^+$ T cells play an important role in immune defence against *Salmonella* infection through multiple mechanisms. Especially, Th1 $CD4^+$ T cells are crucial for effective immune protection. Still, it remains a question to be addressed how $CD4^+$ T_{reg} cells might contribute or interfere with immunity to *Salmonella*. Targeting $CD4^+$ T cells for future vaccine development will likely lead to improved efficacy and protection.

1.3 Aim of the thesis

The chemokine CCL17 has been extensively investigated for its role in numerous inflammatory and allergic diseases, such as contact hypersensitivity, atopic dermatitis, atherosclerosis, colitis and arthritis. In contrast, the closely related chemokine CCL22 has rather been associated with an immunosuppressive environment found for example in cancer. Both chemokines have been demonstrated to interact with the chemokine receptor CCR4 in mice. This receptor is expressed on a variety of immune cells, including effector T cells as well as regulatory T cells. In the immune system, CCL22 is probably best known for its role in the recruitment of regulatory T cells and associated suppression of tumour-specific T cell immunity (Anz et al., 2015; Curiel et al., 2004; Gobert et al., 2009). Whereas, CCL17 is rather known for its ability to attract effector T cells to sites of inflammation (Yoshie and Matsushima, 2015) and to promote DC-T cell interactions (Semmling et al., 2010), as well as for supporting DC migration (Stutte et al., 2010).

In earlier studies, our lab showed that CCL17 is strongly expressed in the Peyer´s patches (Alferink et al., 2003), a site to which *Salmonella* is known to preferentially localise (Carter and Collins, 1974). Previous researchers have suggested DC as the main cell-type responsible for bacterial transmission from the intestine to the draining lymph nodes (Bogunovic et al., 2009; Voedisch et al., 2009). Hence, the first aim of this study was to investigate the role of CCL17 expressing DC in the transmission of *Salmonella*.

Besides the chemokine CCL17, we also wanted to study the chemokine CCL22 and its functions. The association of CCL22 with regulatory T cell recruitment and immune suppression has been well investigated in cancer models (Anz et al., 2015; Curiel et al., 2004; Gobert et al., 2009). Only little is known, however, on the role of CCL22 but also CCL17 in the context of building CD4$^+$ T cell immunity towards an infectious disease. Thus, in the present thesis, regulatory T cells and their effect on effector T cells should be analysed using a *Salmonella* vaccine/challenge model in our recently generated CCL22-deficient as well as CCL17/22 double-deficient mice. Furthermore, the results obtained from our mouse model should be translated into a human context. In cooperation with Prof. A. Pollard we aimed to investigate the levels of CCL22 and CCL17 in plasma samples from a human *Salmonella* challenge study.

Taken together, this thesis had the objective to provide a better understanding of the role of the chemokines CCL17 and CCL22 in the immune defence against *Salmonella* infection.

2 Materials and Methods

2.1 Materials

2.1.1 Equipment

Table 2.1.1: Equipment used in this study

Equipment	Article – (Company)
Automatic tissue processor	Leica TP1020 (Leica Microsystems, Wetzlar, Germany)
Balances	440-35A (Kern & Sohn, Balingen, Germany)
Cell counting chamber	Neubauer improved (La Fontaine via Labotec, Göttingen, Germany)
Centrifuges	5415R (Eppendorf, Hamburg, Germany) 5810R (Eppendorf, Hamburg, Germany)
ELISA washer	CAPP wash 12 (CAPP, Odense, Germany)
Flow Cytometer	BD LSRFortessa^{TM} (BD Biosciences, Heidelberg, Germany) BD LSR II Flow (BD Biosciences, Heidelberg, Germany) BD FACSSymphony^{TM} (BD Biosciences, Heidelberg, Germany)
Fluorescent Imager	MAGPIX® (Luminex Corporation, Austin, USA)
Freezer (-20°C)	Comfort (Liebherr, Biberach, Germany) Bosch GSD12A20 (Bosch, Gerlingen, Germany)
Freezer (-80°C)	New Brunswick Ultra-Low Temperature Freezer (Eppendorf, Hamburg, Germany)
Fridge (+4°C)	MediLine LKUexv1610 (Liebherr, Biberach, Germany)
Gel electrophoresis	PerfectBlue Gel System (Peqlab, Erlangen, Deutschland)
Heating devices	TS1 Thermo Shaker (Biometra, Göttingen, Germany) Heating block Thermostat TH21 (HLC BioTech, Bovenden, Germany) Water bath WNB 22 (Memmert, Schwabach, Germany)
Homogenizer	Stomacher® 80 Biomaster (Seward Limited, Worthing, UK)

Ice machine	Scotsman Flockeneisbereiter AF200 (Hubbard Systems, Birmingham, USA)
Incubator	CB 150 (Binder, Tuttlingen, Germany) ECOCELL (MMM Group, Planegg/München, Germany)
Incubator shaker	Stuart orbital incubator SI500 (Cole-Parmer, Stone, UK)
Laminar flow Workbench	BDK Laminar Flow (BDK, Sonnenbühl, Genkingen, Germany)
Magnetic stirrer	IKA RCT basic (IKA-Werke GmbH & Co. KG, Staufen, Germany)
Measuring cylinder	250ml, 500ml, 1000ml, 2000ml (VWR, Wayne, USA)
Microscope	BZ 9000 Kezence (KEYENCE DEUTSCHLAND GmbH, Neu-Isenburg, Germany) LSM 780 ZEISS (Carl Zeiss Microscopy GmbH, Jena, Germany)
Microtome	Leica CM 3050 S (Leica Microsystems, Wetzlar, Germany)
Microwave	NN-E235M (Panasonic, Osaka, Japan)
Photometer	Bio Photometer 6131 (Eppendorf, Hamburg, Germany)
Pipettes	10µl, 20µl, 200µl, 1000µl (Eppendorf, Hamburg, Germany) 2,5µl ErgoOne (StarLab, Hamburg, Germany) Multichannel DV8-10, DV12-50, DV8-300 (HTL Lab Solutions, Warszawa, Poland)
Spectrophotometer (ELISA)	EL 800 (BioTek, Winooski, USA)
Thermal cycler	T100TM (BioRad, Hercules, USA), T1 Thermocycler (Biometra, Göttingen, Germany)
Threaded bottles	100ml, 250ml, 500ml, 1000ml (Schott, Mainz, Germany)
Transilluminator	Transilluminator UST-30M-8R (BioView, Rehovot, Israel) Biostep Dark Hood DH-40/50 (biostep, Burkhaltsdorf, Germany)
Vortex shaker	Vortex Genie 2 (Scientific Industries, New York, USA)

2.1.2 Consumables

Table 2.1.2: Consumables used in this study

Item	Company
Cell strainer nylon (70µm, 100µm)	VWR, Radnor, USA
Cover slips	Roth, Karlsruhe, Germany
CryoPure Tube 1.8 ml	Sarstedt, Nümbrecht, Germany
Culture plates (6-well/ 24-well/ 48-well/ 96- well, flat bottom)	Greiner, Kremsmünster, Austria
ELISA plate (half-area, 96 K)	Greiner, Kremsmünster, Austria
Filter tips	Sarstedt, Nümbrecht, Germany
Flow cytometry tubes	Sarstedt, Nümbrecht, Germany
Measuring pipettes (5ml, 10ml, 25ml)	Greiner, Kremsmünster, Austria
Micro tube 1.1ml Z-Gel	Sarstedt, Nümbrecht, Germany
Microscope slides (Superfrost plus)	Thermo Scientific, Waltham, USA
Parafilm®	American National Cam, Greenwich, USA
PCR tubes	Sarstedt, Nümbrecht, Germany
Petri dishes	Greiner, Kremsmünster, Austria
Precision wipes	Kimberly-Clark, Reigate, UK
Reaction tubes (15ml, 50ml)	Greiner, Kremsmünster, Austria
Safe seal reaction tubes (0,5, 1.5ml, 2.0ml)	Sarstedt, Nümbrecht, Germany
Sterican needles (0.90x40mm, 19G x 11⁄2)	Braun, Melsungen, Germany
Stomacher® blender bags 80 ml	Seward Limited, Worthing, UK
Syringes Inject-F Tuberkulin (1ml)	Braun, Melsungen, Germany
Syringes Inject® (2ml, 5ml, 10ml, 20ml)	Braun, Melsungen, Germany
Tissue-Tek® Cryomold (15x15mm, 25x20mm)	Sakura Finetek, Torrance, USA
UVette® (220 nm – 1.600 nm)	Eppendorf, Hamburg, Germany

2.1.3 Chemicals and reagents

Table 2.1.3: Chemicals and reagents used in this study

Chemicals/reagents	Company
100bp DNA Ladder	New England BioLabs, Ipswich, USA
10x TAE buffer	Invitrogen, Carlsbad, USA
2-mercaptoethanol	Sigma-Aldrich, Steinheim, German
Acetone	VWR, Darmstadt, Germany
Ammonium chloride	Merck, Darmstadt, Germany
Ampuwa	Fresenius Kabi, Bad Homburg, Germany
Bacto™ Agar	BD Bioscience, Franklin Lakes, USA
Chloramphenicol	Roth, Karlsruhe, Germany
DABCO	Sigma-Aldrich, Steinheim, Germany
DAPI	Sigma-Aldrich, Steinheim, German
Deoxynucleotide (dNTP) Solution Mix	Peqlab, Erlangen, Germany
DNase I	Merck, Darmstadt, Germany
Dulbecco's PBS	Sigma-Aldrich, Steinheim, Germany
Ethanol 70% (methylated)	Roth, Karlsruhe, Germany
Ethylenediaminetetraacetic acid (EDTA)	Sigma-Aldrich, St. Louis, USA
FACS Clean Solution	BD Bioscience, Franklin Lakes, USA
FACS Rinse Solution	BD Bioscience, Franklin Lakes, USA
Foetal Bovine Serum	ThermoFischer, Waltham, USA
Fixable Viability Dye eFluor 780	eBioscience, San Diego, US
Gentamicin	Gibco by Life Technologies, Carlsbad, USA
Glycerol	Roth, Karlsruhe, Germany
Hank's Balanced Salt Solution (HBSS) (10x)	Gibco by Life Technologies, Carlsbad, USA
HEPES	Sigma-Aldrich, St. Louis, USA
Horseradish Peroxidase	Sigma-Aldrich, St. Louis, USA

LB Broth, high salt	Sigma-Aldrich, St. Louis, USA
L-Glutamine	Gibco by Life Technologies, Carlsbad, USA
Liberase™	Merck, Darmstadt, Germany
Mouse BD Fc Block™ (purified rat anti-mouse CD16/CD32)	BD Bioscience, Franklin Lakes, USA
Mowiol	Sigma-Aldrich, St. Louis, USA
SPHERO™ Blank Calibration Particles (6.0 – 6.4 µm)	BD Bioscience, Franklin Lakes, USA
Paraformaldehyde (PFA)	Merck, Darmstadt, Germany
Penicillin-Streptomycin	Gibco by Life Technologies, Carlsbad, USA
Percoll	GE healthcare life science, Chalfont St Giles, GB
peqGOLD Universal Agarose	Peqlab, Erlangen, Germany
Phosphate Buffered Saline Dulbecco	Merck, Darmstadt, Germany
Poly-D-lysine	Invitrogen, Carlsbad, USA
Proteinase K	Sigma-Aldrich, St. Louis, USA
RPMI 1640	ThermoFisher, Waltham, USA
Sodium hydrogen carbonate ($NaHCO_3$)	Sigma-Aldrich, St. Louis, USA
Streptomycin sulfate	Roth, Karlsruhe, Germany
Sucrose	Sigma-Aldrich, St. Louis, USA
Sulfuric acid (H_2SO_4)	Roth, Karlsruhe, Germany
Tissue Freezing Medium	Leica Biosystems, Nussloch, Germany
Tris Buffered Saline	Merck, Darmstadt, Germany
Trypan Blue	Sigma-Aldrich, St. Louis, USA
Tween-20	Roth, Karlsruhe, Germany

2.1.4 Solutions and buffers

Table 2.1.4: Solutions and buffers used in this study

Solutions/buffers	Content
Complete RPMI	RPMI 1640 10% heat-inactivated FCS 2 mM L-Glutamine 10 mM HEPES 100 U/ml Penicillin 100 μg/ml Streptomycin 0.05 mM 2-mercaptoethanol
DC medium	RPMI 1640 10% heat-inactivated FCS 100 U/ml Penicillin 100 μg/ml Streptomycin 2% GMCSF (media from L929 cells)
Digestion buffer	RPMI 1640 5% heat-inactivated FCS 100 U/ml Liberase 5 U/ml DNase
ELISA stopping solution	25% H_2SO_4 in H_2O
ELISA wash buffer	0.05% Tween-20 in PBS
FACS buffer	PBS 5 mM EDTA 2% heat-inactivated FCS
Histology blocking buffer	PBS 1% BSA 2% donkey serum 2% goat serum
Lysis buffer (tail lysis)	5mM EDTA, pH8.0 0.2% SDS 200 mM NaCl 0.1 mg/ml Proteinase K
PFA (4 %)	4g PFA in 100 ml PBS, pH 7.4
RBC lysis buffer	17 mM Tris buffer 140 mM ammonium chloride in ddH_2O, pH 7.2

2.1.5 Kits and assays

Table 2.1.5: Kits and assays used in this study

Kits/assays	Company
eBioscience™ Foxp3 / Transcription Factor Staining Buffer Set	eBioscience, Inc., San Diego, USA
Human Magnetic Luminex® Assay for CCL22/CCL17	R&D Systems, Minneapolis, USA
Mouse IFNγ DuoSet ELISA kit	R&D Systems, Minneapolis, USA
Phycolink R-Phycoerythrin (RPE) conjugation kit	ProZyme, Hayward, USA

2.1.6 Antibodies

Table 2.1.6: Flow cytometry antibodies/reagents used in this study

Antigen	Clone	Conjugate	Dilution	Company
CD3e	17A2	AF700	1/150	BD Biosciences
CD4	GK1.5	BUV496	1/300	BD Biosciences
CD4	GK1.5	BUV563	1/500	BD Biosciences
CD8a	53-6.7	BUV805	1/400	BD Biosciences
CD11b	M1/70	BV711	1/200	BD Biosciences
CD11c	HL3	BV786	1/200	BD Biosciences
CD19	eBio1D3	PE-Cy7	1/200	ebioscience
CD25	PC61	BV605	1/200	BD Biosciences
CD44	IM7	FITC	1/500	BD Biosciences
CD44	IM7	BV570	1/200	BioLegend
CD44	IM7	BV510	1/200	BioLegend
CD45	30-F11	BV605	1/200	BD Biosciences
CD62L	MEL-14	APC-R700	1/200	BD Biosciences
CD62L	MEL-14	BUV737	1/400	BD Biosciences
CD64	X54-5/7.1	AF647	1/200	BD Biosciences

CD103	M290	BV421	1/200	BD Biosciences
CXCR3	CXCR3-173	BV421	1/200	BD Biosciences
CXCR3	CXCR3-173	BV650	1/200	BioLegend
CXCR6	SA051D1	BV711	1/200	BioLegend
CXCR6	SA051D1	PE	1/200	BioLegend
CXCR6	SA051D1	PE-Cy7	1/200	BioLegend
FoxP3	FJK-16s	PE	1/100	ebioscience
FoxP3	FJK-16s	PerCP-Cy5.5	1/200	BD Biosciences
FR4	eBio12A5	PE-Cy7	1/200	ebioscience
ICOS	7E.17G9	PE	1/200	BD Biosciences
IFNγ	XMG1.2	APC	1/100	BioLegend
KLRG1	2F1	BUV395	1/300	BD Biosciences
Ly-6C	AL21	BV605	1/200	BD Biosciences
MHCII	M5/114.15.2	PE-Cy7	1/400	BioLegend
MHCII	M5/114.15.2	PerCP-Cy5.5	1/200	BD Biosciences
RS053-tetramer	-	PE	0.5 μg/ sample	In-house
STM-LPS	1E6	PE	1/600	Abcam
TCRβ	H57-597	BUV737	1/300	BD Biosciences
TCRβ	H57-597	PE-Cy7	1/200	BD Biosciences
TIGIT	1G9	APC	1/200	BioLegend

Table 2.1.7: Histology antibodies used in this study

Antigen	Clone	Conjugate	Dilution	Company
RFP (rabbit)	polyclonal	-	1/250	Rockland
eGFP (rabbit)	polyclonal	-	1/250	Life Technologies
eGFP (rat)	FM264G	-	1/150	BioLegend
Rabbit IgG	polyclonal	AF 488	1/200	Thermo Fischer

Rabbit IgG	polyclonal	AF 594	1/200	Thermo Fischer
Rat IgG	polyclonal	AF488	1/200	Thermo Fischer
CD4	RM4-5	PE	1/100	BioLegend
CD8	53-6.7	PE	1/100	BioLegend
B220	RA3-6B2	APC	1/100	BioLegend

2.1.7 Bacterial strains

Table 2.1.8: Bacterial strains used in this study

Strain	Resistance	Characteristics	Source/Reference
S. Typhimurium			
SL1344	Streptomycin	Wild type strain rpsL hisG	(Wray and Sojka, 1978)
SL13344 *mCherry*	Streptomycin, Chloramphenicol	Expression of mCherry	(Knodler et al., 2014)
TAS2010	Streptomycin		(Kupz et al., 2013)

2.1.8 Mouse strains

Mice were housed under specific pathogen-free (SPF) conditions in the Genetic Resources Center (GRC) of the Life & Medical Sciences (LIMES) Institute, University of Bonn, Germany, or in in the Biological Research Facility in the Department of Microbiology and Immunology, the University of Melbourne, at the Peter Doherty Institute, Australia. Mice were maintained in individually ventilated cages (IVC) under conventional laboratory conditions (12h/12h light/dark cycle, 22 °C), with *ad libitum* access to food and water. Mice were genotyped using PCR. All animal experiments were performed with age- and sex-matched mice using male or female 8-14 weeks-old wt (C57BL/6J) or transgenic mice. All animal experiments performed in Bonn were approved by the government of North Rhine-Westphalia (Az 84-02.04.2013.A084, Az 81-02.04.2018.A094). Experiments performed in Melbourne were approved by the University of Melbourne Animal Ethics Committee (AEC) (project 1613898), and complied with the National Health and Medical Research Council (NHMRC) Australian Code of Practice for the Care and Use of Animals for Scientific Purposes (8th edition, 2013). Mice were euthanised by CO_2 asphyxiation or by cervical dislocation.

Table 2.1.9: Used mouse strains within this study

Mouse line	Genetic background	Reference	Supplier
wt	C57BL/6J-RCCHsd	-	Envigo/ GRC
CCL17$^{E/+}$	C57BL/6J-RCCHsd	Alferink 2013	I. Förster
CCL17$^{E/E}$	C57BL/6J-RCCHsd	Alferink 2013	I. Förster
CCL22$^{-/-}$	C57BL/6J-RCCHsd	I. Förster (unpublished)	I. Förster
CCL17$^{E/E}$ CCL22$^{-/-}$	C57BL/6J-RCCHsd	I. Förster (unpublished)	I. Förster

2.1.9 Software

Table 2.1.10: Used software within this study

Software	Company
BioRender	BioRender, Toronto, Canada
BZ-II Analyzer	Keyence, Montabaur, Germany
CFX Manager^{TM} Software	Bio-Rad, Munich, Germany
FACS Diva	BD, Franklin Lakes, USA
FlowJo 10.4.2	TreeStar, Inc., Ashland, USA
GraphPad Prism 6	GraphPad, La Jolla, USA
ImageJ (Fiji) 1	Rasband, W.S., ImageJ, U. S. National Institutes of Health, Bethesda, USA
Inkscape 0.92.4	Harrington, B. et al, Inkscape
Mendeley Software	Elsevier, Amsterdam, Netherlands
Microsoft Office 2011	Microsoft, Redmond, USA
Xquartz 2.7.11	Open source

2.2 Methods

2.2.1 Bacterial growth conditions

2.2.1.1 Growth of *Salmonella* Typhimurium

Salmonella enterica serovar Typhimurium (STM) strains were grown overnight at 37 °C either shacking in Luria-Bertani broth (LB broth) or on Luria-Bertani agar plates (LB) supplemented with 50 µg/ml streptomycin. If required 100 µg/ml chloramphenicol was added.

2.2.1.2 Growth conditions for oral infection

For oral infection, a culture of the required STM strains was set up overnight at 37°C in 10 ml LB. The following day, a subculture with the required volume was set up by diluting the overnight culture at 1:100 followed by 3 hours (h) incubation shaking at 37°C. The optical density at 600 nm was measured to approximate the bacterial concentration. Bacteria were harvested by centrifugation (3700 rpm for 10 min) followed by two washing steps with sterile phosphate-buffered saline (PBS). Bacteria were diluted in sterile LB broth/ 10% sodium bicarbonate solution at 1:1 ratio to the appropriate concentration (1-2.5x10^9 or 5x10^7 CFU/ml SL1344; 1x10^9 CFU/ml TAS2010).

2.2.1.3 Preparation of glycerol stocks

For long term storage of STM stocks, a culture was set up overnight. The next day 500 µl of the overnight culture was mixed with 500 µl LB/glycerol mix at 1:1 ratio and stored in cryovials at -80 °C.

2.2.1.4 Preparation of heat-killed bacteria

For the preparation of heat-killed *Salmonella* a 10ml culture was set up overnight shaking at 37°C. Bacteria were harvested by centrifugation (3700 rpm for 10 min), washed twice in sterile PBS and resuspended in 10 ml PBS. An aliquot of the bacteria was serially diluted and plated out onto agar plates with 50 µg/ml streptomycin to determine the concentration of bacteria. After 24 h, true bacterial concentration was determined. Bacteria were heat-inactivated at 65 °C for 45 minutes. In order to confirm effective killing, an undiluted aliquot from the heat-killed suspension was cultured on a LB plate. Heat-killed bacteria were diluted to a concentration of $1x10^9$ CFU/ml, aliquoted and stored at -20 °C until use.

2.2.2 Animal experiments

2.2.2.1 Oral infection of mice

For oral infection, mice were scruffed and the inoculum was slowly administered using a 1 ml syringe with a feeding needle in a volume of 200 µl of either LB broth/ 10% sodium bicarbonate solution at 1:1 ratio or PBS.

For short-term acute experiments (19h, 36h or 3 days), mice were infected with $1\text{-}2.5x10^9$ CFU wild type STM for the analysis of myeloid cell populations involved in the transmission of STM and the expression of CCL17 expression. Alternatively, for long term studies (5 and 9 weeks, 14-17 weeks) mice were vaccinated with $1x10^9$ CFU live-attenuated STM vaccine strain TAS2010, and T cell populations were analysed after vaccination or after vaccination and wild type STM challenge.

2.2.2.2 Determination of bacterial loads

To determine the numbers of viable STM in organs, mice were euthanised via cervical dislocation after anaesthesia or CO_2 asphyxiation. Spleen and liver were carefully removed and transferred into sterile stomacher bags. Subsequently, organs were homogenised in 5 ml (spleen) or 10 ml (liver) of sterile ice-cold PBS using a Stomacher® 80 homogeniser or samples were taken from single cell suspension (section 2.2.2.3.1). In the case of PP and mLN, organs were carefully isolated and transferred into sterile ice-cold HBSS with 10% FCS. Following single cell suspension was generated (section 2.2.2.3.2). Homogenates were serially diluted if required and plated onto LB plates containing 50 µg/ml streptomycin to determine the bacterial load. Plates were incubated aerobically for 24h at 37 °C. Bacteria were counted and expressed as viable CFU/organ.

2.2.2.3 Flow cytometry and analysis of cell populations

2.2.2.3.1 Preparation of single cells – spleen and liver

Livers were perfused with PBS to remove circulating cells. Spleen and liver were collected in ice-cold FACS buffer and gently pushed through a 70µm cell strainer to generate single cell suspension. Cells were washed in FACS buffer (1500 rpm for 5 min at 4 °C). Liver lymphocytes were isolated by Percoll gradient (section 2.2.2.3.3). Next, spleen or liver cell pellets were resuspended in 5 ml RBC lysis buffer and incubated for 10 min at RT to lyse erythrocytes. Subsequently, cells were washed in FACS buffer (1500 rpm for 5 min at 4 °C), filtered and resuspended in FACS buffer for staining with fluorescently labelled antibodies.

2.2.2.3.2 Preparation of single cells – mesenteric lymph nodes and Peyer's patches

mLN and small intestines were collected in ice-cold HBSS with 10% FCS. Small intestines were flushed with ice-cold PBS and PP were extracted. Remaining fat tissue was removed from mLN. Organs were stored in ice-cold HBSS with 10% FCS. For intracellular tracking of STM, organs were pre-treated with 100 µg/ml gentamicin for 30 min at RT and then washed three times with PBS. Next, organs were digested in digestion buffer (RPMI with 5% FCS, 100 U/ml Liberase and 5 U/ml DNase) for 20 min shaking at 37 °C, then pushed through a 70µm cell strainer to generate single cell suspension. For analysis of T cell populations, mLN and PP were directly pushed through a 70µm cell strainer to generate a single cell suspension without any prior antibiotic treatment or digestion. Finally, single cells were filtered, washed with FACS buffer (1500 rpm for 5 min at 4 °C) and resuspended in FACS buffer for further processing.

2.2.2.3.3 Separation of hepatocytes from immune cells

Livers were collected, single cell suspension was generated (section 2.2.2.3.1) and samples were subjected to Percoll gradient. For this, 20 ml 33% isotonic Percoll was added to each sample. Samples were spun down (200 rpm for 12 min at RT, no brake) to separate hepatocytes from immune cells. The on top floating hepatocytes were discarded. The pelleted immune cells were washed with FACS buffer, resuspended in 5 ml RBC lysis buffer and incubated for 10 min at RT to lyse erythrocytes. Subsequently, cells were washed in FACS buffer (1500 rpm for 5 min at 4 °C), filtered and resuspended in FACS buffer for further processing.

2.2.2.3.4 Flow cytometry

2.2.2.3.4.1 Surface staining

Single cells from PP, mLN, spleen and liver were transferred to 96-well round-bottom plate and incubated with Fc-block^{TM} in a total volume of 25 µl FACS buffer for 10 min on ice to block non-specific binding. Subsequently, antibodies against surface markers were added in 50 µl FACS buffer and cells were stained for 45 min on ice using either a staining panel for myeloid cell markers (table 2.11) or a T cell marker panel (table 2.12). Following, cells were washed in FACS buffer (1500 rpm for 5 min at 4 °C) and finally resuspended in 150 µl FACS buffer. Approximately 1-2 x 10^4 calibration beads were added to each sample prior acquisition to calculate cell numbers. Total cell numbers were calculated by setting the number of calibration beads acquired in each sample into relation to a beads-only sample, where 100% of events were collected. Compensation was performed using single-stained samples. Data was collected using a BD^{TM} LSR II flow cytometer, a BD LSRFortessa™ cell analyser or a BD FACSSymphony™ cell analyser. Data analysis was done using FlowJo™ software.

Table 2.2.1: The myeloid cell marker panel (antibody details are listed in table 2.1.6)

Myeloid cell marker staining	
Live Dead marker	surface staining
CD3 or TCRβ	surface staining
B220 or CD19	surface staining
CD11b	surface staining
CD11c	surface staining

CD45	surface staining, optional
CD86	surface staining, optional
CD103	surface staining
CD64	surface staining
Ly6C	surface staining
MHCII	surface staining
GFP	intracellular staining, optional
STM-LPS	intracellular staining, optional

Table 2.2.2: The T cell marker panel (antibody details are listed in table 2.1.6)

T cell marker staining	
Live Dead marker	surface staining
CD3 or TCRβ	surface staining
CD4	surface staining
CD8	surface staining
CD25	surface staining, optional
CD44	surface staining
CD62L	surface staining
CXCR3	surface staining
CXCR6	surface staining
FoxP3	intra cellular staining
FR4	surface staining, optional
KLRG1	surface staining
IFNγ	intra cellular staining, optional
Tetramer	surface staining, optional

2.2.2.3.4.2 Tetramer staining

To stain for *Salmonella* specific T cells, MHCII tetramer for a specific *Salmonella* antigen, RS053, was used to stain $CD4^+$ T cells. Single cells were stained with the RS053-tetramer in a total volume of 25 µl RPMI with 5% FCS for 1h at 4 °C. Subsequently, cells were directly subjected to surface staining without any further washing steps.

2.2.2.3.4.3 Intracellular staining

To stain for intracellular cytokines, single cells were prepared and stained for surface markers (section 2.2.2.3.4.1). Subsequently, cells were fixed and permeabilised using the eBioscience™ Foxp3 / transcription factor staining buffer set according to manufacturer’s instructions. Intracellular markers were stained overnight in 200 µl permeabilization buffer. The next day, cells were washed in permeabilization buffer followed by a washing step in FACS buffer (1500 rpm for 5 min at 4 °C) and finally resuspended in 150 µl FACS buffer.

2.2.3 Histology

2.2.3.1 Immunohistochemistry of lymph nodes and Peyer´s patches

mLN and PP were collected in HBSS with 10% FCS. Tissue samples were fixed overnight in 4% PFA, dehydrated 3 h in a 30% sucrose solution, embedded in Tissue-Tek™ Cryomold™ with tissue freezing medium and stored at -20 °C. Frozen samples were cut into 10µm thick sections using the Cryostat Leica CM3050 S, transferred to specimen slides, fixed in acetone for 5 min, washed three times in PBS, air-dried and finally stored at -80 °C.

Samples were thawed immediately before staining and rehydrated in PBS for 5 min. Slides with samples were placed in a humidified chamber for blocking and staining. Tissue sections were covered with 150 µl histo block and incubated at RT for 2 h. Histo block was removed and the samples were then subjected to staining with primary antibodies in 150 µl PBS with 1% FCS overnight at 4 °C. Sections were washed three times with PBS and then covered with secondary antibodies in 150 µl PBS with 1% FCS for 2h at RT. Subsequently, samples were washed with PBS, stained with DAPI (1:1000) for 10 min at RT and washed again. Finally, they were covered with Mowiol and coverslips and stored at 4 °C. Images of stained samples were acquired with the Keyence BX9000 and analysed with ImageJ.

2.2.4 Determination of chemokine levels in human plasma

Plasma samples from Ty21a-vaccinated humans, who had been part of a randomised, controlled trial comparing the typhoid vaccines M01ZH09 with placebo and Ty21a (Darton et al., 2016), were analysed for their serum CCL17 and CCL22 levels using the R&D Luminex® Assay according to the manufacturer's instructions. Three time points were chosen for analysis: pre-vaccination, day 0 (day of challenge), day 7 (7 days post-challenge). Samples were measured in duplicates and the mean was calculated from acquired duplicates. The minimum level of detection was 91.85 pg/ml for CCL17 and 52.26 pg/ml for CCL22. Chemokine concentrations were extrapolated from the standard curve.

2.2.5 Statistical analysis

All acquired data were analysed with GraphPad Prism 6 using unpaired *t*-tests, one-way or two-way ANOVA with Tukey´s post-test for multiple comparisons. Survival studies were analysed using Log-rank (Mantel-Cox) test. The *p*-value was calculated to indicate statistical significance. *P*-values above 0.05 were considered as not significant (ns). Error bars in graphs indicate the mean with 95% confidence intervals (CI), unless otherwise described.

3 Results

3.1 Function of CCL17-expressing cells in an acute invasive *Salmonella* model

The chemokine CCL17 has mainly been studied in the context of inflammatory and allergic diseases (Achuthan et al., 2016; Alferink et al., 2003; Fülle et al., 2018a; Heiseke et al., 2012; Stutte et al., 2010; Weber et al., 2011b). In contrast, the actions of CCL17 in infectious diseases are not well understood (Alferink et al., 2016). From *in vitro* and *in vivo* studies it is known that the major functions of CCL17 are the induction of chemotaxis via the receptor CCR4 and the initiation of DC-T cell interactions (Fülle et al., 2018a; Semmling et al., 2010; Stutte et al., 2010).

In mice, the expression of CCL17 is mainly restricted to DC present within barrier organs like the skin and intestinal mucosa, including Peyer´s patches (PP) and their draining lymph nodes (LN) (Alferink et al., 2003). The PP are a key portal for entry by *Salmonella* spp. (Carter and Collins, 1974). Once pathogenic bacteria like *Salmonellae* have entered the gut they can invade their host via different routes, one involving uptake by intestinal macrophages and DC in the PP. DC have been described as the "Trojan horse" of Salmonellosis, transporting *Salmonella* from the gut to the mLN causing spreading of the bacteria from their site of entry (Broz et al., 2012; Gayet et al., 2017; Palmer and Slauch, 2017).

Given the role of PP in bacterial entry and initial replication, and the observation that CCL17 is highly expressed by DC in the PP, it was hypothesised that CCL17^{+} DC may play a role in the transmission of *Salmonella* from the gut to the mLN. Using the murine model for *S.* Typhimurium (STM) infection and the CCL17$^{E/+}$ reporter and CCL17$^{E/E}$ KO mice, the aim of this study was to determine which mononuclear phagocyte populations are involved in the transmission of STM from the gut to the draining lymph nodes.

3.1.1 Histological analysis of CCL17 in PP and mLN of naïve and infected mice

3.1.1.1 CCL17-expressing cells are localised to the dome area of PP and the T cell zone of PP and mLN

CCL17 is mostly known as an inflammatory chemokine since it has been widely associated with inflammatory and allergic diseases, but it is also a chemokine expressed under homeostatic conditions. In naïve mice, CCL17 is expressed in the thymus, brain and in barrier organs (Alferink et al., 2003; Fülle et al., 2018b). Mice in which *egfp* cDNA was inserted into the murine *ccl17* locus from one allele (CCL17$^{E/+}$) were used as chemokine reporter mice. Mice, where *egfp* cDNA was inserted into the murine *ccl17* locus on both alleles (CCL17$^{E/E}$), are deficient in CCL17.

PP and mLN from naïve CCL17$^{E/+}$ reporter mice were investigated for chemokine expression (Fig 3.1.1). PP consisted mostly of B cells that form the germinal centres, and neighbouring T cell zones. CCL17^{+} cells co-localised to T cell rich areas of PP (Fig 3.1.1 A), and in the gut-lumen facing dome area of PP. Similar to the PP, in mLN CCL17^{+} cells localised within the T cell area and rather not in the B cell area of the mLN (Fig 3.1.1 B). These results were consistent with previous research (Alferink et al., 2003).

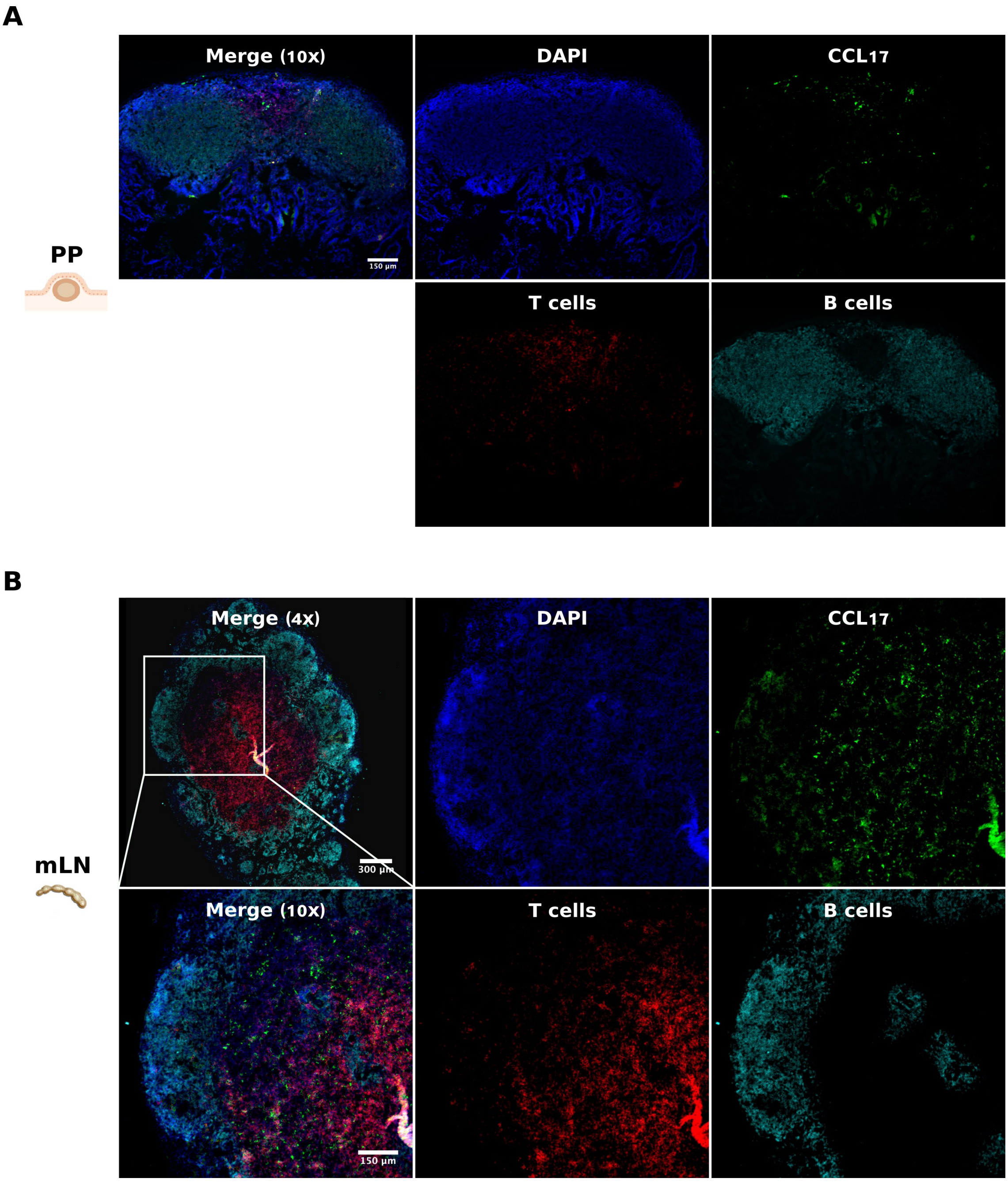

Figure 3.1.1: Histological analysis of CCL17 expression in PP and mLN in naïve mice

mLN and PP were isolated from naïve CCL17$^{E/+}$ reporter mice, fixed and subjected to immunofluorescent staining. Sections were stained with antibodies against EGFP (CCL17), marking endogenous expression of EGFP in CCL17$^{E/+}$ reporter mice, against B220 (for B cells) and CD4/CD8 (for T cells), and also stained with DAPI (for nuclei). Samples were analysed via fluorescent microscopy. Vertical sections through PP (A) or mLN (B) show CCL17^{+} cells (green), B cells (cyan), T cells (red) and nuclei (blue) in pseudocolor. Pseudocolor merged image is depicted in the first left picture of A and B. Scale bars are depicted in merge image. Representative images are shown (n=3, exemplary images are shown).

3.1.1.2 CCL17-expressing cells co-localise with *Salmonella* in the dome area of PP

During STM infection, PP are one of the main entry points for bacteria (Carter and Collins, 1974), a site where CCL17^{+} cells are known to be present (Fig 3.1.1. A). Hence, the potential interactions between CCL17^{+} cells and STM in PP and mLN were investigated. CCL17$^{E/+}$ and CCL17$^{E/E}$ mice were orally infected with mCherry-expressing STM, PP and mLN were isolated 3 days post-infection and evaluated via histology (Fig 3.1.2 A). Histological analysis of PP sections from CCL17$^{E/+}$ and CCL17$^{E/E}$ mice showed STM and EGFP/CCL17-expressing cells localising in close proximity to each other in the dome area of PP (Fig 3.1.2 B and C). In some cases, STM were found inside of EGFP^{+} cells (Fig 3.1.2 C). In contrast to observations made in the PP, the distribution of bacteria in the mLN of CCL17$^{E/+}$ and CCL17$^{E/E}$ mice was not restricted to the areas where EGFP^{+}/CCL17^{+} cells were localised; mCherry-expressing STM were detected in the whole mLN (Fig 3.1.2 D and E).

Overall, these findings demonstrate that CCL17-expressing cells co-localised with STM in the dome area of PP. However, the absence of CCL17 did not interfere with the localisation of EGFP^{+} cells, or STM, in PP or mLN since no difference between CCL17$^{E/+}$ and CCL17$^{E/E}$ mice was observed.

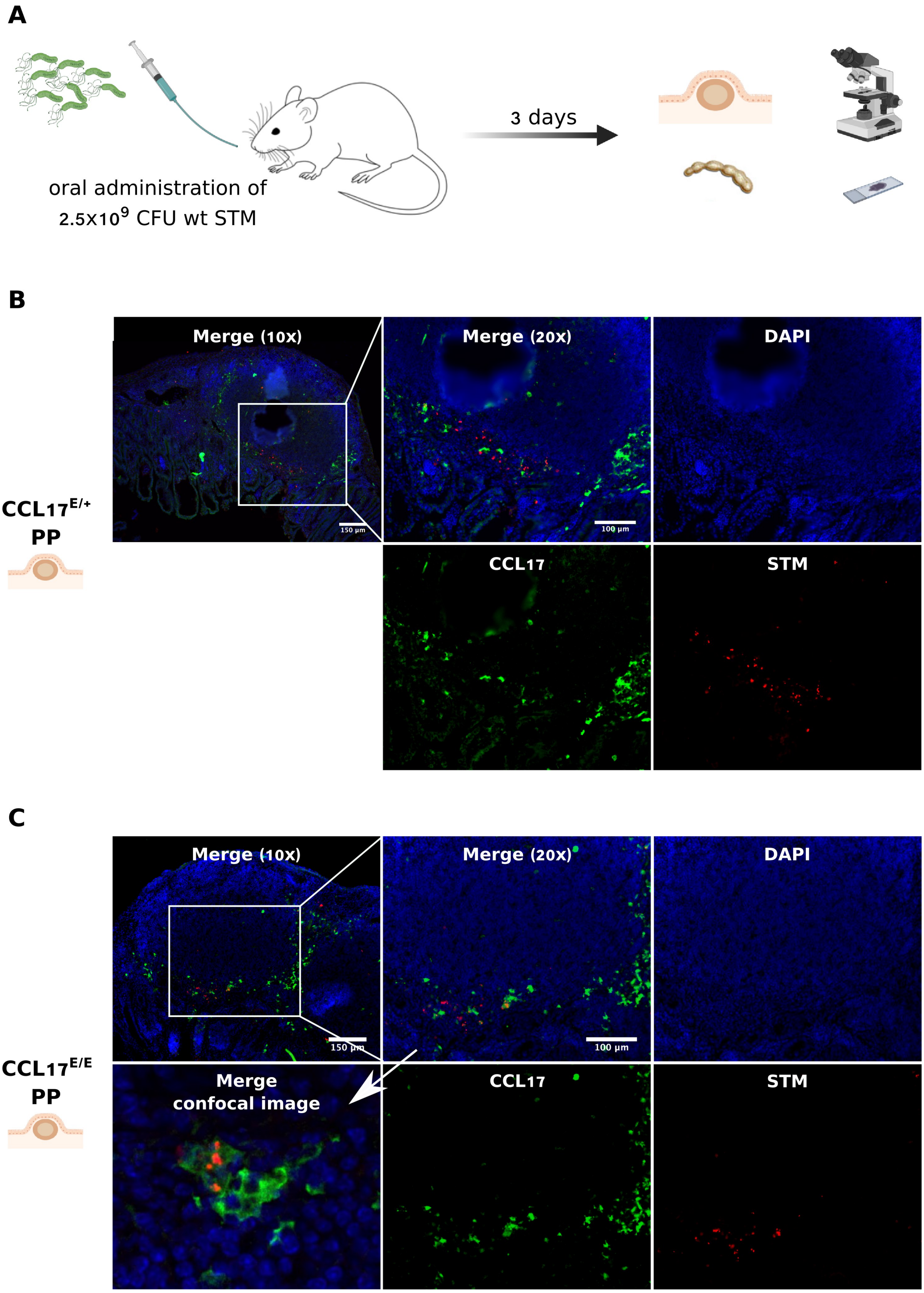
A
oral administration of
2.5x10^9 CFU wt STM
3 days
B
Merge (10x)
Merge (20x)
DAPI
CCL17
STM
150 µm
100 µm
CCL17^E/+
PP
C
Merge (10x)
Merge (20x)
DAPI
150 µm
100 µm
Merge
confocal image
CCL17
STM
CCL17^E/E
PP

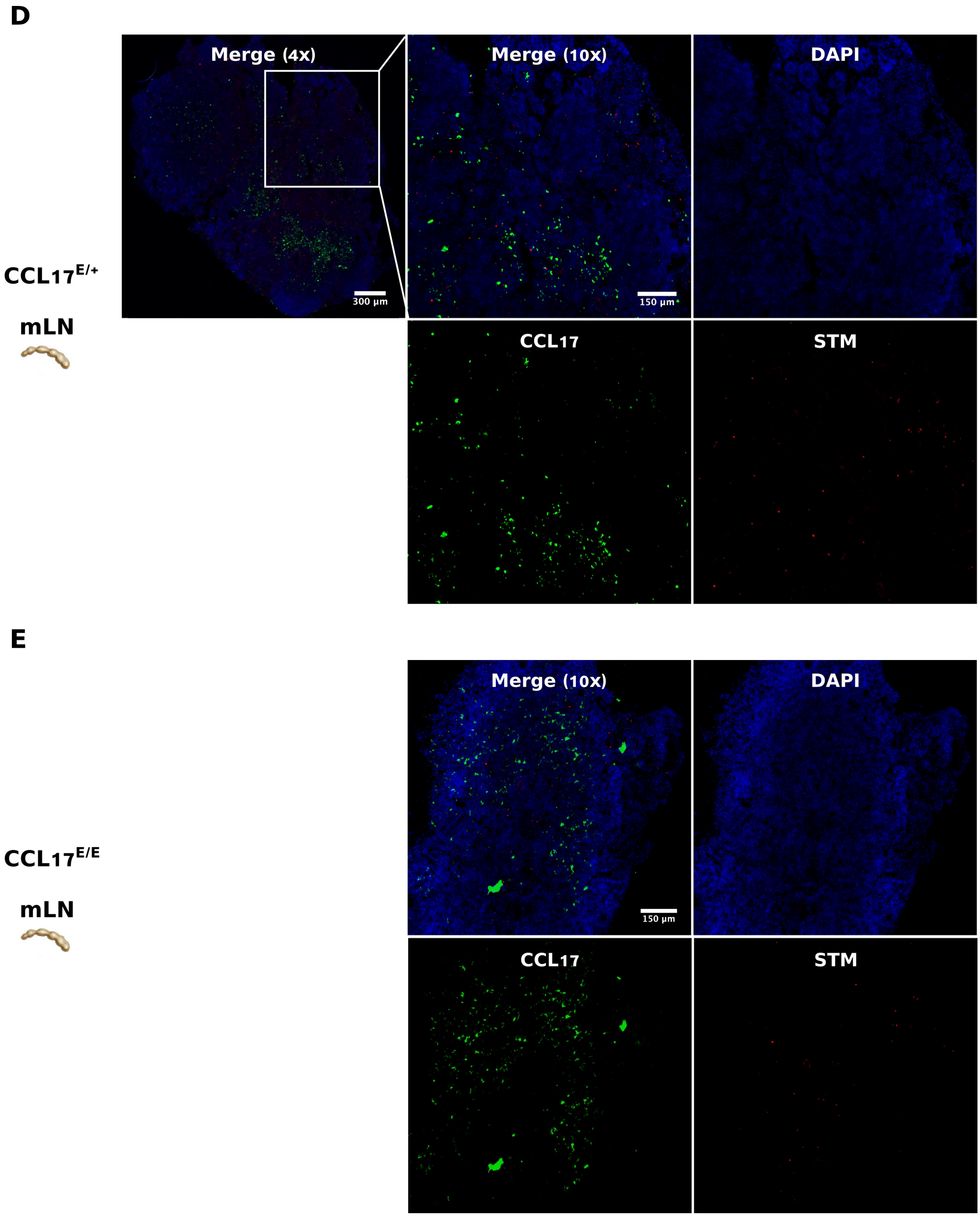

Figure 3.1.2: Histological analysis of CCL17 expression and localisation of STM in PP and mLN in infected mice

CCL17$^{E/+}$ and CCL17$^{E/E}$ mice were orally infected with 2.5x10^{9} STM SL1344 expressing mCherry. PP and mLN were isolated 3 days post-infection (A), fixed and subjected to immunofluorescent staining. Sections were stained with antibodies against EGFP (CCL17) marking endogenous expression of EGFP in CCL17$^{E/+}$ and CCL17$^{E/E}$ mice, against RFP-derivates marking endogenous expression of mCherry in STM and stained with DAPI (nuclei). Samples were analysed via fluorescent microscopy. Vertical sections through

PP from CCL17$^{E/+}$ reporter mice (B) and CCL17$^{E/E}$ deficient mice (C) or through mLN from CCL17$^{E/+}$ mice (D) and CCL17$^{E/E}$ mice (E) show CCL17^{+}/EGFP^{+} cells (green), STM (red) and nuclei (blue) in pseudocolor. Pseudocolor merged image is depicted in the first left picture of B, C, D and E. Vertical sections through PP from and CCL17$^{E/E}$ mouse evaluated with confocal microscope (C). Scale bars are included in merge image. Representative images are shown (n =9, three independent experiments were performed, exemplary images are shown).

3.1.2 CCL17-expressing cells contribute to dissemination of STM from PP to mLN

In a chronic dermatitis model using CCL17-deficient mice, Langerhans cells (LC) are retained in the lesional skin after chronic allergen exposure, since sensitisation for CCR7-dependent DC migration is abrogated (Stutte et al., 2010). Further *in vitro* studies underlined the importance of CCL17 for DC migration to CCR7 ligands (Stutte et al., 2010). In order to investigate the effects of CCL17 on DC migration in the gut, CCL17-deficient mice were infected with invasive *Salmonella*. Since STM are taken up by intestinal DC (Farache et al., 2013; Niess et al., 2005), and then transported to the mLN (Bogunovic et al., 2009; Bravo-Blas et al., 2019; Voedisch et al., 2009), the intracellular bacteria might be used to track bacteria-containing DC that migrate from the intestine/PP to the mLN.

CCL17$^{E/E}$, CCL17$^{E/+}$ and wild type (wt) mice were orally infected with STM SL1344; the PP, mLN, spleen and liver were isolated one- and three days post-infection and evaluated for bacterial counts (Fig 3.1.3 A). STM was detected on day one post-infection in all organs analysed, with PP having the highest counts consistent with oral administration of the bacteria (Fig 3.1.3 B). CFU counts from day one did not vary significantly between mouse strains in the PP, spleen or liver, but were significantly reduced in the mLN from CCL17$^{E/E}$ mice compared to CCL17$^{E/+}$ and wt controls (Fig 3.1.3 B). In all 4 organs, CFU counts from day three were increased compared to day one, but no differences were detected between mouse strains in mLN or the other organs that were investigated (Fig 3.1.3 C).

Taken together, the findings demonstrate that less bacteria are present in the mLN, but not in the PP or other assessed organs, of CCL17-deficient mice compared to control animals on day one post-infection, suggesting an involvement by CCL17 in the migration of STM infected CCL17^{+} cells from PP to mLN, but not to systemic organs.

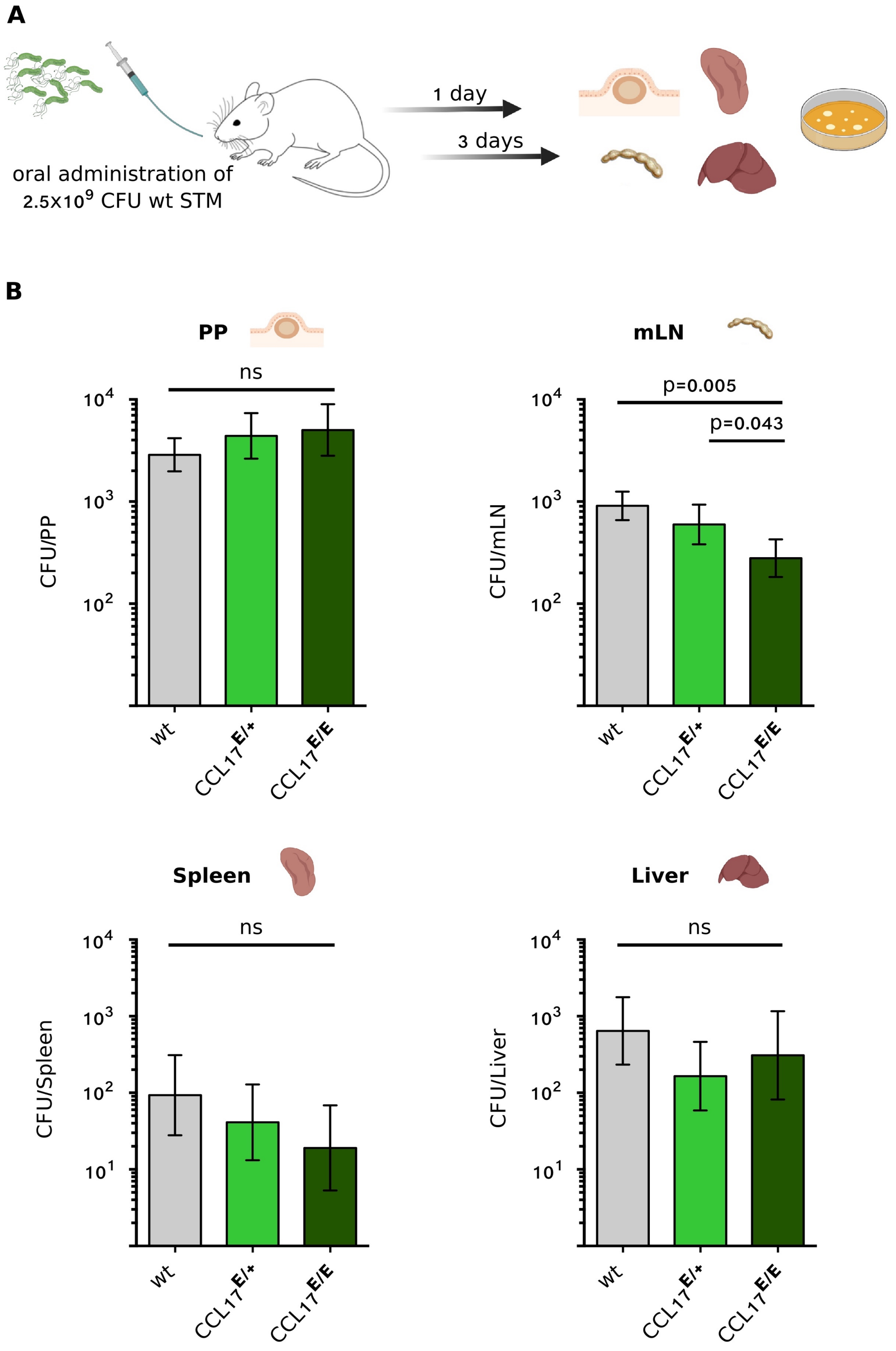
A
oral administration of
$2.5x10^9$ CFU wt STM
1 day
3 days
B
PP
ns
10^4
10^3
10^2
CFU/PP
wt
$CCL17^{E/+}$
$CCL17^{E/E}$
mLN
p=0.005
p=0.043
10^4
10^3
10^2
CFU/mLN
wt
$CCL17^{E/+}$
$CCL17^{E/E}$
Spleen
ns
10^4
10^3
10^2
10^1
CFU/Spleen
wt
$CCL17^{E/+}$
$CCL17^{E/E}$
Liver
ns
10^4
10^3
10^2
10^1
CFU/Liver
wt
$CCL17^{E/+}$
$CCL17^{E/E}$

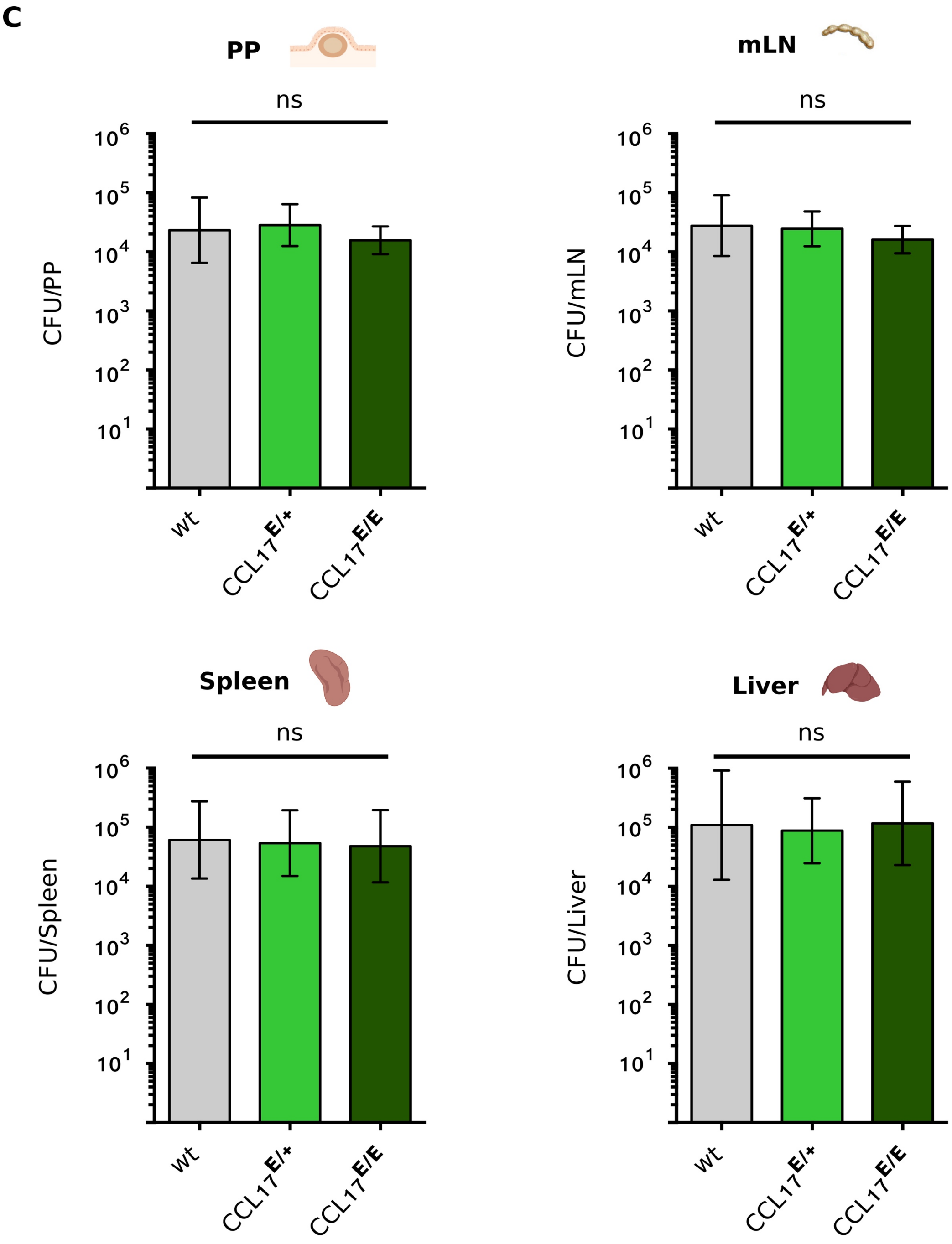

Figure 3.1.3: Analysis of bacterial burden of STM-infected CCL17-deficient mice
Wt, CCL17$^{E/+}$ and CCL17$^{E/E}$ mice were orally infected with 1-2.5x10^{9} STM SL1344. PP, mLN, spleen and liver were isolated one- and three days post-infection (A). CFU counts were determined by plating out organ homogenates from day one (B) and day three (C) post-infection on LB agar with appropriate antibiotics that would help select for STM. Plates were incubated overnight and the colonies counted. Statistical significance was tested using one-way ANOVA with Tukey´s test for multiple comparison. Error bars indicate geometric mean with 95% CI (day 1: n=16-23, pooled from 7 independent experiments; day 3: n=7-20, pooled from 5-7 independent experiments).

3.1.3 CCL17 expression is triggered exclusively in specific intestinal DC subsets by STM infection

Since the experiments suggested that CCL17 may be involved in the spreading of *Salmonella* (Fig 3.1.3 B), it was hypothesised that the level of CCL17 expression might be influenced by STM infection. Since there is only limited information on the expression of CCL17 during infection, expression levels of CCL17 in the gut were analysed after oral STM infection.

CCL17$^{E/+}$ reporter mice were orally infected with STM SL1344. PP and mLN were isolated one day (19h) post-infection and mononuclear phagocytes were analysed for CCL17/EGFP expression via flow cytometry (Fig 3.1.4 A). Naïve CCL17$^{E/+}$ reporter mice were used as control animals. Using a flow cytometric strategy that specifically targeted mononuclear phagocytes (Fig 3.1.4 B), dead and Lin^{+} (T and B cells) cells were excluded, as were doublet cells and autofluorescent (AF)$^{+}$ cells. The target cell populations were analysed for their Ly6C and MHCII expression and further subsets classified as Ly6C^{+} MHCII^{+} (macrophage-like phenotype), Ly6C^{+} MHCII^{-} (monocyte-like phenotype), Ly6C^{-} MHCII^{+} (DC-like phenotype). The level of CCL17 expression was then determined in these different cell populations. Alternatively, MHCII^{+} CD64^{-} cells from live, single Lin^{-} AF^{-} cells were selected. These cells were further analysed for CD11c expression to mark the total DC population, which was further subdivided depending on their CD103 and CD11b expression into the 4 DC subpopulations according to Cerovic et al*.* (Cerovic et al., 2013). All 4 DC subpopulations, as well as the total DC population, were investigated for CCL17 expression (Fig 3.1.4 B).

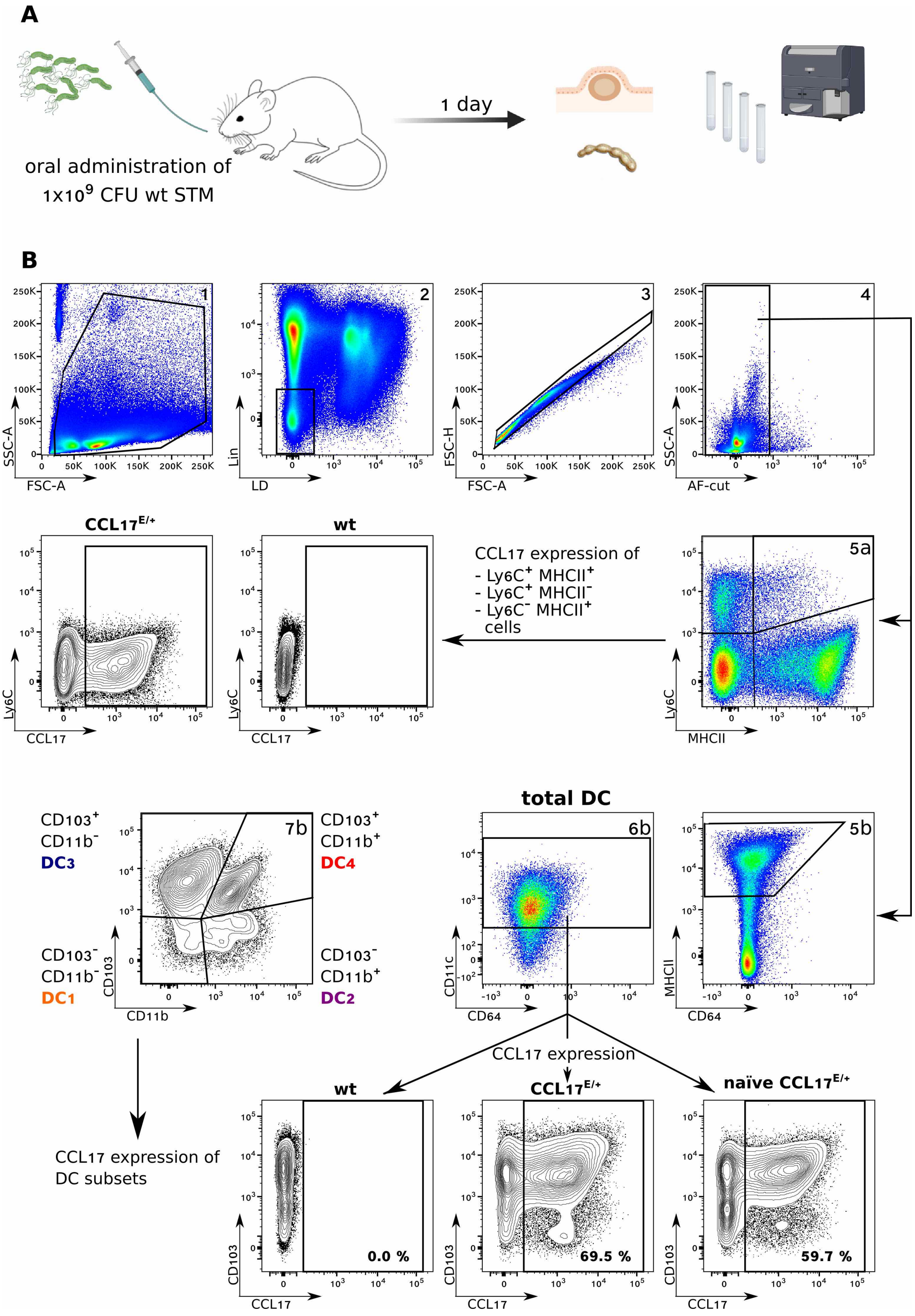
A
oral administration of
1x10⁹ CFU wt STM
1 day
B
1
SSC-A
FSC-A
2
Lin
LD
3
FSC-H
FSC-A
4
SSC-A
AF-cut
CCL17E/+
wt
Ly6C
CCL17
CCL17 expression of
- Ly6C⁺ MHCII⁺
- Ly6C⁺ MHCII⁻
- Ly6C⁻ MHCII⁺
cells
5a
Ly6C
MHCII
total DC
6b
CD11c
CD64
5b
MHCII
CD64
7b
CD103⁺
CD11b⁻
DC3
CD103⁺
CD11b⁺
DC4
CD103⁻
CD11b⁻
DC1
CD103⁻
CD11b⁺
DC2
CD103
CD11b
CCL17 expression
CCL17 expression of
DC subsets
wt
CCL17E/+
naïve CCL17E/+
0.0 %
69.5 %
59.7 %
CD103
CCL17

Figure 3.1.4: Analysis of CCL17 expression in mononuclear phagocytes – experimental setup and gating strategy
CCL17$^{E/+}$ were orally infected with 1x10^{9} CFU STM SL1344. PP and mLN were isolated from 19h infected and control naïve mice; the myeloid cell compartment was analysed via flow cytometry (A). Cells were selected due to their FSC and SSC properties (B1). Live Lin^{-} cells (B and T cells) were selected (B2), single cells identified (B3) and autofluorescent (AF) cells were excluded using an empty fluorescent channel (B4). Remaining cells were analysed for the expression of myeloid cell markers Ly6C and MHCII (B5a) Ly6C^{+} MHCII^{+} cells were identified as macrophage-like population, Ly6C^{+} MHCII^{-} cells were identified as monocyte-like population and Ly6C^{-} MHCII^{+} cells were identified as DC-like population. All 3 mononuclear phagocyte populations were analysed for their CCL17 expression, wt control is shown alongside the sample from infected CCL17$^{E/+}$ mouse. Alternatively, MHCII^{+} CD64^{-} cells were selected from remaining live single Lin^{-} AF^{-} cells (5b) and further evaluated for their CD11c expression (6b). MHCII^{+} CD64^{-} CD11c^{+} cells were identified as DC and were further subdivided into 4 subpopulations depending on their expression of CD103 and CD11b: DC1 (CD103^{-} CD11b^{-}), DC2 (CD103^{-} CD11b^{+}), DC3 (CD103^{+} CD11b^{-}) and DC4 (CD103^{+} CD11b^{+}) (7b). total DC and DC subpopulations were subjected to CCL17 expression analysis, wt and naïve CCL17$^{E/+}$ control are shown alongside the infected sample. Representative gating of mLN from an infected CCL17$^{E/+}$ mouse is depicted.

Depending on their Ly6C and MHCII expression, myeloid cells were categorised as macrophage-like cells (Ly6C^{+} MHCII^{+}), monocyte-like cells (Ly6C^{+} MHCII^{-}) or DC-like cells (Ly6C^{-} MHCII^{+}) and analysed for their CCL17 expression in PP and mLN. The DC-like cell population was the predominant CCL17-expressing cell type in PP and in mLN whereas, in general, the frequency of CCL17-expressing cells was higher in mLN compared to PP (Fig 3.1.5). Also, macrophage-like cells expressed CCL17, but the proportion of CCL17-expressing cells within this population was lower compared to the DC-like population. The monocyte-like population showed the lowest frequency of CCL17^{+} cells, if any. In the PP, no significant differences in CCL17^{+} cells were detected between myeloid cell populations from naïve or STM-infected mice whereas, in the mLN myeloid cell from infected mice, there was an increase of CCL17^{+} cell frequencies compared to naïve controls (Fig 3.1.5).

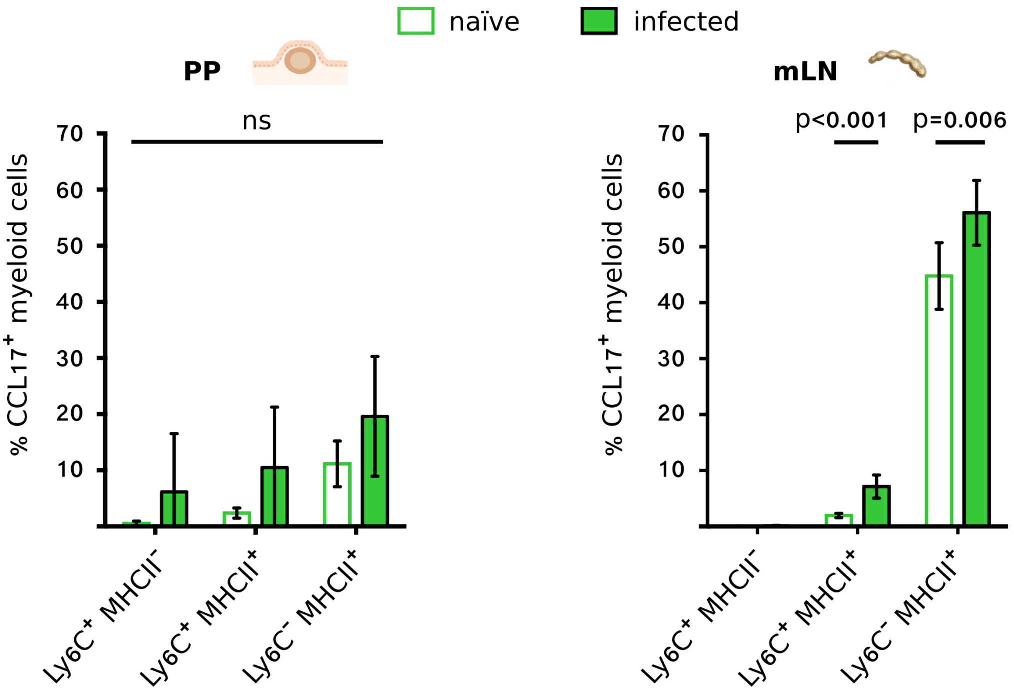

Figure 3.1.5: Analysis of CCL17 expression in myeloid cells
CCL17$^{E/+}$ were orally infected with 1x10^9 CFU STM SL1344. PP and mLN were evaluated for CCL17/EGFP expression in mononuclear phagocytes 19h post-infection, naïve mice were used as the control. Ly6C$^+$ MHCII$^+$ cells were identified as macrophage-like population, Ly6C$^+$ MHCII$^-$ cells were identified as monocyte-like population and Ly6C$^-$ MHCII$^+$ cells were identified as DC-like population. Statistical significance was tested using one-way ANOVA with Tukey´s test for multiple comparison. Error bars indicate mean with 95% CI (n= 7-8, pooled from three independent experiments).

The intestine provides a unique setting where 4 DC subsets with distinctive functions can be identified, depending on their expression of CD103 and CD11b. The increase of CCL17$^+$ DC-like cells observed in mLN after *Salmonella* infection (Fig 3.1.5) led to further investigation of the different DC subpopulations in the intestine. The more stringent flow cytometric strategy for DC using MHCII, CD64 and CD11c (Fig 3.1.4 B plot 5b&6b), instead of MHCII and Ly6C (Fig 3.1.4 B plot 5a), revealed not only a significant increase of CCL17$^+$ total DC in the mLN, but also in the PP after STM infection (Fig 3.1.6 A). In PP, the DC1 subset, and especially the DC3 and DC4 subpopulations showed a significant increase in the frequency of CCL17$^+$ cells compared to naïve controls. In mLN, there were similar increases in DC1, DC2 and DC4 but not in DC3, indicating that infection with STM resulted in an increased percentage of CCL17$^+$ DC after bacterial challenge (Fig

3.1.6 A). The increase in CCL17⁺ DC frequencies was also mirrored in most populations by an increase of MFI (Fig 3.1.6 B) indicating not only an expansion of CCL17⁺ DC after STM infection but also augmented CCL17 expression in these cells.

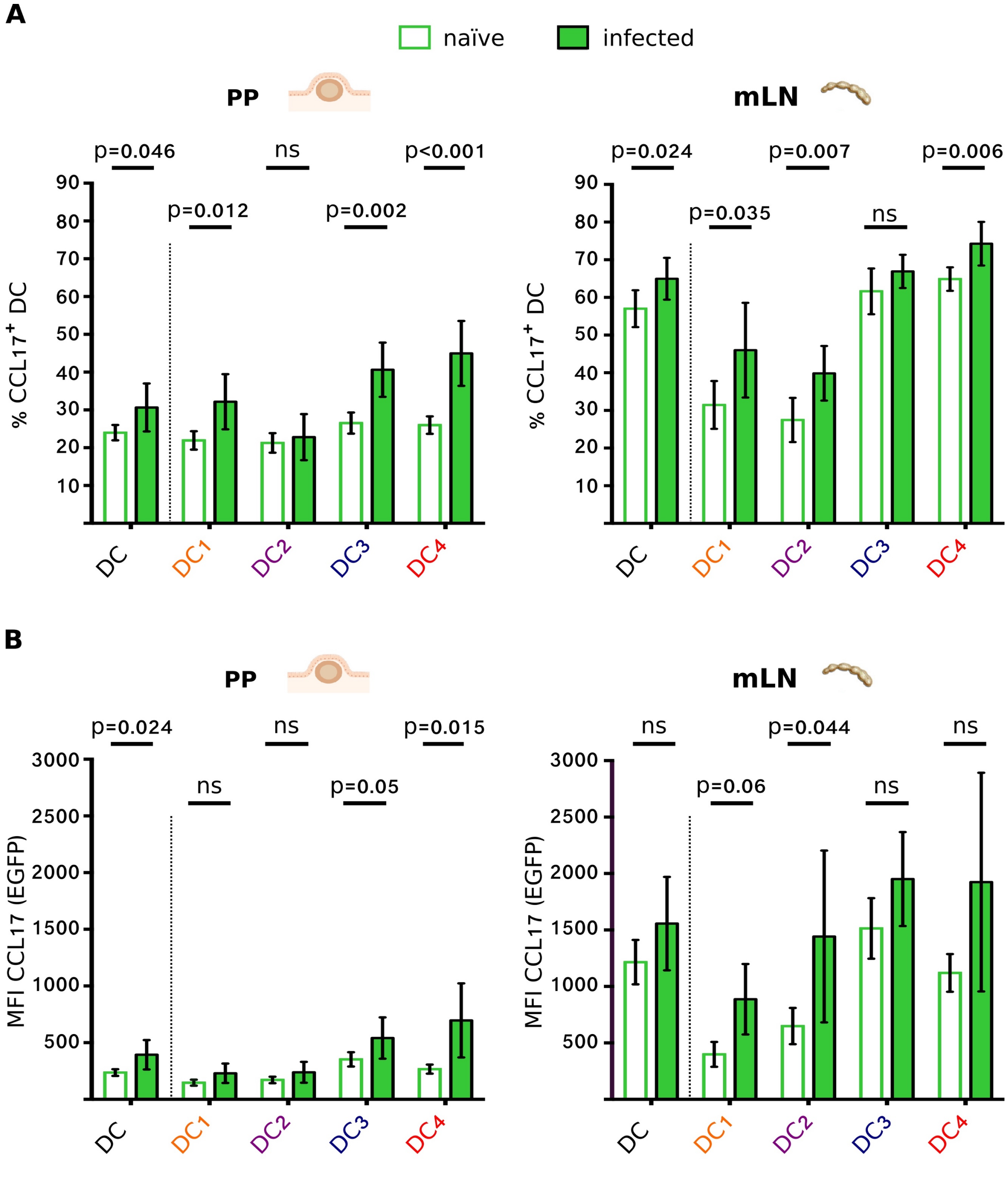

DC: total DC

DC1: CD103⁻ CD11b⁻

DC2: CD103⁻ CD11b⁺

DC3: CD103⁺ CD11b⁻

DC4: CD103⁺ CD11b⁺

Figure 3.1.6: Analysis of CCL17 expression in DC subsets
CCL17$^{E/+}$ mice were orally infected with 1x10^{9} CFU STM SL1344. PP and mLN were evaluated for CCL17/EGFP expression in total DC and DC subsets 19h post-infection, and naïve mice were used as the control. MHCII^{+} CD64^{-} CD11c^{+} cells were identified as DC and were further subdivided into 4 subpopulations depending on their expression of CD103 and CD11b: DC1 (CD103^{-} CD11b^{-}), DC2 (CD103^{-} CD11b^{+}), DC3 (CD103^{+} CD11b^{-}) and DC4 (CD103^{+} CD11b^{+}). CCL17^{+} cell frequencies (A) and MFI (B) of total DC and DC subsets were assessed. Statistical significance was tested using one-way ANOVA with Tukey´s test for multiple comparison. Error bars indicate mean with 95% CI (n= 11, pooled from three independent experiments).

Interestingly, the DC subsets that expressed CD103 (DC3 and DC4) were the subsets that showed an expansion of CCL17^{+} cells, as well as an increase in MFI, after STM challenge in PP. In contrast, in the mLN, the CD103^{-} DC subsets, demonstrated an increase of CCL17^{+}, cells as well as an increase in MFI (Fig 3.1.4.6). These observations suggested a differential STM-induced expression of CCL17 in different DC subsets, depending on the organ analysed. It was noted though that the CD103^{+} DC subsets of mLN were constitutively high for CCL17 expression already before infection with STM.

3.1.4 Different phagocytic myeloid cells harbour STM in mLN

Several studies have investigated the cell populations responsible for the transport and therefore spreading of *Salmonella* from the gut to the mLN. DC have been identified as the cell type ´highjacked´ by STM for intracellular transportation from the intestine to the mLN (Bogunovic et al., 2009; Bravo-Blas et al., 2019; Voedisch et al., 2009). In addition, it is also very likely that bacteria can float freely in the lymph and thereby reach the mLN (Bravo-Blas et al., 2019). In addition to DC, macrophages and monocytes also take up STM after *in vivo* infection (Bravo-Blas et al., 2019; Vazquez-Torres et al., 1999), but only DC are thought to carry bacteria from the gut to the draining lymph nodes (Bogunovic et al., 2009; Bravo-Blas et al., 2019; Voedisch et al., 2009). Since the data presented here demonstrated that CCL17 expression in different intestinal DC subsets is affected by STM infection (Fig 3.1.6), it was of interest to investigate whether CCL17^{+} DC might be specifically targeted by STM. Moreover, the hypothesis that deficiency in CCL17 or in CCL17 and CCL22 might interfere with the uptake of *Salmonella* in mononuclear phagocytes, was tested. An antibody specific to STM-LPS was used to detect intracellular bacteria within mononuclear phagocytes in the mLN of CCL17$^{E/+}$ reporter mice, CCL17-deficient and CCL17/CCL22 double-deficient mice.

Wild type, CCL17$^{E/+}$ reporter mice, CCL17$^{E/E}$ and CCL17$^{E/E}$CCL22$^{-/-}$ mice were orally infected with STM SL1344, mLN were isolated 1.5 days (36h) post-infection and the mononuclear phagocyte compartment was analysed for intracellular bacteria and CCL17/EGFP expression using flow cytometry (Fig 3.1.7 A). In contrast to the previous gating strategy (Fig 3.1.4 B), a slightly different flow cytometric approach was used that allowed for specific targeting of all mononuclear phagocytes (DC/monocytes/macrophages) (Fig 3.1.7 B). Only viable, Lin^{-} (T and B cells) cells were investigated, autofluorescent (AF)$^{+}$ as well as doublet cells were excluded. Subsequently, target cells were analysed for their CD11c and CD64 expression. CD64^{+} cells were further evaluated for their CD11c and MHCII expression and CD11c$^{int/+}$ MHCII^{+} were identified as macrophages (Mφ) (Fig 3.1.7 B plot 5-6a). CD11c^{-} CD64^{-} cells were further assessed for their Ly6C and MHCII expression, Ly6C^{+} MHCII^{-} cells were classified as newly extravasated monocytes (new Mo.) and Ly6C$^-$ MHCII$^+$ cells most likely as monocyte/macrophage intermediates (Mo./Mφ) (Fig 3.1.7 B plot 5-6b). CD11c$^+$ CD64$^-$ cells were additionally assessed for their Ly6C and MHCII expression, Ly6C$^-$ MHCII$^+$ cells were identified as DC (Fig 3.1.7 B plot 5-6c). These cell populations were then investigated for intracellular STM. Naïve animals were used as control, as some background was detected for the monocyte populations (Fig 3.1.7 B). In addition, DC were further subdivided depending on their CD103 and CD11b expression into the 4 DC subsets (Fig 3.1.7 B plot 7), and then analysed for intracellular STM.

DC, newly extravasated monocytes, monocyte/macrophage intermediates and macrophages harboured similar counts of STM$^+$ cells. STM-distribution in mononuclear phagocytes was only moderately affected by the genetic background of mice. Newly extravasated monocytes in CCL17-deficient mice contained the highest count of STM$^+$ cells compared to CCL17$^{E/+}$, CCL17$^{E/E}$CCL22$^{-/-}$ and wt mice (Fig 3.1.7 C). Subsequently, the CCL17/EGFP expression of STM$^+$ DC was assessed (Fig 3.1.7 D-E). Approximately 1/3 of STM$^+$ DC expressed CCL17. In CCL17/22 double-deficient mice, EGFP expression was increased compared to CCL17$^{E/+}$ reporter and CCL17$^{E/E}$ mice (Fig 3.1.7 E).

Intestinal DC can be subdivided into 4 different subpopulations depending on their expression of CD103 and CD11b. In previous studies, all DC subsets have been shown to harbour STM within the mLN, but the CD103$^+$CD11b$^+$ DC (DC4) were the major population (Bogunovic et al., 2009; Bravo-Blas et al., 2019). Therefore, not only the different myeloid cell populations but also the different intestinal DC subsets were investigated for intracellular bacteria (Fig 3.1.7 F-G). All DC subtypes contained STM, but especially the CD103$^+$ CD11b$^-$ DC subset (DC3) showed a high proportion of STM. Approximately 54% of all STM$^+$ DC had a CD103$^+$ CD11b$^-$ phenotype, which was an enrichment compared to the normal distribution of the DC subsets, where CD103$^+$ CD11b$^-$ DC (DC3) represented approximately 40% of total DC (Fig 3.1.7 F). The higher frequency of STM$^+$ CD103$^+$ CD11b$^-$ DC (DC3) was demonstrated in all murine genotypes analysed, and was therefore independent of CCL17 or CCL22 expression. Consistent with the overrepresentation of CD103$^+$ CD11b$^-$ DC (DC3), CD103$^+$ CD11b$^+$ DC (DC4) were underrepresented in the STM$^+$ population, in comparison to the normal distribution of the DC populations (Fig 3.1.7 G).

Taken together, *Salmonella* was detected in many myeloid cell populations within the mLN including DC, monocytes and macrophages and STM did not infect a sole population but rather all of the populations analysed. Approximately 30% of STM$^+$ DC expressed CCL17/EGFP whereas, in CCL17/CCL22 double-deficient mice, the frequency of STM$^+$ EGFP$^+$ cells was increased. Analysis of the STM$^+$ DC subpopulations revealed that all DC subsets did harbour STM, but the CD103$^+$ CD11b$^-$ DC (DC3) were identified as the main STM$^+$ DC-population. In addition, comparison of the STM$^+$ DC to the overall DC population revealed a higher proportion of CD103$^+$ CD11b$^-$ DC (DC3) suggesting a preference of *Salmonella* for this specific DC subset. Finally, the STM-distribution was largely unaffected by the absence of CCL17 or CCL17 and CCL22.

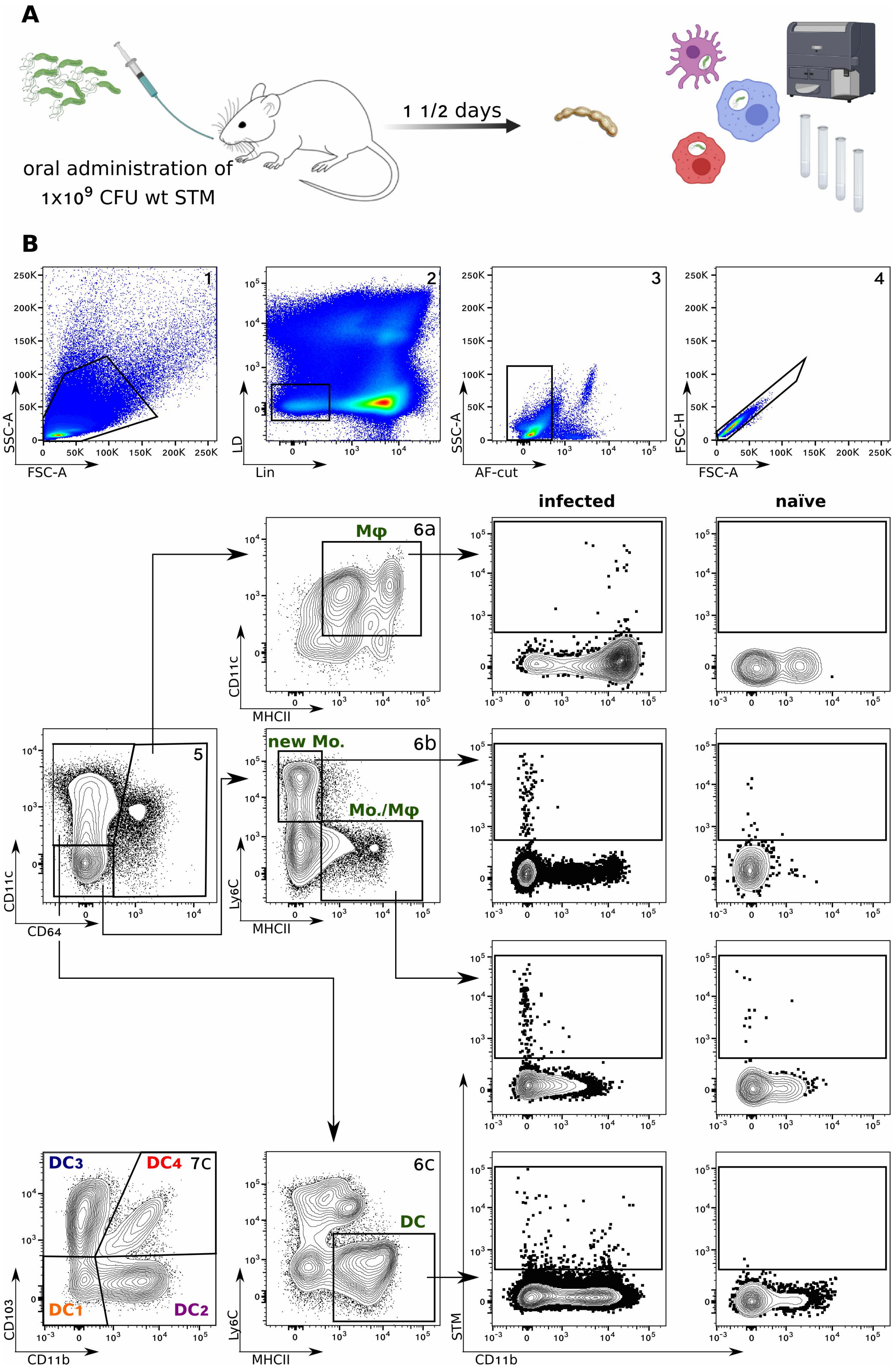
A
oral administration of
1x10⁹ CFU wt STM
1 1/2 days
B
1
SSC-A
FSC-A
2
LD
Lin
3
SSC-A
AF-cut
4
FSC-H
FSC-A
infected
naïve
Mφ
6a
CD11c
MHCII
5
CD11c
CD64
new Mo.
6b
Mo./Mφ
Ly6C
MHCII
DC3
DC4
7C
DC1
DC2
CD103
CD11b
6C
DC
Ly6C
MHCII
STM
CD11b

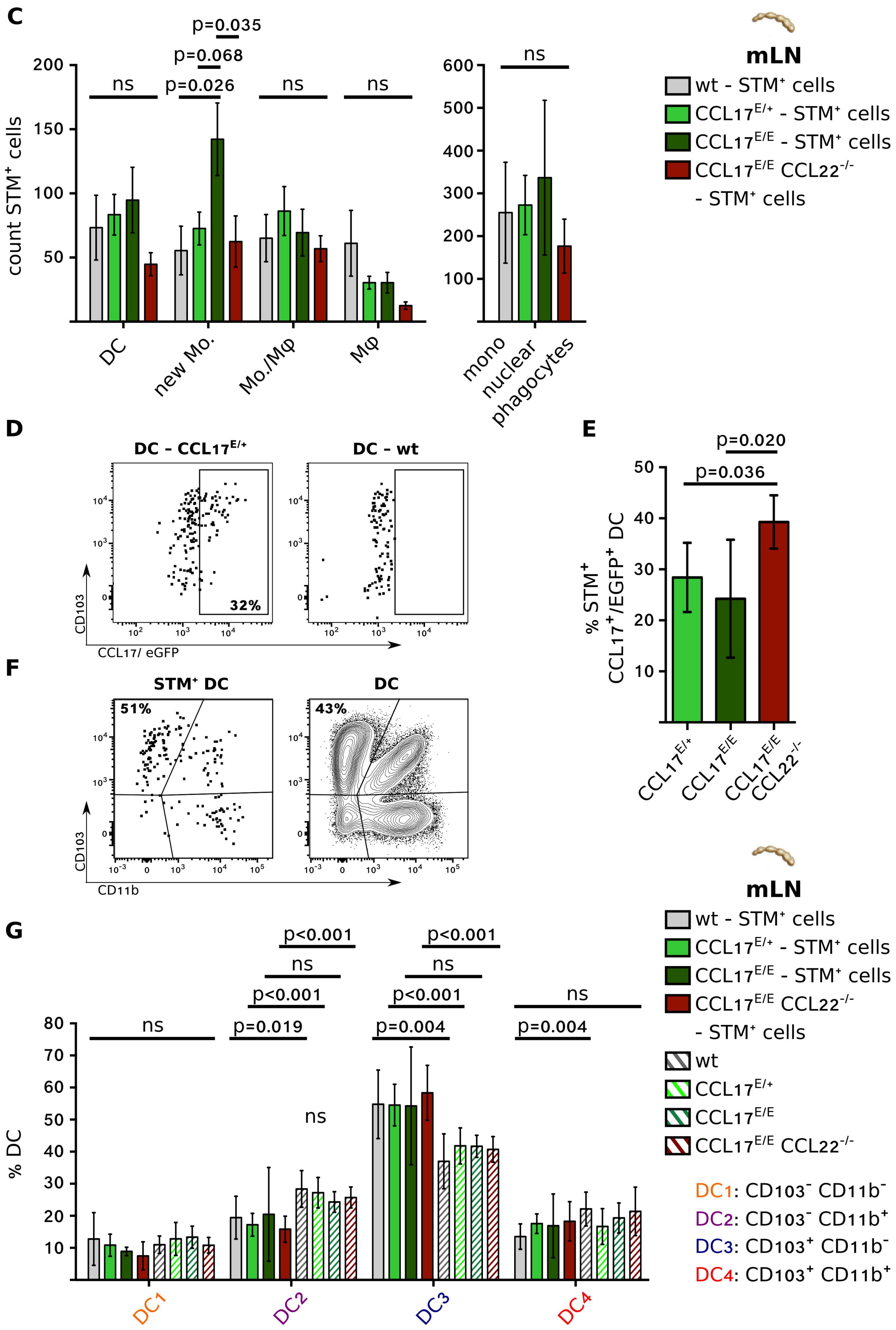
C
mLN
wt - STM+ cells
CCL17E/+ - STM+ cells
CCL17E/E - STM+ cells
CCL17E/E CCL22-/- - STM+ cells
count STM+ cells
200
150
100
50
ns
p=0.035
p=0.068
p=0.026
ns
ns
DC
new Mo.
Mo./Mφ
Mφ
600
500
400
300
200
100
ns
mono nuclear phagocytes
D
DC - CCL17E/+
DC - wt
32%
CD103
CCL17/ eGFP
E
p=0.020
p=0.036
50
40
30
20
10
% STM+ CCL17+/EGFP+ DC
CCL17E/+
CCL17E/E
CCL17E/E CCL22-/-
F
STM+ DC
DC
51%
43%
CD103
CD11b
G
mLN
wt - STM+ cells
CCL17E/+ - STM+ cells
CCL17E/E - STM+ cells
CCL17E/E CCL22-/- - STM+ cells
wt
CCL17E/+
CCL17E/E
CCL17E/E CCL22-/-
DC1: CD103- CD11b-
DC2: CD103- CD11b+
DC3: CD103+ CD11b-
DC4: CD103+ CD11b+
% DC
80
70
60
50
40
30
20
10
ns
p<0.001
ns
p<0.001
p=0.019
p<0.001
ns
p<0.001
p=0.004
ns
p=0.004
ns
DC1
DC2
DC3
DC4

Figure 3.1.7: Analysis of STM$^+$ mononuclear phagocytes
Wt, CCL17$^{E/+}$, CCL17$^{E/E}$ and CCL17/CCL22 double-deficient mice were orally infected with 1x10^9 CFU STM SL1344. mLN were isolated from 36h-infected, and control naïve mice; the STM$^+$ mononuclear phagocytes were analysed via flow cytometry (A). Cells were selected based on their FSC and SSC properties (B1). Live Lin$^-$ cells (B and T cells) were selected (B2), autofluorescent (AF) cells were excluded using an empty fluorescent channel (B3) and single cells identified (B4). Remaining cells were analysed for the expression of DC/macrophage markers CD11c and CD64 (B5). CD64$^+$ cells were further evaluated for their CD11c and MHCII expression and CD11c$^{int/+}$ MHCII$^+$ cells were identified as macrophages (Mφ) (B6a). CD11c$^-$ CD64$^-$ cells were further assessed for their Ly6C and MHCII expression, Ly6C$^+$ MHCII$^-$ cells were classified as newly extravasated monocytes (new Mo.) and Ly6C$^-$ MHCII$^+$ cells as monocyte/macrophage intermediates (Mo./Mφ) (B6b). CD11c$^+$ CD64$^-$ cells were further addressed for their Ly6C and MHCII expression, Ly6C$^-$ MHCII$^+$ cells were identified as DC (B6c). These cell populations were then investigated for intracellular STM using a monoclonal STM-specific anti-LPS antibody, uninfected control is shown alongside infected sample (B). DC were further subdivided into 4 subpopulations depending on their expression of CD103 and CD11b: DC1 (CD103$^-$ CD11b$^-$), DC2 (CD103$^-$ CD11b$^+$), DC3 (CD103$^+$ CD11b$^-$) and DC4 (CD103$^+$ CD11b$^+$) (7c). STM$^+$ DC, monocytes and macrophages were quantified as well as the mononuclear phagocyte compartment in total (sum of STM$^+$ mononuclear phagocytes (DC/ new Mo/ Mo./Mφ/ Mφ)) (C). STM$^+$ DC were subjected to CCL17 expression analysis (D-E) and STM$^+$ DC subpopulations were evaluated (F-G). A representative gating of mLN from an infected mouse is depicted. Detected background in control naïve mice was subtracted from detected STM$^+$ cells for each myeloid cell population in order to obtain STM$^+$ cell counts. Statistical significance was tested using two-way ANOVA with Tukey´s test for multiple comparison (C), one-way ANOVA with Tukey´s test for multiple comparison (E) and unpaired t-test (G). Error bars indicate mean with SEM (C) or 95% CI (E and G) (n=5-15, pooled from two to three independent experiments).

3.2 Influence of CCL17 and CCL22 on T cell immunity against *Salmonella* Typhimurium

Dendritic cells are potent inducers of T cell priming and activation. The chemokine CCL17 and the closely related chemokine CCL22 play an important role in DC-T cell interaction, suggesting a relevant function of these chemokines in building T cell immunity. Both molecules belong to a group of chemokines that are both expressed under homeostatic conditions and induced upon inflammation (Alferink et al., 2003; Vulcano et al., 2001). They act via their receptor CCR4, which is present on a variety of different T cells including regulatory T cells (T_{reg}) (Andrew et al., 2001; Inukai et al., 2007; Latorre et al., 2019; Miltenyi Biotec, 2015; Morimoto et al., 2005; Sugiyama et al., 2013; Yuan et al., 2007). The actions of CCL17 on T cells in the context of various allergy and inflammatory conditions have been well studied using a CCL17-deficient mouse model (Achuthan et al., 2016; Alferink et al., 2003; Fülle et al., 2018a; Heiseke et al., 2012; Stutte et al., 2010). Also, the actions of CCL22 on T cell populations, in particular, T_{reg} cells, have been studied predominantly in cancer models (Anz et al., 2015; Gobert et al., 2009; Layseca-Espinosa et al., 2013). Besides the established CCL17-deficient mouse model, we recently generated CCL22-deficient and CCL17/CCL22 double-deficient mice in-house. They have yet to be used as tools to study the role of these cytokines in infection immunity.

These mouse models will enable us to address the complex relationships between the two CCR4 ligands, CCL17 and CCL22, especially in the context of building T cell immunity through vaccination.

3.2.1 Deficiency in CCL17 and CCL22 results in increased vaccine efficacy vaccine-induced CD4$^+$ T cell immunity after secondary challenge

Relatively little is known about CCL17 and CCL22 in the context of infection or vaccination. Hence, the aim of this study-part was to address whether deficiency in the chemokines CCL17 and CCL22 would interfere with T cell immunity in the context of an infectious disease. We chose the well-established *Salmonella* Typhimurium (STM) vaccine/challenge model. In this model, C57BL/6 mice are vaccinated with an attenuated STM strain such as BRD509 or TAS2010. Mice clear attenuated STM infections within 7 to 10 weeks and are protected from secondary infection with virulent STM, such as STM SL1344 (Kupz et al., 2014), that is otherwise lethal in unvaccinated mice. Non-immune mice typically succumb to STM SL1344 infection within a few days (5-8 days), depending on the dose of bacteria administered. The level of resistance to virulent STM challenge is believed to be correlated with the degree of development of acquired immunity. This model not only allows the analysis of the primary T cell immune response after vaccination, but also the secondary T cell response after challenge and thus is a powerful tool to study the influence of CCL17 and CCL22 on T cell immunity.

The experiments reported used vaccination with TAS2010, since it confers increased protection from secondary challenge compared to the BRD509 vaccine model (Kupz et al., 2013).

3.2.1.1 Deficiency in CCL22, but not CCL17, contributes to better survival after secondary challenge

The first hypothesis tested was that the absence of either or both of CCL17 and CCL22 would interfere with vaccine efficacy. Wt, CCL17$^{E/E}$, CCL22$^{-/-}$ and CCL17/CCL22 double-deficient mice were vaccinated with TAS2010 for 12-15 weeks, and then challenged orally with virulent STM SL1344. Unvaccinated mice served as controls. Mice were monitored regularly over 21 days to evaluate the efficacy of vaccine-mediated immune protection (Fig 3.2.1 A). As expected, all unvaccinated control mice succumbed to infection within 5 to 8 days post-challenge, independent of their genetic background with respect to chemokine expression (Fig 3.2.1 B). Some vaccinated mice were unprotected by the vaccine, but generally vaccinated mice were better protected from secondary virulent challenge than unvaccinated mice. Vaccinated wt and CCL17$^{E/E}$ mice had a survival rate of approximately 50% whereas, all unvaccinated mice were sensitive to challenge. This level of protection in wt mice and CCL17$^{E/E}$ mice was significantly lower than the protection observed in CCL22$^{-/-}$ (100%) and in CCL17/CCL22 double-deficient mice (90%) (Fig 3.2.1 B).

These findings suggest that a deficiency in CCL22, but not CCL17, results in better survival of vaccinated mice compared to wt controls after STM SL1344 challenge. Deficiency in both chemokines did not lead to additional protection.

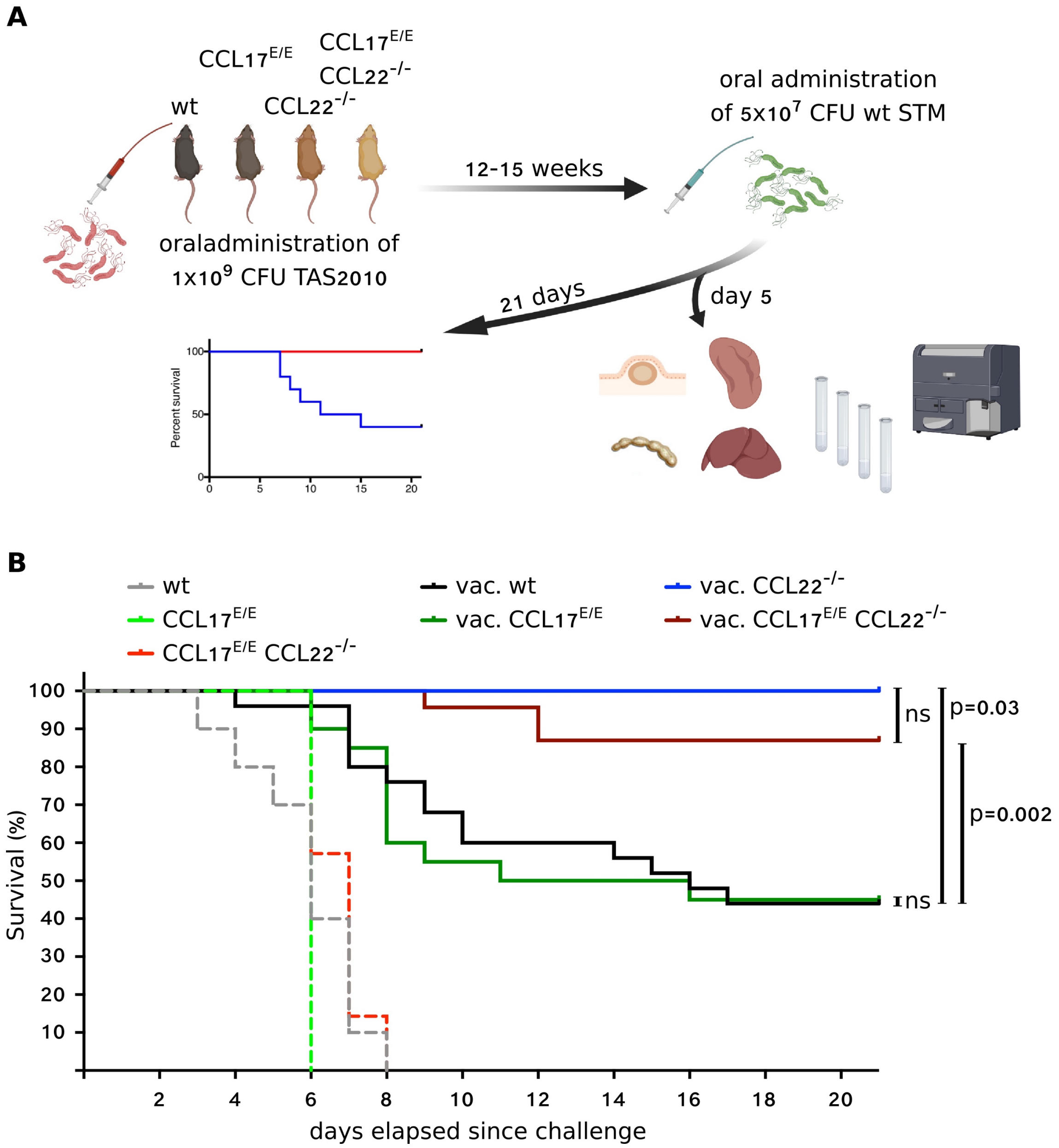

Figure 3.2.1: Survival of TAS2010 vaccinated and challenged wt and KO mice
Wt, CCL17$^{E/E}$, CCL22$^{-/-}$ and CCL17/CCL22 double-deficient mice were orally vaccinated (vac.) with 1x10^{9} CFU TAS2010. 12 to 15 weeks post-vaccination mice were orally challenged with 5x10^{7} CFU STM SL1344. Mice were monitored over 21 days and survival after-challenge was addressed, alternatively PP, mLN, spleen and liver were isolated from KO and wt mice 5 days post-challenge and the T$_{reg}$ and T$_{conv}$ cell compartment was analysed via flow cytometry (A). As controls, naïve CCL17$^{E/E}$, CCL17/CCL22 double-deficient and wt mice (dashed lines) were challenged alongside vaccinated mice. Mice were monitored daily for their health status (body condition, appearance, behaviour and weight) according to animal ethics over 21 days and survival after-challenge was addressed (n= 3-10 unvaccinated mice, n= 20-25 vaccinated mice; pooled from 5 independent experiments; for CCL22$^{-/-}$ n=6; pooled from two independent experiments). For statistical analysis curve comparison with Logrank (Mantel-Cox test) was used.

3.2.1.2 Vaccinated CCL17/CCL22 double-deficient mice possess a superior CD4$^+$ T cell immune response after secondary challenge

In the acquired immune defence against *Salmonella* spp. Infections, a number of different cell types have been shown to be important, including NK cells and B cells, but in particular CD4$^+$ T cells (Kupz et al., 2013, 2014; Lee et al., 2012b; McSorley et al., 2000; Ugrinovic et al., 2003). In order to investigate the reason for the strikingly better survival of mice deficient in CCL22, the cellular foundation of T cell immunity after secondary STM SL1344 challenge was analysed. It was hypothesised that, since CCL22 is associated with the recruitment of regulatory T cells (Anz et al., 2015; Curiel et al., 2004; Gobert et al., 2009), a reduced mobilisation of these suppressive cells in CCL22-deficient mice might contribute to the better survival. Therefore, the analysis focused on suppressive T$_{reg}$ cells and Th1 CD4$^+$ T cells, as these cells play an essential role in immunity to STM infections in mice (Johanns et al., 2010; Mittrücker et al., 2002; Srinivasan et al., 2004).

CD4$^+$ regulatory T cell (T$_{reg}$) and CD4$^+$ conventional T cell (T$_{conv}$) populations from vaccinated KO mice and wt controls were investigated in PP, mLN, spleen and liver 5 days after challenge (Fig 3.2.1 A). These organs were chosen since they represent the main route of infection from the gut to systemic organs. After oral infection, STM enter the gut via the PP and are transported to mLN, before they reach the spleen and liver, the main organs of bacterial replication (Carter and Collins, 1974). The following flow cytometric strategy was used (Fig 3.2.2 A): only viable CD3$^+$ cells were analysed, and autofluorescent (AF)$^+$ as well as doublet cells were excluded. The T cell population analysis focused on the CD4$^+$ FOXP3$^+$ T$_{reg}$ and the CD4$^+$ FOXP3$^-$ T$_{conv}$ cell compartments. CD44$^+$ CD62L$^-$ effector T$_{reg}$ cells were selected and further, KLRG1$^+$ effector T$_{reg}$ cells were analysed in more detail. KLRG1 is a marker for highly activated effector T$_{reg}$ cells and is associated with enhanced suppressive functions (Cheng et al., 2012; Feuerer et al., 2010; Yuan et al., 2014).

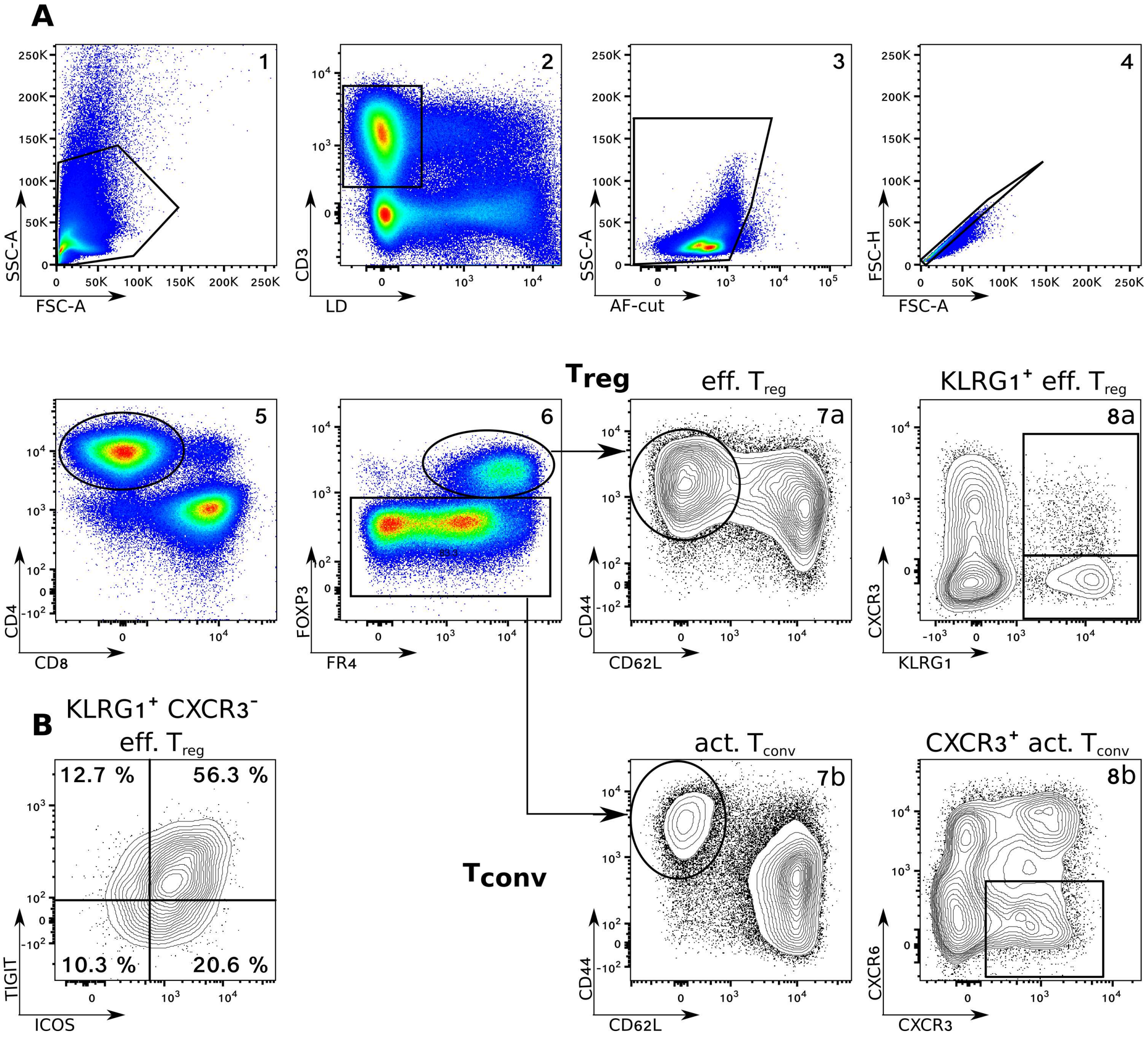

Figure 3.2.2: CD4$^+$ T cell FACS analysis of TAS2010 vaccinated and challenged wt and KO mice – gating strategy

Wt, CCL17$^{E/E}$, CCL22$^{-/-}$ and CCL17/CCL22 double-deficient mice were orally vaccinated with 1x10^9 CFU TAS2010. 12 to 15 weeks post-vaccination, mice were orally challenged with 5x10^7 CFU STM SL1344. PP, mLN, spleen and liver were isolated from wt and KO mice 5 days post-challenge and the T$_{reg}$ and T$_{conv}$ cell compartments were analysed via flow cytometry. Fixed cells were selected based on their FSC and SSC properties (A1). Live T cells were identified as CD3$^+$ LD$^-$ cells (A2). Subsequently, autofluorescent cells were excluded using an empty fluorescent channel (A3). Single cells were identified (A4). CD4$^+$ T cells were selected (A5) and separated into FOXP3$^+$ and FOXP3$^-$ cells (A6). FOXP3$^+$ cells were identified as T$_{reg}$ cells and FOXP3$^-$ as T$_{conv}$ cells. T$_{reg}$ cells were further analysed for CD44 and CD62L expression. CD44$^+$ CD62L$^-$ cells were selected and identified as effector T$_{reg}$ cells (A7a). CD44$^+$ CD62L$^-$ effector (eff.) T$_{reg}$ cells were then addressed for their KLRG1 and CXCR3 expression. KLRG1$^+$ eff. T$_{reg}$ cells were subdivided into CXCR3$^+$ and CXCR3$^-$ KLRG1$^+$ eff. T$_{reg}$ cells (A8a). T$_{conv}$ cells were further analysed for CD44 and CD62L expression. CD44$^+$ CD62L$^-$ cells were selected and identified as activated T$_{conv}$ cells (A7b). Following, CD44$^+$ CD62L$^-$ activated (act.) T$_{conv}$ cells were evaluated for their CXCR3 and CXCR6 expression. CXCR3$^+$ CXCR6$^-$ cells were identified as CXCR3$^+$ act. T$_{conv}$

(A8b). KLRG1$^+$ CXCR3$^-$ eff. T_{reg} cells were investigated for ICOS and TIGIT expression (B). Representative gating of mLN from a vaccinated and challenged wt mouse is depicted.

In the T_{conv} compartment, CD44$^+$ CD62L$^-$ activated T_{conv} cells were selected, and CXCR3$^+$ (CXCR6$^-$) activated T_{conv} cells were further evaluated. CXCR3 is a marker for Th1 T cells (Groom and Luste, 2011; Kim et al., 2001). Also, CXCR6 can be used as Th1 T cell marker (Kim et al., 2001; Latta et al., 2007), but in contrast to CXCR3 which is expressed on 90% of all Th1 polarised cells, CXCR6 is only expressed on 20% of all Th1 T cells (Kim et al., 2001).

In addition to the expression of the T_{reg} activation marker KLRG1, other T_{reg} activation markers such as ICOS and TIGIT were analysed (Joller et al., 2014; Kornete et al., 2012). The data indicated that effector T_{reg} cells that expressed KLRG1 also expressed other T_{reg} activation markers like ICOS and TIGIT, or at least one of these markers, further confirming the activation status of KLRG1$^+$ effector T_{reg} cells (Fig 3.2.2 B).

Firstly, total cell counts from wt and KO animals were calculated. Absolute (abs.) cell counts from PP, mLN, spleen and liver did not differ between wt, CCL17$^{E/E}$, and CCL17/CCL22 double-deficient mice after vaccination and 5 days of challenge (Fig 3.2.3); all were within a 10-fold range and the variation within groups was large.

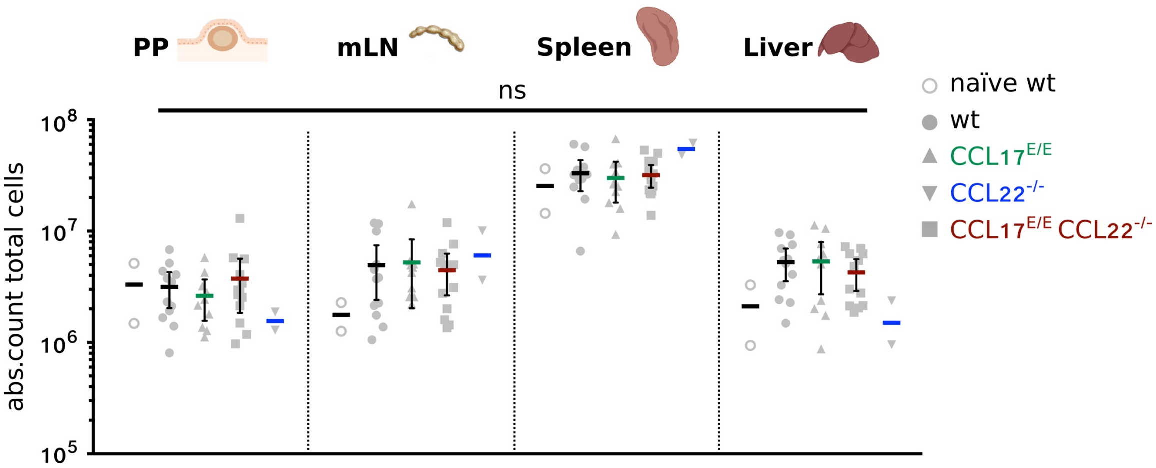

Figure 3.2.3: FACS analysis of TAS2010 vaccinated and challenged wt and KO mice – absolute cell counts of total cells
Absolute cell counts (Fig 3.2.2 A1) were calculated using counting beads. Wt, CCL17$^{E/E}$, CCL22$^{-/-}$ and CCL17/CCL22 double-deficient mice were orally vaccinated with 1x10^9 CFU TAS2010. 12 to 15 weeks post-vaccination mice were orally challenged with 5x10^7 CFU STM SL1344. Cell counts were evaluated for PP, mLN, spleen and liver. Two naïve wt mice were used as controls. Symbols represent individual mice (n= 10-13; pooled from three independent experiments; for CCL22$^{-/-}$ n=2; one experiment). Statistical significance was tested using two-way ANOVA with Tukey´s test for multiple comparison. Naïve mice and vaccinated CCL22$^{-/-}$ mice were not included in the statistical analysis. Error bars indicate mean with 95% CI.

Subsequently, KLRG1$^+$ effector T$_{reg}$ cells were evaluated for their expression of CXCR3 and subdivided into CXCR3$^+$ and CXCR3$^-$ cells. CXCR3 typically is a Th1 marker (Groom and Luste, 2011; Kim et al., 2001), but can also be associated with T$_{reg}$ cells that regulate Th1 response, since CXCR3$^+$ T$_{reg}$ cells and Th1 T cells co-localise to the same tissue (Koch et al., 2009). CXCR3 has also been associated with lymphocyte homing to the gut (Yuan et al., 2014). Therefore, CXCR3$^+$ KLRG1$^+$ effector T$_{reg}$ cells might be cells that recently migrated to the gut-associated lymphoid tissue (GALT), whereas CXCR3$^-$ KLRG1$^+$ effector T$_{reg}$ cells might represent cells that already resided within the gut tissue for some time. In vaccinated and challenged mice KLRG1$^+$ effector T$_{reg}$ cells were mainly CXCR3$^-$ (Fig 3.2.2 A 8a). Both subpopulations (CXCR3$^+$ and CXCR3$^-$) of KLRG1$^+$ effector T$_{reg}$ cells in vaccinated and challenged mice were analysed, but only the CXCR3$^-$ subpopulation exhibited significant differences between chemokine KO mice and wt controls (Fig 3.2.4).

Generally, the frequency of CXCR3$^-$ KLRG1$^+$ effector T$_{reg}$ cells (left panel) from CCL17/CCL22 double-deficient mice was significantly reduced compared to wt controls in PP, mLN and spleen. A similar trend was observed in CXCR3$^+$ cells (right panel) (Fig 3.2.4). In PP, the frequency of CXCR3$^-$ KLRG1$^+$ effector T$_{reg}$ cells from CCL17/CCL22 double-deficient mice was not only significantly reduced compared to wt animals, but also when compared to CCL17$^{E/E}$ mice (Fig 3.2.4 A). In the spleen, the percentage of CXCR3$^-$ KLRG1$^+$ effector T$_{reg}$ cells from CCL17$^{E/E}$ mice exhibited a significant decrease compared to wt controls, and was similar to CCL17/CCL22 double-deficient mice (Fig 3.2.4 C). This trend was also seen in mLN but variability in the observations meant that the differences were not statistically significant (Fig 3.2.4 B). In the liver, the respective T cell populations did not differ in frequency in any of the groups (Fig 3.2.4 D).

These data suggest that both chemokines contribute to the regulation of KLRG1$^+$ effector T$_{reg}$ cells after vaccination and challenge. Mice deficient only in CCL22 could not be properly investigated due to breeding problems. Only one experiment was performed with these mice, and further studies are hence required.

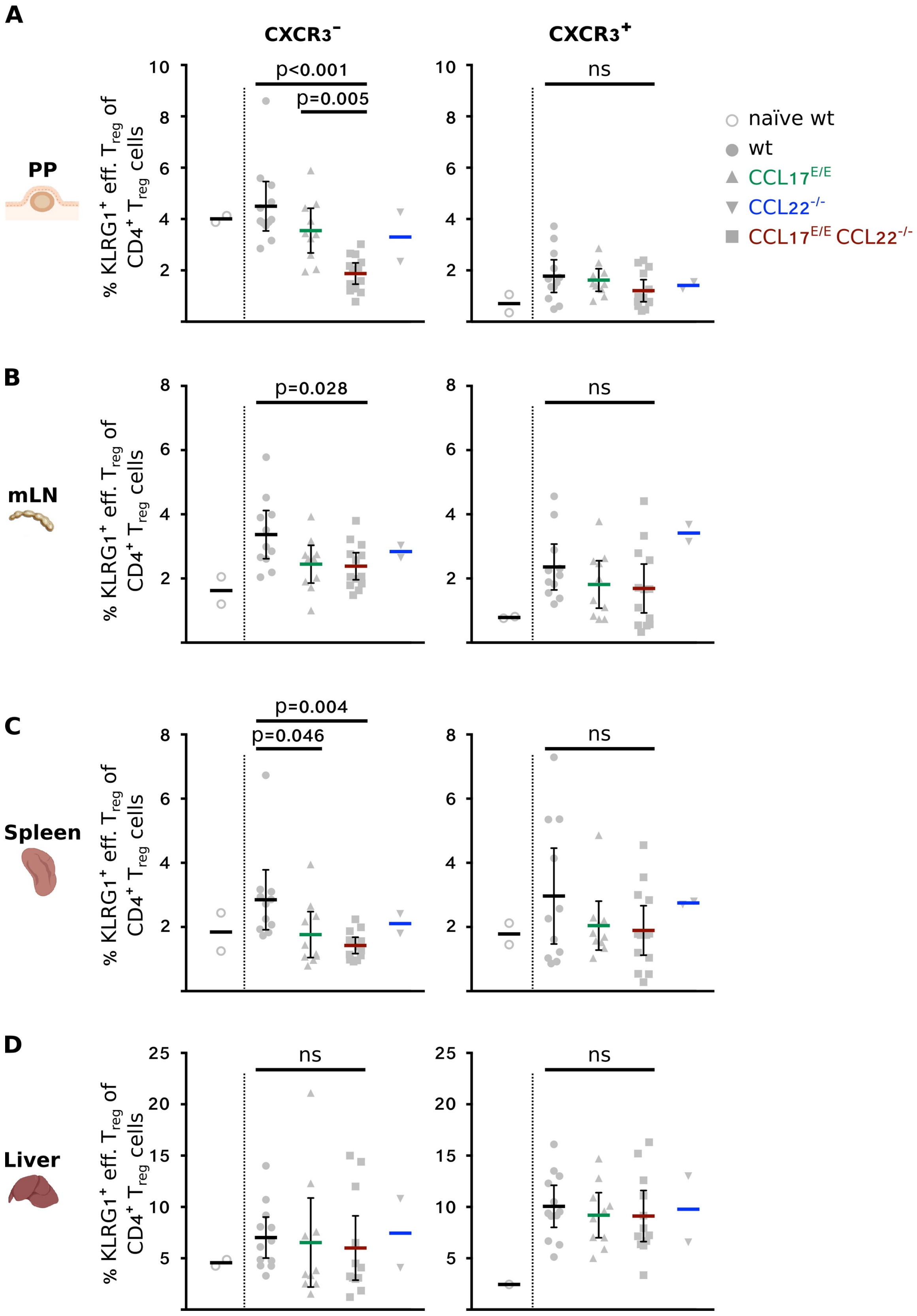
A
B
C
D
CXCR3⁻
CXCR3⁺
PP
mLN
Spleen
Liver
% KLRG1⁺ eff. Treg of CD4⁺ Treg cells
p<0.001
p=0.005
p=0.028
p=0.004
p=0.046
ns
10
8
6
4
2
25
20
15
5
○ naïve wt
● wt
▲ CCL17E/E
▼ CCL22-/-
■ CCL17E/E CCL22-/-

Figure 3.2.4: CD4$^+$ T cell FACS analysis of TAS2010 vaccinated and challenged wt and KO mice – analysis of regulatory T cells
Wt, CCL17$^{E/E}$, CCL22$^{-/-}$ and CCL17/CCL22 double-deficient mice were orally vaccinated with 1x10^9 CFU TAS2010. 12 to 15 weeks post-vaccination mice were challenged with 5x10^7 CFU STM SL1344. The frequency of CXCR3$^-$ or CXCR3$^+$ KLRG1$^+$ eff. T$_{reg}$ from CD4$^+$ T$_{reg}$ cells were analysed 5 days post-secondary challenge, in the PP (A), mLN (B), spleen (C) and liver (D). Two naïve wt mice were used as controls. Symbols represent individual mice (n= 10-13; pooled from three independent experiments; for CCL22$^{-/-}$ n=2; one experiment). Statistical significance was tested using one-way ANOVA with Tukey´s test for multiple comparison Naïve mice and vaccinated CCL22$^{-/-}$ mice were not included in the statistical analysis. Error bars indicate mean with 95% CI.

Since KLRG1$^+$ effector T$_{reg}$ cells were most strongly affected in CCL17/CCL22 double-deficient mice after secondary challenge, experiments were conducted to investigate whether Th1 effector T cells might be suppressed by these effector regulatory T cells. CXCR3$^+$ activated T$_{conv}$ cells were evaluated in vaccinated and challenged animals and CXCR3 was used as a Th1 marker (Fig 3.2.5 A). The frequency of CXCR3$^+$ activated T$_{conv}$ cells from CCL17/CCL22 double-deficient mice appeared to be increased compared to wt controls and CCL17$^{E/E}$ mice in PP, mLN and liver, but the differences were not statistically significant (Fig 3.2.5 A). In the spleen, no differences in CXCR3$^+$ activated T$_{conv}$ cell frequency was observed between the different mouse strains that were vaccinated/challenged and examined (Fig 3.2.5 A).

To correlate the absolute cell counts of CXCR3$^-$ KLRG1$^+$ effector T$_{reg}$ cells to the absolute cell counts of CXCR3$^+$ activated T$_{conv}$ cells, the ratio of CXCR3$^-$ KLRG1$^+$ effector T$_{reg}$ cells to CXCR3$^+$ activated T$_{conv}$ cells was calculated (Fig 3.2.5 B). This ratio was significantly reduced in PP from CCL17/CCL22 double-deficient mice compared to wt control and CCL17$^{E/E}$ mice. Wt mice had a ratio of approximately 5 CXCR3$^-$ KLRG1$^+$ effector T$_{reg}$ cells to 100 CXCR3$^+$ activated T$_{conv}$ cells (5/100), CCL17$^{E/E}$ mice had a ratio of about 3/100 and CCL17/CCL22 double-deficient mice had a ratio of 1/100 (Fig 3.2.5 B). In mLN, the ratio was not only significantly decreased in CCL17/CCL22 double-deficient mice, but also in CCL17$^{E/E}$ mice, compared to wt mice. Wt mice had a ratio of about 17 CXCR3$^-$ KLRG1$^+$ effector T$_{reg}$ cells to 100 CXCR3$^+$ activated T$_{conv}$ cells (17/100), CCL17$^{E/E}$ mice had a ratio of about 9/100 and CCL17/CCL22 double-deficient mice had a ratio of 10/100 (Fig 3.2.5 B). Results obtained for spleen and liver showed a similar trend as in PP and mLN, but the ratio in CCL17/CCL22 double-deficient mice was not significantly reduced compared to wt control animals due to higher variation in individual mice (Fig 3.2.5 B).

A small number of CCL22$^{-/-}$ mice were analysed and demonstrated a similar ratio as wt or CCL17$^{E/E}$ mice. Since only one experiment with two mice was performed, no conclusion can be made.

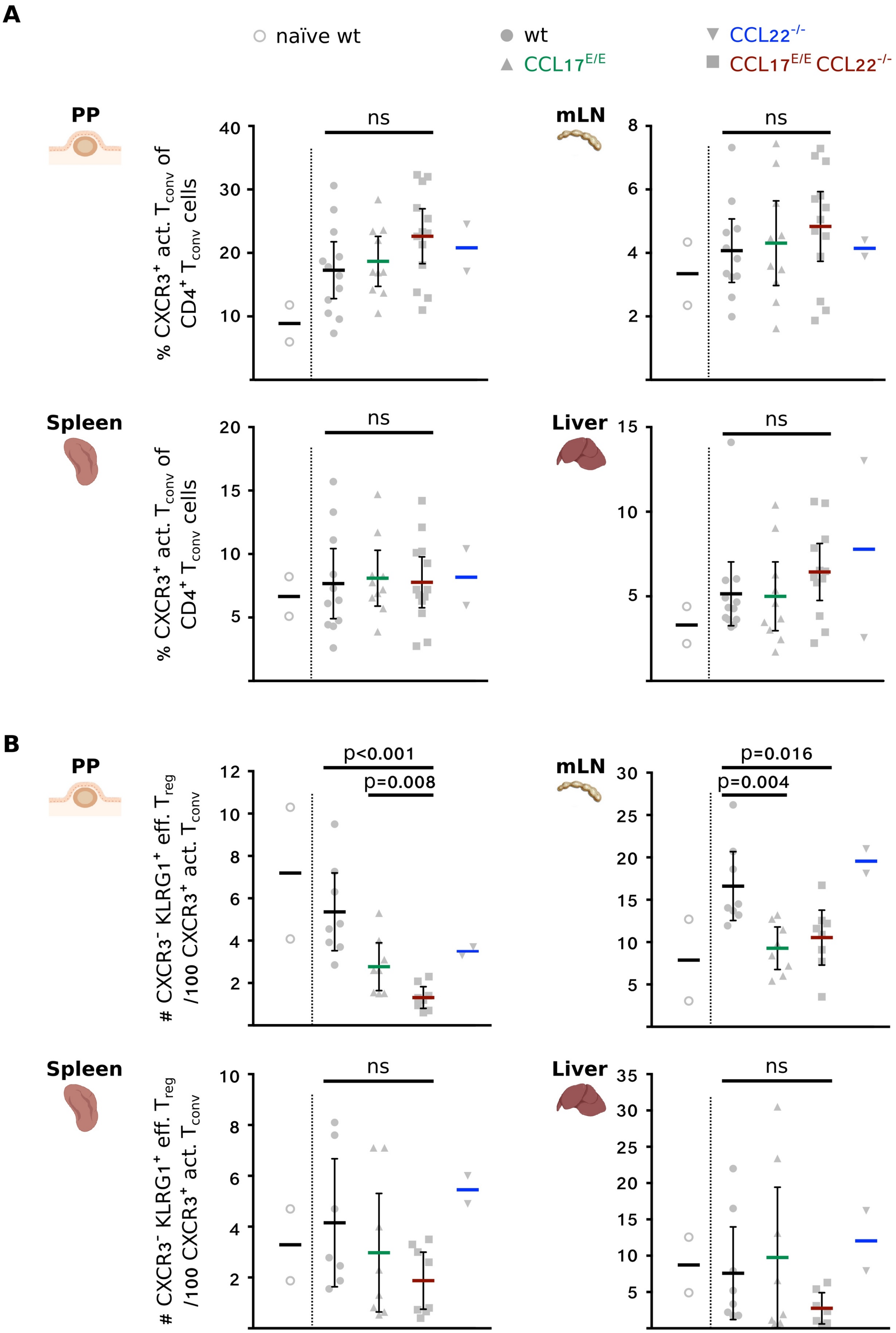
A
○ naïve wt
● wt
▲ CCL17^E/E
▼ CCL22^-/-
■ CCL17^E/E CCL22^-/-
PP
% CXCR3+ act. Tconv of CD4+ Tconv cells
40
30
20
10
ns
mLN
8
6
4
2
ns
Spleen
% CXCR3+ act. Tconv of CD4+ Tconv cells
20
15
10
5
ns
Liver
15
10
5
ns
B
PP
CXCR3- KLRG1+ eff. Treg /100 CXCR3+ act. Tconv
12
10
8
6
4
2
p<0.001
p=0.008
mLN
30
25
20
15
10
5
p=0.016
p=0.004
Spleen
CXCR3- KLRG1+ eff. Treg /100 CXCR3+ act. Tconv
10
8
6
4
2
ns
Liver
35
30
25
20
15
10
5
ns

Figure 3.2.5: CD4$^+$ T cell FACS analysis of TAS2010 vaccinated and challenged wt and KO mice – analysis of conventional T cells
Wt, CCL17$^{E/E}$, CCL22$^{-/-}$ and CCL17/CCL22 double-deficient mice were orally vaccinated with 1x10^9 CFU TAS2010. 12 to 15 weeks post-vaccination mice were challenged with 5x10^7 CFU STM SL1344. The percentage of CXCR3$^+$ eff. T$_{conv}$ of CD4$^+$ T$_{conv}$ cells was analysed 5 days post wt STM challenge in PP, mLN, spleen and liver (A). The ratio from absolute counts of KLRG1$^+$ CXCR3$^-$ eff. T$_{reg}$ cells to absolute counts of CXCR3$^+$ act. T$_{conv}$ cells was calculated for PP, mLN, spleen and liver (B). Two naïve wt mice were used as controls. Symbols represent individual mice (n= 10-13; pooled from three independent experiments; for CCL22$^{-/-}$ n=2; one experiment). Statistical significance was tested using one-way ANOVA with Tukey´s test for multiple comparison. Naïve mice and vaccinated CCL22$^{-/-}$ mice were not included in the statistical analysis. Error bars indicate mean with 95% CI.

Overall, the results from TAS2010 vaccinated and then challenged mice showed that KLRG1$^+$ effector T$_{reg}$ cells were decreased in mice deficient for both chemokines, CCL17 and CCL22, after-challenge with STM SL1344 (Fig 3.2.4). In contrast, CXCR3$^+$ activated T$_{conv}$ cells were slightly increased in CCL17/CCL22 double-deficient mice after challenge (Fig 3.2.5 A). Correlating, the ratio of CXCR3$^-$ KLRG1$^+$ effector T$_{reg}$ cells to CXCR3$^+$ activated T$_{conv}$ cells, revealed that less effector T$_{reg}$ cells were detected per 100 T$_{conv}$ cells in CCL17/CCL22 double-deficient mice compared to wt controls. This skewing of the T$_{reg}$/T$_{conv}$ ratio may have promoted a more potent Th1 T cell immune response (Fig 3.2.5 B) that resulted in better survival of mice deficient in both chemokines.

3.2.2 Deficiency in CCL17/CCL22 supports the development of a strong antigen-specific $CD4^+$ T cell immune response

Studies in the vaccination/challenge model suggested that deficiency in CCL22, or deficiency of both CCL17 and CCL22 resulted in better vaccine efficacy after secondary challenge. Consistent with this observation, there was an apparent increased Th1 cell immune response in animals deficient in CCL17 and CCL22, characterised by a lower number of $KLRG1^+$ effector T_{reg} cells per $CXCR3^+$ activated T_{conv} cells. The potentially enhanced immune environment, which limited STM pathogenesis, most likely led to the enhanced vaccine efficacy.

It was not clear whether the positive differences in CCL17/CCL22 double-deficient mice were established after vaccination or after challenge. In the next series of experiments, the vaccination phase was studied in more detail.

3.2.2.1 Neither CCL17 nor CCL22 interfere with health status or bacterial burden in TAS2010 vaccinated mice

Mice were orally vaccinated with $1x10^9$ CFU TAS2010 and monitored three times per week for health status and weight over 12 weeks. All strains analysed, comprising $CCL17^{E/E}$, $CCL22^{-/-}$, CCL17/CCL22 double-deficient and wt mice, showed similar weight changes over time. Vaccinated mice lost approximately 5% of their body weight within the first week of infection, reaching a plateau phase until week two, where after they gained weight over time (Fig 3.2.6). In addition to the body weight, the body condition, appearance and behaviour of vaccinated mice was assessed. Regarding the later parameters, the different strains of vaccinated mice did not show any abnormalities or differences (data not shown).

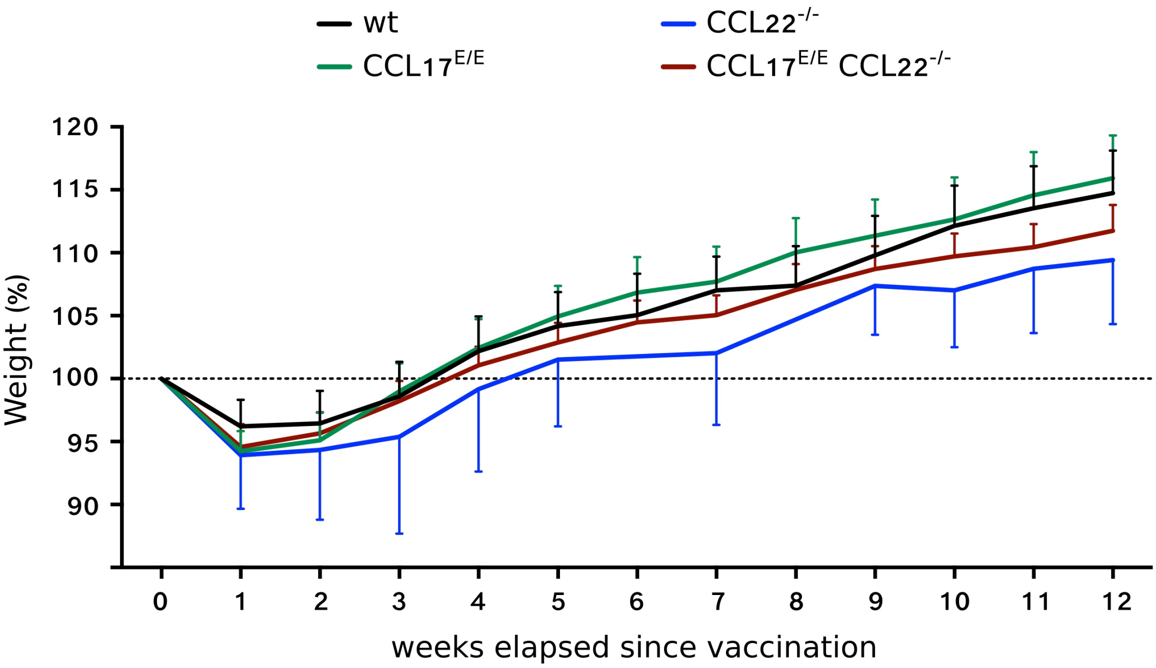

Figure 3.2.6: Weight curve of TAS2010 vaccinated wt and KO mice
Wt, CCL17$^{E/E}$, CCL22$^{-/-}$ and CCL17/CCL22 double-deficient mice were orally vaccinated with 1x10^{9} CFU TAS2010. Mice were monitored 3 times a week for their health status (body condition, appearance, behaviour and weight) according to animal ethics. Recorded weights were normalised to day 0 (pre-vaccination). The geometric mean with 95% CI is depicted (n=42-48 for CCL17$^{E/E}$, CCL17/CCL22 double-deficient and wt mice pooled from 5 independent experiments; n= 8 for CCL22$^{-/-}$ mice pooled from two independent experiments).

Besides weight, also the bacterial burden in TAS2010 vaccinated CCL17$^{E/E}$, CCL22$^{-/-}$, CCL17/CCL22 double-deficient and wt mice was assessed during the vaccination period. TAS2010 is an attenuated STM strain that persists for 8-10 weeks in wt C57BL/6 mice. The bacterial burden in PP, mLN, spleen and liver from CCL17$^{E/E}$ and wt control mice was determined at day one and at 1, 2, 5 and 9 weeks post-vaccination (Fig 3.2.7 A). CCL22$^{-/-}$ and CCL17/CCL22 double-deficient mice were only analysed at week 5 and 9 post-vaccination (Fig 3.2.7 B). Similar to weight change after vaccination, CFU counts did not differ significantly between the different mouse strains. Bacteria were detected on day one post-vaccination, with PP having the highest counts, consistent with oral vaccine administration. One week post-vaccination, CFU counts peaked in all organs analysed, except for the liver, where the peak was reached at week 1. At week 1 and week 2, CFU counts were similar. From week 2 onwards, the bacterial burden in all organs investigated declined continuously, resulting in clearance below the detection level in PP and liver, and almost complete clearance from the spleen and mLN by week 9 post-vaccination (Fig 3.2.7 B).

Taken together, the kinetics of bacterial growth and clearance were similar between all three chemokine KO mouse lines and wt controls, as was the health status of the mice. The peak of bacterial counts (Fig 3.2.7 B) correlated with weight loss (Fig 3.2.6), suggesting that the deficiency for either or both chemokines did not lead to gross abnormalities in host immune control of the attenuated *Salmonella* vaccine strain during the vaccination phase. In short, the increased protection seen in the CCL17/CCL22 double-deficient mice after vaccination and challenge did not appear to result from increased growth of the vaccine, and hence antigen availability, during the vaccination period.

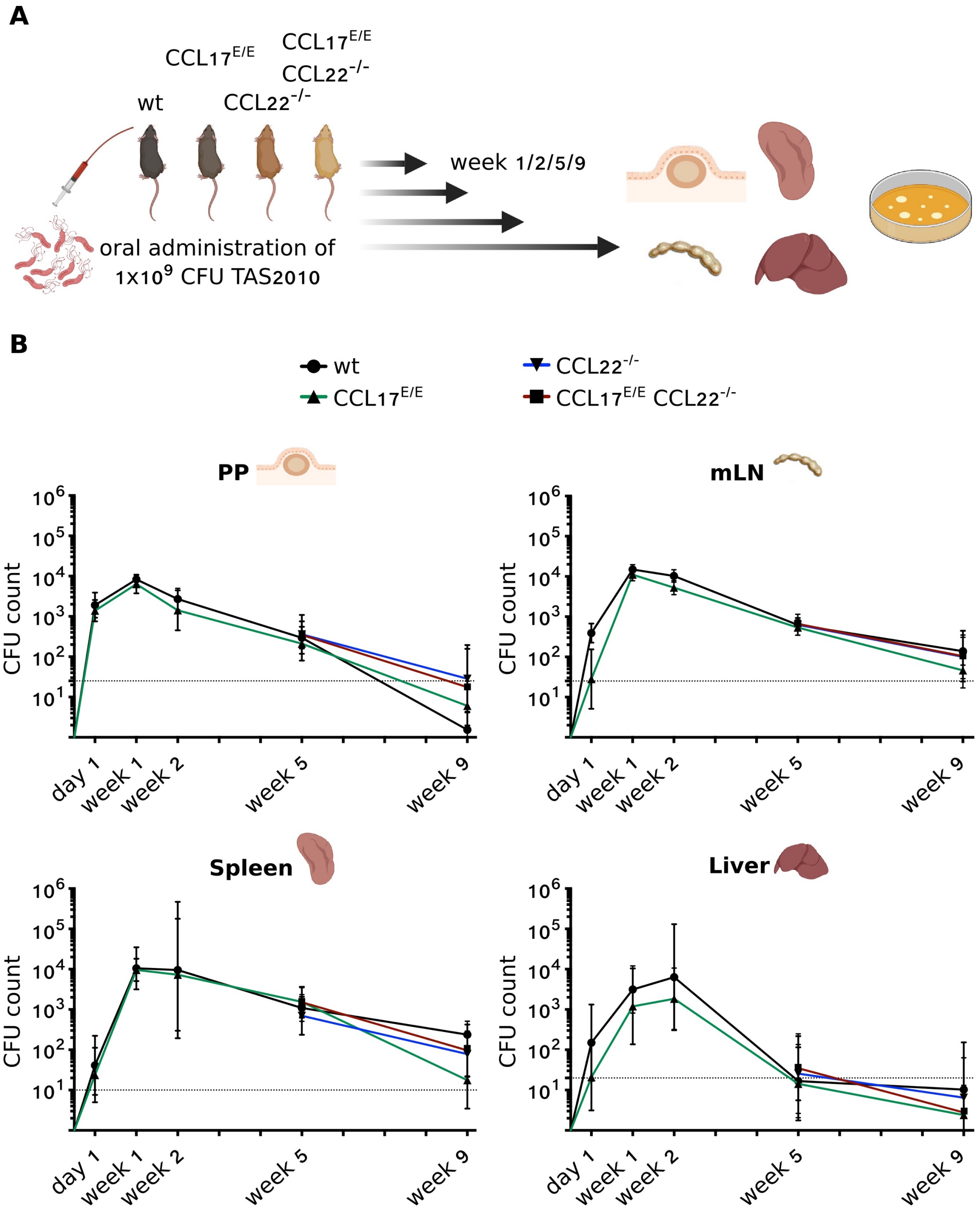

Figure 3.2.7: Bacterial counts of TAS2010 vaccinated wt and KO mice
Wt, CCL17$^{E/E}$, CCL22$^{-/-}$ and CCL17/CCL22 double-deficient mice were orally vaccinated with 1x10^{9} CFU TAS2010. PP, mLN, spleen and liver were collected one day and 1/2/5/9 weeks post-vaccination and bacterial burden was evaluated. Organs were homogenised, plated one LB agar plates with streptomycin, incubated overnight and colonies counted (A). CFU counts were calculated for each organ (B). Dotted lines indicate the cut-off for CFU detection limits. Error bars indicate mean with 95% CI (n=4-10; pooled from seven independent experiments).

3.2.2.2 CCL17/CCL22 double-deficient mice exhibit a superior antigen-specific CD4$^+$ T cell immune response after TAS2010 vaccination

In order to study the functions of CCL17 and CCL22 in the development of CD4$^+$ T cell immunity after vaccination all three chemokine KO mouse strains and wt control animals were analysed 5- and 9 weeks post-vaccination with TAS2010. The T_{reg} and T_{conv} cell compartments were investigated in PP, mLN, spleen and liver (Fig 3.2.8 A). A week 5 time point was selected because (unpublished laboratory) data suggested the peak of STM-antigen-specific CD4$^+$ T cell immune response at this time. Week 9 was chosen as this time point correlates with TAS2010 clearance in wt control animals (Timothy Scott, PhD, University of Melbourne). A similar flow cytometric strategy as in the analysis of CD4$^+$ T cell populations in vaccinated/challenged animals was used (Fig 3.2.8 B). Only viable CD3$^+$ cells were analysed, and autofluorescent (AF)$^+$ as well as doublet cells were excluded. The analysis of the T cell population focused on CD4$^+$ FOXP3$^+$ T_{reg} and the CD4$^+$ FOXP3$^-$ T_{conv} compartments. CD44$^+$ CD62L$^-$ effector T_{reg} cells were selected and KLRG1$^+$ effector T_{reg} were analysed in more detail. In the T_{conv} compartment, CD44$^+$ CD62L$^-$ activated T_{conv} cells were selected, and CXCR3$^+$ (CXCR6$^-$) activated T_{conv} cells were evaluated. In addition to the expression of the T_{reg} activation marker KLRG1, the T_{reg} activation marker, ICOS (Kornete et al., 2012), was analysed for expression on effector T_{reg} cells. Data indicated that effector T_{reg} cells that expressed KLRG1 also expressed ICOS, further confirming the activation status of KLRG1$^+$ effector T_{reg} cells (Fig 3.2.8 C).

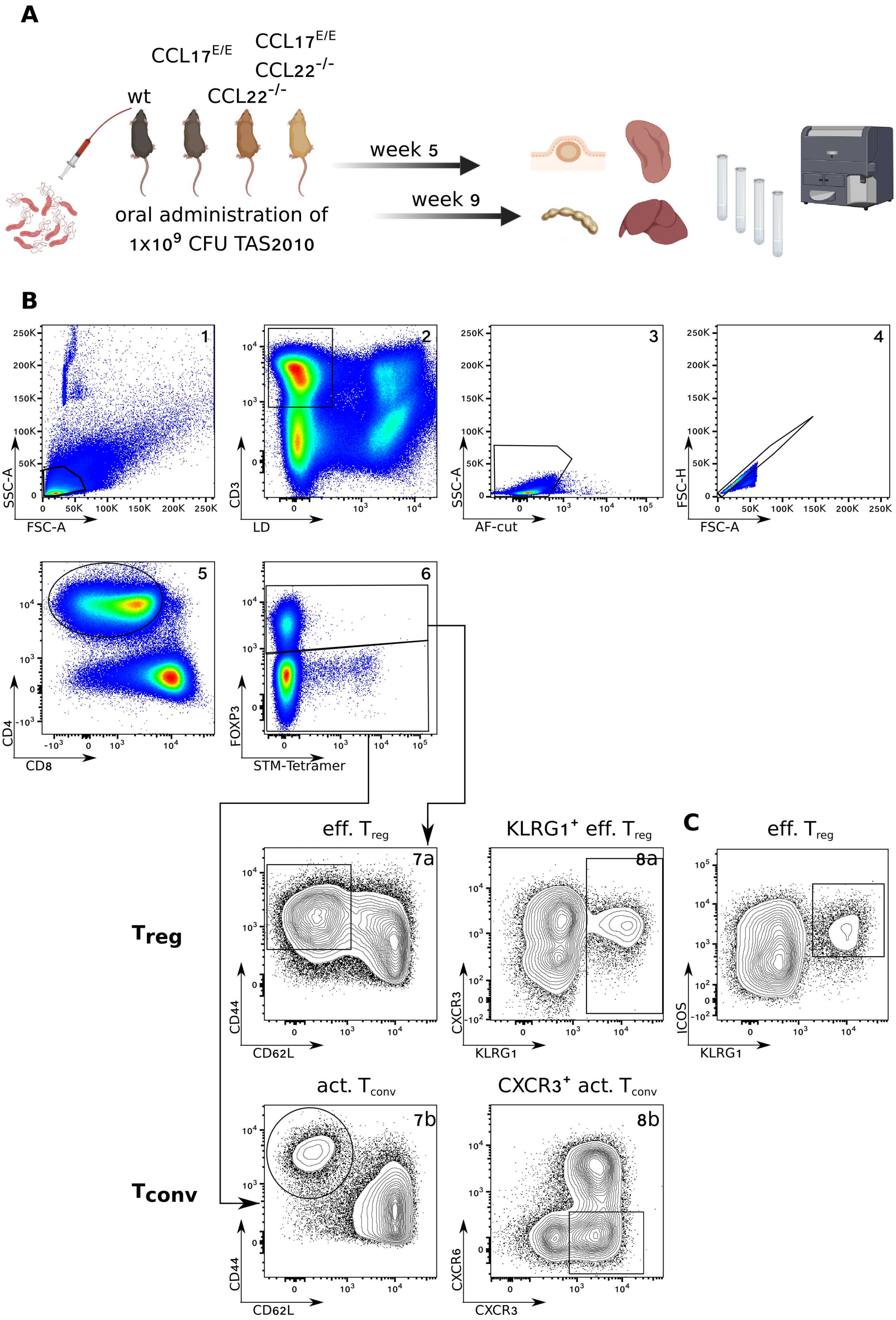
A
wt
CCL17E/E
CCL22-/-
CCL17E/E
CCL22-/-
oral administration of
1x10⁹ CFU TAS2010
week 5
week 9
B
1
SSC-A
FSC-A
2
CD3
LD
3
SSC-A
AF-cut
4
FSC-H
FSC-A
5
CD4
CD8
6
FOXP3
STM-Tetramer
Treg
Tconv
eff. Treg
7a
CD44
CD62L
KLRG1+ eff. Treg
8a
CXCR3
KLRG1
act. Tconv
7b
CD44
CD62L
CXCR3+ act. Tconv
8b
CXCR6
CXCR3
C
eff. Treg
ICOS
KLRG1

Figure 3.2.8: CD4$^+$ T cell FACS analysis of TAS2010 vaccinate wt and KO mice – experimental setup and gating strategy
Wt, CCL17$^{E/E}$, CCL22$^{-/-}$, and CCL17/CCL22 double-deficient mice were orally vaccinated with 1x10^9 CFU TAS2010. PP, mLN, spleen and liver were isolated from wt and KO mice 5- and 9 weeks post-vaccination and the T_{reg} and T_{conv} cell compartment was analysed via flow cytometry (A). Fixed cells were selected based on their FSC and SSC properties (B1). Live T cells were identified as CD3$^+$ LD$^-$ cells (B2). Subsequently, autofluorescent (AF) cells were excluded using an empty fluorescent channel (B3). Single cells were identified (B4). CD4$^+$ T cells were selected (B5) and separated into FOXP3$^+$ and FOXP3$^-$ cells (B6). FOXP3$^+$ cells were identified as T_{reg} cells and FOXP3$^-$ as T_{conv} cells. T_{reg} cells were further analysed for CD44 and CD62L expression. CD44$^+$ CD62L$^-$ cells were selected and identified as effector T_{reg} cells (B7a). CD44$^+$ CD62L$^-$ eff. T_{reg} cells were then assessed for their KLRG1 expression. KLRG1$^+$ cells were identified as KLRG1$^+$ eff. T_{reg} cells (B8a). T_{conv} cells were further analysed for CD44 and CD62L expression. CD44$^+$ CD62L$^-$ cells were selected and identified as activated T_{conv} cells (B7b). Following CD44$^+$ CD62L$^-$ act. T_{conv} cells were evaluated for their CXCR3 and CXCR6 expression. CXCR3$^+$ CXCR6$^-$ cells were identified as CXCR3$^+$ act. T_{conv} cells (B8b). Next to KLRG1 expression also ICOS expression was investigated in eff. T_{reg} cells (C). Representative gating of mLN wt mouse at week 5 post-vaccination is depicted.

Absolute counts of total cells from PP, mLN, spleen and liver did not differ between all mouse strains analysed 5- and 9 weeks post-vaccination (Fig 3.2.9 A and B). In spleen, 9 weeks after vaccination, however, all three chemokine KO mice showed an approximately 50% reduction in cell numbers compared to wt control animals, although cell numbers between the three KO mice were similar (Fig 3.2.9 B).

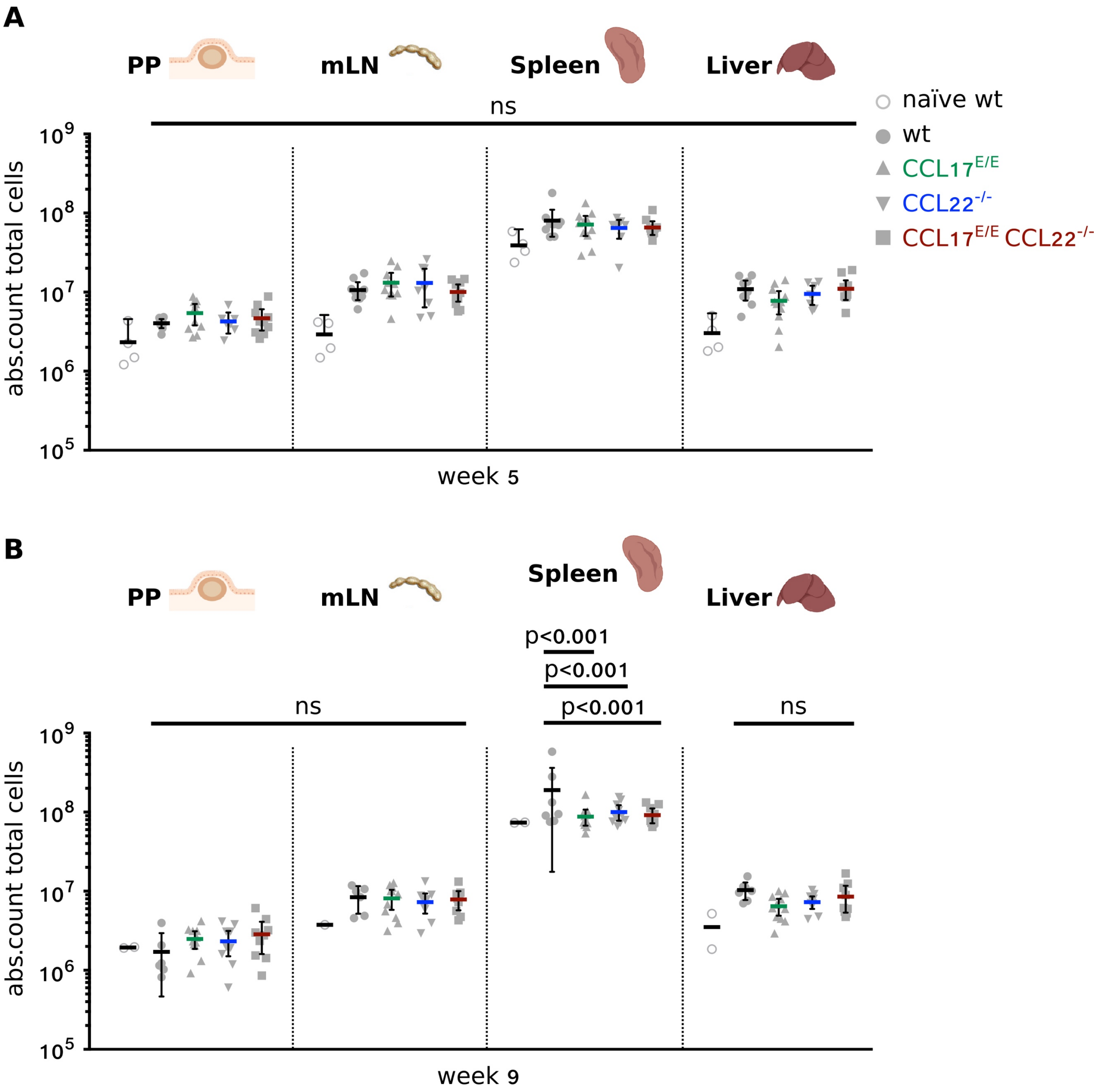

Figure 3.2.9: FACS analysis of TAS2010 vaccinated wt and KO mice – absolute cell counts of total cells

Absolute cell counts (Fig 3.2.7 B1) were calculated using counting beads. Cell counts were evaluated for PP, mLN, spleen and liver of wt, CCL17$^{E/E}$, CCL22$^{-/-}$ and CCL17/CCL22 double-deficient mice 5 weeks (A) and 9 weeks (B) post-vaccination. Two till four naïve wt mice were used as controls. Symbols represent individual mice (n= 6-11; pooled from two independent experiments). Statistical significance was tested using two-way ANOVA with Tukey´s test for multiple comparison. Naïve mice were not included in the statistical analysis. Error bars indicate mean with 95% CI.

Cell frequencies were evaluated to complement cell numbers. Comparison of the 4 mouse strains analysed demonstrated that the frequency of KLRG1$^+$ effector T$_{reg}$ cells was higher in vaccinated mice, compared to naïve wt mice. The percentage of KLRG1$^+$ effector T$_{reg}$ cells was highest at week 5 and then decreased by week 9 post-vaccination (Fig 3.2.10). Examination of the individual mouse strains revealed that the frequency of KLRG1$^+$ effector T$_{reg}$ cells in PP from CCL17/CCL22 double-deficient animals was significantly reduced by approximately 30% compared to wt controls as well as to CCL17$^{E/E}$ mice at week 5 and week 9 post-vaccination. Furthermore, the percentage of KLRG1$^+$ effector T$_{reg}$ cells in CCL22$^{-/-}$ mice was significantly decreased compared to wt animals but not to CCL17/CCL22 double-deficient or CCL17$^{E/E}$ animals, 5 weeks post-vaccination. This effect was still seen 9 weeks after vaccination, albeit the differences were reduced (Fig 3.2.10 A).

The frequency of KLRG1$^+$ effector T$_{reg}$ cells in the spleen of CCL17/CCL22 double-deficient mice was significantly reduced by approximately 25% compared to wt controls as well as to CCL17$^{E/E}$ mice at week 5 post-vaccination. CCL22$^{-/-}$ mice showed no significant differences in the percentage of KLRG1$^+$ effector T$_{reg}$ cells compared to the other mouse strains analysed. Nevertheless, the proportion of KLRG1$^+$ effector T$_{reg}$ cells in CCL22$^{-/-}$ mice was similar to the frequency observed in CCL17/CCL22 double-deficient mice (Fig 3.2.10 C). At week 9, an even stronger decline of KLRG1$^+$ effector T$_{reg}$ cell frequency of almost 50% was observed only in CCL17/CCL22 double-deficient compared to wt control mice. Mice deficient in only one of the two chemokines showed frequencies of KLRG1$^+$ effector T$_{reg}$ cells in between those of wt control mice and CCL17/CCL22 double-deficient animals (Fig 3.2.10 C).

In accordance with the observations made in the PP and spleen, the percentage of KLRG1$^+$ effector T$_{reg}$ cells in the liver of CCL17/CCL22 double-deficient mice was significantly reduced by 30% compared to wt controls but not to CCL17$^{E/E}$ and CCL22$^{-/-}$ mice, at week 5 post-vaccination. In contrast, no changes in this T cell population were observed between the chemokine KO mouse strains and wt control animals, at 9 weeks post-vaccination in the liver (Fig 3.2.10 D).

In mLN, analysis of KLRG1$^+$ effector T$_{reg}$ cell frequency revealed no differences between the KO mouse strains and wt control mice. In contrast to the other organs investigated, there was no decrease in the frequency of KLRG1$^+$ effector T$_{reg}$ cells between week 5 to week 9 (Fig 3.2.10 B).

These data suggest that KLRG1$^+$ effector T$_{reg}$ cells are regulated predominantly by CCL22 during vaccination, especially in the PP, in addition to systemic organs. Deficiency in CCL17 alone did not demonstrate a significant impact on the presence of KLRG1$^+$ effector T$_{reg}$ cells. In contrast, deficiency in CCL22 alone resulted in a reduction of KLRG1$^+$ effector T$_{reg}$ cell frequencies compared to wt control animals, but this reduction was only significant in mice that lacked both chemokines, suggesting also a minor role for CCL17 in the regulation of KLRG1$^+$ effector T$_{reg}$ cells during vaccination.

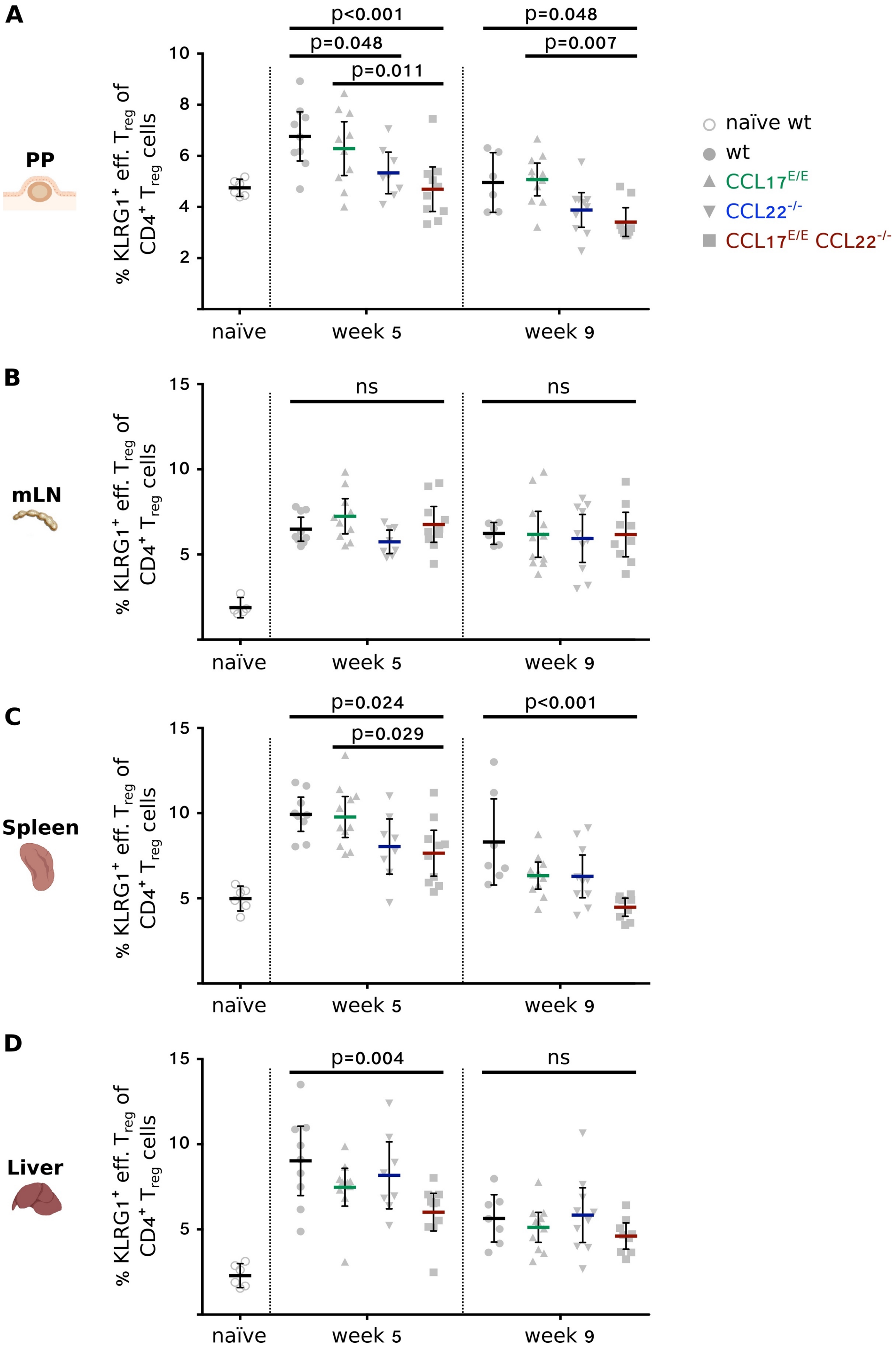
A
PP
B
mLN
C
Spleen
D
Liver
% KLRG1+ eff. Treg of CD4+ Treg cells
naïve
week 5
week 9
p<0.001
p=0.048
p=0.011
p=0.007
p=0.024
p=0.029
p=0.004
ns
○ naïve wt
● wt
▲ CCL17E/E
▼ CCL22-/-
■ CCL17E/E CCL22-/-

Figure 3.2.10: CD4$^+$ T cell FACS analysis of TAS2010 vaccinated wt and KO mice – evaluation of regulatory T cells
Wt, CCL17$^{E/E}$, CCL22$^{-/-}$ and CCL17/CCL22 double-deficient mice were orally vaccinated with 1x10^9 CFU TAS2010. The KLRG1$^+$ eff. T$_{reg}$ frequency of CD4$^+$ T$_{reg}$ cells was analysed 5- and 9 weeks post-vaccination in PP (A), mLN (B), spleen (C) and liver (D). Naïve wt mice were used as controls. Symbols represent individual mice (n= 6-11; pooled from two independent experiments). Statistical significance was tested using two-way ANOVA with Tukey´s test for multiple comparison. Naïve mice were not included in the statistical analysis. Error bars indicate mean with 95% CI.

The CXCR3$^+$ activated T$_{conv}$ cells were investigated in addition to KLRG1$^+$ effector T$_{reg}$ cells. Overall, the percentage of CXCR3$^+$ activated T$_{conv}$ cells did not vary much from week 5 and 9 post-vaccination in the different mouse strains, with the marked exception of cells from CCL17/CCL22 double-deficient animals, in the spleen and liver (Fig 3.2.11).

Analysis of the individual mouse strains showed that the proportion of CXCR3$^+$ activated T$_{conv}$ cells in PP from CCL17/CCL22 double-deficient mice was significantly increased compared to CCL17$^{E/E}$ mice at week 5 post-vaccination. In CCL22$^{-/-}$ mice, the frequency of CXCR3$^+$ activated T$_{conv}$ cells was not significantly different compared to the other mouse strains analysed, but the percentage of cells measured sat between those of CCL17$^{E/E}$ and CCL17/CCL22 double-deficient mice (Fig 3.2.11 A). Nine weeks post-vaccination, similar results to those observed at 5 weeks post-vaccination were obtained, but the increase of CXCR3$^+$ activated T$_{conv}$ cell frequencies from CCL17/CCL22 double-deficient mice was not statistically significant (Fig 3.2.11 A).

In the spleen, the percentage of CXCR3$^+$ activated T$_{conv}$ cells from CCL17/CCL22 double-deficient mice was significantly increased compared to CCL17$^{E/E}$ mice, 5 weeks post-vaccination. In CCL22-deficient mice, the frequency of CXCR3$^+$ activated T$_{conv}$ cells increased 5 weeks post-vaccination, but this difference was not statistically significant. Most notably, the frequency of CXCR3$^+$ activated T$_{conv}$ cells in CCL17/CCL22 double-deficient mice increased further from 5 to 9 weeks and was significantly augmented at week 9 to 12%, compared to 6% in wt control animals, 7% in CCL17$^{E/E}$, and 8% in CCL22$^{-/-}$ animals (Fig 3.2.11 C).

The percentage of CXCR3$^+$ activated T$_{conv}$ cells in the livers of CCL22$^{-/-}$ animals was significantly expanded compared to wt control animals at week 5 post-vaccination. In CCL17/CCL22 double-deficient mice, the frequency of CXCR3$^+$ activated T$_{conv}$ cells was also slightly increased, albeit not significantly, compared to wt control mice (p=0.066) (Fig 3.2.11 D). Similar to observations in the spleen, the population of CXCR3$^+$ activated T$_{conv}$ cells in CCL17/CCL22 double-deficient mice increased strongly over time. The frequency of CXCR3$^+$ activated T$_{conv}$ cells in CCL17/CCL22 double-deficient mice showed the greatest level of expansion 9 weeks post-vaccination with up to 3-fold (200%) increase compared to wt controls and by approximately 50%, compared to CCL17$^{E/E}$ and CCL22$^{-/-}$. In CCL17$^{E/E}$ and CCL22$^{-/-}$ animals, an increase of CXCR3$^+$ activated T$_{conv}$ cell frequencies by roughly 2-fold (100%) compared to wt control animals was detected (Fig 3.2.11 D).

These results suggest an additive effect of CCL17 and CCL22 deficiencies on CXCR3$^+$ activated T$_{conv}$ cells during vaccination, most likely mediated by the reduction of KLRG1$^+$ effector T$_{reg}$ cells (Fig 3.2.10). Mice deficient in only one chemokine did not reach the same level of increase in CXCR3$^+$ activated T$_{conv}$ cells as mice with a combined deficiency. In animals lacking both chemokines, these cells showed further expansion instead of stagnation as seen in the wt controls at week 9 post-vaccination (Fig 3.2.11), even though bacterial clearance occurred at a similar rate in all 4 mouse strains (Fig 3.2.7).

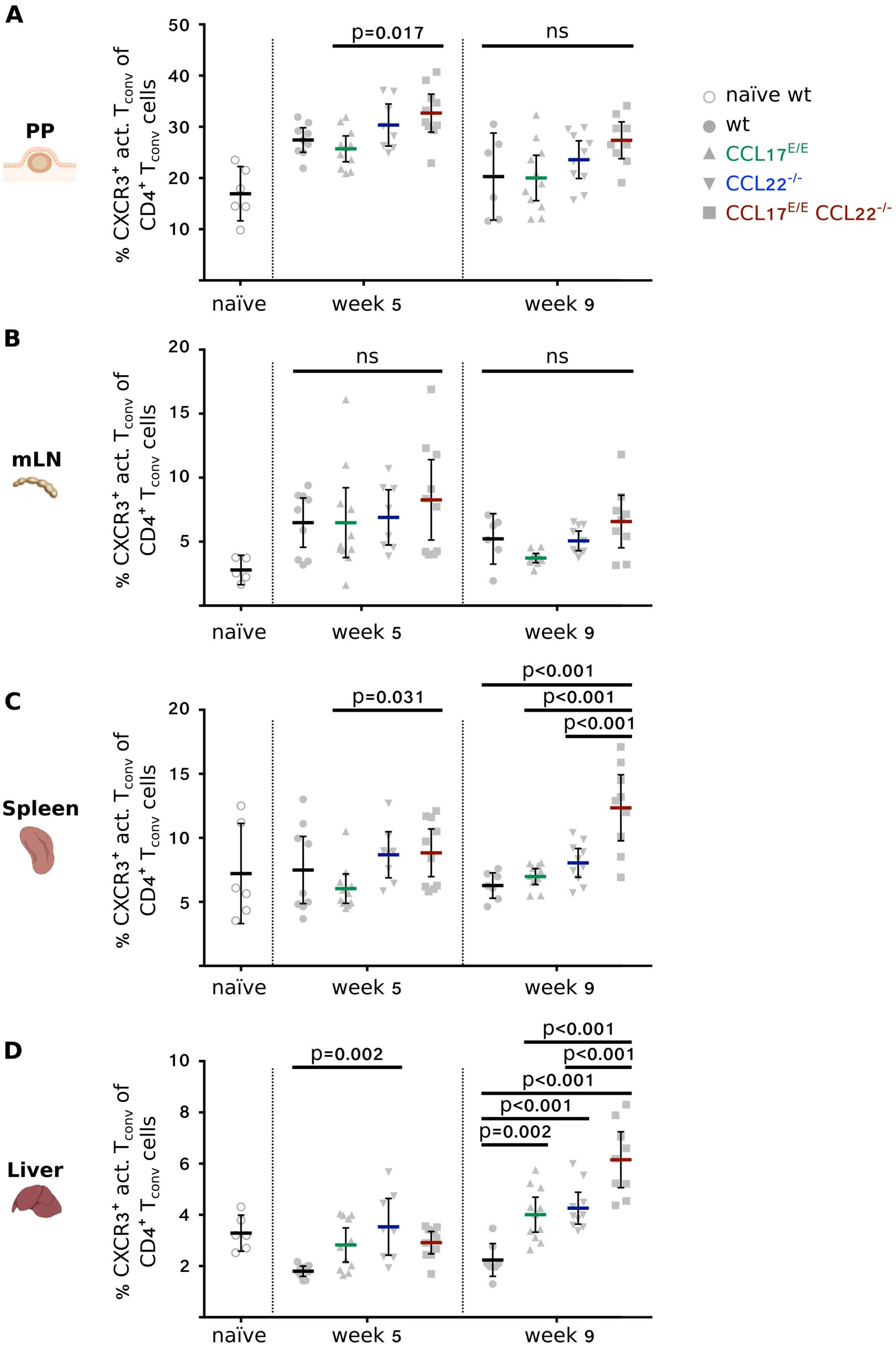
A
PP
% CXCR3⁺ act. Tconv of CD4⁺ Tconv cells
50
40
30
20
10
p=0.017
ns
naïve
week 5
week 9
○ naïve wt
● wt
▲ CCL17E/E
▼ CCL22-/-
■ CCL17E/E CCL22-/-
B
mLN
% CXCR3⁺ act. Tconv of CD4⁺ Tconv cells
20
15
10
5
ns
ns
naïve
week 5
week 9
C
Spleen
% CXCR3⁺ act. Tconv of CD4⁺ Tconv cells
20
15
10
5
p=0.031
p<0.001
p<0.001
p<0.001
naïve
week 5
week 9
D
Liver
% CXCR3⁺ act. Tconv of CD4⁺ Tconv cells
10
8
6
4
2
p=0.002
p<0.001
p<0.001
p<0.001
p<0.001
p=0.002
naïve
week 5
week 9

Figure 3.2.11: CD4$^+$ T cell FACS analysis of TAS2010 vaccinated wt and KO mice – analysis of conventional T cells
Wt, CCL17$^{E/E}$, CCL22$^{-/-}$ and CCL17/CCL22 double-deficient mice were orally vaccinated with 1x10^9 CFU TAS2010. Frequency of CXCR3$^+$ eff. T$_{conv}$ of CD4$^+$ T$_{conv}$ cells was analysed 5- and 9 weeks post-vaccination in PP (A), mLN (B), spleen (C) and liver (D). Naïve wt mice were used as controls. Symbols represent individual mice (n= 6-11; pooled from two independent experiments). Statistical significance was tested using two-way ANOVA with Tukey´s test for multiple comparison. Naïve mice were not included in the statistical analysis. Error bars indicate mean with 95% CI.

With the observations made in the T$_{reg}$ and the T$_{conv}$ cell compartments, the increase in STM-specific T cells was studied using a STM-specific MHCII tetramer (RS053) that was recently generated by Adrian Semeniuk from the Strugnell lab (unpublished) (Fig 3.2.12). Only CD4$^+$ FOXP3$^-$ T$_{conv}$ cells, but not CD4$^+$ FOXP3$^+$ T$_{reg}$ cells were stained with the RS053 tetramer, suggesting that T$_{reg}$ cells were not specific for this particular STM-epitope (Fig 3.2.8 B 6). It was noted that the RS053 epitope was identified by analysis of Th1 IFNγ secreting T cells induced 5 weeks post-vaccination with TAS2010.

Within the activated T$_{conv}$ cell compartment the tetramer stained a clearly distinct population (Fig 3.2.12 A) in PP, mLN and spleen (Fig 3.2.12 B). These tetramer$^+$ activated T$_{conv}$ cells were present at equal frequencies within all 4 mouse strains in PP, mLN, spleen and liver (Fig 3.2.12 B). When these cells were analysed in more detail for the expression of CXCR3 and CXCR6, it was observed that CXCR3 and CXCR6 were differentially expressed within the STM-tetramer$^+$ activated T$_{conv}$ cells. This differential expression of CXCR3 and CXCR6 was dependent on the organ analysed. CXCR3$^+$ (CXCR6$^-$) activated T$_{conv}$ cells, the cells in the focus of our interest, were mainly present within the STM-tetramer$^+$ activated T$_{conv}$ cells in PP (41%) and mLN (29%) (Fig 3.2.12 C). In PP from CCL17/CCL22 double-deficient mice, the frequency of CXCR3$^+$ CXCR6$^-$ within tetramer$^+$ activated T$_{conv}$ cells increased significantly by approximately 20-25%, compared to wt control animals and CCL17$^{E/E}$ mice (Fig 3.2.12 D).

These data indicate that activated T$_{conv}$ cells specific for the investigated epitope are enriched in the CXCR3$^+$ activated T$_{conv}$ cell population in PP, and are increased in the CCL17/CCL22 double deficient mice.

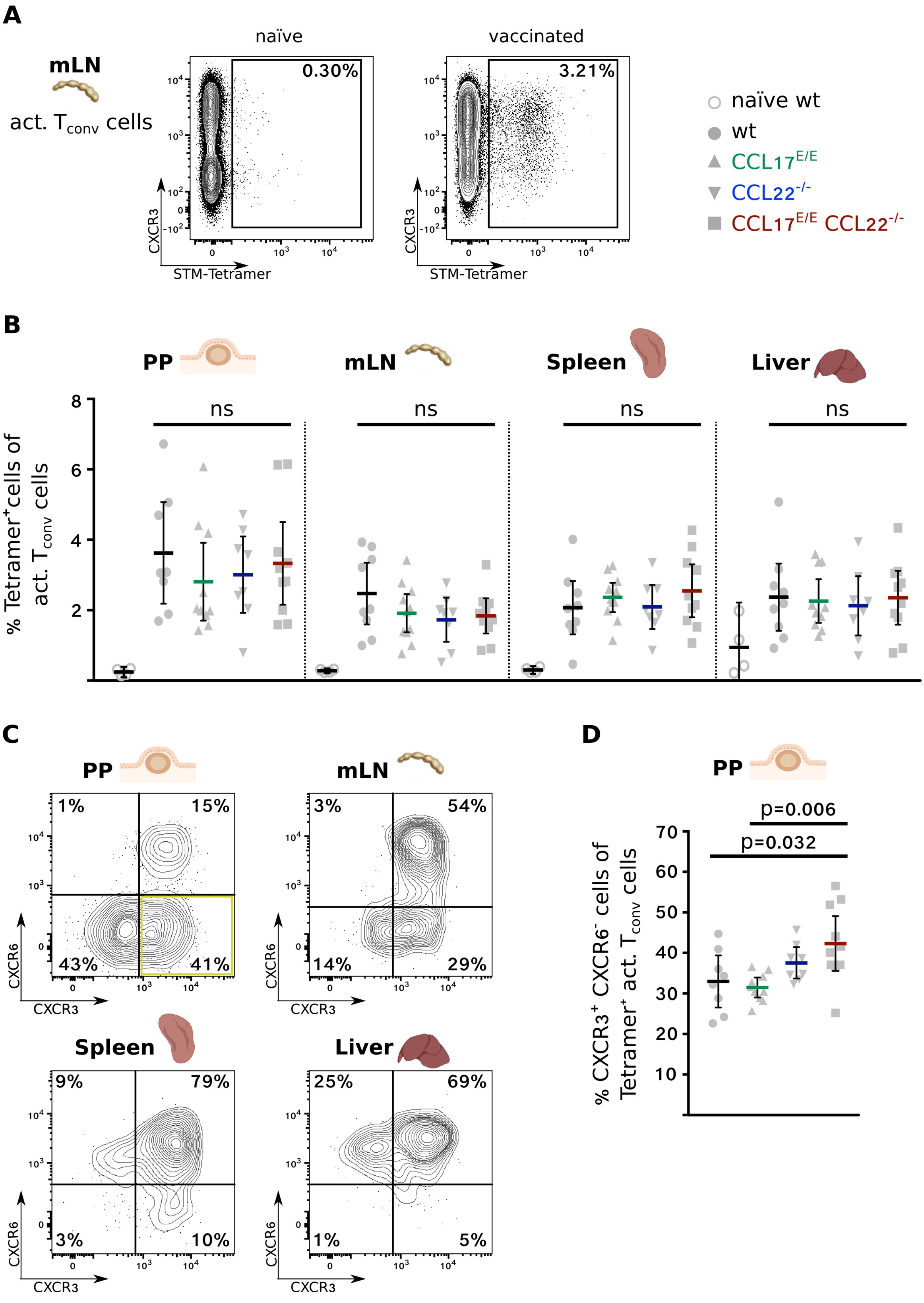
A
mLN
act. T_{conv} cells
naïve
vaccinated
0.30%
3.21%
CXCR3
STM-Tetramer
○ naïve wt
● wt
▲ $CCL17^{E/E}$
▼ $CCL22^{-/-}$
■ $CCL17^{E/E}$ $CCL22^{-/-}$
B
PP
mLN
Spleen
Liver
ns
ns
ns
ns
% $Tetramer^{+}$cells of act. T_{conv} cells
8
6
4
2
C
PP
1%
15%
43%
41%
mLN
3%
54%
14%
29%
Spleen
9%
79%
3%
10%
Liver
25%
69%
1%
5%
CXCR6
CXCR3
D
PP
p=0.006
p=0.032
% $CXCR3^{+}$ $CXCR6^{-}$ cells of $Tetramer^{+}$ act. T_{conv} cells
70
60
50
40
30
20
10

Figure 3.2.12: CD4$^+$ T cell FACS analysis of TAS2010 vaccinated wt and KO mice – STM-antigen specific conventional T cells
Wt, CCL17$^{E/E}$, CCL22$^{-/-}$ and CCL17/CCL22 double-deficient mice were orally vaccinated with 1x10^9 CFU TAS2010. STM-epitope-specific act. T$_{conv}$ cells were investigated 5 weeks post-vaccination using the STM-specific RS053 MHCII tetramer. The RS053 tetramer was used to identify STM-specific activated T$_{conv}$ cells of mLN from 5 weeks TAS2010 vaccinated wt mouse compared to naïve wt mouse (A). The percentage of tetramer$^+$ cells within act. T$_{conv}$ cells was analysed in PP, mLN, spleen and liver (B). Furthermore, the frequency of CXCR3$^+$ CXCR6$^-$ within tetramer$^+$ act. T$_{conv}$ cells was evaluated in PP, mLN, spleen and liver from wt mice (C) and quantified for PP from all 4 mouse strains (D). Four naïve wt mice were used as controls. Symbols represent individual mice (n= 7-11; pooled from two independent experiments). Statistical significance was tested using one-way ANOVA with Tukey´s test for multiple comparison. Naïve mice were not included in the statistical analysis. Error bars indicate mean with 95% CI.

Findings from the T$_{reg}$ compartment showed a decrease of KLRG1$^+$ effector T$_{reg}$ cells in CCL17/CCL22 double-deficient mice compared to wt controls after vaccination (Fig 3.2.10). The T$_{conv}$ compartment in turn, revealed an augmentation of CXCR3$^+$ activated T$_{conv}$ cells (which contained epitope-specific CD4$^+$ T cells) in CCL17/CCL22 double-deficient mice compared to wt controls in corresponding organs (Fig 3.2.11). In order to relate these findings, the ratio of absolute cell counts of KLRG1$^+$ effector T$_{reg}$ cells to absolute cell counts of CXCR3$^+$ activated T$_{conv}$ cells was calculated for PP (Fig 3.2.13 A) and spleen (Fig 3.2.13 B). In both organs, T$_{reg}$ and T$_{conv}$ cells showed the most pronounced differences between CCL17/CCL22 double-deficient and wt control mice.

At 5 weeks post-vaccination, the ratio of KLRG1$^+$ effector T$_{reg}$ cells to CXCR3$^+$ activated T$_{conv}$ cells in PP was equivalent in all 4 mouse strains studied. At 9 weeks post-vaccination, however, a significant reduction was observed in CCL17/CCL22 double-deficient mice compared to wt and CCL17$^{E/E}$ mice. Likewise, a decrease of the ratio of KLRG1$^+$ effector T$_{reg}$ cells to CXCR3$^+$ activated T$_{conv}$ cells was detected in CCL22$^{-/-}$ animals compared to wt mice. Wt mice had a ratio of 70 KLRG1$^+$ effector T$_{reg}$ cells to 1000 CXCR3$^+$ activated T$_{conv}$ cells, CCL17$^{E/E}$ mice had an approximate ratio of 60/1000, CCL22$^{-/-}$ mice had a ratio of roughly 40/1000 and CCL17/CCL22 double-deficient mice of approximately 30/1000, skewing the balance of T_{reg} cells to T_{conv} cells more to the side of the T_{reg} cells in wt mice (Fig 3.2.13 A).

At 5 weeks post-vaccination, the calculated ratio in the spleen was significantly reduced only in CCL22$^{-/-}$ mice compared to CCL17$^{E/E}$ mice. At 9 weeks post-vaccination, however, the ratio of KLRG1^{+} effector T_{reg} cells to CXCR3^{+} activated T_{conv} cells in the spleens of CCL17/CCL22 double-deficient mice was significantly decreased compared to wt controls. Wt mice had a ratio of 13 KLRG1^{+} effector T_{reg} cells to 1000 CXCR3^{+} activated T_{conv} cells and CCL17/CCL22 double-deficient mice of approximately 7/1000, shifting the balance of T_{reg} cells to T_{conv} cells in CCL17/CCL22 double-deficient mice more to the side of the activated T cells. CCL17$^{E/E}$ and CCL22$^{-/-}$ mice had a ratio of approximately 10/1000, and the mean ratio was positioned in between wt and CCL17/CCL22 double-deficient mice (Fig 3.2.13 B).

These results indicate that the deficiency in CCL17 and CCL22 contributes to an environment that supports a potent Th1 immune response, possibly through a relative reduction in regulatory T cells, since mice lacking both chemokines showed lower numbers of KLRG1^{+} effector T_{reg} cells per 1000 CXCR3^{+} activated T_{conv} cells than wt control animals.

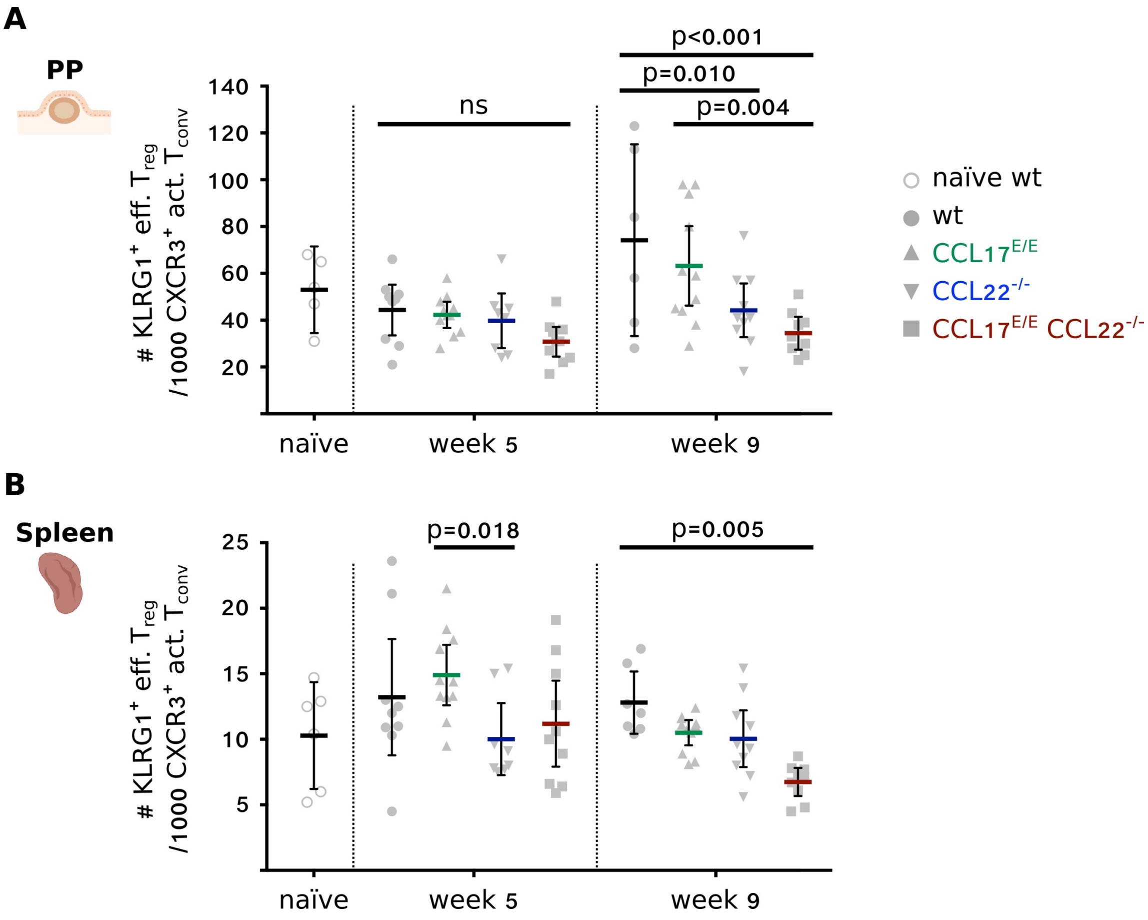

Figure 3.2.13: CD4$^+$ T cell FACS analysis of TAS2010 vaccinated wt and KO mice – ratio KLRG1$^+$ effector regulatory T cells to CXCR3$^+$ activated conventional T cells Wt, CCL17$^{E/E}$, CCL22$^{-/-}$ and CCL17/CCL22 double-deficient mice were orally vaccinated with 1x10^9 CFU TAS2010. The ratio of KLRG1$^+$ eff. T$_{reg}$ cells to CXCR3$^+$ act. T$_{conv}$ cells was calculated from absolute cell counts for PP (A) and spleen (B) 5- and 9 weeks post-vaccination. Naïve wt mice were used as controls. Symbols represent individual mice (n= 6-11; pooled from two independent experiments). Statistical significance was tested using two-way ANOVA with Tukey´s test for multiple comparison. Naïve mice were not included in the statistical analysis. Error bars indicate mean with 95% CI.

In summary, the results obtained from examining the T$_{reg}$ and T$_{conv}$ cell compartments after vaccination of mice with TAS2010, suggested that the combined deficiency of CCL17 and CCL22 leads to a reduction of KLRG1$^+$ effector T$_{reg}$ cells in organs that represent major sites of infection after oral STM vaccination (Fig 3.2.10). In parallel, CXCR3$^+$ activated T$_{conv}$ cells were increased in mice deficient for both chemokines, especially at a late stage of vaccination (week 9) (Fig 3.2.11). The enhanced expansion of CXCR3$^+$ activated T$_{conv}$ cells versus a reduction of KLRG1^{+} effector T$_{reg}$ cells could be more favourable for the induction of a potent Th1 immune response (Fig 3.2.13). Furthermore, it was shown that activated T$_{conv}$ cells included cells that were specific for the epitope investigated (Fig 3.2.12). These findings mirror the results obtained from vaccinated and challenged mice, suggesting that the effect seen after secondary challenge apparently has its origin already during vaccination.

3.2.3 Analysis of $CD4^+$ T cell populations in the gut and systemic organs of naïve CCL17/CCL22 chemokine deficient mice

The chemokines CCL17 and CCL22 belong to the type of chemokines that are induced upon inflammation but are also already expressed under homeostatic conditions (Alferink et al., 2003; Vulcano et al., 2001). Yet, there is limited knowledge on CCL17 and CCL22 and their influence on T cells in steady-state. Mice deficient for both chemokines demonstrate a decrease in effector regulatory T cells and in parallel an increase in activated $CD4^+$ T cells, shown by vaccination and vaccination/challenge. Since CCL17 and CCL22 are also expressed in steady-state, the observations made after vaccination and vaccination/challenge were explored further in naïve animals.

As in the previous experiments, the $CD4^+$ T_{reg} and $CD4^+$ T_{conv} cell compartments were analysed in 4 different organs (PP, mLN, spleen and liver), chosen because they represent key sites for bacterial invasion and replication during *Salmonella* infection. Comparisons were made between $CCL17^{E/E}$, $CCL22^{-/-}$, CCL17/CCL22 double-deficient and wt mice as, using flow cytometry (Fig 3.2.14 A).

It was of particular interest to address whether a deficiency in CCL22 or CCL17/CCL22 would interfere with T cell populations already in steady-state. The following gating strategy was applied (Fig 3.2.14 B): only viable $TCR\beta^+$ cells were analysed, and $CD3^-$, autofluorescent $(AF)^+$ as well as doublet cells were excluded. T cell population analysis focused on the $CD4^+$ $FOXP3^+$ T_{reg} cell compartment and the $CD4^+$ $FOXP3^-$ T_{conv} cell compartment. In addition, $KLRG1^+$ ($CD44^+$ $CD62L^-$) effector T_{reg} cells, activated ($CD44^+$ $CD62L^-$) T_{conv} and $CXCR3^+$ ($CD44^+$ $CD62L^-$) activated T_{conv} cells were analysed in more detail.

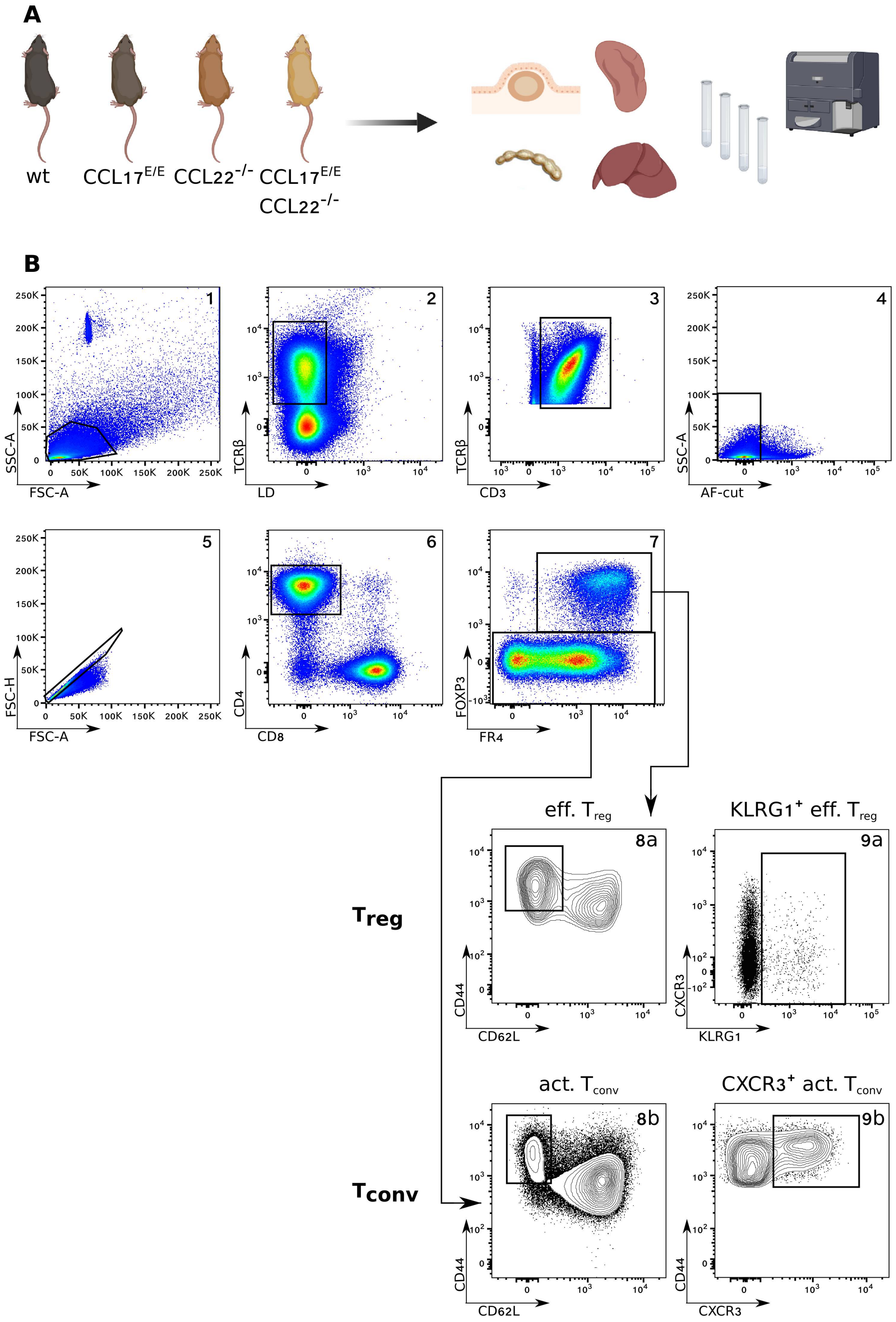
A
wt
CCL17^E/E
CCL22^-/-
CCL17^E/E CCL22^-/-
B
1
SSC-A
FSC-A
2
TCRβ
LD
3
TCRβ
CD3
4
SSC-A
AF-cut
5
FSC-H
FSC-A
6
CD4
CD8
7
FOXP3
FR4
Treg
Tconv
eff. Treg
8a
CD44
CD62L
KLRG1+ eff. Treg
9a
CXCR3
KLRG1
act. Tconv
8b
CD44
CD62L
CXCR3+ act. Tconv
9b
CD44
CXCR3

Figure 3.2.14: FACS analysis of CD4$^+$ T cells of naïve wt and KO mice – experimental setup and gating strategy
PP, mLN, spleen and liver were isolated from wt, CCL17$^{E/E}$, CCL22$^{-/-}$ and CCL17/CCL22 double-deficient mice; the T$_{reg}$ and T$_{conv}$ cell compartment was analysed via flow cytometry (A). Cells from fixed samples were selected based on their FSC and SSC properties (B1). Live $\alpha\beta$-T cells were identified as TCRβ^+ Live-Dead dye negative (LD$^-$) (B2), in addition T cells were further analysed for CD3 expression, selecting CD3$^+$ T cells, thus confirming these cells as T cells (B3). Subsequently, autofluorescent (AF) cells were excluded using an empty fluorescent channel (B4) and single cells were identified (B5). CD4$^+$ T cells were selected (B6) and separated into FOXP3$^+$ FR4$^+$ and FOXP3$^-$ cells (B7). FOXP3$^+$ FR4$^+$ cells were identified as T$_{reg}$ cells and FOXP3$^-$ as T$_{conv}$ cells. T$_{reg}$ cells were further analysed for CD44 and CD62L expression. CD44$^+$ CD62L$^-$ cells were selected and identified as effector T$_{reg}$ cells (B8a). CD44$^+$ CD62L$^-$ eff. T$_{reg}$ cells were then analysed for their KLRG1 expression. KLRG1$^+$ cells were identified as KLRG1$^+$ eff. T$_{reg}$ cells (B9a). T$_{conv}$ cells were further analysed for CD44 and CD62L expression. CD44$^+$ CD62L$^-$ cells were selected and identified as activated T$_{conv}$ cells (B8b). Following CD44$^+$ CD62L$^-$ act. T$_{conv}$ cells were evaluated for their CXCR3 expression. CXCR3$^+$ cells were identified as CXCR3$^+$ act. T$_{conv}$ cells (B9b). Representative gating of mLN from a naïve wt mouse is depicted.

Absolute counts of total cells from mLN, spleen and liver were comparable between all mouse strains analysed. In PP, however, all three KO mice showed an approximately 50% reduction in cell numbers compared to wt controls, although cell numbers did not differ between the three KO mice (Fig 3.2.15 A). It was hypothesised that a reduction in CD4$^+$ T cell populations may, at least in part, contribute to the reduction of cell numbers in the PP. Hence, CD4$^+$ T cells were analysed in more detail. Absolute cell counts of T$_{reg}$ and KLRG1$^+$ effector T$_{reg}$ cells were similar in all mouse strains analysed (Fig 3.2.15 B). In contrast, absolute cell counts of T$_{conv}$ and especially of activated T$_{conv}$ cells were significantly decreased in all three KO mice compared to wt controls. In the activated T$_{conv}$ cell population, the decrease in cell numbers was very prominent, with a 4.5-7-fold reduction in all three KO mice compared to wt controls (Fig 3.2.15 B). CXCR3$^+$ activated T$_{conv}$ cell counts were significantly reduced only in CCL17$^{E/E}$ and CCL22$^{-/-}$ mice, but not in CCL17/CCL22 double-deficient mice compared to wt controls (Fig 3.2.15 B).

In conclusion, the data indicate that the reduction of activated CD4$^+$T$_{conv}$ in PP of KO mice contributed to the overall decrease in absolute cell counts. The reduction of CD4$^+$ T$_{conv}$ cell counts alone, however, did not explain the overall reduction of approximately 1x10^6 cells in KO mice compared to wt animals. Other cell types might be involved and need to be investigated.

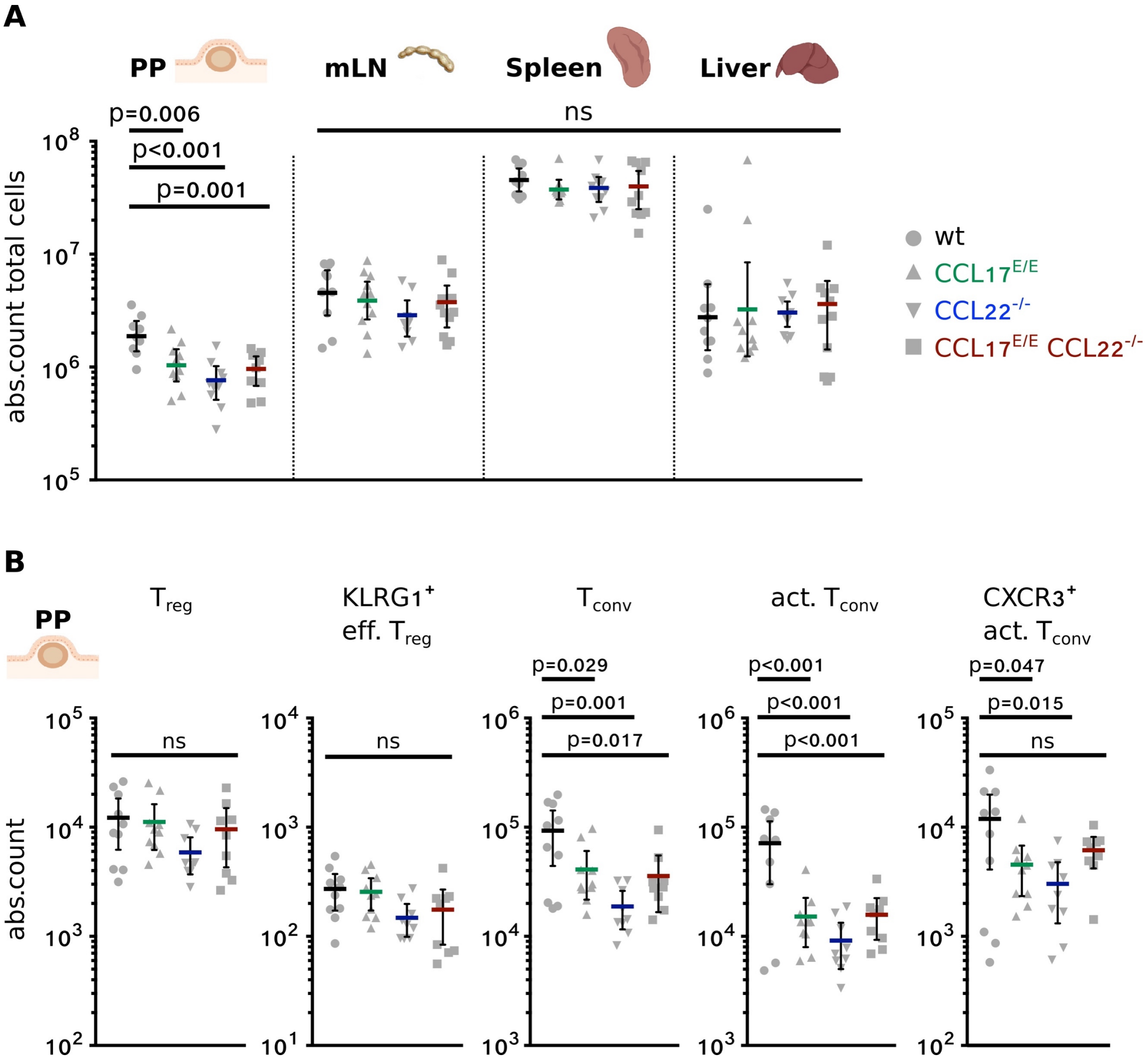

Figure 3.2.15: CD4$^+$ T cell FACS analysis of naïve wt and KO mice – absolute cell counts of T$_{reg}$ and T$_{conv}$ cell populations

Absolute cell counts (Fig 3.2.1 gate in B1) were calculated using counting beads. Cell counts were evaluated for PP, mLN, spleen and liver of wt, CCL17$^{E/E}$, CCL22$^{-/-}$ and CCL17/CCL22 double-deficient mice (A). In addition, absolute cell counts of T$_{reg}$, KLRG1$^+$ eff. T$_{reg}$, T$_{conv}$, act. T$_{conv}$ and CXCR3$^+$ act. T $_{conv}$ cells in PP were analysed (B). Symbols represent individual mice (n= 9-11; pooled from three independent experiments). Statistical significance was tested using one-way ANOVA with Tukey´s test for multiple comparison. Error bars indicate mean with 95% CI.

Besides absolute cell counts of CD4$^+$ T$_{reg}$ and T$_{conv}$ cell populations also the frequencies of CD4$^+$ T$_{reg}$ (Fig 3.2.16) and T$_{conv}$ cells (Fig 3.2.17) were analysed. The percentage of T$_{reg}$ cells in mLN, spleen and liver did not differ in any of the 4 analysed mouse strains. In contrast, in PP, all three KO mice demonstrated a significant increase of T$_{reg}$ cell frequencies compared to wt controls by approximately 2-fold (Fig 3.2.16 A). This was expected since all three chemokine KO mice had shown a reduction of T$_{conv}$ cell counts compared to wt mice but similar T$_{reg}$ cell counts (Fig 3.2.15 B), overall changing the ratio of T$_{reg}$ to T$_{conv}$ cells in PP of KO mice. In addition, the frequency of KLRG1$^+$ effector T$_{reg}$ of total T$_{reg}$ cells was assessed and revealed a decrease of this population in PP of CCL17/CCL22 double-deficient mice compared to wt controls by approximately 25%. Furthermore, a reduction of KLRG1$^+$ effector T$_{reg}$ cell frequency in mLN of CCL22$^{-/-}$ and CCL17/CCL22 double-deficient compared to CCL17$^{E/E}$ animals, was observed (Fig 3.2.16 B). Overall, these findings suggest that even though absolute cell counts of KLRG1$^+$ effector T$_{reg}$ cells were not significantly different, the frequency of KLRG1$^+$ effector T$_{reg}$ among all T$_{reg}$ cells was significantly lower in PP of CCL17/CCL22 double-deficient mice under steady-state conditions.

Similar to the observation made in the T$_{reg}$ cell compartment, the frequency of T$_{conv}$ cells in mLN, spleen and liver did not differ between strains. In PP, T$_{conv}$ cell frequency from all three KO mice depicted a significant reduction compared to wt controls (Fig 3.2.17 A). A similar trend was observed for activated T$_{conv}$ cell frequencies (Fig 3.2.17 B), as expected from previous findings (Fig 3.2.15 A and B). Interestingly, analysis of CXCR3$^+$ activated T$_{conv}$ cell frequencies revealed an opposing outcome. The percentage of CXCR3$^+$ activated T$_{conv}$ cells in CCL17/CCL22 double-deficient mice compared to wt controls, and to CCL17$^{E/E}$ mice, showed a significant increase of approximately 2-fold (Fig 3.2.17 C).

Taken together, no changes were observed in CD4$^+$ T$_{reg}$ and T$_{conv}$ cell populations in CCL17$^{E/E}$, CCL22$^{-/-}$ and CCL17/CCL22 double-deficient mice in systemic organs such as the spleen and liver. The most striking differences in the T$_{reg}$ and the T$_{conv}$ cell compartments were seen in PP, affecting all three KO mice, but particularly CCL17/CCL22 double-deficient mice, which revealed a reduction of KLRG1$^+$ effector T$_{reg}$ cells and an increase of CXCR3$^+$ activated T$_{conv}$ cells compared to wt mice; this observation recapitulated observations made in vaccinated, and vaccinated and challenged animals. The fact that only changes in the T_{reg} and T_{conv} cell compartment were observed in the PP and not in mLN, spleen or liver, suggests that they might be due to the stimuli provided by the gut microbiota.

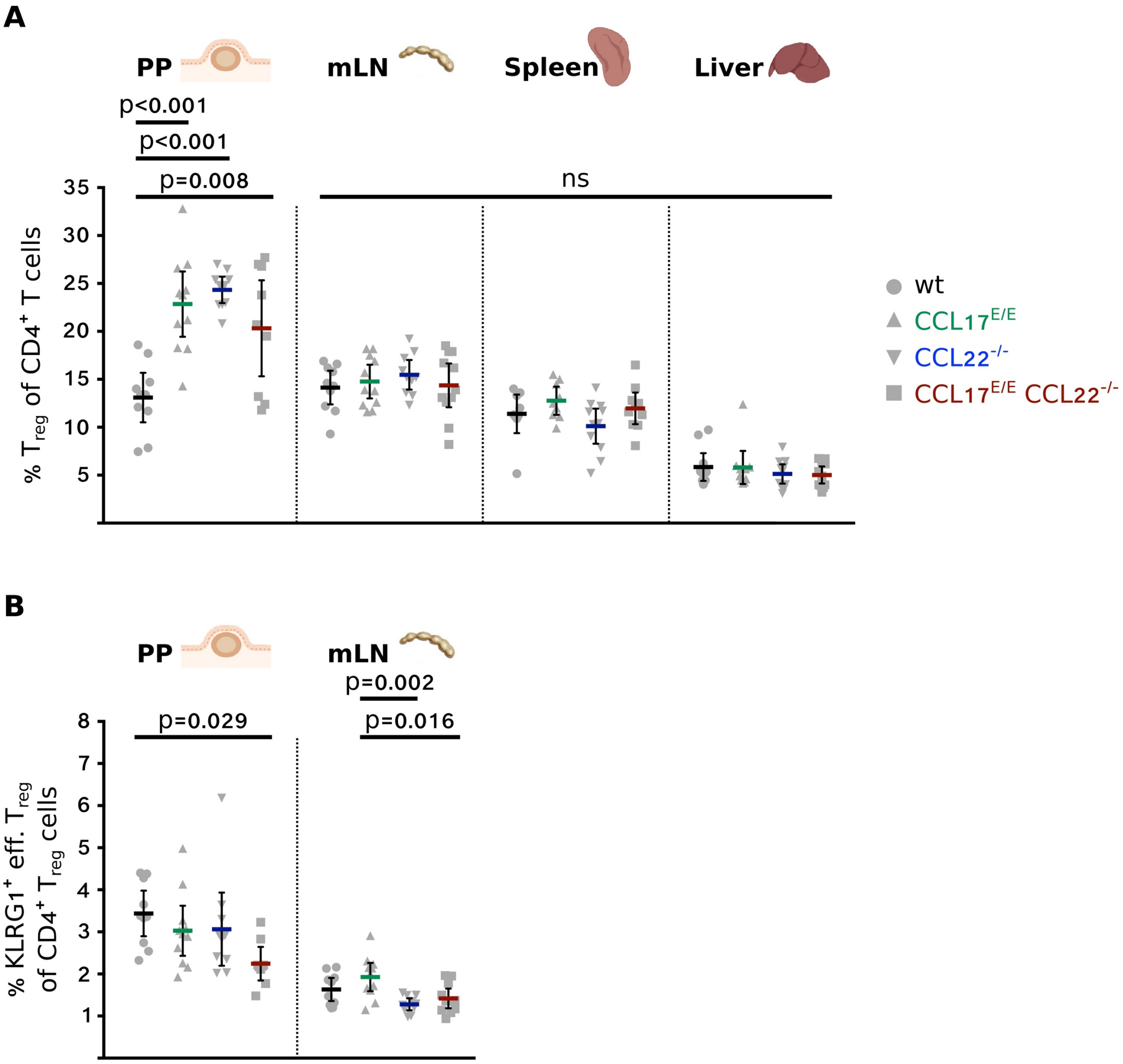

Figure 3.2.16: CD4$^+$ T cell FACS analysis of naïve wt and KO mice – evaluation of regulatory T cells

Percentage of T_{reg} within CD4$^+$ T cells was calculated in PP, mLN, spleen and liver of wt, CCL17$^{E/E}$, CCL22$^{-/-}$ and CCL17/CCL22 double-deficient mice (A). Furthermore, the frequency of KLRG1$^+$ eff. T_{reg} within CD4$^+$ T_{reg} cells was determined in PP and mLN (B). Symbols represent individual mice (n= 9-11; pooled from three independent experiments). Statistical significance was tested using one-way ANOVA with Tukey´s test for multiple comparison. Error bars indicate mean with 95 %CI.

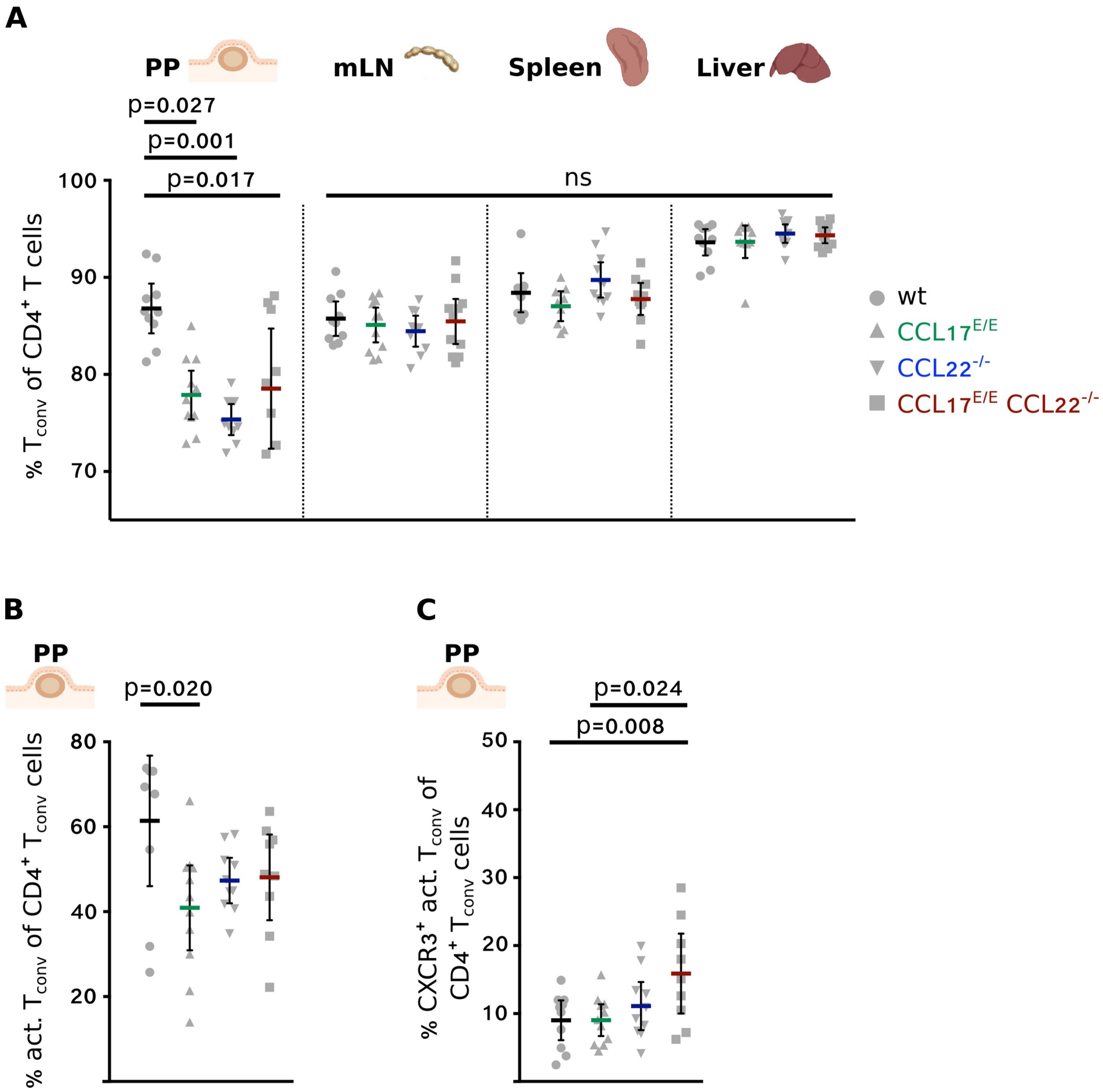

Figure 3.2.17: CD4$^+$ T cell FACS analysis of naïve wt and KO mice – evaluation of conventional T cells

Percentage of T_{conv} within CD4$^+$ T cells was calculated in PP, mLN, spleen and liver of wt, CCL17$^{E/E}$, CCL22$^{-/-}$ and CCL17/CCL22 double-deficient mice (A). In addition, the percentage of act. T_{conv} within CD4$^+$ T_{conv} cells was determined in PP (B). Also, the frequency of CXCR3$^+$ act. T_{conv} within CD4$^+$ T_{conv} cells was analysed in PP(C). Symbols represent individual mice (n= 9-11; pooled from three independent experiments). Statistical significance was tested using one-way ANOVA with Tukey´s test for multiple comparison. Error bars indicate mean with 95% CI.

3.3 Analysis of CCL17 and CCL22 serum levels of humans challenged with *Salmonella* Typhi

Research on *Salmonella* Typhi (STY) has always been challenging since it is a pathogen restricted to the human hosts only. Therefore, mouse models using *Salmonella* Typhimurium (STM) have been used to mimic the human disease; the STM mouse model has been used since the 1960s to investigate the pathogenesis and immunology of STY (Spano, 2016). The aim of this component of the study was to investigate if the observations made in the STM mouse model regarding CCL17 and CCL22 can be observed in humans infected with STY. Data from the murine model suggested that a deficiency in CCL22 and CCL17 leads to an enhanced vaccine efficacy. The experiment evaluated whether lower levels of serum CCL22 and/or CCL17 in volunteers vaccinated with Ty21a, a live attenuated STY vaccine, correlated with a more successful vaccine outcome when the same individuals were challenged with virulent STY (Quailes strain).

Professor Pollard´s group performed a randomised, double-blind, placebo-controlled trial in healthy adult participants at a single centre in Oxford (UK). Participants were assigned to receive one dose of double-blinded M01ZH09-vaccine, or placebo, or 3-doses of open-label Ty21a-vaccine. The 99 participants were randomised to receive M01ZH09 (n = 33), placebo (n = 33) or 3-doses of Ty21a (n = 33). At 28 days after vaccination, participants were orally challenged with 1-5 10^4 CFU *S*. Typhi Quailes strain (Darton et al., 2016). Samples from Ty21a vaccinated participants were analysed for levels of CCL17 and CCL22, since it is a commercially available approved live-attenuated vaccine. M01ZH09 on the other hand, is not approved and still in clinical trial (Darton et al., 2016). Plasma samples used in this thesis were derived from blood samples taken pre-vaccination (PV), at day 0 (pre-challenge) and day 7 (post-challenge) (Fig 3.3 A). The efficacy of the vaccine compared with placebo was assessed as the percentage of participants reaching pre-defined endpoints constituting typhoid diagnosis (fever and/or bacteraemia) during the 14 days after challenge. After challenge, typhoid disease was diagnosed in 20/30 (66.7% [95% CI 47.2 to 87.2]) of placebo recipients and 13/30 (43.3% [95% CI 25.5 to 62.6]) of Ty21a vaccine recipients. Vaccine efficacy for 3-doses of Ty21a was 35% [95% CI -5 to 60] (Darton et al., 2016).

Plasma samples were analysed with the Human Magnetic Luminex® Assay for CCL22/CCL17 from R&D Systems. Concentrations of CCL22 and CCL17 were measured for each individual participant at PV, day 0 and day 7 (Fig 3.3 B).

Chemokine concentrations in plasma from each individual participant were normalised to PV (100 %) due to great differences in chemokine concertations between individual participants already at PV (Fig 3.3 C). Normalised chemokine concentrations were then plotted against the time course of vaccination and challenge (Fig 3.3 D). No significant differences in CCL22 or CCL17 concentration of normalised values were observed between not Typhoid Diagnosed (nTD) participants with a successful vaccine outcome and Typhoid Diagnosed (TD) participants, who had an unsuccessful vaccine outcome. Some trends were observed. Participants diagnosed with Typhi showed a slight drop in CCL22 and a more pronounced drop in CCL17 pre-challenge on day 0 compared to PV. Volunteers who were nTD had a slight increase in CCL22 and a minor decrease in CCL17 on day 0 compared to PV. CCL22 as well as CCL17 then increased on day 7 post-challenge in TD volunteers, which was expected for CCL17, since it is a chemokine known to be associated with inflammation. In participants that became nTD, CCL22 increased slightly where CCL17 stayed at similar levels compared to day 0 (Fig 3.3 C). Furthermore, chemokine levels of the volunteers were plotted in correlation to each other for each time point (Fig 3.3. E-G). Study participants that later showed protection against *Salmonella* challenge (nTD) had, in 10/17 cases either a very high concentration of CCL17 or CCL22 pre-vaccination of approximately 500 pg/ml, whereas TD participants had in, 11/12 cases, lower CCL17 and CCL22 concentrations pre-vaccination (Fig 3.3. E). Chemokine concentrations on day 0 and day 7 showed a less clear picture.

Summarising, no correlation between low CCL22 or CCL17 concentrations and vaccine outcome was observed, but high serum concentrations of CCL17 or CCL22 were associated with disease protection. In addition, serum levels of both chemokines were influenced by vaccination and challenge.

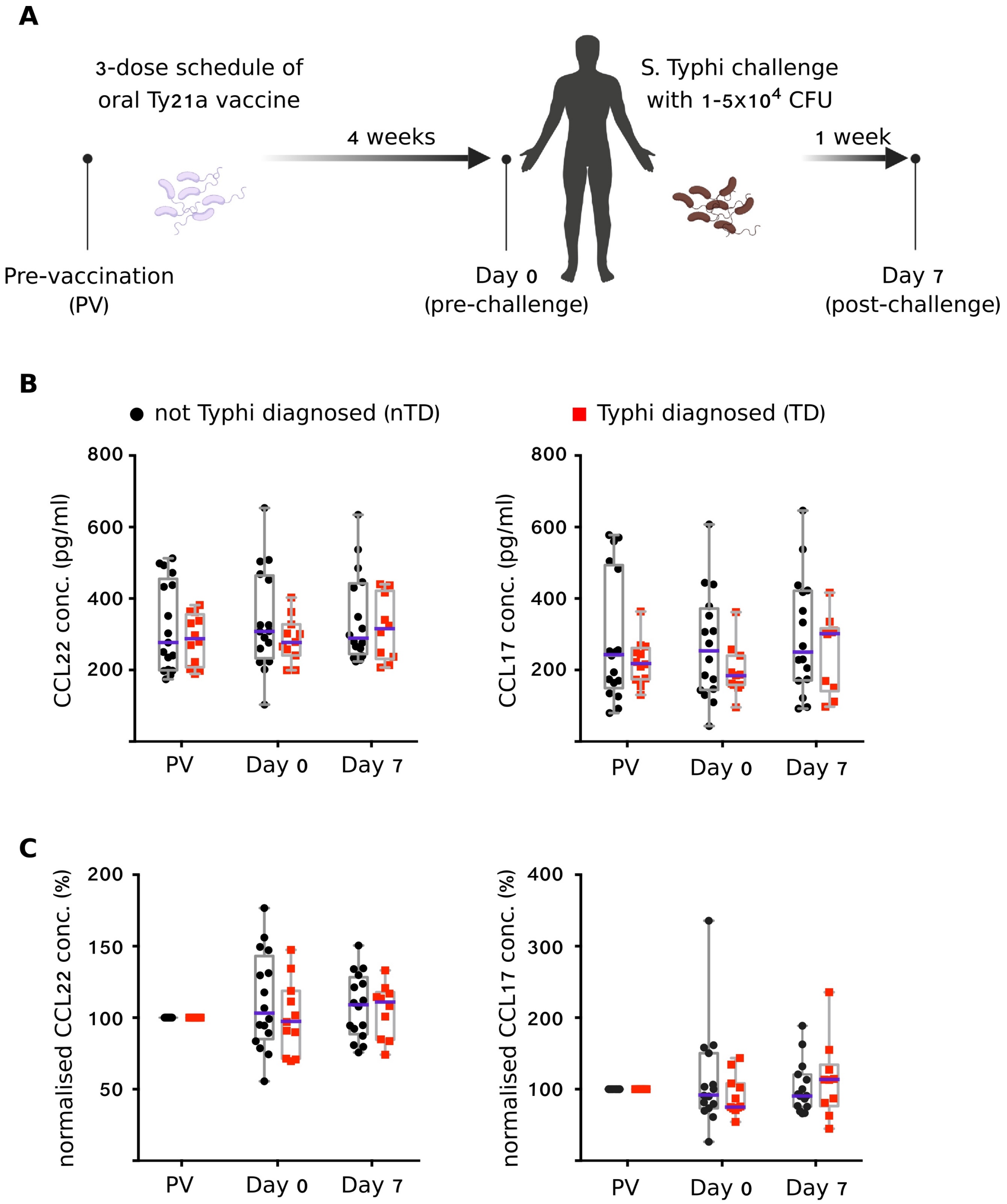
A
3-dose schedule of oral Ty21a vaccine
4 weeks
S. Typhi challenge with 1-5x10^4 CFU
1 week
Pre-vaccination (PV)
Day 0 (pre-challenge)
Day 7 (post-challenge)
B
● not Typhi diagnosed (nTD)
🟥 Typhi diagnosed (TD)
CCL22 conc. (pg/ml)
800
600
400
200
PV
Day 0
Day 7
CCL17 conc. (pg/ml)
800
600
400
200
PV
Day 0
Day 7
C
normalised CCL22 conc. (%)
200
150
100
50
PV
Day 0
Day 7
normalised CCL17 conc. (%)
400
300
200
100
PV
Day 0
Day 7

D

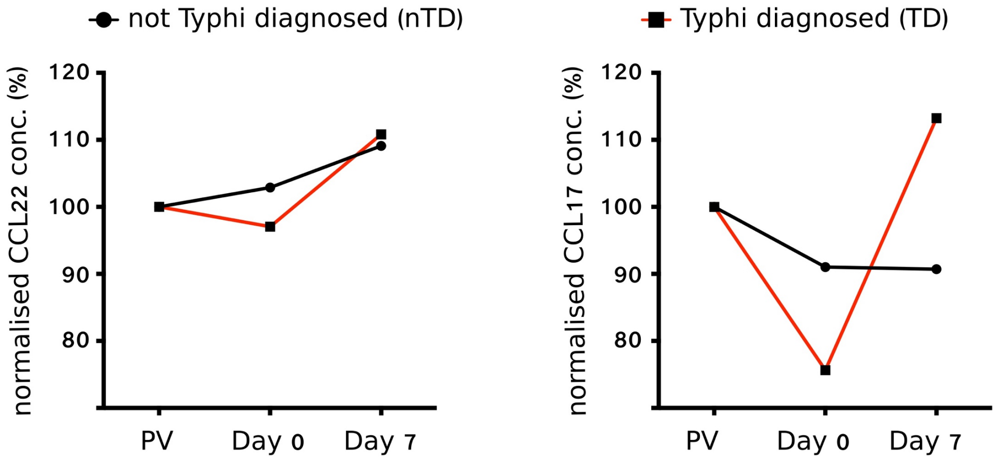
not Typhi diagnosed (nTD)
Typhi diagnosed (TD)
normalised CCL22 conc. (%)
120
110
100
90
80
PV
Day 0
Day 7
normalised CCL17 conc. (%)
120
110
100
90
80
PV
Day 0
Day 7

E

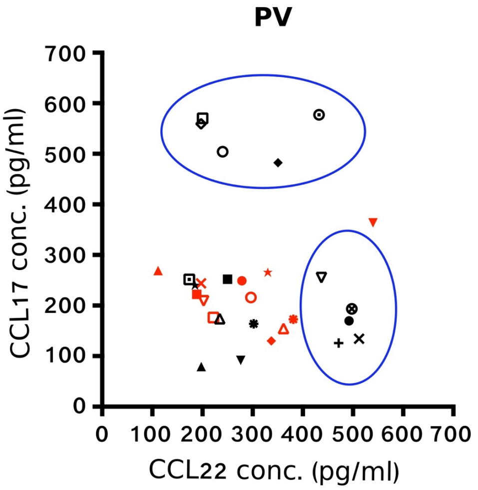
PV
CCL17 conc. (pg/ml)
700
600
500
400
300
200
100
0
0
100
200
300
400
500
600
700
CCL22 conc. (pg/ml)

F

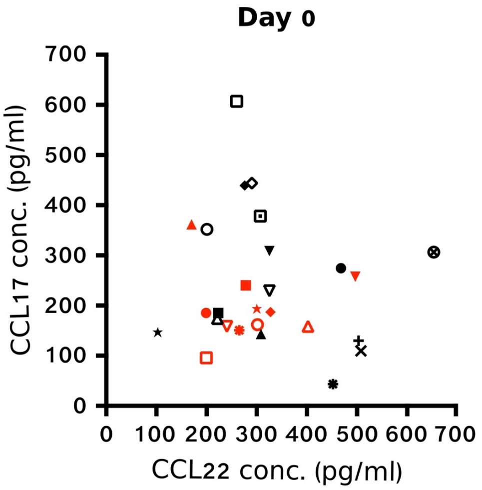
Day 0
CCL17 conc. (pg/ml)
700
600
500
400
300
200
100
0
0
100
200
300
400
500
600
700
CCL22 conc. (pg/ml)

G

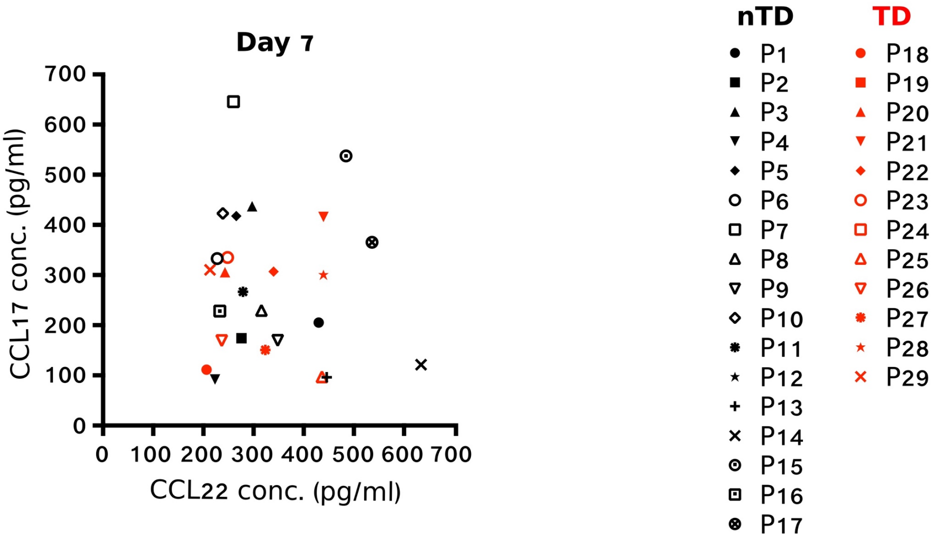
Day 7
CCL17 conc. (pg/ml)
700
600
500
400
300
200
100
0
0
100
200
300
400
500
600
700
CCL22 conc. (pg/ml)
nTD
TD
P1
P2
P3
P4
P5
P6
P7
P8
P9
P10
P11
P12
P13
P14
P15
P16
P17
P18
P19
P20
P21
P22
P23
P24
P25
P26
P27
P28
P29

Figure 3.3: Analysis of CCL22 and CCL17 concentration in human plasma
Human vaccine and challenge trial participants received three doses of oral Ty21a-vaccine. 28 days after vaccination, participants were orally challenged with 1-5 10^4 CFU *S*. Typhi Quailes strain. Analysed plasma samples derived from blood samples taken pre-vaccination (PV), at day 0 (pre-challenge) and day 7 (post-challenge) (A). Plasma samples were analysed with the Human Magnetic Luminex® Assay for CCL22/CCL17 from R&D Systems. Chemokine concentrations were acquired for each time point (B). Furthermore, chemokine concentrations were normalised to PV (100%) (C). Data are depicted as box and whiskers with min. to max. (B and C). In addition, normalised concentrations were plotted as summarised data, median is depicted (D). Individual CCL17 and CCL22 concentrations of each study participant were correlated to each other for different time points (E-G). n=16-17 (nTD), n=11-12 (TD).

4 Discussion

Chemokines play a key role in the trafficking of cells of the innate and adaptive immune systems to their target tissue or niche. Acting as chemoattractants chemokines facilitate cell migration and perform other critical functions such as priming of naïve T cells or supporting cell fate decisions into effector and memory cells (Griffith et al., 2014). The chemokines CCL17 and CCL22 share some of these functions, although CCL17 is associated with an inflammatory environment, whereas CCL22 is linked to an immunosuppressive milieu.

CCL17 is connected to the development of inflammatory and allergic diseases of all major barrier organs, including the intestine, the skin and the lung. In the gut, CCL17 promotes intestinal inflammation (Heiseke et al., 2012). In the skin, the chemokine enhances the development of contact hypersensitivity (CHS) (Alferink et al., 2003; Fülle et al., 2018a; Tsunemi et al., 2006) and atopic dermatitis (Kataoka, 2014; Stutte et al., 2010; Vestergaard et al., 2000). In the lung, CCL17 triggers allergic asthma (Santulli-Marotto et al., 2013a; Yahia et al., 2014). CCL22, in contrast, is associated with autoimmune protection (Bischoff et al., 2015; Montane et al., 2011), and the recruitment of regulatory T cells (T_{reg}) into the tumour microenvironment (Anz et al., 2015; Curiel et al., 2004; Wiedemann et al., 2016). Even though DC are the primary source of CCL17 (Alferink et al., 2003; Globisch et al., 2014) and CCL22 (Godiska et al., 1997; Rapp et al., 2019; Schaniel et al., 1998; Vulcano et al., 2001), and both chemokines bind to the same receptor, CCR4 (Imai et al., 1997, 1998), they are associated with different diseases suggesting that CCL17 and CCL22 may have different roles. This phenomenon, whereby different ligands of the same receptor are able to induce diverse responses, is known as biased agonism (Anderson et al., 2016; Rajagopal et al., 2013).

The key functions of CCL17 include the recruitment of T cells to sites of inflammation (Fülle et al., 2018a; Weber et al., 2011b), the induction of DC-T cell interactions required to initiate an adaptive immune response (Semmling et al., 2010), and the sensitisation of DC for CCR7- and CXCR4-dependent migration (Stutte et al., 2010). Similarly, CCL22 also plays an important role in the recruitment of T cells (Anz et al., 2015; Curiel et al., 2004; Wiedemann et al., 2016), the induction of DC-T cell interactions (Rapp et al., 2019), and the stimulation of DC migration (Bischoff et al., 2015). Interestingly, these CCL22-mediated functions are mainly associated with T_{reg} cells, which explains the correlation between CCL22 expression, autoimmune protection and tumour immune-escape response mechanisms.

In this thesis, a new insight into the field of CCL17/CCL22 biology was provided through investigations of these two chemokines during infection, an area which has been only poorly studied so far. The roles of the chemokines CCL17 and CCL22 in the immune defence against *Salmonella* Typhimurium infection was studied in a murine model.

More specifically, the role of CCL17-expressing DC in the transmission of virulent *Salmonella* Typhimurium from the intestine to the draining lymph nodes was studied and the function of CCL22 and CCL17 in the induction of adaptive immunity against *Salmonella* Typhimurium was investigated. The findings are important in the context of vaccine development.

4.1 CCL17-expressing DC contribute to the transmission of *Salmonella* Typhimurium

CCL17^{+} DC harbouring *Salmonella* migrate from the PP to the mLN

In previous studies of our group (Förster lab, LIMES Institute), the expression of CCL17 in various organs was assessed. The analysis of naïve CCL17$^{E/+}$ reporter mice revealed the presence of CCL17-expressing cells in the dome area of PP as well as in the T cell zone of PP and mLN (Alferink et al., 2003). This and other studies have identified DC in several organs, including the mLN, as the main source of CCL17 (Alferink et al., 2003; Globisch et al., 2014). The results from the present study confirmed these observations. In addition, the identification of the T cell area to which CCL17-expressing cells localised was not only based on anatomic localisation, as has been the case in former studies (Alferink et al., 2003), but also by co-staining for T cells (Fig 3.1.1). The findings presented here gave a new insight into steady-state CCL17 expression in different intestinal mononuclear phagocytes, demonstrating that intestinal DC and to a lesser extent, macrophages, but not monocytes, express CCL17 in the gut in steady-state (Fig 3.1.5).

The primary site of intestinal invasion by *Salmonella* are the PP (Carter and Collins, 1974; Jones et al., 1994), a site to which CCL17-expressing cells localise, as demonstrated in the present work. Once *Salmonella* has breached the epithelial barrier, the bacteria are taken up by macrophages or DC located in the subepithelial dome region (SED) (Broz et al., 2012; Gayet et al., 2017; Hopkins et al., 2000; Niess et al., 2005; Palmer and Slauch, 2017). Here, CCL17$^+$ DC co-localising with STM in the SED of PP were observed (Fig 3.1.2 B+C) which may include cells that have taken up invading bacteria. From the intestine, STM are transported to the draining mLN within DC acting as 'Trojan horses', while hiding from the immune system (Bogunovic et al., 2009; Bravo-Blas et al., 2019; Voedisch et al., 2009). In the mLN they reside within a range of different cells, including macrophages, DC, B cells and neutrophils (Bravo-Blas et al., 2019). These previous studies support the observations in the present work that STM not only localised to the area of CCL17$^+$ cells (T cell zone), but were distributed freely over the whole mLN including the B cell zone (Fig 3.1.2 D+E). In addition, *Salmonella* induces caspase-1-dependent cell death in DC and macrophages (Brennan and Cookson, 2000; van der Velden et al., 2003; Watson et al., 2000) which can release intracellular bacteria to the extracellular space, providing a potential pathway for *Salmonella* to disseminate and infect other cell types in different areas of the mLN.

The identification of CCL17-expressing DC that most likely contained STM by histology lead to the hypothesis that CCL17$^+$ DC harbour STM and facilitate transportation of bacteria from the PP to mLN. Consistent with this hypothesis, flow cytometry analysis of DC after STM infection suggested that CCL17$^+$ DC are able to transport STM from the gut to mLN. Bacteria, however, were not restricted to CCL17$^+$ DC (Fig 3.1.7 D+E). Previous studies have described DC as the cell type responsible for the transport of STM from the gut to the mLN (Bogunovic et al., 2009; Bravo-Blas et al., 2019; Voedisch et al., 2009), but this is the first time that CCL17$^+$ DC were shown to participate in the spreading of STM. The approaches of Bogunovic et al. and Voedisch et al., as well as the approach of the present work, focused on the analysis of STM$^+$ DC in the mLN. A very recent study by Bravo-Blas et al. was able to analyse not only STM$^+$ mononuclear phagocytes within the mLN, but also all cells migrating via the lymphatics from the intestine to the mLN (Bravo-Blas et al., 2019). Cells were directly isolated from the thoracic duct of lymphadenectomised mice. Bravo-Blas and colleagues demonstrated that only DC, but not macrophages, migrate in the lymph after STM infection. A very small proportion of these migratory DC also carry STM. Bravo-Blas et al. showed that the CD103$^+$ CD11b$^+$ DC subset (30% of all STM$^+$ DC) are the main population harbouring STM in the mLN, consistent with the observations made by Bogunovic et al (50% of all STM$^+$ DC). In contrast, data presented here suggested that the CD103$^+$ CD11b$^-$ DC (50% of all STM$^+$ DC) subset was the principal population carrying STM in the mLN (Fig 3.1.7 F+G). Interestingly, all three studies, including the present, demonstrated that STM are not found exclusively within one single DC subpopulation. The differences between the present study, identifying the CD103$^+$ CD11b$^-$ DC population as the main STM$^+$ DC subset, and previous studies, naming the CD103$^+$ CD11b$^+$ DC-population as the main STM$^+$ DC subset (Bogunovic et al., 2009; Bravo-Blas et al., 2019), probably result from the different STM-infection model used (Bogunovic et al. and Bravo-Blas et al. used mice pre-treated with antibiotics prior to oral infection), STM strains, time points as well as slightly different gating strategies used within the three studies.

DC represent perfect ‘Trojan horses’ in which STM can survive (Bueno et al., 2008; Niedergang et al., 2000), and disseminate to systemic tissue by exploiting the intrinsic migration capacity of DC, mostly while hidden from detection by the effector immune response. DC, however, are a key link between innate and adaptive immunity. With their unique ability to prime antigen-specific naïve T cells, DC are vital for initiating adaptive immunity in response to infection. Virulent STM has developed strategies to interfere with the capacity of DC to prime adaptive immunity against bacteria e.g. *Salmonella* is able to inhibit T cell activation by interfering with MHCII antigen presentation on the DC surface (Bayer-Santos et al., 2016; Cheminay et al., 2005; Halici et al., 2008; Tobar et al., 2006). Hence, targeting DC does not only contribute to bacterial dissemination, but may also form part of an evolved immune evasion strategy, which specifically suppresses the adaptive immune response against *Salmonella*.

The present work not only identified the CD103$^+$ CD11b$^-$ DC-population as the main STM$^+$ DC subset, but also revealed the CD103$^+$ CD11b$^-$ DC subset as specifically targeted by *Salmonella* (Fig 3.1.7 F+G). Different intestinal DC subsets are associated with the activation of different effector T cells. The CD103$^+$ CD11b$^-$ DC subset is linked to cross-presentation to CD8$^+$ T cells (Cerovic et al., 2013) as well as to the activation of Th1 (Luda et al., 2016) and T$_{reg}$ cells (Esterházy et al., 2016; Welty et al., 2013). Targeting one specific DC subset such as the CD103$^+$ CD11b$^-$ DC population could ablate the development of specific effector T cell immune responses. In order to understand the dominance of one specific STM-harbouring DC population, more experiments would need to be performed.

Even though only DC can migrate from the gut to the mLN and thereby facilitate the spread of *Salmonella* (Bravo-Blas et al., 2019), also other myeloid cells were found to carry bacteria within the mLN, in the work presented here. *Salmonella* were consistently detected in newly extravasated monocytes, monocyte/macrophage intermediates, and macrophages, in addition to DC. Not a sole population but rather all of the populations analysed harboured bacteria to approximately the same extent (Fig 3.1.7 C). Bravo-Blas and colleagues did not make any statement about STM$^+$ monocytes, however, there is evidence that CD18$^+$ monocytes may harbour bacteria and contribute to the dissemination of *Salmonella* to systemic sites via the bloodstream (Worley et al., 2006). In addition, bacteria were found to travel extracellularly in the lymph (Bravo-Blas et al., 2019). This could explain how cells other than the migrating STM$^+$ DC take up bacteria in the mLN (Bravo-Blas et al., 2019).

CCL17 supports the transmission of *Salmonella* from the PP to the mLN

As outlined earlier, the chemokine CCL17 is required for CCR7-dependent DC migration in the skin (Stutte et al., 2010). Interestingly, In the present study, CCL17 deficiency resulted in decreased bacterial loads in mLN one day, but not three days, post-infection (Fig 3.1.3 B+D). CFU counts in PP, spleen and liver, however, did not differ one day post-infection (Fig 3.1.3 B). In conclusion, CCL17, which is predominately expressed by DC, likely contributes to the dissemination of *Salmonella* from the PP to the mLN, but not to systemic organs at the early stage of infection. The contribution of STM containing CCL17$^+$ DC to the transmission of *Salmonella* is most likely only detectable at an early stage of infection (day 1), because the exponential growth of bacteria at a later stage of infection (day 3) presumably masks the effect of a the incoming CCL17$^+$ STM$^+$ DC.

Consistent with the observations made here, Voedisch et al. demonstrated the impaired DC migration in CCR7$^{-/-}$ animals. They used growth-attenuated STM, and analysed the mLN, spleen and liver two days post-infection. A reduction of the bacterial load was detected in the mLN, but not in the liver or spleen of CCR7$^{-/-}$ mice. Experiments using virulent wt SL1344 STM, however, did not show any differences between CCR7$^{-/-}$ mice and wt controls (Voedisch et al., 2009), most likely because the analysis was performed too late, when the effect seen with growth-attenuated STM was already masked by the exponential growth of virulent *Salmonella* at that time point.

Findings from the present study as well as from Voedisch and colleagues indicate that DC facilitated transmission of *Salmonella* appears to be of significance for the early spreading of the bacteria from the intestine to the draining lymph nodes, but of minor importance for reaching systemic sites. This is probably because STM might also be transported by other cell types than DC such as monocytes, or DC might migrate independently of CCR7 and CCL17.

CCL17 expression is induced in distinct intestinal DC subsets upon *Salmonella* infection

CCL17 is known as an inflammatory chemokine, but only limited information is available on its expression after bacterial infection. Here, in a flow cytometry analysis of different myeloid cells, and in particular DC subsets, the data obtained indicated that CCL17$^+$ DC not only harbour STM and contribute to the transmission of bacteria but also, that upon infection, CCL17/EGFP expression is upregulated (Fig 3.1.5 and Fig 3.1.6). In line with these observations, TLR-stimulation via LPS or other PAMP (CpG-ODN, Poly-(I:C)), as well as TNFα induces CCL17 expression (Alferink et al., 2003; Fülle et al., 2018b; Globisch et al., 2014).

Salmonella infection appears to have a more indirect effect on the CCL17 expression level of DC, since the overall DC population upregulated CCL17/EGFP, not just the few STM$^+$ DC (Fig 3.1.6). It is likely that, extracellular STM may contribute to the overall stimulation of CCL17 expression in DC. In addition, inflammatory cytokines such as IL1β and IL18 released upon STM-induced pyroptotic cell death of infected DC and macrophages (Brennan and Cookson, 2000; van der Velden et al., 2003; Watson et al., 2000) may add to the indirect stimulation of CCL17 expression via the induction of TNFα (Bethea et al., 1992; Ledesma et al., 2004).

Remarkably, CCL17 expression, as well as the frequency of CCL17-expressing cells, increased in distinct DC subsets depending on the organ analysed. The DC populations that upregulated CCL17 in the PP were the cells that expressed CD103 whereas, in the mLN, the CD103$^-$ DC subsets showed the strongest level of upregulation (Fig 3.1.6). It is not clear whether the CD103$^+$ DC in PP that showed upregulation of CCL17 differentiate into the CD103$^-$ DC population with increased CCL17 expression in mLN, after they have migrated from the PP to the mLN and downregulated CD103, or if they represent a completely unrelated DC population. CD103 (α_E integrin), in combination with β_7 integrin, mediates cellular adhesion to E-cadherin, expressed by the epithelium (Cepek et al., 1994; Karecla et al., 1995). Mice deficient in CD103 demonstrated reduced mucosal-homing capabilities in T cells (Schön et al., 1999). In accordance, tissue-resident T cells express high levels of CD103 (Mackay et al., 2012; Wakim et al., 2010), suggesting an important role of CD103 in tissue retention. If CD103 on DC mediates tissue residence, then downregulation of CD103 may enable intestinal DC to migrate from the PP to the lymph nodes. Interestingly, human monocyte-derived DC downregulate CD103 upon bacterial infection (Roe et al., 2017). In conclusion, CD103$^+$ DC demonstrating increased CCL17 expression after STM infection may have migrated from the PP to the mLN in a CCR7-dependent manner, while downregulating CD103, thus becoming part of the CD103$^-$ DC population upon arrival in the mLN.

The upregulation of CCL17 in different DC subsets may not only have supported DC migration to the T cell areas in PP and mLN but, in addition, may have promoted DC-T cell interactions, important for the induction of a potent adaptive immune response. Different intestinal DC subtypes induce different effector T cell responses. Thus, a differential CCL17 expression in DC of PP compared to mLN might represent a way to direct the required T cell response for each site. In the intestine, Th17 cells play an important role in early protective immunity by limiting dissemination of *Salmonella* from PP to the mLN. Raffatellu and colleagues demonstrated increased systemic dissemination of STM from the gut in IL17 receptor-deficient mice, suggesting that defective IL17 responses cause defects in mucosal barrier functions (Raffatellu et al., 2008b). In addition, the induction of a potent Th1 response represents a key element in the defence against *Salmonella* (Johanns et al., 2010; Kupz et al., 2014; Mittrücker et al., 2002; Srinivasan et al., 2004). Both types of immune responses can be primed through CD103$^-$ DC (Cerovic et al., 2013; Scott et al., 2015). The induction of a strong Th1 and Th17 response in the mLN through CD103$^-$ DC might be most favourable. The adequate immune control of bacteria in the PP, the main entry-point of *Salmonella*, however, might not only require Th1 and Th17 T cells, but also T_{reg} cells, since an overshooting inflammatory immune response due to strong bacterial stimulation may be detrimental. Intestinal CD103$^+$ DC do not only activate Th1 and Th17 cells (Cerovic et al., 2013; Luda et al., 2016), but also promote T_{reg} cell differentiation (Esterházy et al., 2016; Welty et al., 2013). T_{reg} cells ensure a controlled immune response upon pathogen encounter in order to prevent immune pathology. In contrast, excessive suppression by T_{reg} cells can interfere with a potent immune response required for pathogen clearance, and hence dampen the effective control of infection (Belkaid, 2007; Rowe et al., 2012).

Taken together, the present work significantly increased our knowledge on CCL17 in the context of infection. CCL17$^+$ DC harbouring STM after infection were identified and may facilitate the dissemination of the bacteria. In addition, the differential upregulation of CCL17 in distinct intestinal DC subsets in response to *Salmonella* infection was revealed.

4.2 Deficiency in the chemokines CCL22 and CCL17 promotes a STM-specific Th1 response through the reduction of effector T_{reg} cells

Deficiency in CCL22 or combined deficiency in CCL22 and CCL17 potently inhibits effector T_{reg} cell expansion

In humans and mice, the CCL17/CCL22/CCR4 axis has attracted great attention in the context of allergic diseases such as asthma and contact dermatitis, but also in tumour therapy (Yoshie and Matsushima, 2015). CCL17 is associated with an inflammatory environment as opposed to CCL22, which acts in an immunosuppressive milieu. Their receptor, CCR4 is present on both, murine and human regulatory T cells (T_{reg}) (Curiel et al., 2004; Gobert et al., 2009; Iellem et al., 2001; Sugiyama et al., 2013; Watanabe et al., 2010; Yuan et al., 2007), next to other activated convectional T cells (Andrew et al., 2001; Inukai et al., 2007; Morimoto et al., 2005). In line, several studies have demonstrated an essential role for CCL22 in the recruitment of T_{reg} cells (Anz et al., 2015; Curiel et al., 2004; Gobert et al., 2009; Montane et al., 2011; Wiedemann et al., 2016). In mice, treatment with an anti-CCL22 antibody specifically reduced T_{reg} cell trafficking to tumours (Curiel et al., 2004). In humans, therapy with CCR4-specific monoclonal antibodies resulted in potent anti-tumour effects (Chang et al., 2012; Ishida et al., 2012; Sugiyama et al., 2013).

The role of CCL22 in the recruitment and/or induction of T_{reg} cells was confirmed through the present study. Here, this was demonstrated for the first time in the setting of a murine STM vaccination/challenge model, in contrast to previous studies that focused on cancer immunity and autoimmunity (Anz et al., 2015; Bischoff et al., 2015; Curiel et al., 2004; Montane et al., 2011; Wiedemann et al., 2016). The present work investigated the T_{reg} compartment of CCL17 and CCL22 single-deficient mice as well as CCL17/CCL22 double-deficient mice in steady-state, after vaccination, and vaccination/challenge. It was demonstrated that effector T_{reg} cells were reduced in CCL17/CCL22 double-deficient mice.

Interestingly, CCL22 single-deficient mice also showed a decrease in T_{reg} cells, but this was not as pronounced (Fig 3.2.10), indicating an essential role for CCL22 in the recruitment and/or induction of T_{reg} cells, and a minor role for CCL17. The knowledge on CCL17 and its potential role in the induction of T_{reg} cells is very limited, but available studies demonstrated that overall deficiency of CCL17 in CCL17$^{E/E}$ mice, or the blocking of CCL17 through an antibody, resulted in T_{reg} cell expansion (Heiseke et al., 2012; Weber et al., 2011b). Based on these findings and those from the present work, it can be concluded that, in the absence of CCL17, dominant immunosuppressive CCL22-CCR4 interactions control T_{reg} cell expansion. This hypothesis is supported by the way both chemokines, CCL22 and CCL17, interact with their receptor CCR4. CCL22 interacts with a different binding domain of CCR4 than CCL17 (Santulli-Marotto et al., 2015). In addition, CCL22 induces a more rapid desensitisation and internalisation of CCR4 compared to CCL17 (Imai et al., 1998; Mariani et al., 2004). In a competitive binding experiment to CCR4, CCL22 demonstrated a clear dominance over CCL17 (Imai et al., 1998). Taken together, these findings define both chemokines as biased at CCR4. Further, evidence suggests, that CCL22 is not only dominant over CCL17 in the activation of CCR4-signalling, but also that two distinct conformations of CCR4 exist: one major receptor-population that is activated by both ligands and one minor population that is activated by CCL22 alone (Anderson et al., 2016). In conclusion, biased agonism of CCL22 and CCL17 towards CCR4 results in CCL22 being the dominant factor attracting T_{reg} cells via CCR4 but not CCL17, however, CCL17 may well support this function. The dominance of CCL22 over CCL17 in this study was especially demonstrated through the strongly increased survival rate after virulent STM challenge of vaccinated CCL22 single-deficient mice, which equalled CCL17/CCL22 double-deficient mice, compared to CCL17 single-deficient mice (Fig 3.2.1). In addition, the dominance of CCL22 over CCL17 would explain why CCL22/CCL17 double-deficient mice performed slightly better in downregulating effector T_{reg} cells than CCL22 single-deficient mice, and why almost no effect was observed in CCL17 single-deficient mice (Fig 3.2.4, Fig 3.2.10).

Although, CCL22 is associated with the induction and/or recruitment of T_{reg} cells for almost two decades, the mechanism how CCL22 controls the T_{reg} response has only recently been discovered by Rapp et al. studying CCL22-deficient mice. They demonstrated that CCL22 expression by DC promotes the formation of stable cell-cell contacts between DC and T_{reg} cells, via the receptor CCR4, supporting potent T cell immunity (Rapp et al., 2019). In general, direct interactions between T_{reg} cells and DC is essential for the immunosuppressive functions of T_{reg} cells (Onishi et al., 2008; Takahashi et al., 1998; Tang et al., 2006; Thornton and Shevach, 1998). These findings could explain why only KLRG1^{+} effector T_{reg} cells, associated with high suppressive functions, were decreased in CCL17/CCL22 double-deficient mice. In the absence of CCL22, the cell-cell contacts between DC and T_{reg} cells are reduced (Rapp et al., 2019), which would probably result in decreased induction of suppressive T_{reg} cells. In addition, a study from Sugiyama et al. demonstrated that CCR4 is specifically expressed by a subset of terminally differentiated, highly suppressive T_{reg} cells, which might be identical to the KLRG1^{+} terminally differentiated effector T_{reg} cells identified in the present study, but not by naive T_{reg} cells from human peripheral blood (Sugiyama et al., 2013).

The frequencies of KLRG1^{+} effector T_{reg} cells in CCL17/CCL22 double-deficient mice were decreased after vaccination and vaccination/challenge in PP, draining lymph nodes and systemic organs. Surprisingly, this effect could also be observed in PP in steady-state. (Fig 3.2.16). CCL22 is expressed in steady-state (Rapp et al., 2019), but expression can be strongly increased by IL4, IL13, but also by LPS or CpG stimulation (Andrew et al., 1998; Inoue et al., 2017; Rapp et al., 2019; Vulcano et al., 2001). Such stimuli can also be provided by the gut microbiota (Lazar et al., 2018). The results of the present work suggest that CCL22 induced T_{reg} cell expansion requires a stimulus such as an infection, vaccination or, in the case of naïve mice, stimulation through the gut microbiota. The local stimulus provided by the gut microbiota, may lead to an expansion of T_{reg} cells restricted to the intestine (PP). In conclusion, the absence of CCL22 would result in a reduced expansion of T_{reg} cells, as it was observed in the present study. T_{reg} cells are essential mediators of immune tolerance, which restrain inappropriately strong inflammatory responses, the malfunction of which can result in autoimmune disorders (Lazar et al., 2018). Accordingly, some studies have already linked CCL22 to protection against autoimmunity (Bischoff et al., 2015; Eby et al., 2015; Montane et al., 2011).

The work of Rapp et al. showed that no obvious phenotypical differences in naïve CCL22-deficient mice can be observed in lymphoid organs, in terms of weight, morphology and proportion of immune cell subsets (Rapp et al., 2019). This could also be confirmed through the work of our lab analysing our in-house generated CCL22-single deficient and CCL17/CCL22 double-deficient mice (unpublished). This is also the case for CCL17-single deficient mice (Alferink et al., 2003). Although, both CCL22 and CCL17, are constitutively expressed under homeostatic conditions (Alferink et al., 2003; Rapp et al., 2019), deficiency in these chemokines does not interfere with the morphology or immune cell composition in lymphoid organs, with one exception observed in this study. All three chemokine KO mice demonstrated a decrease in absolute cell counts of PP, which could be partially accounted for, by the reduction of activated CD4$^+$ conventional T cells. Overall T$_{reg}$ cell counts were not affected (Fig 3.2.15). CCR4 is not only expressed by T$_{reg}$ cells but also by a variety of different activated conventional T cells (Andrew et al., 2001; Inukai et al., 2007; Morimoto et al., 2005; Yoshie and Matsushima, 2015). It might be that under homeostatic conditions the CCL17/CCL22/CCR4 axis is necessary for the homing of conventional T cells to the intestine, although it seems to be dispensable for homing to lymphoid organs (Rapp et al., 2019). Further experiments are required in order to fully understand the mechanisms responsible for the reduction in cell counts of PP. It has yet to be investigated which cell populations are decreased exactly in the PP of chemokine KO mice. Furthermore, it has not yet been determined if these observations are restricted to the PP, or if the cells of the LP are affected as well. Assessing other barrier organs like the skin or the lung, may provide more insights into how the CCL17/CCL22/CCR4 axis regulates homing of T cells to barrier organs, in contrast to lymphoid organs, in the steady-state.

A potent antigen-specific Th1 immune response against *Salmonella* is promoted by the reduction of effector T_{reg} cells

The principal that T_{reg} cells regulate inflammatory immune responses through the direct suppression of activated conventional T cells is well established (Dowling et al., 2018; Onishi et al., 2008; Sakaguchi et al., 2009; Sugiyama et al., 2013; Takahashi et al., 1998). While T_{reg} cells have a critical role in preventing autoimmune diseases, such as type 1 diabetes, and controlling chronic inflammatory diseases, such as inflammatory bowel disease and asthma, they also limit anti-tumour immunity and suppress favourable immune responses to pathogens resulting in pathogen persistence (Vignali et al., 2008). The successful regulation of an inflammatory immune response through T_{reg} cells is a question of balance. In the work presented here, a STM vaccine/challenge model was used in order to investigate the role of the chemokines CCL22 and CCL17 in building T cell immunity to *Salmonella*. The present study demonstrated that deficiency in CCL22 and CCL17 reduced effector T_{reg} cells and, in consequence, led to an increase in the STM-specific Th1 immune response, characterised by an expansion of Th1 T cells (Fig 3.2.5 A, Fig 3.2.11), which strikingly enhanced vaccine efficacy (Fig 3.2.1).

Suppression of conventional T (T_{conv}) cells by effector T_{reg} cells is facilitated via multiple routes, including secretion of anti-inflammatory cytokines (IL10), inducing apoptosis of target cells via the granzyme/perforin pathway, and by inhibition of DC (Vignali et al., 2008; Whibley et al., 2019). In the case of CCL22, a chemokine-specific way of blocking the inflammatory immune response is added. Rapp and colleagues showed that T_{conv} and T_{reg} cells compete for the same DC, and that dominance of T_{reg} over T_{conv} cells in terms of cell-cell contacts with the DC depends on DC-derived CCL22 (Rapp et al., 2019). Hence, CCL22 is required for T_{reg} cells to outcompete T_{conv} cells for space around the DC, a process that is central for suppression by T_{reg} cells. Decreasing the contact time between antigen-presenting DC and the precursors of T_{conv} effector cells, thus preventing activation, results in specific immune suppression (Onishi et al., 2008; Tadokoro et al., 2006). These findings are consistent with the observations made in the present work that demonstrated a reduction in the ratios of effector T_{reg}

cells/activated T_{conv} cells in CCL17/CCL22 double-deficient mice and in CCL22 single-deficient mice (Fig 3.2.5 B, Fig 3.2.13). In the absence of CCL22, DC and T_{reg} cells form less and shorter contacts (Rapp et al., 2019), putting the T_{conv} cells in a better position for the competition for cell-cell interactions with DC that are crucial for T cell activation. Overall, this would result in a change of effector T_{reg} cells/activated T_{conv} ratio, which in the case of STM immunity was clearly more beneficial, as demonstrated in the present study through a better vaccine efficacy (Fig 3.2.1).

Studies in both experimental animal models and humans have demonstrated that T_{reg} cells can accumulate following infection and interfere with the pathogen-specific immune response in a variety of ways that can be favourable for both the host and the pathogen. In a model of microbe-associated gut inflammation using *Helicobacter hepaticus*, adoptively transferred T_{reg} cells inhibited T cell-mediated and innate intestinal inflammation, and thus prevented immune pathology (Maloy et al., 2003). While insufficient inhibition by T_{reg} cells can promote tissue damage, an imbalance in effector T cell versus T_{reg} cell response in favour of suppressive T_{reg} cells can lead to pathogen persistence. Depletion of T_{reg} cells in a model for ongoing pulmonary paracoccidioidomycosis (PCM) rescued infected hosts from progressive and potentially fatal disease outcomes (Galdino et al., 2018). The function of T_{reg} cells in STM infection has only been poorly studied; Johanns and colleagues demonstrated that suppressive T_{reg} cells contribute to the inhibition of activated conventional T cells and to pathogen persistence using a mouse model of persistent STM infection (Johanns et al., 2010). Although the present work was performed in a different STM model, the findings from Johanns et al. that effector T_{reg} cells suppress potent T cell immune response to STM infection are consistent with the presented data. In the study presented here, no reduction in bacterial counts was observed in animals with reduced T_{reg} cells (CCL17/CCL22 double-deficient mice during the vaccination phase), in contrast to the study from Johanns and colleagues, who observed a slight reduction in bacterial counts (Johanns et al., 2010). The differences are most likely based on the fact that, in the present work, effector T_{reg} cells were reduced due to the absence of CCL22, whereas in the study of Johanns et al. FOXP3^{DTR} mice were used and T$_{reg}$ cells were depleted completely.

Interestingly, KLRG1^{+} effector T$_{reg}$ cells, which inhibited activated T$_{conv}$ cells with a Th1 phenotype, were characterised in our model by the expression of CXCR3, but were negative for CXCR6 expression. Like CXCR3 (Groom and Luste, 2011; Kim et al., 2001), CXCR6 can be used as a Th1 T cell marker (Kim et al., 2001; Latta et al., 2007) but, in contrast to CXCR3 which is expressed on 90% of all Th1 polarised cells, CXCR6 is only expressed on 20% of all Th1 T cells (Kim et al., 2001). CXCR6 expression, however, can be connected to CD8^{+} T cell memory formation after infection, especially for tissue-resident cells (Heesch et al., 2014; Tse et al., 2014; Zaid et al., 2017). Hence, CXCR6^{-} T cells might represent effector T cells and CXCR6^{+} cells might represent memory T cells that have turned off their effector gene expression.

Translating findings from the mouse model into the human setting

Prof. A. Pollard and colleagues performed a human challenge study of *Salmonella* Typhi infection in 2016. In a randomised controlled trial, the commercially available Ty21a-vaccine was compared with the new M01ZH09-vaccine and placebo (Darton et al., 2016). This clinical study allowed us to test whether lower CCL22 levels in the blood would correlate with better vaccine efficacy, purportedly due to a reduction in T$_{reg}$ cells and hence an enhancement of T cell immune response, analogous to the mouse model. Human plasma samples from the *Salmonella* Typhi challenge study were analysed for the chemokines CCL22 and CCL17. Unfortunately, no clear correlation between CCL22 or CCL17 concentrations and vaccine outcome was observed but, paradoxically, higher serum levels of CCL17 or CCL22 appeared to be associated with disease protection (Fig 3.3 B).

Animal models, and in particular the mouse model, have been instrumental in establishing a number of conceptual improvements in our understanding of human *Salmonella* disease. A limitation, however, of the mouse model for typhoid-like enteric fever is that *S*. Typhimurium causes acute inflammatory diarrhea in humans rather than a systemic illness, and therefore implies a differential type of immune response to *S*. Typhimurium in humans compared to laboratory mice (Palmer and Slauch, 2017; Santos et al., 2001). The limitations of the mouse model may also be applicable to the present study. The principle of blocking the CCL17/CCL22/CCR4 axis in order to inhibit T_{reg} cells and thus improve immune response, however, is not only applicable in the murine models but also in humans (Chang et al., 2012; Ishida et al., 2012; Sugiyama et al., 2013).

Another reason why no correlations between low CCL22/CCL17 plasma levels and beneficial vaccine outcome were observed could be that the results in the mouse model were obtained by analysing local immunity in the gut and systemic organs. CCL22 and CCL17 concertation in plasma were not determined in the mouse model. It may be useful to analyse serum levels in mice when trying to interpret CCL22 and CCL17 concentrations in human plasma in connection to vaccine protection.

The most likely explanation may certainly be that a naturally occurring low concentration of CCL22 in the circulation may just not be sufficient to inhibit T_{reg} cell induction and to boost the vaccine efficacy. Blocking CCL22 during the vaccination process may be required.

Boosting vaccines – how blocking of the chemokines CCL17 and CCL22 could contribute to vaccine efficacy

Regulatory T cells have an important function in controlling the immune system yet, in some situations, they may be detrimental. T_{reg} cells play a crucial role in suppressing anti-tumour immune responses, hence targeting these cells is of exceptional interest. T_{reg} cells can be targeted through different approaches. Chemotherapeutic agents reduce the quantity of T_{reg} cells and synergise with immune-modulatory drugs to enhance anti-tumour immunity, but this is usually achieved in a T_{reg} cell non-specific way. Epigenetic modifiers promote the conversion of T_{reg} cells into 'effector-like' $CD4^+$ T cells, but such interventions may potentially have off-target effects. Surface markers expressed on T_{reg} cells such as CCR4 can be targeted in order to specifically deplete or block T_{reg} cells, but these could also interfere with non-tumour related T_{reg} cells that express the same markers (Han et al., 2019). In the field of tumour therapy, the use of anti-CCR4 antibodies has proven to be a potent instrument to enhance tumour immunity in humans (Chang et al., 2012; Ishida et al., 2012; Kamada et al., 2019; Sugiyama et al., 2013) e.g. via selectively removing CCR4$^+$ effector T$_{reg}$ cells (Kamada et al., 2019; Sugiyama et al., 2013) or inhibiting chemotaxis and reducing suppressive activity of T$_{reg}$ cells (Chang et al., 2012). The experience and knowledge that has been acquired in cancer therapy with respect to boosting immunity through the inhibition/depletion of T$_{reg}$ cells can be transferred to vaccine research, where a similar aim is pursued. In fact, blocking T$_{reg}$ cells has shown very good results in improving vaccine responses (Bayry et al., 2008; Davies et al., 2009; Espinoza Mora et al., 2014; Knuschke et al., 2016; Moore et al., 2005). In an interesting approach, Bayry and colleagues used a small molecule CCR4-antagonist as vaccine adjuvant to target and decrease local recruitment of CCR4$^+$ T$_{reg}$ cells in order to amplify vaccine responses. They demonstrated that CCR4 antagonists can enhance the response to a poorly immunogenic protein antigen to a level of a commercially available alum-adjuvanted vaccine (Bayry et al., 2008). A very similar approach to block the CCL17/CCL22/CCR4 axis is currently undertaken in our group (Förster lab, LIMES institute). In a proof-of-principle experiment the efficiency of CCL17-specific aptamers for inhibition of CHS reactions during the elicitation phase was shown (Fülle et al., 2018a). High-affinity RNA aptamers with specificity for CCL22 are developed at the moment, as they were developed and tested for CCL17. Targeting CCL22 in a vaccine approach instead of its receptor, CCR4, may represent a more specific way to block CCR4$^+$ T$_{reg}$ cells and thus enhance vaccine responses. Furthermore, unlike vaccines using aluminium phosphate (alum) as adjuvant, which is a good inducer of antibody responses but a poor inducer of cellular immune responses (Hutchings et al., 2005), blocking T$_{reg}$ cells through CCL22 specific aptamers may allow for enhancement of both humoral and cellular immune responses, as has been demonstrated for the CCR4 antagonists (Bayry et al., 2008).

In summary, inhibition of effector T$_{reg}$ cells e.g. through high-affinity RNA aptamers with specificity for CCL22 may represent a powerful tool to enhance immunity and hence boost vaccine responses. This approach may be particularly valuable when used for already existing vaccines with poor protection or for patients with a weak immune system such as infants or the elderly.

5 References

Acharya, I.L., Lowe, C.U., Thapa, R., Gurubacharya, V.L., Shrestha, D.B., Cadoz, M., Schulz, D., Armand, J., Bryla, D.A., Trollfors, B., et al. (1987). Prevention of typhoid fever in Nepal with the Vi capsular polysaccharide of Salmonella typhi. A preliminary report. N. Engl. J. Med. *317*.

Achuthan, A., Cook, A.D., Lee, M.-C., Saleh, R., Khiew, H.-W., Chang, M.W.N., Louis, C., Fleetwood, A.J., Lacey, D.C., Christensen, A.D., et al. (2016). Granulocyte macrophage colony-stimulating factor induces CCL17 production via IRF4 to mediate inflammation. J. Clin. Invest. *126*, 3453–3466.

Agnès, W., Isabelle, V.P., Anne-Marie, C.M., Adam, S., and Philippe, V. (2014). Interactions of salmonella with animals and plants. Front. Microbiol. *5*, 1–18.

Akkaya, B., Oya, Y., Akkaya, M., Al Souz, J., Holstein, A.H., Kamenyeva, O., Kabat, J., Matsumura, R., Dorward, D.W., Glass, D.D., et al. (2019). Regulatory T cells mediate specific suppression by depleting peptide–MHC class II from dendritic cells. Nat. Immunol. *20*, 218–231.

Alferink, J., Lieberam, I., Reindl, W., Behrens, A., Weiß, S., Hüser, N., Gerauer, K., Ross, R., Reske-Kunz, A.B., Ahmad-Nejad, P., et al. (2003). Compartmentalized Production of CCL17 In Vivo: Strong Inducibility in Peripheral Dendritic Cells Contrasts Selective Absence from the Spleen. J. Exp. Med. J. Exp. Med *00*, 585–599.

Alferink, J., Specht, S., Arends, H., Schumak, B., Schmidt, K., Ruland, C., Lundt, R., Kemter, A., Dlugos, A., Kuepper, J.M., et al. (2016). Cannabinoid receptor 2 modulates susceptibility to experimental cerebral malaria through a CCL17-dependent Mechanism. J. Biol. Chem. *291*, 19517–19531.

Anderson, C.A., Solari, R., and Pease, J.E. (2016). Biased agonism at chemokine receptors: obstacles or opportunities for drug discovery? J. Leukoc. Biol. *99*, 901–909.

Andrew, D.P., Chang, M., McNinch, J., Wathen, S.T., Rihanek, M., Tseng, J., Spellberg, J.P., and III, C.G.E. (1998). STCP-1 (MDC) CC Chemokine Acts Specifically on Chronically Activated Th2 Lymphocytes and Is Produced by Monocytes on Stimulation with Th2 Cytokines IL-4 and IL-13 David. J. Immunol. *161*, 5027–5038.

Andrew, D.P., Ruffing, N., Kim, C.H., Miao, W., Heath, H., Li, Y., Murphy, K., Campbell, J.J., Butcher, E.C., and Wu, L. (2001). C-C Chemokine Receptor 4 Expression Defines a Major Subset of Circulating Nonintestinal Memory T Cells of Both Th1 and Th2 Potential. J. Immunol. *166*, 103–111.

Andrews, J.R., and Ryan, E.T. (2015). Diagnostics for invasive Salmonella infections: current challenges and future directions. Physiol. Behav. *19*.

Anz, D., Rapp, M., Eiber, S., Koelzer, V.H., Thaler, R., Haubner, S., Knott, M., Nagel, S., Golic, M., Wiedemann, G.M., et al. (2015). Suppression of intratumoral CCL22 by type I interferon inhibits migration of regulatory T cells and blocks cancer progression. Cancer Res. *75*, 4483–4493.

Arpaia, N., Godec, J., Lau, L., Sivick, K.E., McLaughlin, L.M., Jones, M.B., Dracheva, T., Peterson, S.N., Monack, D.M., and Barton, G.M. (2011). TLR signaling is required for salmonella typhimurium virulence. Cell *144*, 675–688.

Bain, C.C., Scott, C.L., Uronen-Hansson, H., Gudjonsson, S., Jansson, O., Grip, O., Guilliams, M., Malissen, B., Agace, W.W., and Mowat, a M. (2013). Resident and pro-inflammatory macrophages in the colon represent alternative context-dependent fates of the same Ly6Chi monocyte precursors. Mucosal Immunol. *6*, 498–510.

Baker, S., and Dougan, G. (2007). The Genome of Salmonella enterica Serovar Typhi. Clin. Infect. Dis. *45*, S29–S33.

Bayer-Santos, E., Durkin, C.H., Rigano, L.A., Kupz, A., Alix, E., Cerny, O., Jennings, E., Liu, M., Ryan, A.S., Lapaque, N., et al. (2016). The Salmonella Effector SteD Mediates MARCH8-Dependent Ubiquitination of MHC II Molecules and Inhibits T Cell Activation. Cell Host Microbe.

Bayry, J., Tchilian, E.Z., Davies, M.N., Forbes, E.K., Draper, S.J., Kaveri, S. V., Hill, A.V.S., Kazatchkine, M.D., Beverley, P.C.L., Flower, D.R., et al. (2008). In silico identified CCR4 antagonists target regulatory T cells and exert adjuvant activity in vaccination. Proc. Natl. Acad. Sci. U. S. A. *105*, 10221–10226.

Belkaid, Y. (2007). Regulatory T cells and infection: A dangerous necessity. Nat. Rev. Immunol. *7*, 875–888.

Benoun, J.M., Peres, N.G., Wang, N., Pham, O.H., Rudisill, V.L., Fogassy, Z.N., Whitney, P.G., Fernandez-Ruiz, D., Gebhardt, T., Pham, Q.M., et al. (2018). Optimal protection against Salmonella infection requires noncirculating memory. Proc. Natl. Acad. Sci. U. S. A. *115*, 10416–10421.

Bethea, J.R., Gillespie, G.Y., and Benveniste, E.N. (1992). Interleukin-1β induction of TNF-α gene expression: Involvement of protein kinase C. J. Cell. Physiol. *152*, 264–273.

Bhaumik, S., and Basu, R. (2017). Cellular and molecular dynamics of Th17 differentiation and its developmental plasticity in the intestinal immune response. Front. Immunol. *8*, 1–20.

Bilate, A.M., and Lafaille, J.J. (2012). Induced CD4 + Foxp3 + Regulatory T Cells in Immune Tolerance . Annu. Rev. Immunol. *30*, 733–758.

Bischoff, L., Alvarez, S., Dai, D.L., Soukhatcheva, G., Orban, P.C., and Verchere, C.B. (2015). Cellular Mechanisms of CCL22-Mediated Attenuation of Autoimmune Diabetes. J. Immunol. *194*, 3054–3064.

Blanchette, J., Jaramillo, M., and Olivier, M. (2003). Signalling events involved in interferon-γ-inducible macrophage nitric oxide generation. Immunology *108*, 513–522.

Boehm, U., Klamp, T., Groot, M., and Howard, J.C. (1997). Cellular responses to Interferon-γ. Annu. Rev. Immunol. *15*, 749–795.

Bogunovic, M., Ginhoux, F., Helft, J., Shang, L., Hashimoto, D., Greter, M., Liu, K., Jakubzick, C., Ingersoll, M.A., Leboeuf, M., et al. (2009). Origin of the Lamina Propria Dendritic Cell Network. Immunity *18*, 513–525.

Bravo-Blas, A., Utriainen, L., Clay, S.L., Kästele, V., Cerovic, V., Cunningham, A.F., Henderson, I.R., Wall, D.M., and Milling, S.W.F. (2019). Salmonella enterica Serovar Typhimurium Travels to Mesenteric Lymph Nodes Both with Host Cells and Autonomously . J. Immunol. *202*, 260–267.

Brennan, M.A., and Cookson, B.T. (2000). Salmonella induces macrophage death by caspase-1-dependent necrosis. Mol. Microbiol. *38*, 31–40.

Brenner, F.W., Villar, R.G., Tauxe, R., Swaminathan, B., Detec-, O., and National, T. (2000). Guest commentary. *38*, 2465–2467.

Britto, C.D., Wong, V.K., Dougan, G., and Pollard, A.J. (2018). A systematic review of antimicrobial resistance in Salmonella enterica serovar Typhi, the etiological agent of typhoid. PLoS Negl. Trop. Dis. *12*, e0006779.

Broz, P., Ohlson, M.B., and Monack, D.M. (2012). Innate immune response to Salmonella typhimurium, a model enteric pathogen. Gut Microbes.

Bueno, S.M., González, P.A., Carreño, L.J., Tobar, J.A., Mora, G.C., Pereda, C.J., Salazar-Onfray, F., and Kalergis, A.M. (2008). The capacity of Salmonella to survive inside dendritic cells and prevent antigen presentation to T cells is host specific. Immunology *124*, 522–533.

Burton, N.A., Schürmann, N., Casse, O., Steeb, A.K., Claudi, B., Zankl, J., Schmidt, A., and Bumann, D. (2014). Disparate impact of oxidative host defenses determines the fate of salmonella during systemic infection in mice. Cell Host Microbe *15*, 72–83.

Carden, S.E., Walker, G.T., Honeycutt, J., Lugo, K., Pham, T., Jacobson, A., Bouley, D., Idoyaga, J., Tsolis, R.M., and Monack, D. (2017). Pseudogenization of the Secreted EffectorGenesseI Confers Rapid Systemic Dissemination of S. Typhimurium ST313 within Migratory Dendritic Cells. Cell Host Microbe *21*, 182–194,.

Cardona, S.M., Garcia, J.A., and Cardona, A.E. (2013). The fine balance of chemokines during disease: trafficking, inflammation and homeostasis. Methods Mol. Biol. *1013*, 1–16.

Carter, P.B., and Collins, F. (1974). The Route of enteric Infection in normal mice. J. Exp. Med. *139*.

Cellier, M. (2013). Cell-Type Specific Determinants of NRAMP1 Expression in Professional Phagocytes. Biology (Basel). *2*, 233–283.

Cepek, K.L., Shaw, S.K., Parker, C.M., Russell, G.J., Morrow, J.S., Rimm, D.L., and Brenner, M.B. (1994). Adhesion between epithelial cells and T lymphocytes mediated by E-cadherin and the α e β 7 integrin. Nature *372*, 190–193.

Cerovic, V., Houston, S.A., Scott, C.L., Aumeunier, A., Yrlid, U., Mowat, A.M., and Milling, S.W.F. (2013). Intestinal CD103- dendritic cells migrate in lymph and prime effector T cells. Mucosal Immunol. *6*, 104–113.

Cerovic, V., Bain, C.C., Mowat, A.M., and Milling, S.W.F. (2014). Intestinal macrophages and dendritic cells: What’s the difference? Trends Immunol. *35*, 270–277.

Chang, D.-K., Sui, J., Geng, S., Muvaffak, A., Bai, M., Fuhlbrigge, R.C., Lo, A., Yammanuru, A., Hubbard, L., Sheehan, J., et al. (2012). Humanization of an anti-CCR4 antibody that kills Cutaneous T- Cell Lymphoma cells and abrogates suppression by T-regulatory cells. Mol Cancer Ther. *11*, 2451–2461.

Cheminay, C., Möhlenbrink, A., and Hensel, M. (2005). Intracellular Salmonella Inhibit Antigen Presentation by Dendritic Cells . J. Immunol. *174*, 2892–2899.

Cheng, G., Yuan, X., Tsai, M.S., Podack, E.R., Yu, A., and Malek, T.R. (2012). IL-2 Receptor Signaling Is Essential for the Development of Klrg1 + Terminally Differentiated T Regulatory Cells . J. Immunol. *189*, 1780–1791.

Cheng, G., Yuan, X., Tsai, M.S., Podack, E.R., Yu, A., and Malek, T.R. (2014). Interleukin-2 receptor signaling is essential for the development of Klrg1+ terminally differentiated T regulatory cells. J Immunol *27*, 1–19.

Cretney, E., Kallies, A., and Nutt, S.L. (2013). Differentiation and function of Foxp3+ effector regulatory T cells. Trends Immunol. *34*, 74–80.

Curiel, T.J., Coukos, G., Zou, L., Alvarez, X., Cheng, P., Mottram, P., Evdemon-Hogan, M., Conejo-Garcia, J.R., Zhang, L., Burow, M., et al. (2004). Specific recruitment of regulatory T cells in ovarian carcinoma fosters immune privilege and predicts reduced survival. Nat. Med. *10*, 942–949.

Curtis, M.M., and Way, S.S. (2009). Interleukin-17 in host defence against bacterial, mycobacterial and fungal pathogens. Immunology *126*, 177–185.

Darton, T.C., Jones, C., Blohmke, C.J., Waddington, C.S., Zhou, L., Peters, A., Haworth, K., Sie, R., Green, C.A., Jeppesen, C.A., et al. (2016). Using a Human Challenge Model of Infection to Measure Vaccine Efficacy: A Randomised, Controlled Trial Comparing the Typhoid Vaccines M01ZH09 with Placebo and Ty21a. PLoS Negl. Trop. Dis. *10*, 1–27.

Davies, M.N., Bayry, J., Tchilian, E.Z., Vani, J., Shaila, M.S., Forbes, E.K., Draper, S.J., Beverley, P.C.L., Tough, D.F., and Flower, D.R. (2009). Toward the Discovery of Vaccine Adjuvants: Coupling In Silico Screening and In Vitro Analysis of Antagonist Binding to Human and Mouse CCR4 Receptors. PLoS One *4*.

Dougan, G., John, V., Palmer, S., and Mastroeni, P. (2011). Immunity to salmonellosis. Immunol. Rev. *240*, 196–210.

Dowling, M.R., Kan, A., Heinzel, S., Marchingo, J.M., Hodgkin, P.D., and Hawkins, E.D. (2018). Regulatory T Cells Suppress Effector T Cell Proliferation by Limiting Division Destiny. Front. Immunol. *9*, 2461.

Eby, J.M., Kang, H., Tully, S.T., Bindeman, W.E., Daniel, S., Chatterjee, S., Mehrotra, S., and Poole, I.C. Le (2015). CCL22 to activate Treg migration and suppress depigmentation in vitiligo. J Invest Dermatol *135*, 1574–1580.

Edelson, B.T., Wumesh, K.C., Juang, R., Kohyama, M., Benoit, L.A., Klekotka, P.A., Moon, C., Albring, J.C., Ise, W., Michael, D.G., et al. (2010). Peripheral CD103+ dendritic cells form a unified subset developmentally related to CD8α+ conventional dendritic cells. J. Exp. Med. *207*, 823–836.

Edsall, G., Gaines, S., Landy, M., Tigertt, W., Sprinz, H., Trapani, R., Mandel, A., and Benson, A. (1960). Studies on infection and immunity in experimental typhoid fever. J Exp Med *112*, 143–166.

Eisenbarth, S.C. (2019). Dendritic cell subsets in T cell programming: location dictates function. Nat. Rev. Immunol. *19*, 89–103.

Elhussein Mohamed, O.Y., Elazomi, A., Mohamed, M.S., and Abdalla, F.B. (2016). Local elevation of CCL22: A new trend in immunotherapy (skin model). J. Cell. Immunother. *2*, 79–84.

Engels, E.A., Falagas, M.E., Lau, J., and Bennish, M.L. (1998). Typhoid fever vaccines: A meta-analysis of studies on efficacy and toxicity. Br. Med. J. *316*, 110–116.

Espinoza Mora, M.D.R., Steeg, C., Tartz, S., Heussler, V., Sparwasser, T., Link, A., Fleischer, B., and Jacobs, T. (2014). Depletion of regulatory T cells augments a vaccine-induced T effector cell response against the liver-stage of malaria but fails to increase memory. PLoS One *9*.

Esterházy, D., Loschko, J., London, M., Jove, V., Oliveira, T.Y., and Mucida, D. (2016). Classical dendritic cells are required for dietary antigen- mediated peripheral regulatory T cell and tolerance induction. Nat. Immunol. *17*, 545–555.

Farache, J., Koren, I., Milo, I., Gurevich, I., Kim, K.W., Zigmond, E., Furtado, G.C., Lira, S.A., and Shakhar, G. (2013). Luminal Bacteria Recruit CD103+ Dendritic Cells into the Intestinal Epithelium to Sample Bacterial Antigens for Presentation. Immunity.

Feasey, N.A., Dougan, G., Kingsley, R.A., Heyderman, R.S., and Gordon, M.A. (2012). Invasive non-typhoidal salmonella disease: An emerging and neglected tropical disease in Africa. Lancet *379*, 2489–2499.

Feuerer, M., Hill, J.A., Kretschmer, K., Von Boehmer, H., Mathis, D., and Benoist, C. (2010). Genomic definition of multiple ex vivo regulatory T cell subphenotypes. Proc. Natl. Acad. Sci. U. S. A. *107*, 5919–5924.

Forrest, B.D., Labrooy, J.T., Beyer, L., Dearlove, C.E., and Shearman, D.J.C. (1991). The human humoral immune response to salmonella typhi ty2la. J. Infect. Dis. *163*, 336–345.

Fülle, L., Steiner, N., Funke, M., Gondorf, F., Pfeiffer, F., Siegl, J., Opitz, F. V., Haßel, S.K., Erazo, A.B., Schanz, O., et al. (2018a). RNA Aptamers Recognizing Murine CCL17 Inhibit T Cell Chemotaxis and Reduce Contact Hypersensitivity In Vivo. Mol. Ther. *26*, 95–104.

Fülle, L., Offermann, N., Hansen, J.N., Breithausen, B., Erazo, A.B., Schanz, O., Radau, L., Gondorf, F., Knöpper, K., Alferink, J., et al. (2018b). CCL17 exerts a neuroimmune modulatory function and is expressed in hippocampal neurons. Glia *66*, 2246–2261.

Galdino, N.A.L., Loures, F. V., de Araújo, E.F., da Costa, T.A., Preite, N.W., and Calich, V.L.G. (2018). Depletion of regulatory T cells in ongoing paracoccidioidomycosis rescues protective Th1/Th17 immunity and prevents fatal disease outcome. Sci. Rep. *8*, 1–15.

Gambineri, E., Torgerson, T.R., and Ochs, H.D. (2003). Immune dysregulation, polyendocrinopathy, enteropathy, and X-linked inheritance (IPEX), a syndrome of systemic autoimmunity caused by mutations of FOXP3, a critical regulator of T-cell homeostasis. Curr. Opin. Rheumatol. *15*, 430–435.

Gayet, R., Bioley, G., Rochereau, N., Paul, S., and Corthésyb, B. (2017). Vaccination against Salmonella Infection : The Mucosal Way. Microbiol. Mol. Biol. Rev. *81*, 1–26.

Gilchrist, J.J., MacLennan, C.A., and Hill, A.V.S. (2015). Genetic susceptibility to invasive Salmonella disease. Nat. Rev. Immunol. *15*, 452–463.

Globisch, T., Steiner, N., Fülle, L., Lukacs-Kornek, V., Degrandi, D., Dresing, P., Alferink, J., Lang, R., Pfeffer, K., Beyer, M., et al. (2014). Cytokine-dependent regulation of dendritic cell differentiation in the splenic microenvironment. Eur. J. Immunol. *44*, 500–510.

Göbel, K., Bittner, S., Melzer, N., Pankratz, S., Dreykluft, A., Schuhmann, M.K., Meuth, S.G., and Wiendl, H. (2012). CD4 + CD25 + FoxP3 + regulatory T cells suppress cytotoxicity of CD8 + effector T cells: Implications for their capacity to limit inflammatory central nervous system damage at the parenchymal level. J. Neuroinflammation *9*, 1–9.

Gobert, M., Treilleux, I., Bendriss-Vermare, N., Bachelot, T., Goddard-Leon, S., Arfl, V., Biota, C., Doffin, A.C., Durand, I., Olive, D., et al. (2009). Regulatory T cells recruited through CCL22/CCR4 are selectively activated in lymphoid infiltrates surrounding primary breast tumors and lead to an adverse clinical utcome. Cancer Res. *69*, 2000–2009.

Godiska, B.R., Chantry, D., Raport, C.J., Sozzani, S., Allavena, P., Leviten, D., Mantovani, A., and Gray, P.W. (1997). Human Macrophage–derived Chemokine (MDC), a Novel Chemoattractant for Monocytes, Monocyte-derived Dendritic Cells, and Natural Killer Cells. J Exp Med *185*.

Gordon, M.A. (2008). Salmonella infections in immunocompromised adults. J. Infect. *56*, 413–422.

Greaves, D.R., Hakkinen, T., Lucas, a D., Liddiard, K., Jones, E., Quinn, C.M., Senaratne, J., Green, F.R., Tyson, K., Boyle, J., et al. (2001). Linked chromosome 16q13 chemokines, macrophage-derived chemokine, fractalkine, and thymus- and activation-regulated chemokine, are expressed in human atherosclerotic lesions. Arter. Thromb Vasc Biol *21*, 923–929.

Griffin, A.J., and McSorley, S.J. (2011). Development of protective immunity to Salmonella, a mucosal pathogen with a systemic agenda. Mucosal Immunol.

Griffith, J.W., Sokol, C.L., and Luster, A.D. (2014). Chemokines and Chemokine Receptors: Positioning Cells for Host Defense and Immunity. Annu. Rev. Immunol. *32*, 659–702.

Groom, J.R., and Luste, A.D. (2011). CXCR3 in T cell function. Exp. Cell Res. *317*, 620–631.

den Haan, J.M.M., Arens, R., and van Zelm, M.C. (2014). The activation of the adaptive immune system: Cross-talk between antigen-presenting cells, T cells and B cells. Immunol. Lett. *162*, 103–112.

Hadis, U., Wahl, B., Schulz, O., Hardtke-Wolenski, M., Schippers, A., Wagner, N., Müller, W., Sparwasser, T., Förster, R., and Pabst, O. (2011). Intestinal Tolerance Requires Gut Homing and Expansion of FoxP3+ Regulatory T Cells in the Lamina Propria. Immunity *34*, 237–246.

Halici, S., Zenk, S.F., Jantsch, J., and Hensel, M. (2008). Functional analysis of the Salmonella pathogenicity island 2-mediated inhibition of antigen presentation in dendritic cells. Infect. Immun. *76*, 4924–4933.

Han, S.J., Toker, A., Liu, Z.Q., and Ohashi, P.S. (2019). Turning the tide against regulatory T cells. Front. Oncol. *9*, 1–16.

Heesch, K., Raczkowski, F., Schumacher, V., Hünemörder, S., Panzer, U., and Mittrücker, H.W. (2014). The function of the chemokine receptor CXCR6 in the T cell response of mice against Listeria monocytogenes. PLoS One *9*.

Heiseke, A.F., Faul, A.C., Lehr, H.A., Förster, I., Schmid, R.M., Krug, A.B., and Reindl, W. (2012). CCL17 promotes intestinal inflammation in mice and counteracts regulatory T cell-mediated protection from colitis. Gastroenterology *142*, 335–345.

Hess, J., Ladel, C., Miko, D., and Kaufmann, S.H.E. (1996). Salmonella typhimurium aroA- infection in gene-targeted immunodeficient mice: major role of CD4+ TCR-alpha beta cells and IFN-gamma in bacterial clearance independent of intracellular location. J Immunol 3321–3326.

Hoogewerf, A.J., Black, D., Proudfoot, A.E.I., Wells, T.N.C., and Power, C.A. (1996). Molecular cloning of murine CC CKR-4 and high affinity binding of chemokines to murine and human CC CKR-4. Biochem. Biophys. Res. Commun. *218*, 337–343.

Hopkins, S.A., Niedergang, F., Corthesy-Theulaz, I.E., and Kraehenbuhl, J.P. (2000). A recombinant Salmonella typhimurium vaccine strain is taken up and survives within murine Peyer's patch dendritic cells. Cell. Microbiol. *2*, 59–68.

Hughes, C.E., and Nibbs, R.J.B. (2018). A guide to chemokines and their receptors. FEBS J. *285*, 2944–2971.

Hutchings, C.L., Gilbert, S.C., Hill, A.V.S., and Moore, A.C. (2005). Novel Protein and Poxvirus-Based Vaccine Combinations for Simultaneous Induction of Humoral and Cell-Mediated Immunity. J. Immunol. *175*, 599–606.

Iellem, A., Mariani, M., Lang, R., Recalde, H., Panina-Bordignon, P., Sinigaglia, F., and D'Ambrosio, D. (2001). Unique chemotactic response profile and specific expression of chemokine receptors CCR4 and CCR8 by CD4+CD25+ regulatory T cells. J. Exp. Med. *194*, 847–853.

Imai, T., Yoshida, T., Baba, M., Nishimura, M., Kakizaki, M., and Yoshie, O. (1996). Molecular cloning of a novel T cell-directed CC chemokine expressed in thymus by signal sequence trap using Epstein-Barr virus vector. J. Biol. Chem. *271*, 21514–21521.

Imai, T., Baba, M., Nishimura, M., Kakizaki, M., Takagi, S., and Yoshie, O. (1997). The T cell-directed CC chemokine TARC is a highly specific biological ligand for CC chemokine receptor 4. J. Biol. Chem. *272*, 15036–15042.

Imai, T., Chantry, D., Raport, C.J., Wood, C.L., Nishimura, M., Godiska, R., Yoshie, O., and Gray, P.W. (1998). Macrophage-derived Chemokine Is a Functional Ligand for the CC Chemokine Receptor 4. J. Biol. Chem. *273*, 7118–7122.

Inoue, M., Yamada, J., Aomatsu-Kikuchi, E., Satoh, K., Kondo, H., Ishisaki, A., and Chosa, N. (2017). SCRG1 suppresses LPS-induced CCL22 production through ERK1/2 activation in mouse macrophage Raw264.7 cells. Mol. Med. Rep. *15*, 4069–4076.

Inukai, Y., Momobayashi, A., Sugawara, N., and Aso, Y. (2007). Changes in expression of T-helper (Th) 1- and Th2-associated chemokine receptors on peripheral blood lymphocytes and plasma concentrations of their ligands, interferon-inducible protein-10 and thymus and activation-regulated chemokine, after antithyroid d. Eur. J. Endocrinol. *156*, 623–630.

Ishida, T., Joh, T., Uike, N., Yamamoto, K., Utsunomiya, A., Yoshida, S., Saburi, Y., Miyamoto, T., Takemoto, S., Suzushima, H., et al. (2012). Defucosylated anti-CCR4 monoclonal antibody (KW-0761) for relapsed adult T-cell leukemia-lymphoma: A multicenter phase II study. J. Clin. Oncol. *30*, 837–842.

Iwasaki, A., and Medzhitov, R. (2015). Control of adaptive immunity by the innate immune system. Nat. Immunol. *16*, 343–353.

Jabado, N., Picard, V., Gros, P., Jankowski, A., Dougaparsad, S., and Grinstein, S. (2000). Natural resistance to intracellular infections: Natural resistance-associated macrophage protein 1 (NRAMP1) functions as a pH-dependent manganese transporter at the phagosomal membrane. J. Exp. Med. *192*, 1237–1247.

Jang, M.H., Sougawa, N., Tanaka, T., Hirata, T., Hiroi, T., Tohya, K., Guo, Z., Umemoto, E., Ebisuno, Y., Yang, B.-G., et al. (2006). CCR7 Is Critically Important for Migration of Dendritic Cells in Intestinal Lamina Propria to Mesenteric Lymph Nodes. J. OfImmunology 803–810.

Jantsch, J., Chikkaballi, D., and Hensel, M. (2011). Cellular aspects of immunity to intracellular Salmonella enterica. Immunol. Rev. *240*, 185–195.

Joeris, T., Müller-Luda, K., Agace, W.W., and Mowat, A.M.I. (2017). Diversity and functions of intestinal mononuclear phagocytes. Mucosal Immunol. *10*, 845–864.

Johanns, T.M., Ertelt, J.M., Rowe, J.H., and Way, S.S. (2010). Regulatory t cell suppressive potency dictates the balance between bacterial proliferation and clearance during persistent Salmonella infection. PLoS Pathog. *6*, 31–32.

Joller, N., Lozano, E., Burkett, P.R., Patel, B., Xiao, S., Zhu, C., Xia, J., Tan, T.G., Sefik, E., Yajnik, V., et al. (2014). Treg cells expressing the co-inhibitory molecule TIGIT selectively inhibit pro-inflammatory Th1 and Th17 cell responses. Immunity *40*, 569–581.

Jones, B.D., Ghori, N., and Falkow, S. (1994). Salmonella typhlrnurium initiates murine infection by penetrating and destroying the specialized epithelial M cells of the peyer’s patches. J. Exp. Med. *180*, 15–23.

Josefowicz, S.Z., Niec, R.E., Kim, H.Y., Treuting, P., Chinen, T., Zheng, Y., Umetsu, D.T., and Rudensky, A.Y. (2012). Extrathymically generated regulatory T cells control mucosal Th2 inflammation. Nature *482*, 395–399.

Jouanguy, E., Ddffinger, R., Dupuis, S., Pallier, A., Altare, F., and Casanova, J.-L. (1999). IL-12 and IFN-y in host defense against mycobacteria and salmonella in mice and men. Curr. Opin. Immunol. 346–351.

Kamada, T., Togashi, Y., Tay, C., Ha, D., Sasaki, A., Nakamura, Y., Sato, E., Fukuoka, S., Tada, Y., Tanaka, A., et al. (2019). PD-1+ regulatory T cells amplified by PD-1 blockade promote hyperprogression of cancer. Proc. Natl. Acad. Sci. U. S. A. *116*, 9999–10008.

Kambayashi, T., and Laufer, T.M. (2014). Atypical MHC class II-expressing antigen-presenting cells: Can anything replace a dendritic cell? Nat. Rev. Immunol. *14*, 719–730.

Kamsteeg, M., Jansen, P.A.M., Van Vlijmen-Willems, I.M.J.J., Van Erp, P.E.J., Rodijk-Olthuis, D., Van Der Valk, P.G., Feuth, T., Zeeuwen, P.L.J.M., and Schalkwijk, J. (2010). Molecular diagnostics of psoriasis, atopic dermatitis, allergic contact dermatitis and irritant contact dermatitis. Br. J. Dermatol. *162*, 568–578.

Karecla, P.I., Bowden, S.J., Green, S.J., and Kilshaw, P.J. (1995). Recognition of E-cadherin on epithelial cells by the mucosal T cell integrin αM290β7 (αEβ7). Eur. J. Immunol. *25*, 852–856.

Katakura, T., Miyazaki, M., Kobayashi, M., Herndon, D.N., and Suzuki, F. (2004). CCL17 and IL-10 as Effectors That Enable Alternatively Activated Macrophages to Inhibit the Generation of Classically Activated Macrophages. J. Immunol. *172*, 1407–1413.

Kataoka, Y. (2014). Thymus and activation-regulated chemokine as a clinical biomarker in atopic dermatitis. J. Dermatol.

Keddy, K.H., Takuva, S., Musekiwa, A., Puren, A.J., Sooka, A., Karstaedt, A., Klugman, K.P., and Angulo, F.J. (2017). An association between decreasing incidence of invasive non-typhoidal salmonellosis and increased use of antiretroviral therapy, Gauteng Province, South Africa, 2003-2013. PLoS One *12*, 2003–2013.

Keestra-Gounder, A.M., Tsolis, R.M., and Bäumler, A.J. (2015). Now you see me, now you don’t: the interaction of Salmonella with innate immune receptors. Nat. Rev. Microbiol. *13*, 206–216.

Kim, C.H., Rott, L., Kunkel, E.J., Genovese, M.C., Andrew, D.P., Wu, L., and Butcher, E.C. (2001). Rules of chemokine receptor association with T cell polarization in vivo. J. Clin. Invest. *108*, 1331–1339.

Knodler, L.A., Crowley, S.M., Sham, H.P., Yang, H., Wrande, M., Ma, C., Ernst, R.K., Steele-Mortimer, O., Celli, J., and Vallance, B.A. (2014). Non-canonical inflammasome activation of caspase-4/ caspase-11 mediates epithelial defenses against enteric bacterial pathogens. Cell Host Microbe *16*, 249–256.

Knuschke, T., Rotan, O., Bayer, W., Sokolova, V., Hansen, W., Sparwasser, T., Dittmer, U., Epple, M., Buer, J., and Westendorf, A.M. (2016). Combination of nanoparticle-based therapeutic vaccination and transient ablation of regulatory T cells enhances anti-viral immunity during chronic retroviral infection. Retrovirology *13*, 1–11.

Koch, M.A., Tucker-Heard, G., Perdue, N.R., Killebrew, J.R., Urdahl, K.B., and Campbell, D.J. (2009). T-bet controls regulatory T cell homeostasis and function during type-1 inflammation. Nat Immunol *10*, 595–602.

Kornete, M., Sgouroudis, E., and Piccirillo, C.A. (2012). ICOS-Dependent Homeostasis and Function of Foxp3 + Regulatory T Cells in Islets of Nonobese Diabetic Mice . J. Immunol. *188*, 1064–1074.

Krause, P., Morris, V., Greenbaum, J.A., Park, Y., Bjoerheden, U., Mikulski, Z., Muffley, T., Shui, J., Kim, G., Cheroutre, H., et al. (2015). IL-10 producing intestinal macrophages prevent excessive anti- bacterial innate immunity by limiting IL-23 synthesis. Nat Commun.

Kufareva, I., Salanga, C.L., and Handel, T.M. (2015). Chemokine and chemokine receptor structure and interactions: implications for therapeutic strategies. Immunol Cell Biol. *93*, 372–383.

Kupz, A., Scott, T.A., Belz, G.T., Andrews, D.M., Greyer, M., Lew, A.M., Brooks, A.G., Smyth, M.J., Curtiss, R., Bedoui, S., et al. (2013). Contribution of Thy1+ NK cells to protective IFN- production during Salmonella Typhimurium infections. Proc. Natl. Acad. Sci. *110*, 2252–2257.

Kupz, A., Bedoui, S., and Strugnell, R.A. (2014). Cellular requirements for systemic control of Salmonella enterica serovar Typhimurium infections in mice. Infect. Immun. *82*, 4997–5004.

Kurtz, J.R., Goggins, J.A., and McLachlan, J.B. (2017). Salmonella infection: Interplay between the bacteria and host immune system. Immunol. Lett. *190*, 42–50.

Lanh, M.N., Van Bay, P., Ho, V.A., Thanh, T.C., Lin, F.Y.C., Bryla, D.A., Chu, C., Schiloach, J., Robbins, J.B., Schneerson, R., et al. (2003). Persistent efficacy of Vi conjugate vaccine against typhoid fever in young children [7]. N. Engl. J. Med. *349*, 1390–1391.

Latorre, I., Fernández-Sanmartín, M.A., Muriel-Moreno, B., Villar-Hernández, R., Vila, S., De Souza-Galvão, M.L., Stojanovic, Z., Jiménez-Fuentes, M.A., Centeno, C., Ruiz-Manzano, J., et al. (2019). Study of CD27 and CCR4 markers on specific CD4 + T-cells as immune tools for active and latent tuberculosis management. Front. Immunol. *10*, 1–11.

Latta, M., Mohan, K., and Issekutz, T.B. (2007). CXCR6 is expressed on T cells in both T helper type 1 (Th1) inflammation and allergen-induced Th2 lung inflammation but is only a weak mediator of chemotaxis. Immunology *121*, 555–564.

Layseca-Espinosa, E., Korniotis, S., Montandon, R., Gras, C., Bouillié, M., Gonzalez-Amaro, R., Dy, M., and Zavala, F. (2013). CCL22-Producing CD8α − Myeloid Dendritic Cells Mediate Regulatory T Cell Recruitment in Response to G-CSF Treatment . J. Immunol. *191*, 2266–2272.

Lazar, V., Ditu, L.M., Pircalabioru, G.G., Gheorghe, I., Curutiu, C., Holban, A.M., Picu, A., Petcu, L., and Chifiriuc, M.C. (2018). Aspects of gut microbiota and immune system interactions in infectious diseases, immunopathology, and cancer. Front. Immunol. *9*, 1–18.

Ledesma, E., Martínez, I., Córdova, Y., Rodríguez-Sosa, M., Monroy, A., Mora, L., Soto, I., Ramos, G., Weiss, B., and Osorio, E.S. (2004). Interleukin-1 beta (IL-1β) induces tumor necrosis factor alpha (TNF-α) expression on mouse myeloid multipotent cell line 32D cl3 and inhibits their proliferation. Cytokine *26*, 66–72.

Lee, W., and Lee, G.R. (2018). Transcriptional regulation and development of regulatory T cells. Exp. Mol. Med. *50*, e456-10.

Lee, S.J., Dunmire, S., and McSorley, S.J. (2012a). MHC class-I-restricted CD8 T cells play a protective role during primary Salmonella infection. Immunol. Lett. *148*, 138–143.

Lee, S.J., McLachlan, J.B., Kurtz, J.R., Fan, D., Winter, S.E., Baumler, A.J., Jenkins, M.K., and McSorley, S.J. (2012b). Temporal expression of bacterial proteins instructs host CD4 T cell expansion and Th17 development. PLoS Pathog. *8*.

Levine, M.M., Ferreccio, C., Black, R.E., Lagos, R., Martin, O.S., and Blackwelder, W.C. (2007). Ty21a Live Oral Typhoid Vaccine and Prevention of Paratyphoid Fever Caused by Salmonella enterica Serovar Paratyphi B. Clin. Infect. Dis. *45*, S24–S28.

Li, M.O., and Rudensky, A.Y. (2016). T Cell Receptor Signaling in the Control of Regulatory T Cell Differentiation and Function. Clin. Res. Hepatol. Gastroenterol. *16*, 220–233.

Lieberam, I., and Förster, I. (1999). The murine β-chemokine TARC is expressed by subsets of dendritic cells and attracts primed CD4+ T cells. Eur. J. Immunol. *29*, 2684–2694.

Lin, F.Y.C., Ho, V.A., Khiem, H.B., Trach, D.D., Bay, P. Van, Thanh, T.C., Kossaczka, Z., Bryla, D.A., Shiloach, J., Robbins, J.B., et al. (2001). The Efficacy of a Salmonella typhi Vi Conjugate Vaccine in Two-to-Five-Year-Old Children. N. Engl. J. Med. *344*, 1263–1269.

Luda, K.M., Joeris, T., Persson, E.K., Rivollier, A., Demiri, M., Sitnik, K.M., Pool, L., Holm, J.B., Melo-Gonzalez, F., Richter, L., et al. (2016). IRF8 Transcription-Factor-Dependent Classical Dendritic Cells Are Essential for Intestinal T Cell

Homeostasis. Immunity *44*, 860–874.

Luu, M., Steinhoff, U., and Visekruna, A. (2017). Functional heterogeneity of gut-resident regulatory T cells. Clin. Transl. Immunol. *6*, e156.

Mackay, L.K., Stock, A.T., Ma, J.Z., Jones, C.M., Kent, S.J., Mueller, S.N., Heath, W.R., Carbone, F.R., and Gebhardt, T. (2012). Long-lived epithelial immunity by tissue-resident memory T (TRM) cells in the absence of persisting local antigen presentation. Proc. Natl. Acad. Sci. U. S. A. *109*, 7037–7042.

MacLennan, C.A., Martin, L.B., and Micoli, F. (2014). Vaccines against invasive Salmonella disease . Hum. Vaccin. Immunother. *10*, 1478–1493.

MacMicking, J.D. (2012). Interferon-inducible effector mechanisms in cell-autonomous immunity. Nat Rev Immunol. *12*, 367–382.

Maloy, K.J., Salaun, L., Cahill, R., Dougan, G., Saunders, N.J., and Powrie, F. (2003). CD4+CD25+ TR cells suppress innate immune pathology through cytokine-dependent mechanisms. J. Exp. Med. *197*, 111–119.

Mariani, M., Lang, R., Binda, E., Panina-Bordignon, P., and D'Ambrosio, D. (2004). Dominance of CCL22 over CCL17 in induction of chemokine receptor CCR4 desensitization and internalization on human Th2 cells. Eur. J. Immunol. *34*, 231–240.

Marmion, D.E., Naylor, G.R.E., and Stewart, I.O. (1953). Second attacks of typhoid fever. J. Hyg. (Lond). *51*, 260–267.

Marsal, J., and Agace, W.W. (2012). Targeting T-cell migration in inflammatory bowel disease. J. Intern. Med. *272*, 411–429.

Mason, K.L., Huffnagle, G.B., Noverr, M.C., and Kao, J.Y. (2008). Overview of gut immunology. Adv. Exp. Med. Biol. *635*, 1–14.

Mastroeni, P., Villarreal-Ramos, B., and Hormaeche, C.E. (1993). Adoptive transfer of immunity to oral challenge with virulent salmonellae in innately susceptible BALB/c mice requires both immune serum and T cells. Infect. Immun. *61*, 3981–3984.

Mastroeni, P., Grant, A., Restif, O., and Maskell, D. (2009). A dynamic view of the spread and intracellular distribution of Salmonella enterica. Nat. Rev. Microbiol. *7*, 73–80.

McCoy, M.W., Moreland, S.M., and Detweiler, C.S. (2012). Hemophagocytic macrophages in murine typhoid fever have an anti-inflammatory phenotype. Infect. Immun. *80*, 3642–3649.

McGhie, E.J., Brawn, L.C., Hume, P.J., Humphreys, D., and Koronakis, V. (2009). Salmonella takes control: effector-driven manipulation of the host. Curr. Opin. Microbiol. *12*, 117–124.

McNally, A., Hill, G.R., Sparwasser, T., Thomas, R., and Steptoe, R.J. (2011). CD4+CD25+ regulatory T cells control CD8+ T-cell effector differentiation by modulating IL-2 homeostasis. Proc. Natl. Acad. Sci. U. S. A. *108*, 7529–7534.

McSorley, S.J. (2014). The role of non-cognate T cell stimulation during intracellular bacterial infection. Front. Immunol. *5*, 1–6.

McSorley, S.J., and Jenkins, M.K. (2000). Antibody is required for protection against virulent but not attenuated Salmonella enterica serovar typhimurium. Infect. Immun. *68*, 3344–3348.

McSorley, S.J., Cookson, B.T., and Jenkins, M.K. (2000). Characterization of CD4 + T Cell Responses During Natural Infection with Salmonella typhimurium . J. Immunol. *164*, 986–993.

Meltzer, E., Sadik, C., and Schwartz, E. (2006). Enteric fever in Israel travelers: A nationwide study. J. Travel Med. *13*, 327.

Miltenyi Biotec (2015). Flow cytometry analysis of Th subsets.

Mittrucker, H.W., and Kaufmann, S.H.E. (2000). Immune response to infection with Salmonella typhimurium in mice. J. Leukoc. Biol. *67*, 457–463.

Mittrücker, H.-W., Raupach, B., Koehler, A., and Kaufmann, S.H.E. (2000). Cutting Edge: Role of B Lymphocytes in Protective Immunity Against Salmonella typhimurium Infection. J. Immunol. *164*, 1648–1652.

Mittrücker, H.W., Köhler, A., and Kaufmann, S.H.E. (2002). Characterization of the murine T-lymphocyte response to Salmonella enterica serovar typhimurium infection. Infect. Immun. *70*, 199–203.

Mohan, V.K., Varanasi, V., Singh, A., Pasetti, M.F., Levine, M.M., Venkatesan, R., and Ella, K.M. (2015). Safety and Immunogenicity of a Vi Polysaccharide-Tetanus Toxoid Conjugate Vaccine (Typbar-TCV) in Healthy Infants, Children, and Adults in Typhoid Endemic Areas: A Multicenter, 2-Cohort, Open-Label, Double-Blind, Randomized Controlled Phase 3 Study. Clin. Infect. Dis. *61*, 393–402.

Monack, D.M., Bouley, D.M., and Falkow, S. (2004). Salmonella typhimurium Persists within Macrophages in the Mesenteric Lymph Nodes of Chronically Infected Nramp1+/+ Mice and Can Be Reactivated by IFNγ Neutralization. J. Exp. Med. *199*, 231–241.

Montane, J., Bischoff, L., Soukhatcheva, G., Dai, D.L., Hardenberg, G., Levings, M.K., Orban, P.C., Kieffer, T.J., Tan, R., and Verchere, C.B. (2011). Prevention of murine autoimmune diabetes by CCL22-mediated Treg recruitment to the pancreatic islets. J. Clin. Invest. *121*, 3024–3028.

Moore, A.C., Gallimore, A., Draper, S.J., Watkins, K.R., Gilbert, S.C., and Hill, A.V.S. (2005). Anti-CD25 Antibody Enhancement of Vaccine-Induced Immunogenicity: Increased Durable Cellular Immunity with Reduced Immunodominance. J. Immunol. *175*, 7264–7273.

Morimoto, Y., Bian, Y., Gao, P., Yashiro-Ohtani, Y., Zhou, X.-Y., Ono, S., Nakahara, H., Kogo, M., Hamaoka, T., and Fujiwara, H. (2005). Induction of surface CCR4 and its functionality in mouse Th2 cells is regulated differently during Th2 development. J. Leukoc. Biol. *78*, 753–761.

Mowat, A.M., and Agace, W.W. (2014). Regional specialization within the intestinal immune system. Nat. Rev. Immunol. *14*, 667–685.

Mowat, A.M.I., Parker, L.A., Beacock-Sharp, H., Millington, O.R., and Chirdo, F. (2004). Oral tolerance: Overview and historical perspectives. Ann. N. Y. Acad. Sci. *1029*, 1–8.

Muotiala, A., and Mäkelä, P.H. (1990). The role of IFN-γ in murine Salmonella typhimurium infection. Microb. Pathog. *8*, 135–141.

Murai, M., Turovskaya, O., Kim, G., Cheroutre, H., Kronenberg, M., and Madan, R. (2009). Interleukin 10 acts on regulatory t cells to maintain expression of the transcription factor foxp3 and suppressive function in mice with colitis. Nat. Immunol. *10*, 1178–1184.

Muraille, E., Leo, O., and Moser, M. (2014). Th1/Th2 paradigm extended: Macrophage polarization as an unappreciated pathogen-driven escape mechanism? Front. Immunol. *5*, 1–12.

Murphy, K., and Weaver, C. (2017). Janeway's Immunibiilogy 9Th Edition (Garland Science, Taylor & Francis Group).

Nanton, M.R., Way, S.S., Shlomchik, M.J., and McSorley, S.J. (2012). B cells are essential for Protective Immunity against Salmonella Independent of Antibody Secretion. J Immunol. *15*, 5503–5507.

Nauciel, C. (1990). Role of CD4+ T cells and T-independent mechanisms in acquired resistance to Salmonella typhimurium infection. J. Immunol. *145*, 1265–1269.

Nelson, R.W., McLachlan, J.B., Kurtz, J.R., and Jenkins, M.K. (2013). CD4 + T Cell Persistence and Function after Infection Are Maintained by Low-Level Peptide:MHC Class II Presentation . J. Immunol. *190*, 2828–2834.

Niedergang, F., Sirard, J.C., Blanc, C.T., and Kraehenbuhl, J.P. (2000). Entry and survival of Salmonella typhimurium in dendritic cells and presentation of recombinant antigens do not require macrophage-specific virulence factors. Proc. Natl. Acad. Sci. U. S. A. *97*, 14650–14655.

Niess, J.H., Brand, S., Gu, X., Landsman, L., Jung, S., McCormick, B.A., Vyas, J.M., Boes, M., Ploegh, H.L., Fox, J.G., et al. (2005). CX3CR1-mediated dendritic cell access to the intestinal lumen and bacterial clearance. Science (80-.). *307*, 254–258.

Olson, B.M., Jankowska-Gan, E., Becker, J.T., Vignali, D.A.A., Burlingham, W.J., and McNeel, D.G. (2012). Human Prostate Tumor Antigen-Specific CD8+ Regulatory T Cells are Inhibited by CTLA-4 or IL-35 Blockade. J Immunol *189*, 5590–5601.

Onishi, Y., Fehervari, Z., Yamaguchi, T., and Sakaguchi, S. (2008). Foxp3+ natural regulatory T cells preferentially form aggregates on dendritic cells in vitro and actively inhibit their maturation. Proc. Natl. Acad. Sci. U. S. A. *105*, 10113–10118.

Palmer, A.D., and Slauch, J.M. (2017). Mechanisms of Salmonella pathogenesis in animal models. Hum. Ecol. Risk Assess. *23*, 1877–1892.

Persson, E., Uronen-Hansson, H., Semmrich, M., Rivollier, A., Hägerbrand, K., Marsal, J., Gudjonsson, S., Håkansson, U., Reizis, B., Kotarsky, K., et al. (2013). IRF4 Transcription-Factor-Dependent CD103+CD11b+ Dendritic Cells Drive Mucosal T Helper 17 Cell Differentiation. Immunity *38*, 958–969.

Pham, O.H., and McSorley, S.J. (2015). Protective host immune responses to Salmonella infection. Futur. Microbiol. *10*, 101–110.

Pham, O.H., O'Donnell, H., Al-Shamkhani, A., Kerrinnes, T., Tsolis, R.M., and McSorley, S.J. (2017). T cell expression of IL-18R and DR3 is essential for non-cognate stimulation of Th1 cells and optimal clearance of intracellular bacteria. PLoS Pathog. *13*, 1–22.

Platt, A.M., Bain, C.C., Bordon, Y., Sester, D.P., and Mowat, A.M. (2010). An Independent Subset of TLR Expressing CCR2-Dependent Macrophages Promotes Colonic Inflammation. J. Immunol. *184*, 6843–6854.

Raffatellu, M., Wilson, R.P., Winter, S.E., and Bäumler, A.J. (2008a). Clinical pathogenesis of typhoid fever. J. Infect. Dev. Ctries. *2*, 260–266.

Raffatellu, M., Santos, R.L., Verhoeven, D.E., George, M.D., Paul, R., Winter, S.E., Godinez, I., Sankaran, S., Paixao, T.A., Gordon, A., et al. (2008b). Simian immunodeficiency virus–induced mucosal interleukin-17 deficiency promotes Salmonella dissemination from the gut. Nat Med. *14*, 421–428.

Rajagopal, S., Bassoni, D.L., Campbell, J.J., Gerard, N.P., Gerard, C., and Wehrman, T.S. (2013). Biased agonism as a mechanism for differential signaling by chemokine receptors. J. Biol. Chem. *288*, 35039–35048.

Rapp, M., Wintergerst, M.W.M., Kunz, W.G., Vetter, V.K., Knott, M.M.L., Lisowski, D., Haubner, S., Moder, S., Thaler, R., Eiber, S., et al. (2019). CCL22 controls immunity by promoting regulatory T cell communication with dendritic cells in lymph nodes. J. Exp. Med. *216*, 1170–1181.

Ravindran, R., Foley, J., Stoklasek, T., Glimcher, L.H., and McSorley, S.J. (2005). Expression of T-bet by CD4 T Cells Is Essential for Resistance to Salmonella Infection . J. Immunol. *175*, 4603–4610.

Roe, M.M., Swain, S., Sebrell, T.A., Sewell, M.A., Collins, M.M., Perrino, B.A., Smith, P.D., Smythies, L.E., and Bimczok, D. (2017). Differential regulation of CD103 (αE integrin) expression in human dendritic cells by retinoic acid and Toll-like receptor ligands. J. Leukoc. Biol. *101*, 1169–1180.

Rowe, J.H., Ertelt, J.M., and Way, S.S. (2012). Foxp3 + regulatory T cells, immune stimulation and host defence against infection. Immunology *136*, 1–10.

Sabbagh, P., Karkhah, A., Nouri, H.R., Javanian, M., and Ebrahimpour, S. (2018). The significance role of regulatory T cells in the persistence of infections by intracellular bacteria. Infect. Genet. Evol. *62*, 270–274.

Sahastrabuddhe, S., and Saluja, T. (2019). Overview of the Typhoid Conjugate Vaccine Pipeline: Current Status and Future Plans. Clin. Infect. Dis. *68*, S22–

S26.

Sakaguchi, S., Sakaguchi, N., Asano, M., Itoh, M., and Toda, M. (1995). Immunologic self-tolerance maintained by activated T cells expressing IL-2 receptor alpha-chains (CD25). J. Immunol. *155*, 1151–1164.

Sakaguchi, S., Wing, K., Onishi, Y., Prieto-Martin, P., and Yamaguchi, T. (2009). Regulatory T cells: How do they suppress immune responses? Int. Immunol. *21*, 1105–1111.

Sander, L.E., Davis, M.J., Boekschoten, M. V, Amsen, D., Christopher, C., Ryffel, B., Swanson, J. a, Müller, M., and Blander, J.M. (2012). Sensing prokaryotic mRNA signifies microbial viability and promotes immunity. Nature *474*, 385–389.

Santos, R.L., Zhang, S., Tsolis, R.M., Kingsley, R.A., Garry Adams, L., and Bäumler, A.J. (2001). Animal models of Salmonella infections: Enteritis versus typhoid fever. Microbes Infect. *3*, 1335–1344.

Santulli-Marotto, S., Boakye, K., Lacy, E., Wu, S.J., Luongo, J., Kavalkovich, K., Coelho, A., Hogaboam, C.M., and Ryan, M. (2013a). Engagement of two distinct binding domains on CCL17 is required for signaling through CCR4 and establishment of localized inflammatory conditions in the lung. PLoS One *8*.

Santulli-Marotto, S., Fisher, J., Petley, T., Boakye, K., Panavas, T., Luongo, J., Kavalkovich, K., Rycyzyn, M., Wu, B., Gutshall, L., et al. (2013b). Surrogate Antibodies That Specifically Bind and Neutralize CCL17 But Not CCL22. Monoclon. Antib. Immunodiagn. Immunother. *32*, 162–171.

Santulli-Marotto, S., Wheeler, J., Lacy, E.R., Boakye, K., Luongo, J., Wu, S.-J., and Ryan, M. (2015). CCL22-specific Antibodies Reveal That Engagement of Two Distinct Binding Domains on CCL22 Is Required for CCR4-mediated Function. Monoclon. Antib. Immunodiagn. Immunother. *34*.

Schaniel, C., Pardali, E., Sallusto, F., Speletas, M., Ruedl, C., Shimizu, T., Seidl, T., Andersson, J., Melchers, F., Rolink, A.G., et al. (1998). Activated murine B lymphocytes and dendritic cells produce a novel CC chemokine which acts selectively on activated T cells. J. Exp. Med. *188*, 451–463.

Schlitzer, A., McGovern, N., Teo, P., Zelante, T., Atarashi, K., Low, D., Ho, A.W.S., See, P., Shin, A., Wasan, P.S., et al. (2013). IRF4 Transcription Factor-Dependent CD11b+ Dendritic Cells in Human and Mouse Control Mucosal IL-17 Cytokine Responses. Immunity *38*, 970–983.

Schlitzer, A., Sivakamasundari, V., Chen, J., Sumatoh, H.R. Bin, Schreuder, J., Lum, J., Malleret, B., Zhang, S., Larbi, A., Zolezzi, F., et al. (2015). Identification of cDC1- and cDC2-committed DC progenitors reveals early lineage priming at the common DC progenitor stage in the bone marrow. Nat. Immunol. *16*, 718–728.

Schoenborn, J.R., and Wilson, C.B. (2007). Regulation of Interferon-γ During Innate and Adaptive Immune Responses. Adv. Immunol. *96*, 41–101.

Schön, M.P., Arya, A., Murphy, E.A., Adams, C.M., Strauch, U.G., Agace, W.W., Marsal, J., Donohue, J.P., Her, H., Beier, D.R., et al. (1999). Mucosal T lymphocyte numbers are selectively reduced in integrin alpha E (CD103)-

deficient mice. J. Immunol. *162*, 6641–6649.

Scott, C.L., Bain, C.C., Wright, P.B., Sichien, D., Kotarsky, K., Persson, E.K., Luda, K., Guilliams, M., Lambrecht, B.N., Agace, W.W., et al. (2015). CCR2 + CD103 - Intestinal dendritic cells develop from DC-committed precursors and induce interleukin-17 production by T cells. Mucosal Immunol. *8*, 327–339.

Semmling, V., Lukacs-Kornek, V., Thaiss, C.A., Quast, T., Hochheiser, K., Panzer, U., Rossjohn, J., Perlmutter, P., Cao, J., Godfrey, D.I., et al. (2010). Alternative cross-priming through CCL17-CCR4-mediated attraction of CTLs toward NKT cell-licensed DCs. Nat. Immunol. *11*, 313–320.

Shaw, M.H., Kamada, N., Kim, Y.G., and Núñez, G. (2012). Microbiota-induced IL-1β, but not IL-6, is critical for the development of steady-state T H17 cells in the intestine. J. Exp. Med. *209*, 251–258.

Smith, J.L. (2003). The Role of Gastric Acid in Preventing Foodborne Disease and How Bacteria Overcome Acid Conditions. J. Food Prot. *66*, 1292–1303.

Spano, S. (2016). Mechanisms of Salmonella Typhi Host Restriction. In Biophysics of Infection, pp. 129–156.

Srinivasan, A., Foley, J., and McSorley, S.J. (2004). Massive Number of Antigen-Specific CD4 T Cells during Vaccination with Live Attenuated Salmonella Causes Interclonal Competition . J. Immunol. *172*, 6884–6893.

Srinivasan, A., Salazar-Gonzalez, R.-M., Jarcho, M., Sandau, M.M., Lefrancois, L., and McSorley, S.J. (2007). Innate Immune Activation of CD4 T Cells in Salmonella -Infected Mice Is Dependent on IL-18 . J. Immunol. *178*, 6342–6349.

Strugnell, R.A., Scott, T.A., Wang, N., Yang, C., Peres, N., Bedoui, S., and Kupz, A. (2014). Salmonella vaccines: Lessons from the mouse model or bad teaching? Curr. Opin. Microbiol. *17*, 99–105.

Sturge, C.R., Benson, A., Raetz, M., Wilhelm, C.L., Mirpuri, J., Vitetta, E.S., and Yarovinsky, F. (2013). TLR-independent neutrophil-derived IFN- is important for host resistance to intracellular pathogens. Proc. Natl. Acad. Sci. *110*, 10711–10716.

Stutte, S., Quast, T., Gerbitzki, N., Savinko, T., Novak, N., Reifenberger, J., Homey, B., Kolanus, W., Alenius, H., and Förster, I. (2010). Requirement of CCL17 for CCR7- and CXCR4-dependent migration of cutaneous dendritic cells. Proc Natl Acad Sci U S A *107*, 8736–8741.

Stutte, S., Gerbitzki, N., Novak, N., and Frster, I. (2012). Expression and Function of CCL17 in Atopic Dermatitis. Atopic Dermat. - Dis. Etiol. Clin. Manag.

Sugiyama, D., Nishikawa, H., Maeda, Y., Nishioka, M., Tanemura, A., Katayama, I., Ezoe, S., Kanakura, Y., Sato, E., Fukumori, Y., et al. (2013). Anti-CCR4 mAb selectively depletes effector-Type FoxP3+CD4+ regulatory T cells, evoking antitumor immune responses in humans. Proc. Natl. Acad. Sci. U. S. A. *110*, 17945–17950.

Sztein, M.B., Salerno-Goncalves, R., and McArthur, M.A. (2014). Complex adaptive immunity to enteric fevers in humans: Lessons learned and the path forward. Front. Immunol. *5*.

Tadokoro, C.E., Shakhar, G., Shen, S., Ding, Y., Lino, A.C., Maraver, A., Lafaille, J.J., and Dustin, M.L. (2006). Regulatory T cells inhibit stable contacts between CD4+ T cells and dendritic cells in vivo. J. Exp. Med. *203*, 505–511.

Takahashi, T., Kuniyasu, Y., Toda, M., Sakaguchi, N., Itoh, M., Iwata, M., Shimizu, J., and Sakaguchi, S. (1998). Immunologic self-tolerance maintained by CD25 + CD4 + naturally anergic and suppressive T cells: Induction of autoimmune disease by breaking their anergic/suppressive state. Int. Immunol. *10*, 1969–1980.

Tang, Q., Adams, J.Y., Tooley, A.J., Bi, M., Fife, B.T., Serra, P., Santamaria, P., Locksley, R.M., Krummel, M.F., and Bluestone, J.A. (2006). Visualizing regulatory T cell control of autoimmune responses in nonobese diabetic mice. Nat. Immunol. *7*, 83–92.

Thornton, A.M., and Shevach, E.M. (1998). CD4+CD25+ immunoregulatory T cells suppress polyclonal T cell activation in vitro by inhibiting interleukin 2 production. J. Exp. Med. *188*, 287–296.

Tobar, J.A., Carreño, L.J., Bueno, S.M., González, P.A., Mora, J.E., Quezada, S.A., and Kalergis, A.M. (2006). Virulent Salmonella enterica serovar typhimurium evades adaptive immunity by preventing dendritic cells from activating T cells. Infect. Immun. *74*, 6438–6448.

Tse, S.W., Radtke, A.J., Espinosa, D.A., Cockburn, I.A., and Zavala, F. (2014). The chemokine receptor CXCR6 is required for the maintenance of liver memory CD8$^+$ T cells specific for infectious pathogens. J. Infect. Dis. *210*, 1508–1516.

Tsolis, R.M., Xavier, M.N., Santos, R.L., and Bäumler, A.J. (2011). How to become a top model: Impact of animal experimentation on human Salmonella disease research. Infect. Immun. *79*, 1806–1814.

Tsunemi, Y., Saeki, H., Nakamura, K., Nagakubo, D., Nakayama, T., Yoshie, O., Kagami, S., Shimazu, K., Kadono, T., Sugaya, M., et al. (2006). CCL17 transgenic mice show an enhanced Th2-type response to both allergic and non-allergic stimuli. Eur. J. Immunol. *36*, 2116–2127.

Uche, I.V., MacLennan, C.A., and Saul, A. (2017). A Systematic Review of the Incidence, Risk Factors and Case Fatality Rates of Invasive Nontyphoidal Salmonella (iNTS) Disease in Africa (1966 to 2014). PLoS Negl. Trop. Dis. *11*, 1–28.

Ugrinovic, S., Ménager, N., Goh, N., and Mastroeni, P. (2003). Characterization and Development of T-Cell Immune Responses in B-Cell-Deficient (Igh-6-/-) Mice with Salmonella enterica Serovar Typhimurium Infection. Infect. Immun. *71*, 6808–6819.

Vazquez-Torres, A., Jones-Carson, J., Baumler, A.J., Falkow, S., Valdivia§k, R., Brown, W., Le, M., Berggren, R., Parks, W.T., and Fang, F.C. (1999). Extraintestinal dissemination of Salmonella by CD18-expressing phagocytes.

Nature *401*.

van der Velden, A.W.M., Velasquez, M., and Starnbach, M.N. (2003). Salmonella Rapidly Kill Dendritic Cells via a Caspase-1- Dependent Mechanism . J. Immunol. *171*, 6742–6749.

van der Velden, A.W.M., Copass, M.K., and Starnbach, M.N. (2005). Salmonella inhibit T cell proliferation by a direct, contact-dependent immunosuppressive effect. Proc. Natl. Acad. Sci. *102*, 17769–17774.

Vestergaard, C., Bang, K., Gesser, B., Yoneyama, H., Matsushima, K., and Larsen, C.G. (2000). A Th2 chemokine, TARC, produced by keratinocytes may recruit CLA+CCR4+ lymphocytes into lesional atopic dermatitis skin. J. Invest. Dermatol. *115*, 640–646.

Vignali, D.A.A., Collison, L.W., and Workman, C.J. (2008). How regulatory T cells work. Nat. Rev. Immunol. *8*, 523–532.

Voedisch, S., Koenecke, C., David, S., Herbrand, H., Förster, R., Rhen, M., and Pabst, O. (2009). Mesenteric lymph nodes confine dendritic cell-mediated dissemination of Salmonella enterica serovar typhimurium and limit systemic disease in mice. Infect. Immun. *77*, 3170–3180.

Vulcano, M., Albanesi, C., Stoppacciaro, A., Bagnati, R., D’Amico, G., Struyf, S., Transidico, P., Bonecchi, R., Prete, A. Del, Allavena, P., et al. (2001). Dendritic cells as a major source of macrophage-derived chemokine/CCL22 in vitro and in vivo. Eur. J. Immunol. *31*, 812–822.

Wain, J., Walsh, A.M., Parry, C.M., White, N.J., Diep, T.S., Hoa, N.T.T., and Ho, V.A. (1998). Quantitation of bacteria in blood of typhoid fever patients and relationship between counts and clinical features, transmissibility, and antibiotic resistance. J. Clin. Microbiol. *36*, 1683–1687.

Wakim, L.M., Woodward-Davis, A., and Bevan, M.J. (2010). Memory T cells persisting within the brain after local infection show functional adaptations to their tissue of residence. Proc. Natl. Acad. Sci. U. S. A. *107*, 17872–17879.

Watanabe, Y., Katou, F., Ohtani, H., Nakayama, T., Yoshie, O., and Hashimoto, K. (2010). Tumor-infiltrating lymphocytes, particularly the balance between CD8+ T cells and CCR4+ regulatory T cells, affect the survival of patients with oral squamous cell carcinoma. Oral Surgery, Oral Med. Oral Pathol. Oral Radiol. Endodontology *109*, 744–752.

Watson, P.R., Gautier, A. V., Paulin, S.M., Bland, A.P., Jones, P.W., and Wallis, T.S. (2000). Salmonella enterica serovars Typhimurium and Dublin can lyse macrophages by a mechanism distinct from apoptosis. Infect. Immun. *68*, 3744–3747.

Wawrzyniak, M., O´Mahony, L., and Akdis, M. (2017). Role of Regulatory Cells in Oral Tolerance. AAIR *9*, 107–115.

Weber, B., Saurer, L., Schenk, M., Dickgreber, N., and Mueller, C. (2011a). CX3CR1 defines functionally distinct intestinal mononuclear phagocyte subsets which maintain their respective functions during homeostatic and inflammatory conditions. Eur. J. Immunol. *41*, 773–779.

Weber, C., Meiler, S., Doring, Y., Koch, M., Drechsler, M., Megens, R.T., Rowinska, Z., Bidzhekov, K., Fecher, C., Ribechini, E., et al. (2011b). CCL17-expressing dendritic cells drive atherosclerosis by restraining regulatory T cell homeostasis in mice. J Clin Invest *121*, 2898–2910.

Welty, N.E., Staley, C., Ghilardi, N., Sadowsky, M.J., Igyártó, B.Z., and Kaplan, D.H. (2013). Intestinal lamina propria dendritic cells maintain T cell homeostasis but do not affect commensalism. J. Exp. Med. *210*, 2011–2024.

Whibley, N., Tucci, A., and Powrie, F. (2019). Regulatory T cell adaptation in the intestine and skin. Nat. Immunol. *20*, 386–396.

Wiedemann, G.M., Knott, M.M.L., Vetter, V.K., Rapp, M., Haubner, S., Fesseler, J., Kühnemuth, B., Layritz, P., Thaler, R., Kruger, S., et al. (2016). Cancer cell-derived IL-1α induces CCL22 and the recruitment of regulatory T cells. Oncoimmunology *5*, 1–11.

Worley, M.J., Nieman, G.S., Geddes, K., and Heffron, F. (2006). Salmonella typhimurium disseminates within its host by manipulating the motility of infected cells. Proc. Natl. Acad. Sci. U. S. A. *103*, 17915–17920.

Wray, C., and Sojka, W.J. (1978). Experimental Salmonella typhimurium infection in calves. Sci. Res. Vet. *25*, 139–143.

Wu, M., Fang, H., and Hwang, S.T. (2001). Cutting Edge: CCR4 Mediates Antigen-Primed T Cell Binding to Activated Dendritic Cells. J. Immunol. *167*, 4791–4795.

Yahia, S.A., Azzaoui, I., Everaere, L., Vorng, H., Chenivesse, C., Marquillies, P., Duez, C., Delacre, M., Grandjean, T., Balsamelli, J., et al. (2014). CCL17 production by dendritic cells is required for NOD1-mediated exacerbation of allergic asthma. Am. J. Respir. Crit. Care Med. *189*, 899–908.

Yoshie, O., and Matsushima, K. (2015). CCR4 and its ligands: From bench to bedside. Int. Immunol. *27*, 11–20.

Yuan, Q., Bromley, S.K., Means, T.K., Jones, K.J., Hayashi, F., Bhan, A.K., and Luster, A.D. (2007). CCR4-dependent regulatory T cell function in inflammatory bowel disease. J. Exp. Med. *204*, 1327–1334.

Yuan, X., Cheng, G., and Malek, T.R. (2014). The importance of regulatory T-cell heterogeneity in maintaining self-tolerance. Immunol Rev. *259*, 103–114.

Zaid, A., Hor, J.L., Christo, S.N., Groom, J.R., Heath, W.R., Mackay, L.K., and Mueller, S.N. (2017). Chemokine Receptor–Dependent Control of Skin Tissue–Resident Memory T Cell Formation. J. Immunol. *199*, 2451–2459.